

BULGARIAN CHEMICAL COMMUNICATIONS

2024 Volume 56 / Special Issue D2

Selected papers presented on the 12th Chemistry Conference of Paisii
Hilendarski University of Plovdiv, 12 - 13 October 2023

*Journal of the Chemical Institutes
of the Bulgarian Academy of Sciences
and of the Union of Chemists in Bulgari*

Factors affecting the 5-hydroxymethyl-2-furfural content in the gas-phase of tobacco smoke of commercial cigarette brands

M. H. Docheva*, D. M. Kirkova, L. S. Stoyanova

Tobacco and Tobacco Products Institute, Agricultural Academy, Markovo 4108, Bulgaria

Received: November 3, 2023; Revised: April 11, 2024

Carbonyl compounds are some of the most harmful substances in tobacco smoke. They have mutagenic and carcinogenic properties and because of that, carbonyls are part of the controlled compounds in tobacco smoke in some countries. They cause burning and irritation of the upper respiratory tract of people during the smoking process. Acetaldehyde, acetone, acrolein, formaldehyde and 5-hydroxymethyl-2-furfural (5-HMF) are present in the largest quantities in tobacco smoke. 5-HMF is a product of the Maillard reaction and is found in many foods. In tobacco smoke, 5-HMF, together with the other carbonyl compounds, is formed by thermal combustion of the soluble sugars and the polysaccharides contained in the tobacco blends. 5-HMF has proven toxic and mutagenic properties. In this study, the factors affecting the 5-HMF content in the gas phase of tobacco smoke of different types of commercial cigarette brands are established. Three factors influencing the content of 5-HMF are investigated - type of blend, filter ventilation and type of filter. Higher content of 5-HMF is produced by Virginia blend cigarettes ($63.0 \pm 5.1 \mu\text{g}/\text{cig}$) compared to American blend cigarettes ($28.0 \pm 2.2 \mu\text{g}/\text{cig}$ and $48.0 \pm 3.8 \mu\text{g}/\text{cig}$). The cigarette brands with 30 - 40 % filter ventilation reduced the content of 5-HMF in tobacco smoke between 43 % and 58 % compared to the non ventilation filters. The content of 5-HMF is not significantly affected by the type of cigarette filter.

Key words: 5-hydroxymethyl-2-furfural (5-HMF), cigarette brands, cigarette blends, filter ventilation, cigarette filter

INTRODUCTION

There is a wide variety of smoking tobacco products on the world market to choose from, including cigarettes, cigars, cigarillos, bidis, chuttas and kreteks. Cigars, cigarillos, bidis, chuttas and kreteks consist only of tobacco leaves. Cigarillos are short, narrow cigars and are wrapped in tobacco leaves or brown, tobacco-based paper. They are smaller than regular cigars but usually larger than cigarettes. Bidis consist of a small amount of sun-dried, flaked tobacco hand wrapped in dried temburni or tendu leaf and tied with string. Despite their small size, bidis deliver more tar and carbon monoxide than manufactured cigarettes. Chuttas are homemade cigars and have a higher content of nicotine and total particulate matter as compared to cigarettes and Bidi. Kreteks are clove-flavored cigarettes. They may contain a wide range of exotic flavorings and eugenol, which have an anesthetic effect, allowing for deeper and more harmful smoke inhalation [1].

In the production of cigarettes, blended tobaccos are used - a mixture of two or more types of tobaccos in different proportions. The type of tobacco used in tobacco products has a decisive influence on the physicochemical nature and taste of the tobacco smoke they produce [1].

Tobacco smoke is a multicomponent system consisting of a solid-liquid phase, a gas phase, and environmental tobacco smoke. The qualitative composition of tobacco smoke is the same. The differences are only quantitative [2].

Tobacco smoke of the commercially sold cigarettes contains more than 6000 chemicals. They are formed during smoking processes, through pyrolysis, intra- or intermolecular interactions of the substances contained in tobacco. Most of these substances are potential toxicants, such as components of the groups of volatile organic compounds, polycyclic aromatic hydrocarbons, aromatic amines, tobacco-specific nitrosamines, phenolic compounds, carbonyl compounds [2-6].

More than 500 carbonyl compounds are identified in tobacco smoke, but ten of them are classified as probably and possibly carcinogenic to humans by the International Agency for Research of Cancer [3]. They cause burning and irritation of the upper respiratory tract of people when smoking. Carbonyls, including acetaldehyde, acetone, acrolein, formaldehyde, 5-hydroxymethyl-2-furfural (5-HMF), are present at high levels in the tobacco smoke [5].

5-HMF is formed in many food items - dried fruit, fruit juice, caramel products. It is also detected in cigarette smoke [7]. Tobacco smoke is produced

* To whom all correspondence should be sent:
E-mail: margarita_1980@abv.bg

by the thermal combustion of sugars in tobacco products, including complex polysaccharides such as cellulose, along with other carbonyl compounds [8]. 5-HMF has proven carcinogenic, hepatotoxic, nephrotoxic, neurotoxic, genotoxic, mutagenic, cytotoxic effect, reproductive and developmental toxicity [7].

The aim of this study is to investigate the factors affecting the content of 5-HMF in the gas phase of tobacco smoke in commercial cigarette brands.

EXPERIMENTAL

Material

The content of 5-HMF in tobacco smoke of 3 commercial cigarette brands (Virginia blends and two American blends) with different types of cigarette filters and filter ventilation were investigated. The cigarettes were purchased from the markets. The description of the investigated cigarettes is presented on Table 1.

Table 1. Description of the cigarette brands

Cigarettes
<i>Brand A</i>
Virginia blend A-nV-A –non-ventilation, acetate filter A-V35-A - 35 % ventilation, acetate filter A-nV-M –non-ventilation, menthol capsule
<i>Brand B</i>
American blend B-nV-A –non-ventilation, acetate filter B-nV-Ach –non-ventilation, acetate and charcoal filter (two sectors filter) B-V30-Ach – 30 % ventilation, acetate and charcoal filter (two sectors filter)
<i>Brand C</i>
American blend C ₁ -nV-A –non-ventilation, acetate filter C ₁ -V40-A – 40 % ventilation, acetate filter C ₂ -nV-ARCh – non-ventilation, acetate, recessed and charcoal filter system (three sectors filter) C ₂ -V40-ARCh – 40 % ventilation, a cetate, recessed and charcoal filter system (three sectors filter)

Three factors influencing the content of 5-HMF were investigated:

- Tobacco blends - Virginia blend and American blend (cigarette brands A-nV-A, B-nV-A and C₁-nV-A).

- Filter ventilation – non-ventilation, 30 % ventilation, 35 % ventilation, 40 % ventilation (cigarette brands A-nV-A and A-V35-A; B-nV-ACh and B-V30-Ach; C₁-nV-A and C₁-V40-A; C₂-nV-ARCh and C₂-V40-ARCh).

- Filter types – acetate; acetate and charcoal (two sectors); acetate, recessed and charcoal (three sectors) -A-nV-A and A-nV-M; B-nV-A and B-nV30-Ach; C₁-nV-A and C₂-nV-ARCh; C₁-V40-A and C₂-V40-ARCh.

Reagents

5-Hydroxymethyl furfural, 2,4-dinitrophenylhydrazine, acetonitrile, perchloric acid, glacial acetic acid, hydrochloric acid 37 %, sodium hydroxide, calcium chloride hexahydrate, *p*-hydroxybenzoic acid hydrazide (PAHBAH), citric acid monohydrate, D-glucose were purchased from Sigma Aldrich.

Methods

- *Determination of carbonyl compounds in tobacco smoke by HPLC-UV/VIS –Coresta recommended method №74, 2018 with some modifications* [9]. Two cigarettes were smoked according to ISO 3308-2012 [10] on an 8-channel linear smoking machine Filtrona 302 fitted with an impinger containing 40 ml of an acidified solution of 2,4-dinitrophenylhydrazine with a concentration of 3.396 mg/ml. The carbonyls in tobacco smoke were trapped by passing each puff through an impinger. The solution was left in the dark for at least 5 hours until the reaction is completed and the carbonyl hydrazone formed. The high-performance liquid chromatograph Perkin Elmer equipped with binary pump and UV/VIS detector was used. The chromatographic analysis was performed on an analytical column “Kromasil” C18, 5 µm, 150 mm. The mobile phase composition was: A = CH₃OH:H₂O (60:40); B = CH₃OH:H₂O (80:20). Gradient elution profile was 100% A, 0 min; 30 min to 0 % A, λ=360 nm.

- *Determination of the content of total sugars by continuous-flow analysis method using hydrochloric acid/p-hydroxybenzoic acid hydrazide (PAHBAH) – Coresta recommended method №89, 2019* [11]. An aqueous extract of the tobacco was prepared and the total sugar content of the extract was analyzed by continuous-flow analysis on Autoanalyzer AA3. The extract was heated in the presence of HCl at 90 °C, which hydrolyses any sucrose present to glucose and fructose. The reduced sample extract was passed through a dialyzer to eliminate interference from colored compounds in the sample and then reacted with PAHBAH in alkaline medium at 85 °C to produce a yellow

osazone complex. All measurements were performed at 420 nm.

All experiments were performed at least three times. 5-HMF yield in tobacco smoke was calculated as mg per cigarette. Total sugars in tobacco blends were calculated as %. All data are presented as mean \pm standard deviation.

RESULTS AND DISCUSSION

Type of blend

The most commonly used cigarette blends are American blend and Virginia blend [1, 12].

The content of 5-HMF in tobacco smoke of two brands of American blend cigarettes and one brand of Virginia blend cigarettes were investigated. In order to eliminate the influence of the filter type and filter ventilation, cigarettes were selected with the same type of filter – non-ventilation, acetate filter (Table 1). The results are presented in Table 2. The higher 5-HMF emissions were produced by Virginia blend cigarettes (63.0 ± 5.1 $\mu\text{g}/\text{cig}$ - A-nV-A) compared to American blend cigarettes (48.0 ± 3.8 $\mu\text{g}/\text{cig}$ – C₁-nV-A and 28.0 ± 2.2 $\mu\text{g}/\text{cig}$ – B-nV-A). It was found that the difference between the highest and the lowest content of 5-HMF in tobacco smoke is 35 $\mu\text{g}/\text{cig}$.

Table 2. Content of 5-HMF in tobacco smoke of different cigarette blends, $\mu\text{g}/\text{cig} \pm \text{SD}$

Tobacco blend	Cigarette brands	5-HMF
Virginia blend	A-nV-A	63.0 ± 5.1
American blend	B-nV-A	28.0 ± 2.2
American blend	C ₁ -nV-A	48.0 ± 3.8

The obtained results can be explained by the composition of the different tobaccos included in the tobacco blends. In Virginia blends there is an approximate ratio on a weight-weight basis (w/w) of Virginia tobacco and Burley 68:27 (w/w). The ratio can be skewed in favor of either tobacco type or manipulation of the deliveries. Oriental tobacco makes up less than 5% w/w of the tobacco blend [13]. The American blend consists of Virginia, Burley and Oriental tobacco in a ratio of approximately 50:37:13 (w/w/w) [13]. In the Virginia blend, the total amount of Virginia and Oriental tobacco is higher than in the American blend. Kirkova *et al.* found that the highest content of 5-HMF was produced in tobacco smoke by Virginia tobaccos (between 56 $\mu\text{g}/\text{cig}$ and 76 $\mu\text{g}/\text{cig}$) and Oriental tobaccos (between 34.2 $\mu\text{g}/\text{cig}$ and 108 $\mu\text{g}/\text{cig}$), compared to the Burley tobacco (between 15.6 $\mu\text{g}/\text{cig}$ and 35.0 $\mu\text{g}/\text{cig}$) [14].

Filter ventilation

Filter ventilation dilutes tobacco smoke with air, which is achieved through filter holes, which are usually one or more rings of small holes or perforations and serve to dilute the smoke with air [12]. Ventilated filters are now common on cigarettes sold in EU countries. Filter ventilation reduces standard toxin yields, such as tar, nicotine and CO [12, 15], but the influence of filter ventilation on the content of 5-HMF in tobacco smoke is not investigated. In this regard, ventilated cigarettes A-V35-A, B-V30-ACh, C₁-V40-A and C₂-V40-ARCh were selected. In the research both ventilated cigarettes and closed ventilated cigarettes were used.

The content of 5-HMF in cigarette brands with non-ventilated filters varied between 63.0 ± 5.1 $\mu\text{g}/\text{cig}$ (A-nV-A) and 28.0 ± 2.2 $\mu\text{g}/\text{cig}$ (B-nV-ACh), while the content of 5-HMF with filter ventilation varied from 12.2 ± 0.9 $\mu\text{g}/\text{cig}$ (B-V30-ACh) to 32.6 ± 2.6 $\mu\text{g}/\text{cig}$ (A-V35-A) – Table 3. The data revealed that the cigarette brands with 30% - 40% filter ventilation reduced the content of 5-HMF in tobacco smoke between 43% (Brand B) and 58% (Brand C) compared to non-ventilated filters. The results are presented in Table 3.

Table 3. Content of 5-HMF in tobacco smoke of cigarette brands with different filters ventilation, $\mu\text{g}/\text{cig} \pm \text{SD}$

Filter ventilation	Cigarette brands	5-HMF
Non ventilation	A-nV-A	63.0 ± 5.1
35 % ventilation	A-V35-A	32.6 ± 2.6
Non ventilation	B-nV-ACh	28.0 ± 2.2
30 % ventilation	B-V30-ACh	12.2 ± 0.9
Non ventilation	C ₁ -nV-A	48.0 ± 3.8
40 % ventilation	C ₁ -V40-A	20.0 ± 2.8
Non ventilation	C ₂ -nV-ARCh	40.0 ± 3.2
40 % ventilation	C ₂ -V40-ARCh	22.8 ± 3.5

The content of 5-HMF in the gas phase of tobacco smoke decreases in proportion to the decrease in the content of tar, nicotine and CO in the solid-liquid phase of tobacco smoke. Docheva *et al.* 2022 established that the content of tar and CO in cigarettes with 30 % ventilation decreased by about 92 %, while the nicotine content - by 36 % compared to non-ventilation cigarettes [16].

Type of filters

To determine the effect of the type of cigarette filters on the content of 5-HMF, cigarette brand A and cigarette brand B were smoked with block vents

(non-ventilation filter). Cigarette brand C was smoked with filter ventilation and filter non-ventilation. The results are presented in Table 4.

Table 4. Content of 5-HMF in tobacco smoke of cigarette brands with different filter types, $\mu\text{g}/\text{cig} \pm \text{SD}$

Filter types	Cigarette brands	5-HMF
Acetate	A-nV-A	63.0 \pm 5.1
Acetate menthol capsule	A-nV-M	70.0 \pm 6.2
Acetate	B-nV-A	28.0 \pm 2.3
Acetate and charcoal filter (two sectors filter)	B-nV-ACh	39.0 \pm 3.2
Acetate	C ₁ -nV-A	48.0 \pm 3.8
Acetate, recessed and charcoal filter system (three sectors filter)	C ₂ -nV-ARCh	40.0 \pm 3.2
Acetate filter	C ₁ -V40-A	20.0 \pm 2.8
Acetate, recessed and charcoal filter system(three sectors filter)	C ₂ -V40-ARCh	22.8 \pm 3.5

Cigarette filters with an activated menthol capsule (A-nV-M) and acetate and charcoal filter (two sectors) (B-nV-ACh) increased the content of 5-HMF in tobacco smoke. The amount of 5-HMF in cigarette brands with acetate filter with activated menthol capsule (A-nV-M) is 70.0 \pm 6.2 $\mu\text{g}/\text{cig}$ and it is 7.0 $\mu\text{g}/\text{cig}$ more than the acetate filter (A-nV-A). Cigarettes with acetate and charcoal filter (B-nV-ACh) produced 39.0 \pm 3.2 $\mu\text{g}/\text{cig}$ 5-HMF, while those with acetate filter (B-nV-A) - 28.0 \pm 2.3 $\mu\text{g}/\text{cig}$. For cigarette brand C with non-vented three-sector filter (C₂-nV-ARCh) a reduction in content of 5-HMF of 8.0 $\mu\text{g}/\text{cig}$ is reported compared to non-vented acetate filter C₁-nV-A. Cigarette brand with three-sector ventilated filter (C₂-V40-ARCh) showed approximately the same 5-HMF content (22.8 \pm 3.2 $\mu\text{g}/\text{cig}$) compared to acetate ventilated filter (C₁-V40-ARCh) - 20.0 \pm 0.8 $\mu\text{g}/\text{cig}$.

The content of 5-HMF in tobacco smoke in one cigarette is significantly lower than that of the toxic effect of 5-HMF - 2–30 mg per person/day [17, 18].

Content of soluble sugars in cigarette tobacco blends

The main degradation product in the caramelization reaction of sugars is 5-HMF [8]. In this regard the content of soluble (total) sugars in tobacco blends A, B and C was analyzed. The results are presented in Table 5. The content of soluble sugars in the Virginia blend (13.7 \pm 0.14 %) is higher than in the American blend – 8.5 \pm 0.08 % and

10.8 \pm 0.11 %. The results obtained are consistent with the ratio of the different types of tobacco in the blends and the content of total sugars in tobaccos. Virginia blend has more than 68% Virginia tobacco content, while American blend has less Virginia tobacco content - about 50% [13].

Table 5. Content of soluble sugars in tobacco of cigarette brands, % \pm SD

Tobacco blend	Total sugars
Virginia blend (A)	13.7 \pm 0.14
American blend (B)	8.5 \pm 0.08
American blend (C)	10.8 \pm 0.11

Correlation between 5-HMF in tobacco smoke and soluble sugars in cigarette brands

Additionally, the ratio between the content of 5-HMF in tobacco smoke and total sugars in cigarette brands with different type of blends and different filter ventilation was investigated. The correlation (R^2) between the content of 5-HMF in tobacco smoke and total sugars in cigarette brands with different type of blends and different filter ventilation is presented in Table 6.

Table 6. Correlation (R^2) between the content of 5-HMF in tobacco smoke and soluble sugars in cigarette brands with different type of blends, different filter ventilation and different filter type.

Correlation	Soluble sugars, %		
	Type of blends	Filter ventilation	Filter type
5-HMF, $\mu\text{g}/\text{cig}$	0.978	0.9864	0.2283

A high correlation between the content of 5-HMF in tobacco smoke and total sugars in cigarette brands with different type of blends and different filter ventilation was found. The content of 5-HMF is not affected by the type of filter.

CONCLUSION

In this study three factors affecting the 5-HMF content in the gas phase of tobacco smoke in different types of commercial cigarette brands were investigated - type of blend, filter ventilation and type of filter. 5-HMF is a degradation product on the caramelization reaction of sugars during the smoking process. The highest content of 5-HMF was found in tobacco smoke of Virginia blend cigarettes, followed by American blend cigarettes. Filter ventilation reduced the 5-HMF content between 43 % and 58 % compared to the non ventilation filters. Cigarette filters with an activated menthol capsule and acetate and charcoal filter increased the content

of 5-HMF in tobacco smoke. Cigarette brand with acetate, recessed and charcoal filter system showed approximately the same 5-HMF content compared to acetate ventilated filter.

Acknowledgement: This research is supported by the Bulgarian Ministry of Education and Science under the National Program “Young Scientists and Postdoctoral Students – 2”.

REFERENCES

1. IARC Monographs on the Evaluation of Carcinogenic Risks to Humans, No. 83. IARC Working Group on the Evaluation of Carcinogenic Risks to Humans, Lyon (FR), International Agency for Research on Cancer 2004.
2. F. Soleimani, S. Dobaradarn, G. Torre, T. Schmidt, R. Saeedi, *Sci Total Environ.*, **813**, 152667 (2022).
3. A. Rodgman, A. Perfetti A. The Chemical Components of Tobacco and Tobacco Smoke, 2nd edn., CRC Press; Boca Raton, Florida, 2013.
4. J. Leffingwell, Chemical Constituents of Tobacco Leaf and Differences among Tobacco Types, Science Direct Working Paper No S1574-0331 (04) 70433-6, 1–60 (2001).
5. T. Horinouchi, T. Higashi, Y. Mazaki, S. Miwa, *Biol Pharm Bull.*, **39** (6), 909 (2016).
6. WHO Elaboration of guidelines for implementation of the Convention (decision FCTC/COP1(15)) Article 9: Product regulation Conference of the Parties to the WHO Framework Convention on Tobacco Control Second session, 2007
7. M. Farag, M. Alagawany, M. Bin-Jumah, S. Othman, A. Khafaga, H. Shaheen, D. Samak, A. Shehata, A. Allam, M. El-Hack, *Molecules*, **25**: 1941 (2020).
8. M. Banožic, S. Jokic, D. Ackar, M. Blažic, D. Šubaric, *Molecules*, **25**, 1734 (2020).
9. CRM 74 Determination of Selected Carbonyls in Mainstream Cigarette Smoke by High Performance Liquid Chromatography (HPLC), 2019.
10. ISO 3308:2012. Routine analytical cigarette-smoking machine - Definitions and standard conditions, 2012.
11. CRM 89 Tobacco – Determination of the content of total sugars – continuous-flow analysis method using hydrochloric acid / *p*-hydroxybenzoic acid hydrazide (PAHBAH), 2019.
12. D. Hoffmann, I. Hoffmann, in: Risks Associated with Smoking Cigarettes with Low Machine-Measured Yields of Tar and Nicotine (Smoking and Tobacco Control Monograph No. 13; NIH Publ. No. 02-5074), Bethesda, MD, National Cancer Institute, p. 159 2001.
13. J. Wigand, Additives, Cigarette Design and Tobacco Product Regulation. A Report to World Health Organization, Tobacco Free Initiative, Tobacco Product Regulation Group, 28 June-2 July 2006, Kobe, Japan, 2006.
14. D. Kirkova, M. Docheva, Y. Kochev, *Proceed. of National Sci. Conf. with Intern. Participation “Ecology and Health”* 25-26 June 2020, Plovdiv, Bulgaria, 100 (2020).
15. L. Kozłowski, R. O'Connor, *Tobacco Control*, **11**:i40-i50 (2002).
16. M. Docheva, Y. Kochev, M. Kasheva, H. Bozakov *Kem. Ind.*, **71** (3-4): 157–161 (2022).
17. K. Appel, R. Gürtler, K. Berg, G. Heinemeyer, A. Lampen, K. Appel, *Mol. Nutr. Food Res.*, **55**: 667–678 (2011).
18. S. De La Cueva, J. Álvarez, A. Vegvari, J. Montilla-Gómez, O. Cruz-López, C. Delgado-Andrade, J. Henares, R. Ángel, *Mol. Nutr. Food Res.*, **61**, 1600773 (2016)

Persistent pollutants in marine organisms: assessment of the state of the Black Sea environment

S. K. Georgieva*, Zl. Peteva, S. Valkova

Department of Chemistry, Faculty of Pharmacy, Medical University - Varna, 55 Marin Drinov Str., Varna, Bulgaria

Received: November 3, 2023; Revised: April 11, 2024

In the last decades, the residues of persistent pollutants such as organochlorine pesticides and polycyclic aromatic hydrocarbons (PAHs) are ubiquitous in marine ecosystems and continue to bioaccumulate in animal tissues. The present study investigated the presence of pollutants in biota with the aim to assess the current environmental state of the Black Sea using benthic fish species as sentinel organisms. The biota samples: goby (*Neogobius melanostomus*), grey mullet (*Mugil cephalus*) and turbot (*Psetta maxima maeotica*) were collected from different sites along the Bulgarian Black Sea coast in the period 2021 – 2022. The concentrations of 13 PAHs and organochlorine pesticides such as DDTs and its metabolites, hexachlorocyclohexane and its isomers (HCHs), hexachlorobenzene (HCB) and hexachlorobutadiene (HCBd) were determined in fish tissues by simultaneous extraction of persistent compounds in an accelerated solvent extractor (ASE) and were detected by gas chromatography with mass spectrometry (GC-MS).

The highest levels of PAHs in fish were found in goby samples: 14.2 ng/g ww (wet weight). The results showed that low-molecular weight (LMW) PAHs (3 and 4 aromatic rings) were predominant accounting 94% of total PAH levels, suggesting petrogenic origin of pollution. Benzo(a)pyrene was not detected in fish samples from the Bulgarian Black Sea coast. Lindane and other HCHs isomers have very low concentrations in all samples investigated. DDT is present mainly in the form of its metabolites p,p'-DDE and p,p'-DDD, suggesting contamination in the past. The HCB and HCBd levels in the fish species did not exceed the EQS of the Directive 2013/39/ EU. These results confirm that the persistent organic pollutants continue to be present in the Black Sea marine environment.

Keywords: polycyclic aromatic hydrocarbons, organochlorine pesticides, fish, the Black Sea

INTRODUCTION

Various studies have shown that persistent pollutants such as organochlorine pesticides and polycyclic aromatic hydrocarbons (PAHs) are ubiquitous in different parts of marine ecosystems (water column, sediment and biota) and exhibit different types of toxicity to humans and marine organisms depending on their persistence, mobility and bioavailability [1-3].

The Marine Strategy Framework Directive (MSFD) aims at maintaining the state of the marine environment by preventing the long-term deterioration of marine ecosystems [4]. Assessments on the environmental status of marine waters and the anthropogenic pressures were based on the Good Environmental Status (GES) definitions. Determination of the GES which defines the environmental quality to be assessed for 11 descriptors: these are either descriptors for pressure (non-indigenous species, eutrophication, hydrographical changes, contaminants in the environment, contaminants in the seafood, marine litter and underwater noise) or 'State' descriptors

(biodiversity, commercially exploited fish and shellfish, food webs and sea-floor integrity) [4]. Evaluation of the presence, control and effects of pollutants in the marine organisms according to MSFD was considered by descriptor 8 (Concentrations of contaminants give no effects) and descriptor 9 (Contaminants in seafood are below safe levels) [3, 4].

Plastic particles, pharmaceuticals, polycyclic aromatic hydrocarbons (PAHs), polychlorinated biphenyls (PCBs), pesticides and other endocrine disruptors, are only some examples of persistent pollutants that are permanently present in the coastal ecosystems [2, 5, 6]. The physicochemical properties of pollutants such as molecular size, high liposolubility and volatility, determine their availability, distribution and environmental persistence in the aquatic ecosystems and biota [1, 7].

The EU Directive 2008/105/EC established the Environmental Quality Standards (EQS) for 33 priority substances and other 8 pollutants with the aim to achieve a good chemical status of surface

* To whom all correspondence should be sent:
E-mail: stgeorgieva@mu-varna.bg

waters [8, 9]. The EQS were set for prey tissue (ww) and EU member states were being able to choose “the most appropriate indicator from among fish, molluscs, crustaceans and other biota” [8]. Fish concentrate pollutants in their tissues directly from water, but also through their diet, thus enabling the assessment of the transfer of pollutants through the trophic web [10].

The specific morphological, climatic and hydrological properties of the Black Sea as a semi-enclosed water basin make it very vulnerable to the impact of anthropogenic pollution. The Bulgarian Black Sea coast is subject to high levels of pollution from various sources – inflow of large rivers, agriculture, intensive shipping, tourism and recreation [11]. The war in Ukraine, which has been going on for almost two years, also poses an environmental risk and is likely to have long-term negative consequences for the Black Sea ecosystem.

PAHs are ubiquitous pollutants in shallower and coastal waters, especially in areas highly subjected to anthropogenic inputs: harbors and river mouths [12, 13]. Of the hundreds of known PAHs, 16 have been listed as priority pollutants by the United States Environmental Protection Agency (US EPA) [2, 14]. The International Agency for Research on Cancer (IARC) has classified sixteen PAHs as probable or possible human carcinogens which can cause mutagenic effects in humans and animal species [15, 16].

HCB and HCBd were pointed as priority substances under EC Directive 2013/39/EU [17]. The main source of this hydrophobic and highly persistent compound HCB today is the chemical industry from which this compound can be emitted as a product in high-temperature processes [18]. Hexachlorobutadiene (HCBd) is currently generated in large quantities as an unintentional by-product in the manufacture of other chlorinated hydrocarbons and polymers [19, 20]. DDT (1,1,1-trichloro - 2, 2 - bis (4-chlorophenyl) ethane) and its metabolites (DDTs) rapidly accumulated in living organisms due to their high lipophilicity [21]. DDT was among the initial persistent organic pollutants listed under the Stockholm Convention (2001) [22] and continues to be used for control of malaria in tropical and subtropical countries [23]. Hexachlorocyclohexane (HCH) isomers were added to the list of the Stockholm Convention in 2009 [22]. Lindan (γ -HCH) and the isomers α -HCH and β -HCH were indicated by the Integrated Risk Information System (IRIS) online database of the Environmental Protection Agency (EPA) as carcinogenic for humans [24].

Data on the presence and distribution of persistent contaminants in fish and especially edible fish species are important not only from ecological, but also human health perspective [25]. To our knowledge, the data on levels of PAHs in fish from the Bulgarian Black Sea coast are very scarce in the literature. The study investigated the presence of persistent organic pollutants in biota with the aim to assess the current environmental state of the Black Sea using benthic fish species goby (*Neogobius melanostomus*), grey mullet (*Mugil cephalus*) and turbot (*Psetta maxima maeotica*) as sentinel organisms.

MATERIALS AND METHODS

Sampling

Benthic fish species were sampled from different stations of the Black Sea coast of Bulgaria: goby (*Neogobius melanostomus*), grey mullet (*Mugil cephalus*) and turbot (*Psetta maxima maeotica*). Samples were caught by local professional fishermen in the period Spring 2021 – Spring 2022. All fish samples were transported into the laboratory in foam boxes filled with ice. In the laboratory, for every fish species a pooled sample of muscle tissue from each individual was compiled by filleting and dissecting. The muscle fish tissue from 10-12 individuals (except turbot) was homogenized by a blender.

Analytical method

The concentrations of 13 PAHs and organochlorine pesticides such as DDTs and its metabolites, hexachlorocyclohexane and its isomers (HCHs), hexachlorobenzene and hexachlorobutadiene were determined in fish tissues with a mixture of hexane:acetone by simultaneous extraction of POPs in an accelerated solvent extractor. The accelerated solvent extraction (ASE) method requires a small amount of organic reagent, and the extraction can be performed rapidly.

A cellulose filter (Thermo Scientific) was placed at the bottom of a 66 mL extraction cell, followed by 10 g Al₂O₃ (acid, Brockmann Activity 1) and another cellulose filter. A 4 g sample was homogenized with an equal weight (10 g) of Thermo Scientific Dionex ASE Prep DE (Thermo Scientific) in a mortar and transferred into the extraction cell. Into this mixture, 25 μ L hexane solution containing the two internal standards (PCB30, PCB204 and 9,10 dihydroanthracene, Dr. Ehrenstorfer Laboratory, Augsburg, Germany, 10 μ g/mL) was added for quantifying the overall recovery of the analytical procedures.

Optimized ASE parameters (4:1, v/v n-hexane/acetone, 80 °C, 1500 psi, 10 min static time, two-cycle extraction, and 90 % rinse volume). Total extraction time and total solvent volume per sample: ~ 30 min and ~ 100 mL, respectively. The extracts were collected in 250 mL vials and were treated with sodium sulfate to remove any possible humidity. After filtration, the organic phase was concentrated to dryness on a rotary evaporator (Hei-Vap Precision Heidolph, Heidolph Instruments GmbH & CO. KG, Germany). The lipid content of each sample was measured gravimetrically.

The clean-up of the samples was conducted according to the previously described method [5]. The extract was cleaned-up on a self-packed multilayer glass column filled with neutral silica and acid silica. PAHs and OCPs were eluted with 10 mL of n-hexane followed by 20 mL of n-hexane/dichloromethane (9:1 v/v). The purified extracts were concentrated to near dryness, reconstituted in 0.5 mL of n-hexane and submitted to analysis by GC-MS. The GC conditions are summarized below.

The analytical determination of individual compounds was carried out on a gas chromatograph GC FOCUS with a POLARIS Q Ion Trap mass spectrometer (Thermo Electron Corporation, USA). A TG-5ms capillary column (Thermo Electron Corporation, USA) with a length of 30 m, 0.25 mm ID and a film thickness of 0.25 µm was used for GC separation of individual compounds. The temperature program for separation of PAHs was as follows: 40°C (1 min), 40°C/min to 130°C (3 min), 12°C/min to 180°C, 7°C/min to 280°C, 10°C/min to 310°C and a final hold for 5.0 min. For DDTs, HCHs, HCB and HCBd determination, the oven was programmed as follows: 60°C (1 min), 30°C/min to 180°C, 5°C/min to 260°C, 30°C/min to 290°C and final hold - 3.0 min. Helium at a flow rate of 1 mL/min was used as carrier gas.

For instrument calibration, recovery determination and quantification of compounds were used pure reference standard solutions: EPA 525 PAH Mix B, 500 µg/mL of each component in acetone (Sigma Aldrich, USA) and EPA 625/CLP Pesticides Mix 2000 µg/mL each component in hexane: toluene (1:1) (Supelco, USA). GC-MS was applied to the analysis of compounds: 13 PAHs: acenaphthylene (ACL), anthracene (AN), benz[a]anthracene (BaA), benzo[b]fluoranthene (BbFA), benzo[k]fluoranthene (BkFA), benzo[ghi]perylene (BghiP), benzo[a]pyrene (BaP),

chrysene (CHR), dibenzo[a,h]anthracene (DbahA), fluorene (FL), indeno[1,2,3-cd]pyrene (IP), phenanthrene (PHE) and pyrene (PY). Organochlorine compounds (OCs): p,p'-DDT, p,p'-DDD and p,p'-DDE, HCB, HCBd; isomers of hexachlorocyclohexane (HCH): γ-HCH (Lindane), α-HCH, β-HCH and δ-HCH. All measurements were performed in triplicate in order to ensure the accuracy of the analytical procedures. Multi-level calibration curves (range 5 – 100 ng/mL) were used for the quantification and good linearity ($R^2 > 0.996$) was achieved for the tested intervals that included the whole concentration range found in the samples (Table 1).

The identification of target analytes by GC with Ion Trap - MSn (IT-MSn) detection was based on a selected parent ion and the whole mass spectrum of its daughter ions. The IT-MSn detection was performed by isolation of the selected parent (precursor) ion for each compound inside the Ion trap MS analyzer followed by application of an adequate excitation voltage for its subsequent fragmentation to its daughter ions (Figs. 1 and 2). Parent ions were selected from the EI-MS spectra (Full scan) based on high m/z values and the peak abundance as well as the chromatographic signal obtained after its isolation in the Ion trap [7]. The PAHs and organochlorine compounds were identified by the relative retention time and the intensity ratios of the monitored extracted ions for GC-MS - Table 1.

Quality control

Quality control procedures included procedural blanks, analysis of replicate samples, use of recovery surrogates, and analysis of certified reference materials BCR - 598 (DDTs in Cod liver oil) - Institute for Reference Materials and Measurements, European Commission). Recovery of DDTs from certified reference material varied in the range 85 - 109% for individual congeners. The blanks did not contain traces of contaminants. The repeatability of the method (evaluated as the relative standard deviation, RSD) was <20%, calculated on 6 replicates of sample at the lowest spiked level.

The method limits of detection (LOD) were calculated as 3 times the standard deviation, based on the low concentrations of PAHs and OCs in fish tissue. The LOQ is the analyte concentration corresponding to ten times the standard deviation. The limit of detection (LOD) of the method was from 0.02 to 0.15 ng/g and the limit of quantification (LOQ) from 0.07 to 0.5 ng/g ww.

Statistical analysis

The statistical analysis of the data was based on the comparison of average values by a t-test. The p-value below 0.05 was considered statistically significant ($p < 0.05$). Concentrations below LODs were considered as LOD/2 for all statistical analyses.

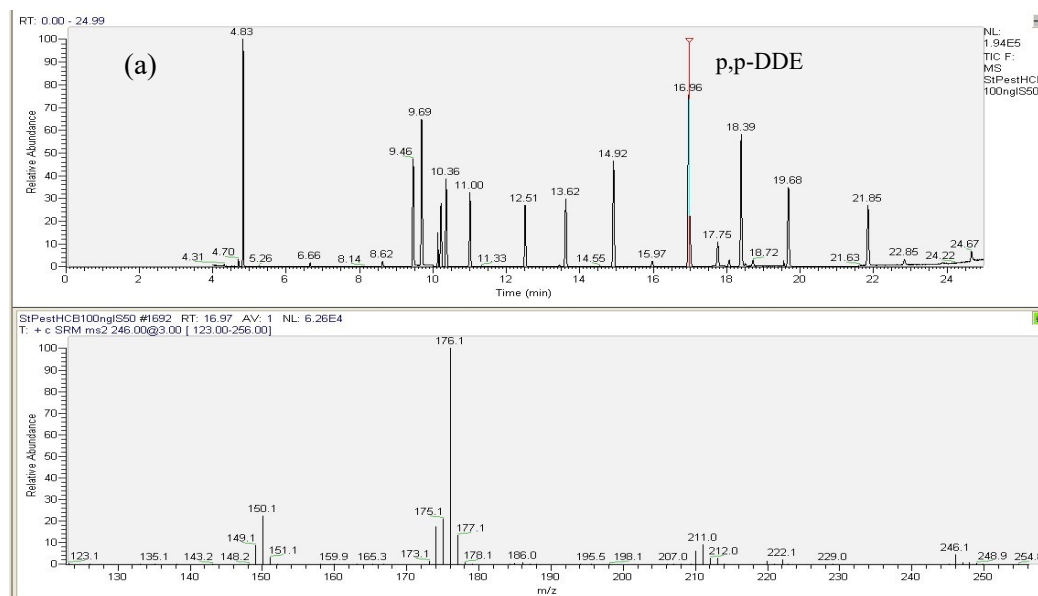
All statistical tests were performed using the SPSS V19.0 package for Windows (SPSS Inc., Chicago, IL, USA).

The chromatograms and mass spectra of reference standard solutions of OCPs and PAHs and fish extract samples are presented in Figs. 1(a, b) and 2(a, b), respectively.

Table 1. Retention time, linearity (correlation coefficient), precursor ions, extracted ions, recovery of individual organochlorine compounds and PAHs.

Compounds	Retention time (s)	Linearity	Recovery	Precursor ions	Extracted ions selected
	min	R ²	(%)	m/z	m/z
HCBD	4.79	0.9966	97.5	225	153.0, 190.0, 225.0
HCB	9.67	0.9979	99.1	284	214.0, 249.0, 284.0
α-HCH	9.44	0.9968	96.5	181	109; 145; 147
γ-HCH	10.34	0.9977	97.8	181	109; 145; 147
β-HCH	10.14	0.9976	86.9	181	109; 145; 147
δ-HCH	10.99	0.9991	89.3	181	109; 145; 147
p,p' - DDE	16.94	0.9956	98.1	246	176.1; 150.1
p,p' - DDD	18.37	0.9985	96.2	235	165.1; 199.1
p,p' - DDT	19.66	0.9999	95.9	235	165.1; 199.1
ACL	9.47	0.9984	97.5	152.1	98.1; 126.1; 152.1
FL	11.08	0.9991	96.1	165.1	139.1; 165.2
PHE	13.56	0.9992	96.3	178.1	98.1; 152.1; 176.1
AN	13.68	0.9997	91.4	178.1	98.1; 152.1; 176.1
PY	17.73	0.9998	93.9	202.2	122.1; 174.1; 200.1
BaA*	21.63	0.9986	89.3	228.2	146.0; 200.1; 226.1
CHR*	21.76	0.9978	88.1	228.2	170.1; 202.1; 224.1
BbFA*	24.99	0.9971	86.2	252.2	193.1; 179.1; 224.1
BkFA	25.06	0.9995	85.9	252.2	193.1; 179.1; 224.1
BaP*	25.85	0.9986	87.5	252.2	193.1; 179.1; 224.1
IP	28.52	0.9978	89.1	276.2	222.1; 248.2; 274.2
DBahA	28.60	0.9998	84.5	276.2	224.2; 248.2; 274.2
BghiP	29.13	0.9965	83.8	276.2	222.1; 248.2; 274.2

* - group of the priority 4PAHs; PAHs: polycyclic aromatic hydrocarbons



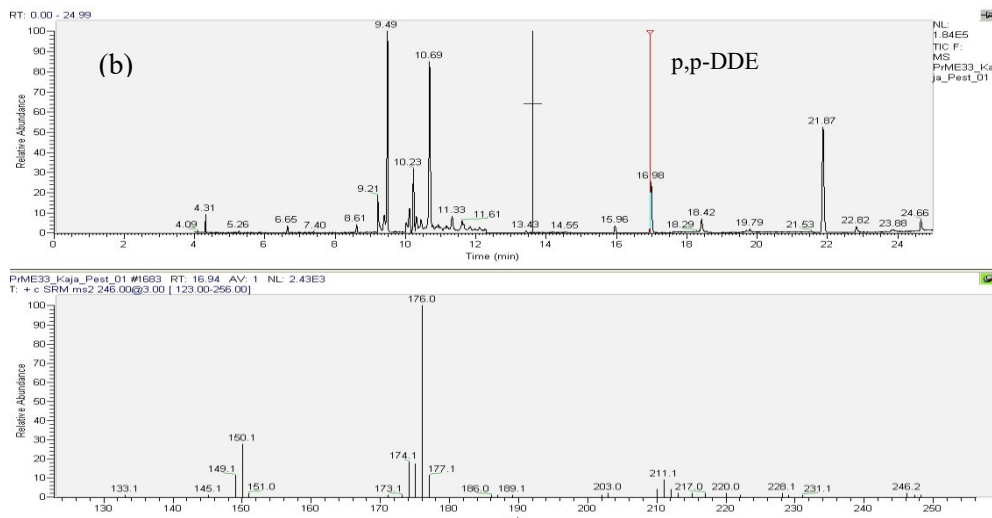


Figure 1. Chromatograms of reference standard solutions of OCPs 100 ng/mL (a) and fish extract sample (b); mass spectra of DDE in standard and sample.

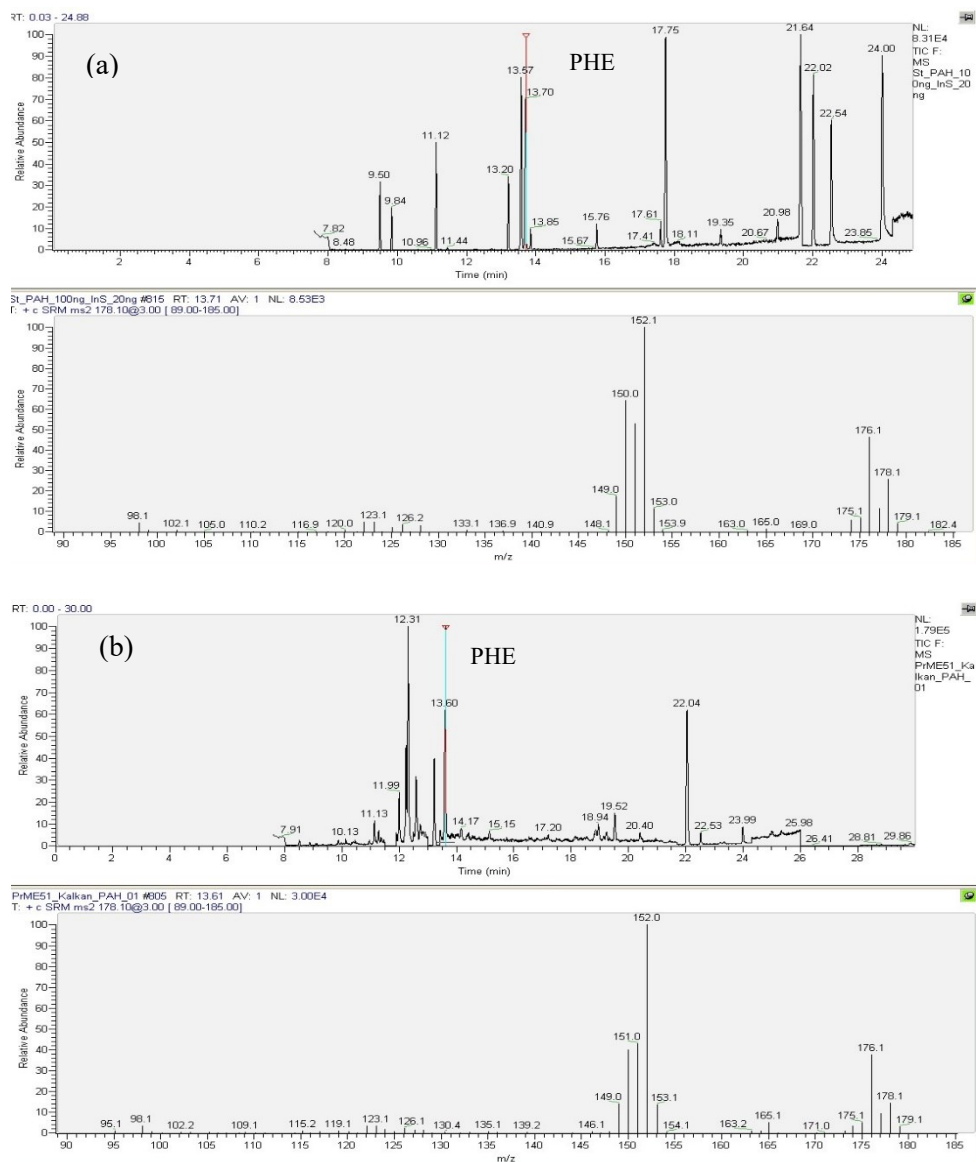


Figure 2. Chromatograms of reference standard solutions of PAHs, 100 ng/mL (a) and fish extract sample (b); mass spectra of PHE in standard and sample.

RESULTS AND DISCUSSION

The assessment of the state of the marine environment regarding the pressure of priority pollutants in the biota was made in accordance with the Marine Strategy under Descriptors 8, 9 and 10 and the Environmental Quality Standards (EQS) for priority substances [4, 8].

Organochlorine compounds (OCs)

The obtained results for the mean concentrations of organochlorine compounds in different fish species from the Black Sea are summarized in Table 2.

Hexachlorobenzene (HCB) is regulated as a hazardous priority pollutant by the Water Framework Directive (WFD) and is ubiquitously distributed in the environment and assumed to mildly biomagnify in aquatic food webs [26]. The highest HCB level was found in turbot, 0.18 ng/g of ww. HCB was detected in only 20% of the goby samples, while in the grey mullet samples, HCB was determined in 75% of the samples examined. HCB was not found in the investigated fish species goby, grey mullet and turbot both from the North and the South sampling areas. To protect the most sensitive organisms from harmful effects of hazardous substances, Environmental Quality Standards (EQS) have been developed within the European Commission [8, 17]. The HCB and HCB concentrations in the fish species did not exceed the EQS of the Directive 2013/39/ EU - 10 and 55 ng/g ($\mu\text{g}/\text{kg}$) ww for biota, respectively [17]. Based on the

results obtained for HCH and HCB in biota, we could conclude that a good chemical status of the marine environment has been achieved.

In general, our results were lower than the data reported in recent years by a number of authors: Spanish authors reported HCB in salmon and mackerel from Mediterranean Sea 1.68 and 0.80 ng/g ww, respectively [27].

Among compounds of the OCs class, the highest quantified value of the sum of DDT and metabolites was 7.73 ng/g ww and was found in turbot samples from the north part (Krapec, cape Kaliakra) of the Black Sea coast. The main metabolite p,p'-DDE was present in much higher concentrations than the other DDTs, while p,p'-DDT was detected in only 12% of the analyzed samples at levels close to the LOQ. This suggests that recently these pesticides have not been used in agriculture after their ban.

The γ isomer of HCHs (Lindane) is one of the most used insecticides in the past. It was considered as carcinogenic to humans (IARC group 1) for professional exposures [15, 28]. The highest value of Lindane was found in a sample of turbot at 1.22 ng/g ww and the sum of the three HCH isomers was quantified as 2.93 ng/g ww. The levels of HCHs in fish samples (mean value 2.5 ng/g ww) were found higher than results reported for sea bass from Lake Como, Italy [28].

The comparison of OCs levels by sampling area was made with aim of assessing the current state of organochlorine pollution along the Bulgarian part of the Black Sea coast (Fig. 3).

Table 2. Lipid content (%) and mean concentrations of HCB, HCB, HCHs and DDTs, (ng/g ww) determined in fish species from the Black Sea coast

Fish species	Goby (N=5)	Grey mullet (N=5)	Turbot (N=3)
Lipids, %	0.40±0.01	2.3±0.21	1.2±0.10
HCB	0.08±0.01	0.11±0.01	0.18±0.02
HCB	nd	nd	nd
p,p' - DDE	1.08±0.16	2.56±0.27	4.52±0.56
p,p' - DDD	0.66±0.08	1.42±0.16	3.01±0.36
p,p' - DDT	nd	0.56±0.08	0.20±0.02
Sum DDTs	1.74	4.54	7.73
α -HCH	1.06±0.12	0.48±0.06	1.05±0.09
β -HCH	nd	nd	nd
γ -HCH	0.77±0.09	0.46±0.06	1.22±0.14
δ -HCH	0.95±0.09	0.85±0.10	0.66±0.07
Sum HCHs	2.78	1.79	2.93

N – number of samples, nd – not detected

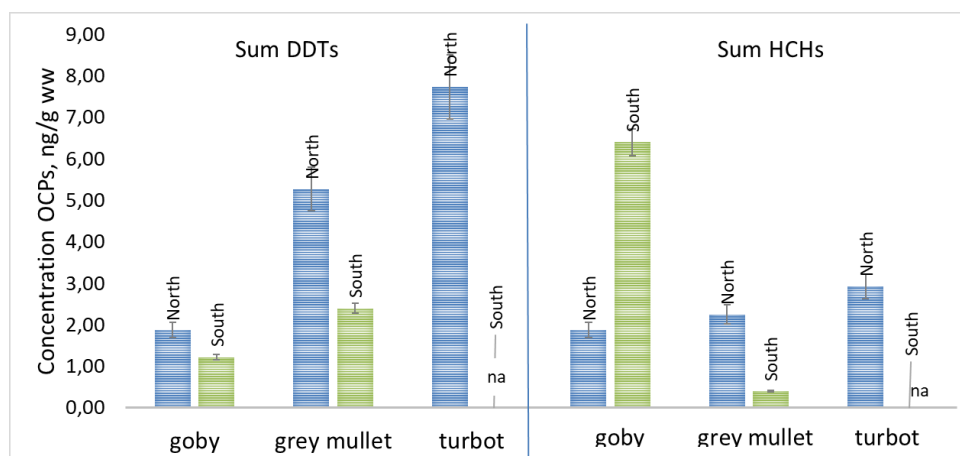


Figure 3. Comparison of DDTs and HCHs levels, ng/g ww in fish from North and South coast of the Black Sea.

Table 3. Individual PAHs concentrations (mean values, ng/g ww) in fish species from the Bulgarian Black Sea coast

PAH compounds	Aromatic rings	Goby (N=5)	Grey mullet (N=5)	Turbot (N=3)
ACL	3	0.40±0.03	0.18±0.02	0.49±0.03
FL	3	2.34±0.15	1.80±0.19	1.87±0.22
PHE	3	11.01±1.13	10.30±1.12	10.08±0.92
AN	3	nd	nd	nd
PY	4	0.42±0.05	nd	1.25 ± 0.14
BaA*	4	nd	nd	nd
CHR*	4	nd	nd	nd
BbFA*	5	nd	nd	nd
BkFA	5	nd	nd	nd
BaP*	5	nd	nd	nd
IP	6	nd	nd	nd
DBahA	5	nd	nd	nd
BghiP	6	nd	nd	nd

nd – not detected; * - group of the priority 4PAHs; PAHs: polycyclic aromatic hydrocarbons

The sum of DDT and its metabolites (Sum DDTs) was found higher in fish samples from the North coast of the Black Sea (mean 4.96 ng/g ww) than in samples from South sampling sites – 1.81 ng/g ww ($p < 0.002$). In contrast, the sum of the three HCH isomers in goby samples from the South sampling area (south of Cape Emine) was quantified higher than HCHs levels in goby from the North area (6.40 and 1.86 ng/g ww, respectively).

Levels of PAHs in fish

The distribution pattern of individual PAHs showed similar profiles in all fish species investigated and was as follows: phenanthrene > fluorene > pyrene > acenaphthylene (Table 3). In all samples anthracene, chrysene, benzo[a]anthracene, benzo[b]fluoranthene, benzo[k]fluoranthene, benzo[a]pyrene, indeno[1,2,3-cd]pyrene, and dibenz[a,h]anthracene showed levels below the detection limit (LOD) of the method. Phenanthrene

is one of the most widespread PAHs in the environment, due to its stable structure and persistence. Due to its high lipophilicity, phenanthrene was the most predominant PAH component in fish tissues (11.01 ng/g ww in goby). Four of the polycyclic hydrocarbons have been identified as indicators by EFSA (designated as 4 PAHs - benzo[a]pyrene, benz[a]anthracene, benzo[b]fluoranthene and chrysene) [29]. Benzo[a]pyrene, known as the most toxic PAH, was not detected in fish samples from the Black Sea, Bulgaria.

The results showed that low-molecular weight (LMW) PAHs (3 and 4 rings) were predominant (accounting 94% of total PAH levels), while high-molecular weight (HMW) PAHs (5- and 6- rings) were below LOD and not detected in the fish samples investigated (Table 3). PAHs are produced by a variety of sources: LMW PAHs are defined as petrogenic compounds (resulting from spillage of

diesel and fuel oil), and HMW PAHs are products of the incomplete combustion of organic matter - they have pyrolytic origin [30].

The ratio of LMW and HMW PAHs indicates the sources of PAHs pollution in the environment [31]. Our results showed that the ratio LMW/HMW PAHs is higher than 1 (mean 19.4), suggesting that PAH pollution of the Bulgarian Black Sea coast was predominantly of petrogenic origin.

The low levels of HMW PAHs found in the present study are logical because it has been found that fish have the ability to metabolize PAHs, in contrast to clams that accumulate them in their tissues [32, 33]. However, they can be used to assess the current state of the marine environment.

The mean PAHs levels in fish species sampled from the northern (north of Cape Emine) and southern (south of Cape Emine) locations of the Bulgarian Black Sea coast are presented in Fig. 4. Comparison of the levels of PAHs in fish by sampling area was made and statistical analysis showed that there is no statistically significant difference in the levels of PAHs in grey mullet from the North and South regions.

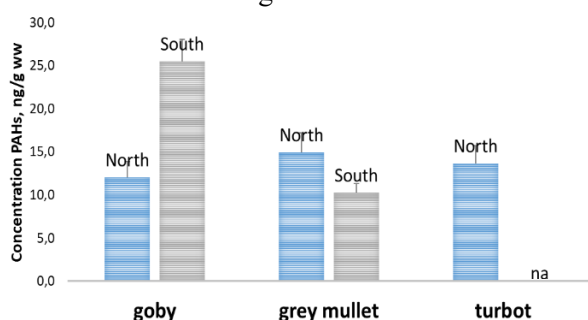


Figure 4. Total PAHs levels, ng/g ww in fish from different sampling regions.

The highest level of Sum PAHs in fish was found in goby samples from Chernomorets (southern sampling area). This result is consistent with a recent study on PAHs in white clam (*Donax trunculus*) [34] which revealed a higher concentration of these pollutants in samples from the Sozopol area. The authors suggest that these levels have been related to marine fuel spill incidents. This confirms that the PAH levels found in the Black Sea biota have a petrogenic origin.

Comparison with other studies on the Black Sea

Recent studies carried out on the Black Sea coast in species such as goby, turbot and red mullet [36] and in turbot in 2021 [3] showed higher concentrations in the DDT and the HCH groups than those determined in the present study. Romanian researchers [36] in 2019 determined concentrations of OCPs in fish (*Neogobius melanostomus*, *Psetta*

maeotica, and *Mullus barbatus ponticus*) from the southern part of the Romanian Black Sea coast (Mangalia region): mean values for HCB - 66.06 ng/g ww, Lindane - 19.72 ng/g ww and sum DDT and its metabolites - 23.11 ng/g ww). The results of the present study were lower than the data from the Romanian project [36].

The findings in our study regarding PAHs were comparable with results obtained from a recent international project on pollution monitoring of the Black Sea. The most important contributors to PAH components in fish from Yeşilirmak and Sakarya Rivers (the Black Sea coast of Turkey) were phenanthrene (43%) and naphthalene (20%) and their distribution profile corresponds to a petrogenic origin of contamination [36]. Total PAH in fish samples showed a distribution between 30.4-285.7 µg/kg ww in Sakarya River and 25.6-842.6 µg/kg ww in Yeşilirmak [36].

Recent study reported PAHs concentrations from 0.001 to 147.45 ± 9.28 µg/kg ww in pelagic fish species (*Sprattus sprattus* and *Trachurus mediterraneus ponticus*) and from 0.0001 to 45.73 ± 5.28 µg/kg ww in benthic fish species (*Neogobius cephalarges*) from the Romanian Black Sea coast [35]. The average sum of 13PAHs in fish species from the Bulgarian Black Sea coast was 13.38 ng/g ww and it is comparable to the results of a recent study by Romanian scientists within the ANEMONE project, which found an average value for the sum of 9 PAHs - 8.15 ng/g ww [36]. The results in our study were lower than the data from a Spanish investigation in the period 2011 - 2018: 16 PAHs were measured in fatty tissues from Mediterranean dolphins and marine turtles (100±59 and 136±47 ng/g ww, respectively) and the tissue pattern of PAHs eminently suggested a petrogenic origin [13].

CONCLUSION

The pollution assessment of the Bulgarian Black Sea showed a good chemical status with regard to HCB and HCBd in benthic fish species, which were found in low levels and did not exceed the European EQS. The organochlorine pesticide DDT was present mainly in the form of its metabolites p,p'-DDE and p,p'-DDD in all samples investigated, suggesting contamination in the past. Low-molecular weight (LMW) PAHs (3 and 4 aromatic rings) were predominant, suggesting petrogenic origin of pollution. The most toxic PAH compound benzo[a]pyrene was not detected in fish samples from the Bulgarian Black Sea coast. In general, concentrations of HCB, HCHs, DDTs, and PAHs in fish species goby, grey mullet and turbot from the

Black Sea were found lower than levels measured in the fish species by other studies.

The monitoring data of OCPs and PAHs levels in the Black Sea ecosystem is important with a view to implementing measures to reduce their widespread distribution and protecting the biodiversity of aquatic organisms and human health. Future research should be directed towards the combined effects of numerous POPs due to serious concerns regarding the potential chronic human exposure.

Acknowledgement: This work was supported by the Maritime Affairs and Fisheries Programme 2014-2020 co-financed by the European Union through the European Maritime Affairs and Fisheries Fund. Project No BG14MFOP001-6.004-0006, contract No МДР-III-01-13/25.01.2021.

REFERENCES

1. M. C. Vagi, A. S. Petsas, M. N. Kostopoulou, *Water*, **13** (18), 2488 (2021). <https://doi.org/10.3390/w13182488>
2. C. L. Chişescu, A. Ene, E.-I. Geana, A. M. Vasile, C.T. Ciucure, *Applied Sciences*, **11**(20), 9721 (2021) <https://doi.org/10.3390/app11209721>
3. D. Danilov, L. Dediu, N. A. Damir, V. Coatu, L. Lazar, *Fishes*, **8** (5), 265 (2023). <https://doi.org/10.3390/fishes8050265>
4. European Commission, Directive 2008/56/EC, Establishing a framework for community action in the field of marine environmental policy (Marine Strategy Framework Directive), *Off. J. Eur. Comm.*, **L 164/19**, 1 (2008).
5. S. K. Georgieva, Zl. V. Peteva, *Bulgarian Chemical Communications*, **49** (Special Issue G), 205 (2017)
6. S. K. Georgieva, Z. V. Peteva, M. D. Stancheva, *BioRisk*, **20**, 59 (2023). <https://doi.org/10.3897/biorisk.20.97555>
7. R. Serrano, M. Barreda, E. Pitarch, F. Hernández, *J. Sep. Sci.*, **26**, 75 (2003).
8. European Commission, Directive 2008 /105/ EC, Environmental Quality Standards in the Field of Water Policy, *Off. J. Eur. Union*, **L348**, 84 (2008)
9. L. I. Majoros, R. Lava, M. Ricci, B. Binici, F. Sandor, A. Held, H. Emons, *Talanta*, **116**, 251 (2013). <https://doi.org/10.1016/j.talanta.2013.04.080>
10. A. T. Fisk, K. A. Hobson, R.J. Norstrom, *Environ Sci Technol*, **35**, 732 (2001). <https://doi.org/10.1021/es001459w>
11. A. Simeonova, R. Chuturkova, V. Yaneva, *Marine Pollution Bulletin*, **119** (1), 110 (2017). <https://doi.org/10.1016/j.marpolbul.2017.03.035>
12. N. Berrojalbiz, J. Dachs, M. J. Ojeda, M. C. Valle, J. Castro-Jimenez, J. Wollgast, et al., *Global Biogeochem. Cycles* **25** (4), (2011). <https://doi.org/10.1029/2010GB003775>
13. G. López-Berenguer, A. Acosta-Dacal, O. P. Luzardo, J. Peñalver, E. Martínez-López, *Chemosphere*, **336**, 139306 (2023). <https://doi.org/10.1016/j.chemosphere.2023.139306>
14. U.S. EPA. Provisional Guidance for Quantitative Risk Assessment of Polycyclic Aromatic Hydrocarbons (PAH). Available online: <https://cfpub.epa.gov/ncea/risk/recordisplay.cfm?deid=49732> (accessed on 17 July 2021).
15. IARC, Monographs on the evaluation of carcinogenic risks to humans. Some non-heterocyclic polycyclic aromatic hydrocarbons and some related exposures. Lyon, (2010). <http://monographs.iarc.fr/ENG/Monographs/vol92/mono92.pdf>
16. M. Ferrante, G. Zanghi, A. Cristaldi, C. Copat, A. Grasso, M. Fiore, S.S. Signorelli, P. Zuccarello, G. Oliveri Conti, *Food and Chemical Toxicology*, **115**, 385 (2018). <https://doi.org/10.1016/j.fct.2018.03.024>
17. European Commission Directive 2013/39/EU as regards priority substances in the field of water policy *Off. J. Eur. Union*, **L 226/1**, (2013). <https://eur-lex.europa.eu/LexUriServ/LexUriServ.do?uri=OJ:L:2013:226:0001:0017:en:PDF>, (accessed on 12/08/2013)
18. F. M. Jaward, N. J. Farrar, T. Harner, A. J. Sweetman, K. C. Jones, *Environ. Sci. and Technol.*, **38**, 34 (2004). <https://doi.org/10.1021/es034705n>
19. J. E. Balmer, H. Hung, K. Vorkamp, R. J. Letcher, D. C.G. Muir, *Emerging Contaminants*, **5**, 116 (2019). <https://doi.org/10.1016/j.emcon.2019.03.002>
20. M. D. Jürgens, A.C. Johnson, K. C. Jones, D. Hughes, A. J. Lawlor, *Sci. of the Total Environ.*, **461–462**, 441 (2013). <https://doi.org/10.1016/j.scitotenv.2013.05.007>
21. W. Masmoudi, M. S. Romdhane, S. Kherriji, M. E. Cafsi, *Food Chem.*, **105**, 72 (2007). <https://doi.org/10.1016/j.foodchem.2007.03.037>
22. Stockholm Convention on Persistent Organic Pollutants (POPs)-Texts and Annexes. United Nations Environ Program. Available online: <http://chm.pops.int/TheConvention/ThePOPs/AllPOPs/tabid/2509/Default.aspx> (accessed on 22 June 2022).
23. H. van den Berg, G. Manuweera, F. Konradsen, *Malar J.*, **16**, 401 (2017). <https://doi.org/10.1186/s12936-017-2050-2>
24. IRIS. Available online: <https://cfpub.epa.gov/ncea/iris/search/index.cfm> (accessed on 22 June 2022).
25. K. Macgregor, I. W. Oliver, L. Harris, I. M. Ridgway, *Environmental Pollution* **158**, 2402 (2010). <https://doi.org/10.1016/j.envpol.2010.04.005>
26. I. J. Allan, B. Vrana, A. Ruus, *Environmental Science & Technology* **56** (12), 7945 (2022). <https://doi.org/10.1021/acs.est.2c00714>
27. G. Falcó, J. M. Llobet, A. Bocio, J. L. Domingo, *The Science of the Total Environment*, **389**(2-3), 289 (2008). <https://doi.org/10.1016/j.scitotenv.2007.09.025>
28. G. Mosconi, F. Di Cesare, F. Arioli, M. Nobile, D. E. A. Tedesco, L. M. Chiesa, S. Panzeri. *Foods*, **11**(15), 2241 (2022). <https://doi.org/10.3390/foods11152241>
29. European Food Safety Authority (EFSA). *EFSA J.*, **6**, 724 (2008). <https://doi.org/10.2903/j.efsa.2008.724>

30. K. Srogi, *Environ. Chem. Lett.*, **5**, 169 (2007).
<https://doi.org/10.1007/s10311-007-0095-0>
31. R. Mercogliano, S. Santonicola, A. De Felice, A. Anastasio, N. Murru, M. C. Ferrante, M. L. Cortesi, *Mar. Pollut. Bull.*, **104(1-2)**, 386 (2016)
<https://doi.org/10.1016/j.marpolbul.2016.01.015>
32. T. Cappello, M. Maisano, A. D'Agata, A. Natalotto, A. Mauceri, S. Fasulo, *Mar. Environ. Res.*, **91**, 52 (2013).
<https://doi.org/10.1016/j.marenvres.2012.12.010>
33. S. Fasulo, F. Iacono, T. Cappello, C. Corsaro, M. Maisano, A. D'Agata, et al., *Ecotoxicol Environ. Saf.*, Oct; **84**, 139 (2012)
<https://doi.org/10.1016/j.ecoenv.2012.07.001>
34. S. K. Georgieva, M. D. Stancheva, Z. V. Peteva, T. I. Ivanova, A. V. Alexandrova, *BioRisk*, **17**, 95 (2022)
<https://doi.org/10.3897/biorisk.17.77343>
35. N.-A. Damir, V. Coatu, E. D. Pantea, M. Galățchi, E. Botez S. Birghilă, *Polycyclic Aromatic Compounds*, **42 (10)**, 7595 (2022)
<https://doi.org/10.1080/10406638.2021.2006243>
36. Project ANEMONE Deliverable 3.1, “Hazardous substances assessment in Black Sea biota”, A. Oros (ed.). CD PRESS, p. 96, 2021. ISBN 978-606-528-531-6

Fatty acid composition in kefir from milk of Bulgarian white dairy goat breed and its crossings

Ts. M. Dimitrova^{1*}, S. A. Ivanova² S. T. Stoycheva¹

¹Agricultural Academy of Sofia, Research Institute of Mountain Stockbreeding and Agriculture, 281 Vasil Levski Str., 5600, Troyan, Bulgaria

²Agricultural Academy-Sofia, Institute of Cryobiology and Food Technology, 53 Cherni vrah Blvd., 1407, Sofia, Bulgaria

Received: November 3, 2024; Revised: April 11, 2024

An analysis was conducted on the fatty acid composition of kefir at the 24th hour of production, obtained from goat's milk of Bulgarian White Dairy (BWD) breed and its crossings with Anglo-Nubian (AN) and Toggenburg (TG) goats during the lactation period. Saturated fatty acids (SFAs) were found to decrease in the milk in all three kefir batches with 1.93 g/ 100 g fat for BWD, with 1.84 g/ 100 g fat for BWDxTG and with 0.98 g/ 100 g fat for BWDxAN, whereas the monounsaturated fatty acids (MUFAs) and polyunsaturated fatty acids (PUFAs) predominated in BWD batches. The essential fatty acids, such as omega-3 and omega-6, had low values in the studied samples. The values of the lipid indices indicate a well-balanced fatty acid composition of goat's milk and the products derived from it. The atherogenic index in all three batches of kefir (2.20; 2.25; 2.47) was lower compared to the raw material (2.48; 2.54; 2.68), which defined them as healthier in terms of lipid content. The data on saturated fatty acids in the studied kefir batches at the 24th hour of production varied from 3.40 g/ 100 g product for BWD to 3.83 g/ 100 g product for BWDxTG, whence they refer to products with a high content of saturated fatty acids and low content of trans fatty acids (0.9 g/ 100 g product), according to Regulation (EC) No. 1924/2006.

Key words: goat's milk, kefir, fatty acids, lipid indices

INTRODUCTION

Milk and milk products are one of the most consumed foods in Bulgaria. They are obtained through various fermentation technologies with the participation of lactic acid bacteria, which increases their dietary potential. The consumption of goat's milk products is associated with beneficial health effects. Beyond its nutritional value and compared to other types of milk, goat's milk is characterized by a high buffer capacity, digestibility, alkalinity and certain therapeutic properties related to healthy nutrition [1].

Kefir is one of the most useful products for human health in the group of fermented lactic acid foods. It is a traditional drink originating from the Caucasus region, but consumed worldwide, resulting from two fermentations with kefir grains – lactic acid and alcoholic [2]. It has all the beneficial properties of lactic acid drinks, providing the body's calcium needs, and at the same time it is a dietary lactic acid product, with high absorption, rich in many beneficial bacteria and suitable for all age groups [3]. Kefir has a smooth creamy consistency, a slightly sour taste mainly due to the presence of lactic acid and a low concentration of ethanol produced by the yeast cells present in the grains.

In addition, a variety of aromatic substances, including acetaldehyde, acetoin, and diacetyl, contribute to its distinctive flavor [4]. The yeasts involved in the fermentation of kefir are important for its physicochemical and sensory characteristics and exhibit antibacterial activity against colonic flora [4]. Milk fat also plays an important role in the production of fermented beverages, as recently there has been an increasing interest in the various fatty acids from the omega-3 group and CLA, which have a significant effect on the metabolism. The possibilities for the inclusion of goat's milk as a component in products with a functional purpose are limited in nature and have not been sufficiently researched. Therefore, the aim of the present study is to produce kefir from goat's milk of Bulgarian White Dairy (BWD) and its crossings with Toggenburg (BWDxTG) and Anglo-Nubian (BWDxAN), to determine its fatty acid composition at the 24th hour of the process of production in view of its health impact on the human body.

MATERIALS AND METHODS

Milk from experimental animals at the Research Institute of Mountain Stockbreeding and Agriculture - Troyan are used, that have been raised in one herd under the same production conditions consisting of three groups - 'Bulgarian White Dairy' and its crossings with 'Toggenburg' and 'Anglo-Nubian'.

* To whom all correspondence should be sent:

E-mail: c.dimitrova@abv.bg

The rearing system is pasture-barn based, as in the period of April-November the animals were on a natural pasture of transitional type and in the barn, during the rest of the year. Several batches of kefir were prepared at the beginning (April), the middle (June) and the end (September) of the lactation period.

Several batches of kefir were prepared from goat's milk of these breed groups for the lactation period. For this purpose, the milk was pasteurized at a temperature of 85-90°C, with a delay of 10-15 s., cooled to 29°C and leavened with dry starter culture for kefir (*Lactococcus lactis* sp. *lactis*, *Lactococcus lactis* sp. *diacetylactis*, *Lactococcus lactis* sp. *cremoris*, *Leuconostoc mesenteroides* sp. *cremoris*, *Lactobacillus kefir*.). It was poured into suitable vessels and allowed to ferment at 29°C for 16 - 18 hours. After that, it was cooled and transferred for refrigerated storage at 0-4°C. Samples from the kefir batches were tested to determine the content of fatty acids at the 24th hour of the production process and were presented as arithmetic mean. Based on the obtained fatty acid composition, the following indices were calculated:

1) Atherogenic index (AI) - calculated based on the content of medium-long fatty acids - C12:0, C14:0 and C16:0 and the groups of monounsaturated fatty acids (MUFAs) and polyunsaturated fatty acids (PUFAs) [5]:

$$AI = \frac{C12:0 + 4 \times C14:0 + C16:0}{MUFAs + PUFAs}$$

2) Thrombogenic index (TI) according to Ulbricht and Southgate [6]:

$$TI = (C14:0 + C16:0 + C18:0) / 0.5 \times \Sigma C18:1 + 0.5 \times \Sigma MUFAs + 0.5 \times \Sigma PUFAn6 + 3 \times PUFAn-3 + (PUFn3 / PUFAn6)$$

3) Lipid preventive score (LPS) according to the equation of Richard and Charbonnier [7]:

$$LPS = TL + 2 \times SFAs - MUFAs - 0.5 \times PUFAs,$$

where: LPS is lipid preventive score;

TL - total lipids;

SFAs - saturated fatty acids;

MUFAs - monounsaturated fatty acids;

PUFAs - polyunsaturated fatty acids.

4) Ratio between hyper and hypocholesterolemic fatty acids (h/H):

$$h/H = (C18:1n-9 + C18:1n-7 + C18:2n-6 + C18:3n-3 + C18:3n-6 + C20:3n-6 + C20:4n-6 + C20:5n-3 + C22:4n-6 + C22:5n-3 + C22:6n-3) / (C14:0 + C16:0).$$

Variational statistical processing of the data was conducted by the Statistica software package.

RESULTS AND DISCUSSION

Milk fat has a significant impact on the biological and nutritional value of milk and the taste qualities of the produced dairy products.

The content of saturated fatty acids in milk and kefir at the 24th hour showed no significant differences between the three groups of goats (Table 1), with the highest amounts being found for C-16:0, followed by C-18:0, C-10:0 and C-14:0.

The levels of lauric (C-12:0), myristic (C-14:0) and palmitic (C-16:0) fatty acids were decreased in milk in all three kefir batches, suggesting a better health effect of the product. Higher results were obtained by Nacheva *et al.* [8] for stearic acid (C-18:0), which increased in the present research work by 0.43g/100g fat in BWD kefir, by 0.22 g/100g fat in BWDxTG and by 0.40 g/100g fat in BWDxAN compared to the original raw material.

A high content of short-chain fatty acids in the diet leads to an increase in the level of LDL-cholesterol in the blood and to an increase in the risk of cardiovascular diseases in humans [9, 10]. Their amount in the milk of the groups studied by us varies from 18.70% (BWD) to 22.39% (BWDxAN).

Of the monounsaturated fatty acids (Table 2), the spectrum of cis- and trans-isomers of C-18:1 is the most diverse, with oleic (C-18:1c9) and vaccenic acids (C-18:1t11) predominating, and the remaining cis- and trans-forms of oleic acid are in concentrations lower than 1%. The highest content of both acids was found in kefir from the BWD breed - 23.01 g/ 100 g fat, 0.89 g/ 100 g fat, whereas the lowest was in BWDxTG - 21.45 and 0.78 g/ 100 g fat, as their concentration in the milk kefir rose slightly. The presence of all trans isomers, with the exception of trans-vaccenic acid (C-18:1t11), are considered "undesirable" due to their varying degrees of carcinogenicity [11]. The significance of this acid (C-18:1t11) is due to its role also as a precursor in the synthesis of the major isomer of the nutritionally valuable conjugated linoleic acid (CLA), namely cis-9 trans-11 C-18:2, which takes place in the mammary gland [12].

Table 1. Saturated fatty acids, g/ 100 g fat, (n=9)

Fatty acids	Breed groups					
	BWD		BWDxTG		BWDxAN	
	x±Sx		x±Sx		x±Sx	
	goat's milk	kefir	goat's milk	kefir	goat's milk	kefir
C-4:0	3.23±0.002	3.29±0.014	3.29±0.005	3.68±0.122	4.02±0.016	4.27±0.013
C-6:0	2.87±0.234	2.69±0.231	3.63±0.321	3.28±0.212	3.77±0.123	3.72±0.010
C-7:0	0.02±0.003	0.01±0.004	0.02±0.003	0.01±0.005	0.02±0.004	0.01±0.002
C-8:0	2.99±0.213	2.72±0.218	3.66±0.132	3.27±0.132	3.70±0.234	3.57±0.201
C-9:0	0.04±0.142	0.03±0.421	0.03±0.198	0.07±0.212	0.04±0.010	0.04±0.205
C-10:0	9.55±0.403a*	9.04±0.342	10.70±0.531a*	10.14±0.345	10.84±0.416	10.26±0.403
C-11:0	0.07±0.05	0.04±0.006	0.05±0.003	0.07±0.005	0.05±0.001	0.06±0.004
C-12:0	4.41±0.198	3.84±0.209	4.53±0.563	4.26±0.305	4.23±0.431	4.17±0.324
C-13:0	0.08±0.065	0.07±0.403	0.06±0.432	0.07±0.236	0.06±0.631	0.06±0.457
C-14:0	9.82±0.132	9.42±0.412	10.20±0.221	9.95±0.642	9.13±0.301	9.02±0.290
C-15:0	0.08±0.076	0.07±0.062	0.09±0.068	0.06±0.078	0.07±0.074	0.04±0.054
C-16:0	27.72±1.234	27.15±1.234	27.69±1.096	27.24±1.064	27.21±1.079	27.12±1.127
C-17:0	0.62±0.032	0.72±0.045	0.57±0.076	0.52±0.031	0.58±0.065	0.056±0.098
C-18:0	12.55±1.678	12.98±1.423	12.83±1.423	13.05±1.076	12.87±1.68	13.27±0.067
C-20:0	0.10±0.016	0.09±0.042	0.04±0.035	0.07±0.043	0.06±0.023	0.04±0.056
C-21:0	0.02±0.036	0.14±0.087	0.08±0.076	0.03±0.065	0.04±0.043	0.02±0.211
C-22:0	0.05±0.009	0.01±0.003	0.03±0.076	0.01±0.043	0.02±0.022	-
C-23:0	-	-	0.01±0.006	0.01±0.312	0.01±0.067	0.01±0.312
C-24:0	0.01±0.009	0.02±0.017	0.02±0.004	0.01±0.010	0.01±0.012	0.01±0.002
C-25:0	0.01±0.15	-	0.02±0.009	0.01±0.017	0.01±0.018	0.01±0.010
C-26:0	0.02±0.019	0.01±0.013	0.01±0.016	-	0.02±0.006	0.01±0.010

Note: a- BWD/BWDxTG; *P<0.05

Polyunsaturated fatty acids in the studied samples (Table 3) have low values with the exception of linoleic and α -linolenic acid.

C18:2c9,12/19:0 ranges from 2.22 g/100 g of fat in kefir from BWDxAN to 2.98 g/100 g of fat in kefir from BWD, whereas C-18:3n3 from 0.52 g/100 g of fat in BWDxTG up to 0.56 g/ 100 g of fat in BWD kefir. The values of linoleic (C-18:2) and linolenic (C-18:3) acids in milk fat depend on the nutrition of the animals, since they are not synthesized in the organism and their absence causes a number of biological disorders [13] Differences for C-18:3n6 are minimal between breeds, from 0.12 g/ 100 g fat in BWD to 0.18 g/ 100 g fat in BWDxAN,

The content of CLA in milk and the mechanisms of impact of individual isomers have been investigated by many authors (Bauman, [14], An *et al.* [15], Schroeder *et al.* [16]). According to Jahreis *et al.* [17] CLA values in milk from different animal species are closely related to feeding regime and ration composition. Relatively low amounts of CLA isomers, some of which are trace amounts, are found in goat's milk and the investigated kefir. The biologically active isomer C-18:2 cis-9, trans-11

(CLA9c,11t), which occupies 80% of the total amount of CLA [18] has the highest content in kefir of BWD breed with 0.47%, whereas the lowest is registered for BWDxTG with 0.37%, as an increase was observed in all three batches compared to the original raw material.

The content of branched-chain saturated fatty acids in the studied samples was low (Table 4), but they are of great interest regarding their potential role as non-invasive biomarkers of rumen function, since their variations in milk may reflect changes in bacterial populations induced by dietary ration composition [19].

The data for the main groups of fatty acids (Table 5) indicate that the levels of SFAs, MUFAs and PUFAs in kefir at the 24th hour do not differ significantly compared to the original goat's milk. A high content of SFAs was found from 72.34 g/100 g of fat in kefir from BWD to 75.81% in BWDxTG. The amount of MUFAs and PUFAs in the product increases by 1.07 respectively; 0.10 g/ 100 g fat for BWD, 1.14; 0.21 g/ 100 g fat for BWDxTG and with 1.86; 0.61 g/ 100 g fat for BWDxAN. Results close to the present were obtained by Wojtowski *et al.* [20] for kefir from goat's milk of a Polish White Goat.

Table 2. Monounsaturated fatty acids, g/ 100 g fat, (n=9)

Fatty acids	Breed groups					
	BWD		BWDxTG		BWDxAN	
	x±Sx		x±Sx		x±Sx	
	goat's milk	kefir	goat's milk	kefir	goat's milk	kefir
C-10:1	0.21±0.024	0.19±0.043	0.18±0.065	0.16±0.021	0.19±0.015	0.15±0.022
C-12:1n1	0.09±0.004	0.03±0.002	0.06±0.004	0.03±0.006	0.07±0.002	0.05±0.001
C-14:1n5	0.07±0.015	0.08±0.013	0.04±0.018	0.05±0.023	0.05±0.0043	0.04±0.075
C-15:1n5	0.02±0.007	0.01±0.012	0.02±0.008	0.06±0.012	0.02±0.004	0.02±0.03
C-16:19tr	0.30±0.022	0.29±0.018	0.34±0.054	0.30±0.012	0.32±0.076	0.22±0.021
C-16:1n7	0.47±0.059	0.58±0.021	0.49±0.033	0.57±0.044	0.52±0.076	0.59±0.014
C-16:2n4	0.01±0.002	-	0.01±0.002	0.01±0.032	0.01±0.021	-
C-17:1n7	0.26±0.016	0.28±0.021	0.24±0.005	0.27±0.043	0.17±0.034	0.17±0.020
C-16:3n4	0.01±0.002	0.01±0.002	0.02±0.003	0.01±0.002	0.01±0.003	0
C-18:1t4	0.06±0.001	0.15±0.003	0.07±0.002	0.18±0.002	0.18±0.001	0.25±0.003
C-18:1t5/6/7	0.16±0.102	0.18±0.038	0.14±0.056	0.17±0.078	0.17±0.013	0.19±0.015
C-18:1t9	0.22±0.043	0.25±0.034	0.24±0.054	0.26±0.098	0.21±0.065	0.24±0.010
C-18:1t10	0.20±0.015	0.28±0.065	0.19±0.170	0.22±0.016	0.17±0.012	0.23±0.013
C-18:1t11	0.84±0.208	0.89±0.140	0.76±0.130	0.78±0.234	0.73±0.134	0.78±0.127
C-18:1c9/C-18:1t12/13/	22.30±0.765	23.01±0.543a*	20.34±0.634	21.45±0.876a*	20.21±0.875	21.91±0.976
C-18:1t15	0.11±0.012	0.27±0.014	0.25±0.089	0.28±0.064	0.19±0.014	0.23±0.026
C-18:1c12	0.03±0.005	0.04±0.007	0.05±0.006	0.06±0.005	0.05±0.007	0.06±0.004
C-18:1c13	0.09±0.007	0.03±0.002	0.10±0.009	0.08±0.006	0.08±0.006	0.06±0.003
C-18:1t16	0.04±0.012	0.03±0.010	0.03±0.012	0.03±0.014	0.03±0.013	0.03±0.012
C-18:1c14	0.03±0.014	0.02±0.007	0.04±0.003	0.03±0.005	0.04±0.002	0.04±0.006
C-18:1c15	0.07±0.010	0.05±0.007	0.05±0.006	0.03±0.004	0.04±0.006	0.02±0.004
C-20:1n9	0.01±0.004	0.02±0.003	0.01±0.002	0.02±0.003	0.01±0.002	0.02±0.003
C-22:1n11	0.04±0.004	0.02±0.003	0.02±0.004	0.01±0.003	0.03±0.004	0.02±0.003
C-22:1n9	0.02±0.012	0.02±0.013	0.03±0.014	0.01±0.015	0.01±0.007	0.01±0.016

Note: a- BWD/BWDxTG; *P<0.05

Table 3. Polyunsaturated fatty acids, g/ 100 g fat, (n=9)

Fatty acids	Breed groups					
	BWD		BWDxTG		BWDxAN	
	x±Sx		x±Sx		x±Sx	
	goat's milk	kefir	goat's milk	kefir	goat's milk	kefir
C-18:2t9,12	0.14±0.023	0.02±0.003	0.10±0.015	0.06 ±0.012	0.11±0.013	0.07±0.015
C-18:2c9,12/19:0	2.78±0.035	2.98±0.065	2.18±0.022	2.40±0.034	2.18±0.089	2.22±0.075
gC-18:3n6	0.09±0.015	0.12±0.013	0.14±0.018	0.16±0.017	0.16±0.018	0.18±0.003
aC-18:3n3	0.53±0.065	0.56±0.045	0.50±0.076	0.52±0.043	0.54±0.045	0.55±0.076
CLA9c,11t	0.42±0.033	0.47±0.030	0.32±0.024	0.37±0.029	0.37±0.017	0.40±0.019
CLA10t,12c	-	-	-	-	-	-
C-18:4n3	-	-	-	-	-	-
CLA9c,11c	0.02±0.006	0.01±0.004	0.01±0.004	0.01±0.003	0.02±0.005	0.01±0.003
CLA9t,11t	0.01±0.002	0.02±0.005	0.02±0.003	0.02±0.001	0.02±0.004	0.01±0.002
C-20:2n6	0.05±0.015	0.04±0.005	0.04±0.009	0.04±0.010	0.05±0.012	0.05±0.012
C-20:3n6	0.01±0.002	0.02±0.005	0.01±0.008	0.02±0.003	0.01±0.002	0.02±0.005
C-20:4n6	0.02±0.006	0.01±0.004	0.03±0.006	0.01±0.012	0.02±0.006	0.01±0.004
C-20:3n3	0.26±0.008	0.18±0.019	0.25±0.032	0.20±0.045	0.21±0.065	0.16±0.034
C-22:5n3	0.06±0.012	0.07±0.011	0.09±0.65	0.08±0.011	0.06±0.004	0.06±0.013
C-22:6n3	0.03±0.017	0.02±0.004	0.02±0.013	0.01±0.004	0.02±0.014	0.02±0.002

Table 4. Branched fatty acids, g/ 100 g fat, (n=9)

Fatty acids	Breed groups					
	BWD		BWDxTG		BWDxAN	
	x±Sx		x±Sx		x±Sx	
	goat's milk	kefir	goat's milk	kefir	goat's milk	kefir
C-13iso	0.05±0.010	0.03±0.004	0.03±0.002	0.04±0.001	0.04±0.002	0.03±0.001
C-13aiso	-	-	-	-	-	-
C-14iso	0.11±0.013	0.19±0.022	0.10±0.015	0.15±0.017	0.08±0.006	0.10±0.017
C-15iso	0.30±0.027	0.26±0.035	0.27±0.023	0.25±0.021	0.26±0.019	0.24±0.021
C-15aiso	0.22±0.022	0.25±0.024	0.23±0.018	0.24±0.022	0.24±0.015	0.26±0.029
C:16iso	0.28±0.013	0.26±0.010	0.25±0.012	0.23±0.016	0.23±0.019	0.20±0.017
C-17iso	0.31±0.24	0.35±0.028	0.35±0.023	0.40±0.032	0.30±0.024	0.32±0.021
C-17aiso	0.42±0.036	0.40±0.035	0.39±0.017	0.35±0.021	0.37±0.018	0.35±0.023
C-18iso	0.01±0.002	0.02±0.001	0.03±0.004	0.03±0.002	0.02±0.005	0.02±0.001

Table 5. Groups of fatty acids, g/ 100 g fat, (n=9)

Fatty acids	Breed groups					
	BWD		BWDxTG		BWDxAN	
	x±Sx		x±Sx		x±Sx	
	goat's milk	kefir	goat's milk	kefir	goat's milk	kefir
ΣCLA	0.45±0.038	0.50±0.076	0.35±0.064	0.40±0.078	0.41±0.098	0.44±0.054
Σ C-18:1 trans isomers	1.93 ±0.231	2.05±0.210	1.68±0.210	1.84±0.201	1.88±0.034	1.95±0.078
Σ C-18:1 cis isomers	22.52±0.878	23.15±0.675	20.58±0.766	21.65±0.543	20.42±0.089	22.09±0.832
Σ SFAs	74.27±0.956a*	72.34±0.786	77.65±0.943a*	75.81±0.589	76.74±0.569	75.76±0.0570
Σ MUFAs	25.66±0.876	26.73±0.786	23.72±0.765	24.86±0.766	23.47±0.899	25.33±0.769
Σ PUFAs	4.42±0.234	4.52±0.187	3.71±0.179	3.92±0.867	3.77±0.767	4.38±0.656
Σ omega-3	0.88±0.087	0.53±0.089	0.86±0.078	0.51±0.066	0.83±0.075	0.55±0.054
Σ omega-6	2.90±0.065	2.88±0.078	2.72±0.045	2.68±0.076	2.64 ±0.075	2.60±0.098
Σ omega-6/Σomega-3	3.31±0.453	5.43±0.798	3.16±0.423	5.25±0.954	3.18±0.876	5.10±0.768
Branched fatty acids	1.70±0.090	1.73±0.056	1.62±0.065	1.65±0.034	1.50±0.076	1.40±0.023

Note: a- BWD/BBWDxTG; *P<0.05

Table 6. Indices for goat's milk and kefir

Indices	BWD		BWDxTG		BWDxAN	
	goat's milk	kefir	goat's milk	kefir	goat's milk	kefir
LPS (g/100 g product)	9.98± 0.875	10.1±0.981	11.02±0.675	11.33±0.943	10.25 ± 0.523	10.44±0.923
AI	2.54±0.542	2.20±0.342	2.68±0.450	2.47±0.453	2.48 ±0.564	2.25±0.470
TI	2.76±0.365	2.43±0.423	2.98±0.576	2.65±0.598	2.80±0.498	2.72±0.761
h/H	0.61±0.923	0.63±0.123	0.60±0.879	0.62±0.267	0.62±0.834	0.65±0.343
TFAs (g/100 g product)	0.08±0.024	0.09±0.021	0.08± 0.043	0.09±0.012	0.08±0.0321	0.09±0.016
SFAs+TFAs (g/100 g product)	3.09 ±0.507	3.40±0.520	3.47±0.487	3.83±0.421	3.57±0.489	3.73±0.321

The biologically significant omega 6/omega 3 ratio is recommended by nutritionists to be in the range of 5 [21], as in the present study an increase was registered to 5.10 g/ 100 g fat in BWDxAN, 5.25 g/ 100 g fat in BWDxTG and 5.43 for kefir from BWD, compared to raw milk. ΣCLA increased slightly by 0.05 g/100 g fat in the final product.

The qualitative assessment of milk fat was conducted on the basis of lipid indices in connection with determining the health impact of the product (Table 6).

The lipid preventive score used to evaluate the preventive activity of a given fat against the risk of cardiovascular diseases varies from 10.01 g/ 100 g of product for kefir from BWD to 11.33 g/ 100 g of product for BWDxTG. The lower content of myristic and palmitic acid in the final product suggests a lower value of the atherogenic index [8] in the separate batches of kefir (2.20 for BWD, 2.25 for BWDxAN, 2.47 for BWDxTG), compared to the original milk. The thrombogenic index is in the range of 2.43 for BWD to 2.72 for BWDxAN,

whereas the cholesterolemic index is in low values below 1, both in milk and in the obtained product at the 24th hour.

Trans fatty acids (TFAs), obtained naturally, have a significant role in human nutrition and in the tested milk and kefir samples from different groups of goats, they have values of 0.08/0.09g/100 g of product, which gives us reason to refer them to products with a low TFAs content, according to Regulation (EC) No. 1924/2006.

CONCLUSIONS

The results for the fatty acid profile of the studied samples show that SFAs are reduced in milk kefir by 1.93 g/ 100 g fat for BWD, 1.84 g/ 100 g fat for BWDxTG and by 0.98 g/ 100 g fat for BWDxAN, whereas MUFAs and PUFAs prevailed in the milk from BWD breed. Essential fatty acids, omega-3 and omega-6, were low in all three batches.

The values of the lipid indices indicate a well-balanced fatty acid composition of goat's milk and its products. The atherogenic index of all three batches of kefir (2.20; 2.25; 2.47) was lower compared to the raw material (2.48; 2.54; 2.68), which defines them as healthier in terms of lipid content.

The data on saturated fatty acids in the studied kefirs at the 24th hour of production varied from 3.40 g/ 100 g product for BWD to 3.83 g/ 100 g product for BWDxTG, whence they refer to products with a high content of saturated fatty acids and low content of trans fatty acids (0.9 g/ 100 g product), according to Regulation (EC) No. 1924/2006.

REFERENCES

1. Y. W. Park, G. F. W. Haenlein, Goat milk its products and nutrition, in: Y. H. Hui (ed.), Handbook of food products manufacturing, New York, USA, John Wiley and Sons, Inc. Publishing House, 2007, p. 32.
2. Z. B. Guzel-Seydim, T. Kok-Tas, A. K. Greene, A. C. Seydim, *Critical Reviews in Food Science and Nutrition*, **51**, 261 (2011).
3. N. Roshtunkina, *Food Ingredients Business*, 1. (2010).
4. E. R. Farnworth, I. Mainville, Kefir: A fermented milk product. Handbook of Fermented Functional Foods, E. R. Farnworth (ed.) CRC Press, London, UK. 2003, p. 77.
5. Y. Chilliard, A. Ferlay, J. Rouel, G. Lamberet, *J. Dairy Sci.*, **86**, 1751 (2003).
6. T. Ulbricht, D. Southgate, *Lancet*, **338**, 985 (1991).
7. J. Richard, A. Charbonnier, *Cahiers de Nutrition et de Di t tique*, **4**, 234 (1994).
8. I. Nacheva, A. Valchkov, K. Loginovska, S. Ivanova, *J. of Mount. Agri. on the Balkans*, **21**(1), 21 (2018).
9. M. Wahlqvist, *Asia Pacific Journal of Clinical Nutrition*, **14** (4), 313 (2005).
10. S. McNaughton, K. Ball, G. Mishra, D. Crawford. *Asia Pacific Journ. of Clinical Nutr.*, **15** (3), S63. (2006).
11. A. Nudda, M. A. Mc Guire, G. Battcone, G. Pulina. *J. Dairy Sci.*, **88**, 1311 (2005).
12. J.M. Griinari, D. E. Bauman, *Advances in Conjugated Linoleic Acid Research, Champaign, Illinois*, **1**, 180 (1999).
13. G. Gerchev, N. Naydenova, Ts. Dimitrova, G. Mihailova, N. Markov, *Journ. of Mount. Agri on the Balkans*, **21**(4), 15 (2018).
14. D. E. Bauman, *J. Dairy Sci.*, **84**(3), 680 (2001).
15. B. C. An, C. W. Kang, Y. Izumi, Y. Kobayashi, K. Tanaka, *Asian- Australasian J. Animal Sci.*, **16**(2), 222 (2003).
16. G. F. Schroeder, G. A. Gagliostro, F. Bargo, J. E. Delahoy, L. D. Muller, *Livestock Prod. Sci.*, **86**(1-3), 1 (2004).
17. G. Jahreis, J. Fritsche, P. Mockel, F. Schone, U. Moller, H. Steinhart, *Nutr. Res.*, **19**(10), 1541 (1999).
18. P. Secchiari, M. Mele, A. Serra, A. Buccioni, M. Antongiovanni, G. Ferruzzi, F. Paoletti, L. Andreotti, *Progress in Nutrition*, **3** (4), 37 (2001).
19. V. Fievez, E. Colman, J. M. Castro-Montoya, I. Stefanov, B. Vlaeminck, *Anim. Feed Sci. Technol.*, **172**, 51 (2012)
20. J. W jowski, R. Dank w, R. Skrzypek, R. Fahr, *Milchwissenschaft*, **58** (11/12) (2003)
21. Y.  zogul, F.  zogul. *Food Chemistry*, **100**, 1634 (2007).

Phenothiazine Schiff bases containing chlorine: synthesis, characterization and antimicrobial study

I. Nikolova^{1*}, I. Kostova¹, M. Marinov²

¹Department of Chemical, Food and Biotechnologies, "Angel Kanchev" University of Ruse, Razgrad Branch, 47 Aprilsko Vastanie Blvd., 7200 Razgrad, Bulgaria

²Faculty of Plant Protection and Agroecology, Department of Chemistry and Phytopharmacy, Agricultural University – Plovdiv, 12 Mendeleev Blvd., 4000 Plovdiv, Bulgaria

Received: November 3, 2024; Revised: April 11, 2024

This article presents the synthesis, structural and spectral (IR and NMR) characterization of some new phenothiazine Schiff bases containing chlorine. The target compounds (Figs. 1a-1d) were obtained as a result of the reaction between 2-amino-6-(10*H*-phenothiazin-10-yl)-1*H*-benzo[*de*]isoquinoline-1,3(2*H*)-dione and the corresponding chlorobenzaldehydes. The antimicrobial activity of the synthesized Schiff bases was evaluated against Gram-positive bacteria *Staphylococcus aureus* and *Bacillus subtilis*, Gram-negative bacteria *Escherichia coli*, *Pseudomonas aeruginosa* and *Salmonella abony*, yeasts *Saccharomyces cerevisiae* and *Candida albicans*, molds *Aspergillus brasiliensis* and *Fusarium moniliforme*.

Keywords: phenothiazine, Schiff bases, antimicrobial activity

INTRODUCTION

Compounds containing the -C=N- (azomethine) group in their structure are known as Schiff bases, and are synthesized by condensation of primary amines and active carbonyl compounds [1]. Schiff bases are known for a broad range of biological activities, such as antitubercular [2], anticancer [3-5], analgesic [6, 7], anti-inflammatory [8, 9], anticonvulsant [10, 11], antibacterial [12], antifungal [13] antioxidant [14, 15], antitumor [16, 17] and anthelmintic [18] activities.

In previous studies of ours, we have presented the synthesis [19, 20], and studies of antimicrobial and corrosion inhibition properties of some phenothiazine products. The results of these studies have prompted us to continue working in this direction, and to synthesize and study new compounds from the group of phenothiazine Schiff bases, not previously described in the literature.

MATERIALS AND METHODS

All used chemicals were purchased from Merck and Sigma-Aldrich. The melting points were determined on a SMP-10 digital melting point apparatus. The IR spectra were taken on Perkin-Elmer FTIR-1600 spectrometer in KBr discs. The NMR spectra were taken on a Bruker DRX-250 spectrometer operating at 250.13 and 62.90 MHz for ¹H and ¹³C, respectively, using the standard Bruker software. The chemical shifts were referenced to tetramethylsilane (TMS). The measurements in

DMSO-*d*₆ solutions were carried out at ambient temperature (300 K).

EXPERIMENTAL

The synthesis of the initial compound 2-amino-6-(10*H*-phenothiazin-10-yl)-1*H*-benzo[*de*]isoquinoline-1,3(2*H*)-dione is presented in Scheme 1 [21].

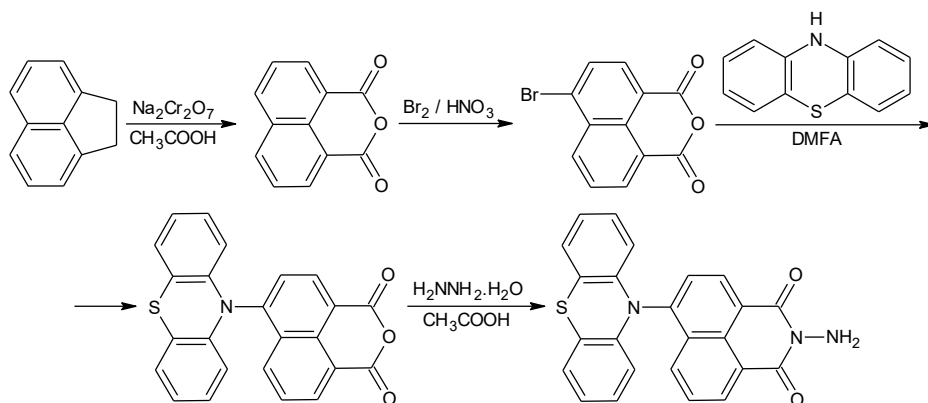
Synthesis of Schiff bases containing chlorine (Scheme 2)

0.005 mol of 2-amino-6-(10*H*-phenothiazin-10-yl)-1*H*-benzo[*de*]isoquinoline-1,3(2*H*)-dione (1) is dissolved in 40 mL of MeOH and 0.005 mol of the corresponding chlorobenzaldehyde (2a-2d) is added. The reaction mixture is heated in a water bath for 1 h (~100°C). After cooling, the product formed (3a-3d) is filtered off and washed with MeOH.

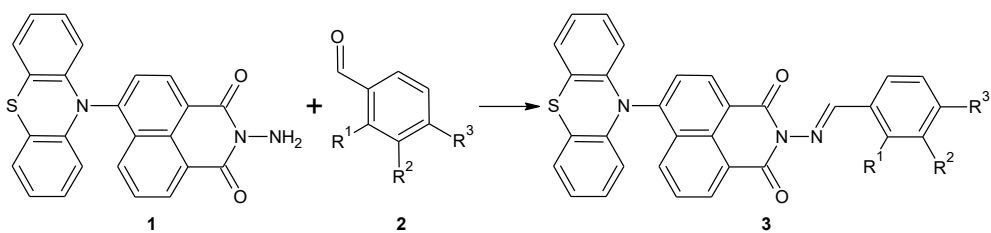
Antimicrobial study

Agar diffusion method and test microorganisms: Gram-positive bacteria *Staphylococcus aureus* ATCC 6538, *Bacillus subtilis* ATCC 6633, Gram-negative bacteria *Escherichia coli* ATCC 8739, *Pseudomonas aeruginosa* ATCC 9027 and *Salmonella abony* NTCC 6017, yeast *Candida albicans* ATCC 10231, *Saccharomyces cerevisiae* ATCC 2601, molds *Aspergillus brasiliensis* ATCC 16404 and *Fusarium moniliforme*, were used to determine the antimicrobial action of the synthesized compounds. 1% solutions in solvent dimethyl sulfoxide (DMSO) were prepared from the compounds tested.

* To whom all correspondence should be sent:
E-mail: inikolova@uni-ruse.bg



Scheme 1



- a) $R^1 = \text{Cl}, R^2 = R^3 = \text{H}$; b) $R^1 = R^2 = \text{Cl}, R^3 = \text{H}$; c) $R^1 = R^3 = \text{Cl}, R^2 = \text{H}$;
d) $R^1 = R^2 = \text{H}, R^3 = \text{Cl}$

Scheme 2

The experiments were performed in nutrient medium Tryptic soy agar (Merck) for bacteria and Sabouraud dextrose agar (Merck) for yeast and molds.

The agar media were melted in a Koch apparatus. They were cooled down to a temperature of 50-48°C and inoculated with 1% of the prepared suspensions of the test microorganisms, then mixed well. 20 mL of the inoculated media were poured into sterile Petri dishes ($\varnothing=90$ mm). The agar was allowed to solidify. Cork borer was used to punch holes ($\varnothing=8$ mm) in the agar plate. 50 μL of the prepared solutions were added dropwise to the wells, and after 30 min of pre-fusion at room temperature, the petri dishes were placed in a thermostat at 37°C for 24 h for bacteria; 28°C for 24 h for yeasts and for 72 h for molds [22]. Diameters of the zones of growth inhibition were taken into account after cultivation as follows: up to 15 mm the microbial culture is weakly sensitive; from 15 to 25 mm – sensitive and over 25 mm – highly sensitive.

RESULTS AND DISCUSSION

Four Schiff base derivatives of phenothiazine with the structure shown in Fig. 1 were synthesized in accordance with Scheme 2 (see the Experimental part).

The yields and melting points of the obtained compounds (3a-3d) are given in Table 1. The spectral data (IR, ^1H NMR and ^{13}C NMR including

^{13}C DEPT 135) of the compounds 3a-3d are presented in Tables 2-4.

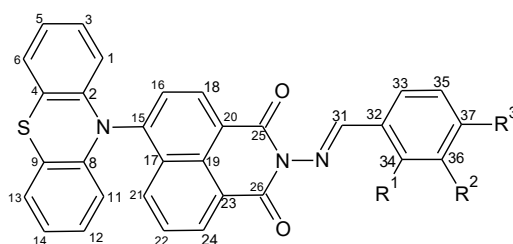


Figure 1. a) $R^1 = \text{Cl}, R^2 = R^3 = \text{H}$; b) $R^1 = R^2 = \text{Cl}, R^3 = \text{H}$; c) $R^1 = R^3 = \text{Cl}, R^2 = \text{H}$; d) $R^1 = R^2 = \text{H}, R^3 = \text{Cl}$
(The numbering of the atoms is only for spectral assignments)

Table 1. Yields and melting points

No	Systematic name	M. p., °C	Yield, %
3a	2-[(2-hlorophenyl)methyleneamino]-6-phenothiazin-10-yl-benzo[de]isoquinoline-1,3-dione	204-205	30
3b	2-[(2,3-dichlorophenyl)methyleneamino]-6-phenothiazin-10-yl-benzo[de]isoquinoline-1,3-dione	163-164	46
3c	2-[(2,4-dichlorophenyl)methyleneamino]-6-phenothiazin-10-yl-benzo[de]isoquinoline-1,3-dione	206-207	46
3d	2-[(4-chlorophenyl)methyleneamino]-6-phenothiazin-10-yl-benzo[de]isoquinoline-1,3-dione	199-200	38

Table 2. Selected IR spectral data (KBr, cm⁻¹)

№	ν C=O	ν C=N	ν C-N	ν Arom.	ν C-Cl
3a	1707, 1697	1612	1340	3089	775
3b	1704, 1671	1609	1338	3061	774, 741
3c	1704, 1671	1613	1340	3090	774, 741
3d	1703, 1654	1618	1341	3034	778

Table 3. Selected ¹H NMR spectroscopic data (DMSO-*d*₆, δ , ppm)

№	
3a	5.80-7.69 (m, 8H, CH, phenoth. core), 8.01-8.24 (m, 4H, CH, benz. core), 8.28 (s, 1H, CH), 8.34-8.77 (m, 5H, CH, naphth. core)
3b	6.67-6.75 (m, 8H, CH, phenoth. core), 6.90-6.99 (t, 3H, CH, benz. core), 8.27 (s, 1H, CH), 8.29-8.64 (m, 5H, CH, naphth. core)
3c	5.80-6.91 (m, 8H, CH, phenoth. core), 6.98-8.05 (t, 3H, CH, benz. core), 8.28 (s, 1H, CH), 8.38-8.64 (m, 5H, CH, naphth. core)
3d	5.80-6.91 (m, 8H, CH, phenoth. core), 6.98-8.00 (t, 3H, CH, benz. core), 8.25 (s, 1H, CH), 8.35-8.80 (m, 5H, CH, naphth. core)

Table 4. Selected ¹³C NMR and ¹³C DEPT 135 spectroscopic data (DMSO-*d*₆, δ , ppm)

Position	Compounds							
	3a	3b	3c	3d	3a	3b	3c	3d
	¹³ C NMR				¹³ C DEPT-135			
1 11	122.2	122.2	114.9	129.5	CH	CH	CH	CH
2 8	135.5	135.5	142.6	143.3				
3 12	132.4	133.9	132.1	129.8	CH	CH	CH	CH
4 10	123.7	122.9	132.2	131.7				
5 14	128.5	126.7	129.6	131.8	CH	CH	CH	CH
6 13	128.7	129.6	128.0	132.0	CH	CH	CH	CH
15	134.8	128.0	133.9	137.9				
16	122.9	116.2	122.2	114.9	CH	CH	CH	CH
17	123.7	125.5	126.7	129.9				
18	133.3	130.5	132.9		CH	CH	CH	CH
19	129.4	130.6	130.6					
20	129.9	132.2	122.9					
21	130.2	132.9	133.9	130.9	CH	CH	CH	CH
22	130.4	132.2	133.9	132.5	CH	CH	CH	CH
23	131.5	133.2	122.2					
24	131.8			133.5	CH		CH	CH
25 26	160.3	161.7	161.7	160.3				
31	168.6	168.6	168.6	171.3	CH			
32	131.9	131.2	116.8	128.5				
33	130.8	118.7		121.4	CH	CH	CH	CH
34	131.9	133.6	134.2	121.4				CH
35	132.1	129.4		125.5	CH	CH	CH	CH
36	122.1	133.8	136.6	125.5	CH		CH	CH
37	133.4				CH	CH		

Table 5. Antimicrobial activity of compounds 3a-3d

Test microorganisms	Diameter of the inhibition zone (mm)			
	3a	3b	3c	3d
<i>Staphylococcus aureus</i> ATCC 6538	0	0	0	0
<i>Bacillus subtilis</i> ATCC 6633	10.4	0	0	12.8
<i>Escherichia coli</i> ATCC 8739	0	0	0	0
<i>Pseudomonas aeruginosa</i> ATCC 9027	0	0	0	0
<i>Salmonella abony</i> NTCC 6017	0	0	0	11.6
<i>Saccharomyces cerevisiae</i> ATCC 2601	0	0	0	0
<i>Candida albicans</i> ATCC 10231	0	0	0	0
<i>Aspergillus brasiliensis</i> ATCC 16404	0	0	0	0
<i>Fusarium moniliforme</i>	0	0	0	0

The IR and ¹H-NMR spectral data of the compound 2-amino-6-(10*H*-phenothiazin-10-yl)-1*H*-benzo[*de*]isoquinoline-1,3(2*H*)-dione [23] show the signals for NH₂ group as follows: 3441 cm⁻¹ and 3324 cm⁻¹ and 2.51 ppm and 3.35 ppm. These signals are absent for the compounds 3a-d. In the synthesized Schiff bases, signals for >C=N group appear in the region 1609-1618 cm⁻¹. The ¹H-NMR spectra of the compounds showed signals for a CH group (№ 31, Figure 1) in the region 8.25-8.28 ppm. This confirms the interaction between the corresponding amine and the aromatic aldehyde leading to the formation of the Schiff bases 3a-d. In the ¹³C-NMR spectra, a new signal for the >C=N group appears, which for compounds 3a-c is around 168.6 ppm, only in compound 3d it is at 171.3 ppm, which is most likely due to the *p*-chlorine atom in the aromatic aldehyde.

Compound 3a shows weak antibacterial activity against the Gram-positive bacterium *Bacillus subtilis*. Compound 3d demonstrates weak activity against *Bacillus subtilis* and the Gram-negative bacterium *Salmonella abony* (Table 5). No activity of these compounds was established against any other test microorganisms used. Compounds 3b and 3c show no activity towards the microorganisms used.

CONCLUSION

Four new phenothiazine derivatives, previously not described in the literature, have been synthesized and their structures have been proven by IR and ¹H, ¹³C and DEPT-135 spectroscopy. Their antimicrobial activity has been investigated, where two of the compounds have shown weak activity against *Bacillus subtilis*, and one is also active against *Salmonella abony*. Two of the compounds have demonstrated no activity towards the microorganisms used.

Acknowledgement: The authors acknowledge the support by the Science Fund of the University of Ruse, Bulgaria (project 2023-BRz-01).

REFERENCES

- R. Nirmal, C. R. Prakash, K. Meenakshi, P. Shanmugapandiyan, *J. Young Pharm.*, **2**(2), 162 (2010).
- K. K. Sivakumar, A. Rajasekaran, *J. Pharm. Bioallied. Sci.*, **5**(2), 126 (2013).
- D. Sunil, A. M. Isloor, P. Shetty, P. G. Nayak, K. S. R. Pai, *Arab. J. Chem.*, **6**(1), 25 (2013).
- A. A. Osowole, I. Ott, O. M. Ogunlana, *Int. J. Inorg. Chem.*, **2012**, 1 (2012).
- S. S. Mohamed, A. R. Tamer, S. M. Bensaber, M. I. Jaeda, N. B. Ermeli, A. A. Allafi, I. A. Mrema, M. Erhuma, A. Hermann, A. M. Gbaj, *Naunyn-Schmiedeberg's Arch. Pharmacol.*, **386**, 813 (2013).
- M. A. Alafeefy, M. A. Bakht, M. A. Ganaie, M. N. Ansarie, N. N. El-Sayed, A. Awaad, *Bioorg. Med. Chem. Lett.*, **25**(2), 179 (2015).
- S. Murtaza, M. S. Akhtar, F. Kanwal, A. Abbas, S. Ashiq, S. Shamim, *J. Saudi Chem. Soc.*, **21**, 359 (2017).
- R. Nirmal, C. R. Prakash, K. Meenakshi, P. Shanmugapandiyan, *J. Young Pharm.*, **2**(2), 162 (2010).
- I. Vazzana, E. Terranova, F. Mattioli, F. Sparatore, *ARKIVOC* (v) 364 (2004).
- C. R. Prakash, S. Raja, G. Saravanan, *Int. J. Pharm. Pharm. Sci.*, **2**(4), 177 (2010).
- C. Ajit kumar, S. N. Pandeya, *Int. J. Pharmtech. Res.*, **4**(2), 590 (2012).
- S. Tiwari, V. Mujalda, V. Sharma, P. Saxena, M. Shrivastava, *Asian J. Pharm. Clin. Res.*, **5**(1), 98 (2012).
- R. A. Sheikh, M. Y. Wani, S. Shreaz, A. A. Hashmi, *Arab. J. Chem.*, **9**, 743 (2016).
- R. N. Gacche, D. S. Gond, N. A. Dhole, B. S. Dawane, *J. Enzyme Inhib. Med. Chem.*, **21**(2), 157 (2006).
- P. Praveen Kumar, B. L. Rani, *Int. J. Chemtech. Res.*, **3**(1), 155 (2011).

16. K. Venkatesan, V. S. V. Satyanarayana, A. Sivakumar, *Polycycl. Aromat. Compd.*: **43**(1), 850 (2022).
17. K. Venkatesan, V. S. V. Satyanarayana, A. Sivakumar, C. Ramamurthy, C. Thirunavukkarasu, *J. Heterocycl. Chem.*, **57**, 2722 (2020).
18. B. Mathew, S. S. Vakketh, S. S. Kumar, *Der Pharma Chem.*, **2**(5), 337 (2010).
19. T. Haralanova, M. Marinov, I. Kostova, I. Nikolova, S. Damyanova, N. Stoyanov, *IOP Conf. Ser. Mater. Sci. Eng.*, **1031**, 1 (2021).
20. I. Kostova, I. Nikolova, M. Marinov, *Proc. Univ. Ruse*, **59**(10.2.), 56 (2020).
21. I. Nikolova, I. Kostova, T. Haralanova, G. Borisov, M. Marinov, N. Stoyanov, *AIP Conf. Proc.*, **2889**: 080022-1-080022-8 (2023).
22. K. N. Hussein, T. Molnar, R. Pinter, A. Toth, E. Ayari, L. Friedrich, I. Dalmadi, G. Kisko, *Prog. Agric. Eng. Sci.*, **16**(S2), 163 (2021).
23. M. Marinov, I. Nikolova, I. Kostova, N. Stoyanov, *Phosphorus Sulfur Silicon Relat. Elem.*, **198**, 128 (2022).

The modification of [¹⁸F]FDG for further click reactions

G. V. Simeonova^{1,2*}, B. R. Todorov²

¹ UMHAT "St. Marina", Department of Nuclear Medicine, 1 Hristo Smirnenski Blvd., Varna, Bulgaria

² Sofia University St. Kliment Ohridski, Faculty of Chemistry and Pharmacy, Department of Analytical Chemistry, 1 James Bourchier Str, Sofia, Bulgaria

Received: November 3, 2023; Revised: April 11, 2024

The synthesis of new fluorinated PET radiopharmaceuticals is facilitated by various strategies for ¹⁸F labeling reactions. [¹⁸F]FDG, as a basic PET radiopharmaceutical (glucose analog), can be used as a building block for indirect radiofluorination under mild reaction conditions, due to the presence of a carbonyl group where chemoselective formation of an oxime bond can take place for conjugation with target moieties. The glycosylation is one of the used modification strategies that can increase the hydrophilicity of the radiotracer, and shorten the period between injection and imaging. Also, glycosylation of biomolecules such as peptides or proteins can improve *in vivo* pharmacokinetics and blood stability.

We have developed a procedure for modification of [¹⁸F]FDG with bifunctional tetrazine derivatives, by oxime bond formation and all experiments were done with standard clinical equipments. For this purpose, [¹⁸F]FDG was produced using a biomedical baby-cyclotron at the Nuclear Medicine Clinic at the University Hospital "St. Marina" – Varna. Successful modification with [¹⁸F]FDG was achieved at a temperature of 70-75°C, in a slightly acidic environment (pH= 4-4.2), in the presence of a *p*-diaminobenzene catalyst for 25-30 minutes. TLC chromatography was used as a fast and available in clinic method to monitor the synthesis process. This is a prerequisite for the development of new PET radiopharmaceuticals and for the refinement of diagnostics and therapy in nuclear medicine.

Keywords: [¹⁸F]-FDG, bifunctional compounds, tetrazine, trans-cyclooctene, oxime formation, click reactions, personal medicine

INTRODUCTION

The early diagnosis of malignant tumors plays a leading role in the choice of treatment approach and the survival prognosis of cancer patients. This task is solved to a significant extent with the help of radionuclide diagnostics (nuclear medicine) [1-3]. The use of molecular imaging agents plays an important role in the advancement of medical procedures and is an essential part of ongoing research. At the forefront of molecular imaging is the use of positron emission tomography (PET-CT) which relies on a biomarker labeled with a short-lived positron-emitting radionuclide [4]. The molecular imaging aims to non-invasively visualize, characterize and quantify biological processes at the cellular and molecular level *in vivo* [5]. When considering the clinical applications of pre-targeted PET imaging, the ideal isotope would be fluorine-18 (¹⁸F) due to its general availability and optimal physical properties [6].

There are various chemical methods of introducing ¹⁸F to the desired molecule. The main synthetic strategies can be divided into two main categories: direct fluorination, i.e. ¹⁸F is directly attached to the molecule to be labeled, and indirect fluorination, in which ¹⁸F is introduced in the form of an ¹⁸F-containing prosthetic group, which usually

requires multistep synthesis [7]. In recent years, various strategies for chemoselective ¹⁸F-labeling reactions have been successfully developed, facilitating the accessibility to novel PET radiopharmaceuticals. These synthesis strategies have been improved, especially due to the development of various ¹⁸F-labeled prosthetic groups designed mainly for chemoselective peptide labeling [8]. The use of a prosthetic group overcomes the inability to radiofluorinate certain compounds by nucleophilic ¹⁸F-substitution of a suitable leaving group. The development of ¹⁸F prosthetic groups makes extensive use of the concept of click chemistry [9]. The click chemical reactions should be simple, fast and modular. They are characterized by high chemical (and radiochemical) yields and production of stable products [9, 10]. Among the reactions that meet these requirements, carbonyl condensation reactions such as imine, hydrazone and oxime formation can be mentioned [11].

The molecule of 2-fluoro-deoxyglucose ([¹⁸F]FDG) is an analogue of glucose, in which the hydroxyl group at the second carbon atom is replaced by ¹⁸F, and finds application in nuclear medicine. [¹⁸F]FDG allows the evaluation of glycolytic activity, which is more enhanced in tumor cells compared to normal cells. It also finds applica-

* To whom all correspondence should be sent:
E-mail: gerimm@abv.bg

tion in the evaluation of cardiac and neurological diseases [12]. In addition to being a basic PET radiopharmaceutical, the molecule can also be used as a building block for indirect radiofluorination under mild reaction conditions. The [¹⁸F]FDG molecule has been reported as a suitable prosthetic group for indirect labeling of various aminoxy-functionalized peptides by chemoselective oxime formation [13]. The glycosylation of biomolecules such as peptides or proteins can improve *in vivo* pharmacokinetics and stability in blood [1]. The glycosylation is one of the most commonly used modification strategies that can increase the hydrophilicity of the radiomarker, increase the proportion of renal elimination, decrease the physiological uptake of the radiopharmaceutical into the digestive system, and shorten the time interval from injection of the tracer to imaging. It can also improve the contrast and usefulness of PET imaging [2]. Of particular interest are studies in which [¹⁸F]FDG has been used as a building block for other, more complex compounds such as peptides that cannot be directly labeled with ¹⁸F due to the harsher conditions required for their radiofluorination (high temperature, highly alkaline conditions) [3]. The glycosylation strategies for anticancer drugs have attracted considerable attention in the scientific community. This strategy improves the pharmacokinetic properties, selectivity of cytotoxic aglycones and is very useful for targeted drug delivery [14]. By a simple one-step method, [¹⁸F]FDG has been applied to fluorinate aminoxy- or hydrazine-functionalized peptides by formation of oxime or hydrazone [15, 16]. The main advantages of oxime formation by a click reaction between aminoxy- and carbonyl-functional groups used for ¹⁸F-fluoroglycosylation are: its high chemoselectivity, the application of unprotected aminoxy precursors and the fact that binding to the carbonyl component can take place in aqueous media (pH 4-7) [1]. The acidic environment facilitates the unblocking of the acetal functional group, and promotes the formation of an oxime bond between the aldehyde and the aminoxy group [17]. The radiochemistry of oxime formation and the relatively high stability, both chemical and *in vivo*, allow the potential use of this approach to rapidly generate the desired [¹⁸F]-labeled macromolecules for application in PET-CT imaging [18]. Another possibility for the reaction with aldehydes is the formation of hydrazones with hydrazine derivatives, which is similar to the formation of oximes - selective towards the formation of Schiff bases, but proceeds relatively slower than the reaction with aminoxy functionals [19]. The hydrazines react

more slowly with aldehydes than aminoxy derivatives, making them less common click partners in ¹⁸F-labeling of peptides [9]. The reaction efficiency in oxime and hydrazone bond formation can be dramatically increased by using a range of catalysts [20]. Bifunctional catalysts are being developed that use intramolecular proton transfer from acid-base groups near a nucleophilic amino group to facilitate rapid hydrazone and oxime formation [21]. The reactions of this type are becoming an essential tool for the preparation of chemically engineered bioconjugates for applications in chemical biology. Biocompatible click reactions have the potential to be used to perform *in situ* ligation in living organisms [11].

The oxime or hydrazone formation reactions in combination with other bioorthogonal click reactions, such as the cycloaddition between bifunctional tetrazine and trans-cyclooctene (TTCO), may play an important role in the development of new radiopharmaceuticals with high specific activity and selectivity. This, in turn, will make a step towards the development of personalized medicine related to early and accurate diagnosis and refinement of therapy. The highly efficient reaction between 1,2,4,5-tetrazines and strained dienophiles is a fast and clean bioorthogonal conjugation method. Moreover, the reaction proceeds without catalyst, which is beneficial in easier purification of the final radioactive tracer [9]. The reaction proceeds rapidly at room temperature and is practically irreversible. It produces N₂ as the only by-product [22]. This type of cycloaddition of heterocyclic azadienes provides a powerful methodology for the synthesis of highly substituted and functionalized heterocycles widely used in organic synthesis and pharmaceutical industries [23]. The ligation of tetrazine with trans cyclooctene can be applied to radiolabel large biomolecules such as ¹⁸F-labeled proteins and the resulting PET biomarker retains good binding ability to the desired target [24, 25]. Currently, the most promising reaction for pretargeted imaging is the ligation between tetrazine (Tz) and trans-cyclooctene (TCO). From a clinical point of view, ¹⁸F-labeled Tz would be ideal for positron emission tomography (PET) applications, as ¹⁸F possesses nearly perfect physical characteristics for molecular imaging [26]. The radionuclide ¹⁸F can be pre-introduced into one of the two molecules involved in the click reaction, tetrazine or dienophile. A difficulty, however, is the delicate stability of tetrazines in general, which can pose a problem for the conjugation of tetrazines to biomolecules [9]. The synthesis of a fluorinated tetrazine starting from an ¹⁸F-containing prosthetic

group is necessary, as tetrazines are unstable under the commonly used direct radiofluorination conditions. The resulting ¹⁸F-labeled tetrazine can be used for pretargeted PET imaging [16, 27]. The glycosylated ¹⁸F-labeled tetrazine is an excellent candidate for *in vivo* bioorthogonal chemistry applications in pretargeted PET imaging approaches [6]. A combination of the two chemoselective (click) reactions, in which functionalized tetrazines with a free aminoxy group capable of forming an oxime bond, have been successfully applied for indirect radiofluorination of monoclonal antibodies [28]. These bifunctional, clickable compounds are a new class of conjugates with promising applications in the nuclear medicine, providing a step towards the development of the personalized medicine related to early and accurate diagnosis and precision therapy.

In the pretargeted imaging approach based on the click reaction between bifunctional tetrazine and trans cyclooctene, one of the reagents can be a carrier of a specific biomolecule and the other of the radionuclide. The biomolecule will be responsible for the accumulation of the complex in the specific organ, and the radionuclide - for the visualization of the areas of interest. The variant in which the tetrazine derivative is indirectly radiolabeled by forming an oxime bond with the [¹⁸F]FDG molecule is proposed. Glycosylated ¹⁸F-labeled bifunctional tetrazine will provide a reagent for indirect radiolabeling of sensitive macromolecules *via* a click reaction with trans-cyclooctene. Figure 1 shows the general reaction scheme between [¹⁸F]FDG-modified tetrazine and bifunctional trans-cyclooctene. Such reactions are easy, fast, and practically irreversible. Most often, they take place at equivalent amounts of the reactants, under physiological conditions and room temperature, without the presence of a catalyst [29, 30]. As part of the implementation of a project with contract No. KP-06-H29/4 (Scientific Research Fund of the Ministry of Education and Science), the kinetic

parameters of "cold click" reactions with some of the pharmacologically most relevant TCO derivatives and Tz are investigated. The corresponding rate constants are experimentally determined. Studying the kinetics of a cold (non-radioactive) click reaction is an important step in the development of a radiolabeling procedure using TTCO. From the obtained results, clarity is obtained about the speed of the reaction and the applicability of the procedure for the purposes of nuclear medicine. The experimentally determined rate constants of the bimolecular "click" reaction in ethanol are of the same order in the range of 150-300 M⁻¹.s⁻¹, which ensures that the reaction takes place within seconds. This second-rate is quite sufficient for the purposes of the pre-target radio tagging strategy.

New bifunctional compounds have been synthesized within the framework of the above-mentioned project. Appropriately functionalized tetrazine derivatives containing a free hydroxylamine group capable of forming an oxime bond were selected. In addition, a suitable spacer was selected between the tetrazine ring and the functional group. By varying the spacer, the lipophilicity and pharmacokinetic properties of the compound can be influenced. The products were purified by polar phase column chromatography and characterized by ¹H-NMR, then provided and used for modification with [¹⁸F]FDG.

The aim of the study is to develop and optimize a highly efficient and rapid method for indirect radiofluorination of bifunctional tetrazine structures with an aminoxy group by [¹⁸F]FDG conjugation under standard clinical laboratory conditions. In our previous research, we mention the development of a modification procedure using another tetrazine (O-{10-[4-(6-phenyl-[1,2,4,5]tetrazin-3-yl)-phenoxy]-decyl}-hydroxylamine), which can be seen in more detail in reference [32]. The established procedure was applied to the successful radiolabeling of another tetrazine derivative.

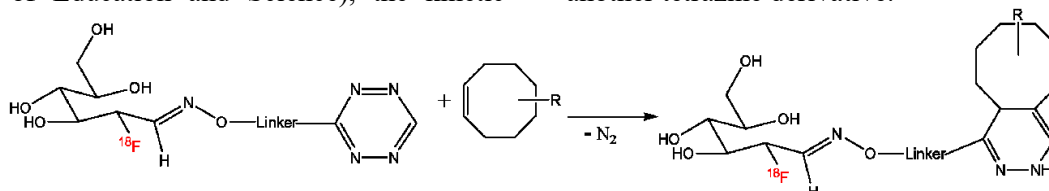


Figure 1. Scheme of the click reaction between modified tetrazine and trans-cyclooctene

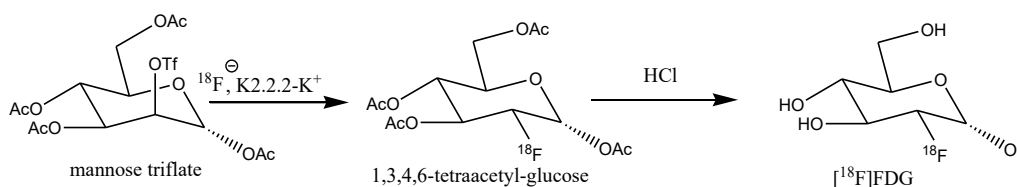
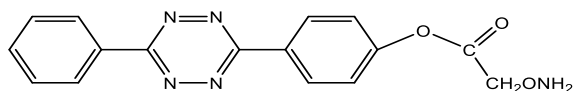


Figure 2. Synthesis of [¹⁸F]FDG

EXPERIMENTAL

A procedure is proposed to modify the most common and widely used radiopharmaceutical [¹⁸F]FDG by oxime bond formation. The procedure is performed at a temperature between 70 and 80 °C and is fully adapted to the clinical conditions and the equipment available in the clinic. The synthesis procedures were performed entirely at the Clinic of Nuclear Medicine at St. Marina University Hospital, Varna, Bulgaria. For this purpose, [¹⁸F]FDG was synthesized using a small biomedical cyclotron (ABT Molecular Imaging biomedical, model ABT BG-75) equipped with an automated radiochemical synthesis module and a quality control system. In the first stage, the radionuclide ¹⁸F is produced by proton bombardment of ¹⁸O-enriched water, and the following ¹⁸O(p,n)¹⁸F nuclear reaction is performed. The production of [¹⁸F]FDG was based on a nucleophilic radiofluorination method with mannose triflate as precursor followed by acid hydrolysis with 2M HCl [31]. All reagents required for the production of radiopharmaceuticals were commercially obtained and used without further purification. Figure 2 shows the reaction scheme of the process.

In this paper, we present the modification of the following aminoxy-functionalized tetrazine: aminoxy-acetic acid 4-(6-phenyl-[1,2,4,5]tetrazin-3-yl)-phenyl ester, which we will denote as R1 for brevity. Its structure is shown in Figure 3.



Aminoxy-acetic acid 4-(6-phenyl-[1,2,4,5]tetrazin-3-yl)-phenyl ester

Figure 3. Structure of used tetrazine R1

Since we are provided with a BOC (tert-butyloxycarbonyl) group-protected bifunctional compound, an additional deprotection step is required before labeling it with [¹⁸F]FDG. A small amount of the protected tetrazine was mixed with 0.5 ml of 10% trifluoroacetic acid in anhydrous ethyl acetate for 12 hours at room temperature, after which the vials were placed in an air oven to evaporate the solvent. The reaction scheme of this preliminary step to obtain R1 is presented in Figure 4.

After elimination of the BOC protection, the bifunctional tetrazine was dissolved in acetonitrile. The resulting solution was used to modify [¹⁸F]FDG by forming an oxime bond. We performed the syntheses in a large excess of tetrazine over radiofluorinated glucose (approximately 10⁴:1), suggesting its complete conversion. The following procedure was used. From a previously prepared 0.25 M solution of the catalyst p-diaminobenzene

acidified with acetic acid to a pH of about 4, 0.5 ml were transferred into the reaction vessel. To this was added 0.1 ml of [¹⁸F]FDG of radioactivity between 5 and 25 MBq. This was followed by heating at 70-75 °C for 15 minutes to activate the molecule and open the glucopyranose ring. As an intermediate, the corresponding Schiff base was obtained with the catalyst. In the next step, 0.2 ml of the prepared R1 solution was added and further heated for another 10-15 minutes at the same temperature [32]. As an inexpensive and clinically available method of analysis, we used radio-TLC to follow the course of the reaction and confirm the production of the labeled product [¹⁸F]FDG-R1. The TLC analysis was performed with silica gel-coated aluminium plates (ALUGRAM Sorbent Silica G/UV254, 40×80 mm) and ethyl acetate was used as eluent. After addition of the sample and subsequent elution, the plates were scanned using a Scan-Ram PET/SPECT radio TLC-scanner.

RESULTS AND DISCUSSION

According to literature data, the most suitable conjugation for [¹⁸F]FDG is *via* oxime or hydrazone bond formation, and this is reported to be an efficient and chemoselective reaction occurring in aqueous media under mildly acidic conditions in the presence of a catalyst. The aim of the presented research was to verify the applicability of such a modification under standard conditions and equipment of a clinical laboratory. By forming an oxime bond, we were able to modify the bifunctional derivative of tetrazine.

The modification of R1 in the presence of p-diaminobenzene proceeds in two steps. In the first step, a Schiff base is obtained as an intermediate between the catalyst and the [¹⁸F]FDG molecule, which after addition of R1 turns into the desired oxime product [¹⁸F]FDG-R1. In Figure 5 the reaction scheme is presented. After the synthesis, a sample of the reaction mixture was taken and spotted onto the TLC plate. After eluting it with ethyl acetate, we obtained the TLC chromatogram presented in Figure 6. Under these elution conditions, the catalyst and unreacted tetrazine move to the front as a brown and pink spot, respectively. The unreacted [¹⁸F]FDG remains at the start (at the drip point), where we also detect a radioactive peak. A new pink spot with reported activity corresponding to the labeled oxime product [¹⁸F]FDG-R1 is observed close to the start. The distribution of spots corresponding to the reaction components after modification of R1 is as follows: 1 is unreacted [¹⁸F]FDG if present in the system, 2 - labeled oxime product, 3 is starting tetrazine, and 4 is catalyst used.

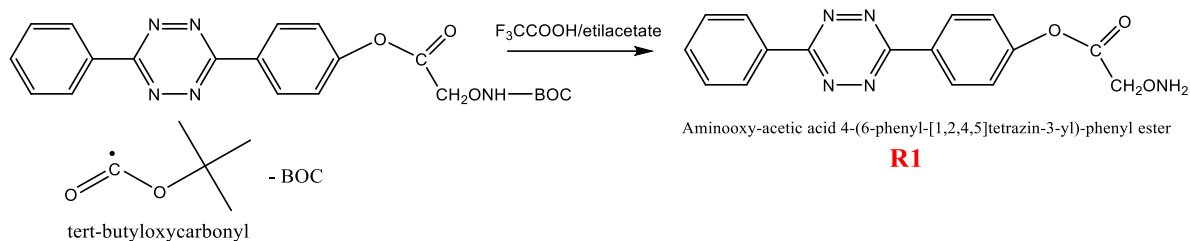


Figure 4. Preparation of tetrazine R1

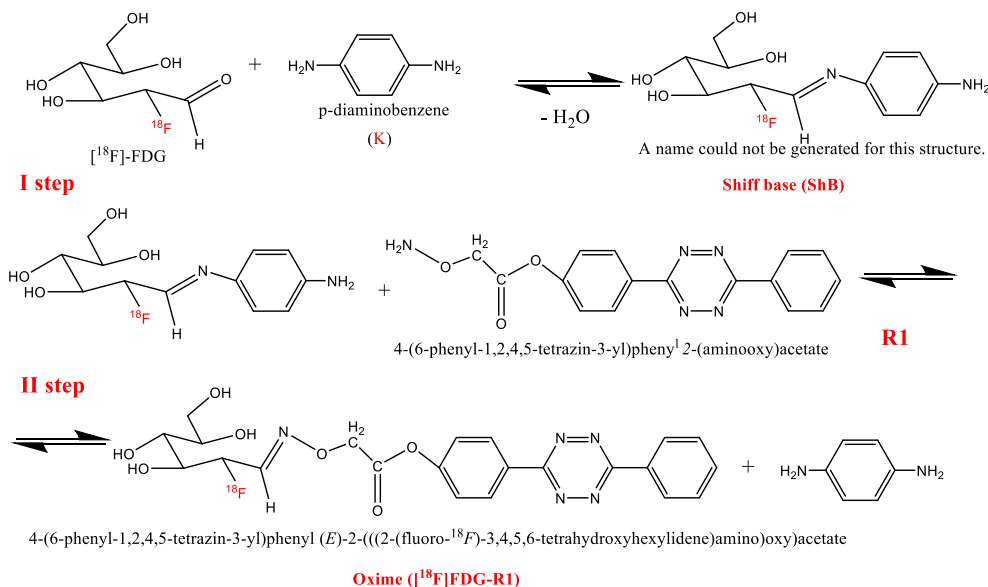


Figure 5. Modification of R1 in the presence of p-diaminobenzene

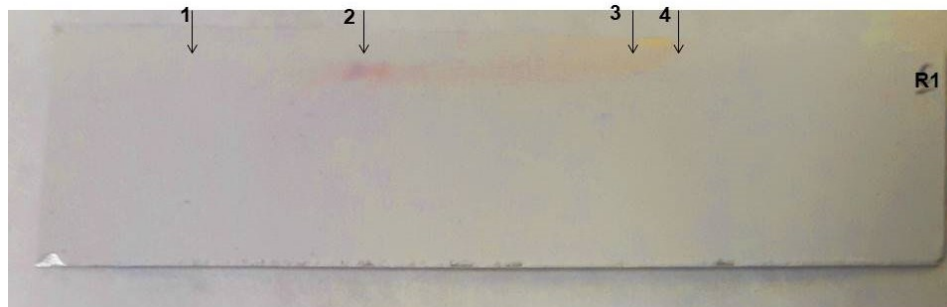


Figure 6. TLC chromatogram showing the distribution of the reaction components after labeling R1

The plate was then scanned and the radio-TLC chromatogram shown in Figure 7 was obtained. Based on it, we determined the retention factor ($R_f = 0.41$) of the obtained product [¹⁸F]FDG-R1 and an approximate radiochemical yield (RCY = 85%), which is uncorrected for radioactive decay. A single radioactive peak was obtained because tetrazine was used in a very large excess ($10^4:1$) over [¹⁸F]FDG, which under optimal conditions undergoes almost complete conversion to the corresponding radiolabeled product. For comparison, a radio-TLC chromatogram of the initial [¹⁸F]FDG, which, after elution under the same conditions, is retained at the start (at the drop point) with $R_f = 0.06$ is also attached. The resulting product was confirmed by radio-HPLC. Since the labeling of R1 is carried out in a

large excess of tetrazine relative to [¹⁸F]FDG, the concentration of the resulting radiolabeled product in the reaction system is negligible. As a result, the obtained products are fully confirmed on the basis of the data from the RAD detector, which has a significantly higher sensitivity. The RAD detector data confirms the successful reaction. The initial [¹⁸F]FDG was recorded as a peak at $t_r = 1.08$ min, and upon analysis of the reaction mixture a new radioactive peak appeared at $t_r = 2.24$ min corresponding to the labeled product Pr2. Figure 8 presents the HPLC chromatograms obtained from the RAD detector of unmodified [¹⁸F]FDG (chromatogram A) and reaction mixture (chromatogram B).

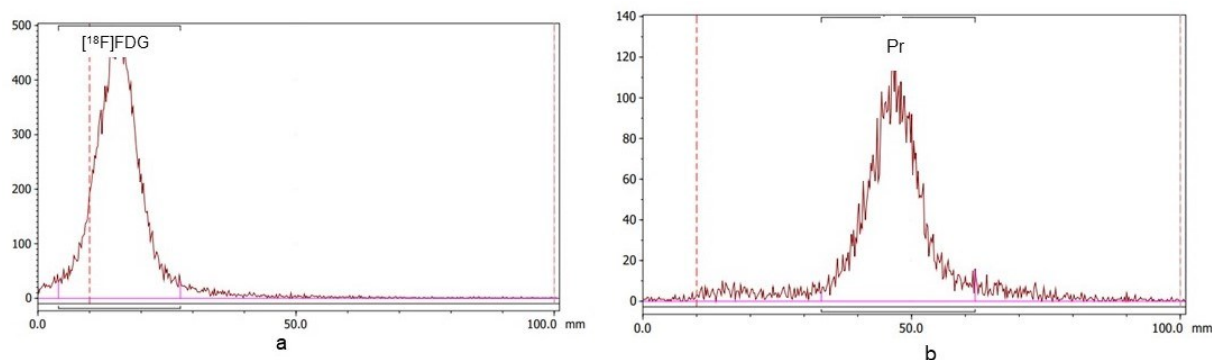


Figure 7. Radio-TLC chromatogram: a) unreacted [¹⁸F]FDG; Rf=0.06; b) modified R1: Rf=0.41; RCY=85.4%



Figure 8. Radio-HPLC analysis of modified R1

CONCLUSIONS

Based on the experiments, the following conclusions can be drawn:

1) The aminoxy-functionalized tetrazine aminoxy-acetic acid 4-(6-phenyl-[1,2,4,5]tetrazin-3-yl)-phenyl ester was successfully modified under soft reaction conditions with good radiochemical yield;

2) The oxime formation with [¹⁸F]-FDG is a practical method for indirect radiofluorination;

3) The developed method is fully applicable to standard clinical laboratory conditions.

REFERENCES

1. S. Maschauer, O. Prante, *BioMed. Research International*, **2014** (2014).
2. X. Yang, F. Wang, H. Zhu, Z. Yang, T. Chu, *Mol. Pharm.*, **16(5)**, 2118 (2019).
3. V. M. Petriev, V. K. Tishchenko, R. N. Krasikova, *Pharm. Chem. J.*, **50**, 209 (2016).
4. P. Carberry, B. P. Lieberman, K. Ploessl, S. R. Choi, D. N. Haase, H. F. Kung, *Bioconj. Chem.*, **22(4)**:642 (2011).
5. J. Y. Choi, B. C. Lee, *Nucl. Med. Mol. Imaging*, **49(4)**, 258 (2015).
6. O. Keinänen, X. G. Li, N. K. Chenna, D. Lumen, J. Ott, C. F. Molthoff, M. Sarparanta, K. Helariutta, T. Vuorinen, A. D. Windhorst, A. J. Airaksinen, *ACS Med. Chem. Lett.*; **7(1)**, 62 (2015).
7. Z. Li, P. S. Conti, *Advanced Drug Delivery Reviews* **62**, 1031 (2010).
8. S. Maschauer, O. Prante, *Carbohydr. Res.*, **344(6)**, 753 (2009).
9. R. Schirmacher, B. Wängler, J. Bailey, V. Bernard-Gauthier, E. Schirmacher, C. Wängler, *Semin. Nucl. Med.*, **47(5)**, 474 (2017).
10. S. Richter, F. Wuest, *Molecules*, **19(12)**, 20536 (2014).
11. S. Ulrich, D. Boturyn, A. Marra, O. Renaudet, P. Dumy, *Chemistry*, **20(1)**, 34 (2014).
12. M. A. Áliva-Rodríguez, H. A. Sanchez, *Unidad PET, Facultad de Medicina, Universidad Nacional Autónoma de México*, **5(3)**, 103 (2010).
13. V. R. Bouvet, F. Wuest, *Lab Chip*, **13(22)**, 4290 (2013).
14. F. Horssain, PhD Thesis, The University of Toledo, 2019.
15. S. Khoshbakht, D. Beiki, P. Geramifar, F. Kobarfard, O. Sabzevari, M. Amini, S. Shahhossein, *J. Radioanal. Nucl. Chem.* **310**, 413 (2016).
16. D. Van der Born, A. Pees, A. J. Poot, R. V. A. Orru, A. D. Windhorst, D. J. Vugts, *Chem. Soc. Rev.*, **46(15)**, 4709 (2017).
17. P. Carberry, A. P. Carpenter, H. F. Kung. *Bioorg. Med. Chem. Lett.*, **21(23)**, 6992 (2011).
18. M. Namavari, O. Padilla De Jesus, Z. Cheng, A. De, E. Kovacs, J. Levi, R. Zhang, J. K. Hoerner, H.

- Grade, F. A. Syud, S. S. Gambhir, *Mol. Imaging Biol.*, **10(4)**, 177 (2008).
19. C. Wängler, R. Schirrmacher, P. Bartenstein, B. Wängler, *Curr. Med. Chem.*, **17(11)**, 1092 (2010).
20. X. G. Li., M. Haaparanta, O. Solin, *Journal of Fluorine Chemistry*, **143**, 49 (2012).
21. D. Larsen, A. M. Kietrys, S. A. Clark, H. Sh. Park, A. Ekebergh, E. T. Kool, *Chem. Sci.*, **9**, 5252 (2018).
22. IAEA (International Atomic Energy Agency) TECDOC SERIES N°1968, Vienna, 2021.
23. Z. C. Wu, D. L. Boger, *J Am Chem Soc.*, **141(41)**, 16388 (2019).
24. M. Wang, PhD Thesis, The University of North Carolina at Chapel Hill, 2019.
25. M. Wang, D. Svatunek, K. Rohlfing, Y. Liu, H. Wang, B. Giglio, H. Yuan, Z. Wu, Z. Li, J. Fox, *Theranostics.*, **6(6)**, 887 (2016).
26. R. García-Vázquez, J. T. Jørgensen, K. E. Bratteby, V. Shalgunov, L. Hvass, M. M. Herth, A. Kjær, U. M. Battisti, *Pharmaceuticals (Basel)*, **15(2)**, 245 (2022).
27. O. Keinänen, D. Partelová, O. Alanen, M. Antopolsky, M. Sarparanta, A. J. Airaksinen, *Nucl. Med. Biol.*, **67**, 27 (2018).
28. O. Keinänen, K. Fung, J. Pourat, V. Jallinoja, D. Vivier, N. K. Pillarsetty, A. J. Airaksinen, J. S. Lewis, B. M. Zeglis, M. Sarparanta, *EJNMMI Res.*, **7(1)**, 95 (2017).
29. G. Simeonova, B. Todorov, V. Lyubomirova, *RAP Conf. Proc.*, **6**, 11 (2021).
30. G. Simeonova, B. Todorov, V. Lyubomirova, *Eur. Phys. J. Spec. Top.*, **232**, 1555 (2023).
31. S. Dall'Angelo, Q. Zhang, I. N. Fleming, M. Piras, L. F. Schweiger, D. O'Hagan, M. Zanda, *Org. Biomol. Chem.*, **11(27)**, 4551 (2013).
32. M. Rashidian, E. Keliher, M. Dougan, P. K. Juras, M. Cavallari, G. R. Wojtkiewicz, J. T. Jacobsen, J. G. Edens, J. M. J. Tas, G. Victora, R. Weissleder, H. Ploegh, *ACS Cent. Sci.*, **1(3)**, 142 (2015).

Phytonutrients in black nightshade fruit (*Solanum nigrum* L.) growing in Bulgaria

Zh. Y. Petkova^{1*}, V. T. Popova², N. T. Petkova³, T. A. Ivanova², P. A. Merdzhanov²,
A. S. Stoyanova²

¹University of Plovdiv "Paisii Hilendarski", Department of Chemical Technology, 24 Tzar Asen Str., 4000 Plovdiv, Bulgaria

²University of Food Technologies, Department of Tobacco, Sugar, Vegetable and Essential Oils, 26 Maritza Blvd., 4002 Plovdiv, Bulgaria

³University of Food Technologies, Department of Organic Chemistry and Inorganic Chemistry, 26 Maritza Blvd., 4002 Plovdiv, Bulgaria

Received: Ножембер 3, 2023; Revised: April 11, 2024

Black nightshade (*Solanum nigrum* L.) belongs to the Solanaceae family and is a medicinal plant with wild populations found in different regions of Bulgaria. The aim of this study was to analyze the availability of selected phytonutrients in the fruits, and, in particular, their presence in two individual fruit structures (seeds and peels) regarded as by-products in juice production. Fresh fruits were characterized by their diameter (8.42±0.62 mm) and absolute weight (393.75±38.00 g/1000 pcs). The seeds contained 9.81% lipids, while their content in the peels was negligible. The main fatty acids in the extracted lipid fraction were linoleic (48.0%), oleic (27.8%) and palmitic (19.6%), with 76.6% share of unsaturated fatty acids. β -Sitosterol (70.80%) predominated in the sterol fraction, and γ -tocopherol (100%) – in the tocopherol fraction of the extracted oil. The main soluble carbohydrates in the seeds were glucose (2.78%) and fructose (2.42%), while the respective quantities in the peels were 4.21% and 3.82%. The cellulose content of the two fruit parts was 14.90% and 15.70%, respectively. The most abundant macro minerals in the seeds were K (15109.34 mg/kg) and Mg (1988.07 mg/kg), and the main micro minerals – Fe (53.68 mg/kg) and Zn (37.77 mg/kg). The peels contained the respective dietary minerals in substantially higher quantities; K (31373.32 mg/kg), Na (3348.46 mg/kg), Ca (2365.82 mg/kg). The results from the study contribute to a more complex appreciation of the nutritional potential of black nightshade fruit available in Bulgaria and the prospects for their processing into value-added products.

Key words: *Solanum nigrum* L., black nightshade, lipids, fatty acids, minerals

INTRODUCTION

Black nightshade (*Solanum nigrum* L.) is an annual plant belonging to the genus *Solanum* of the Solanaceae family. Nowadays it is found throughout the world, being adapted to various soil types, altitudes and climatic conditions [1, 2]. The plant usually grows as a weed in moist, shady places, bushes, forest edges, around waste and cultivated lands, along rivers and streams, etc. [3-5]. Black nightshade is common to Bulgaria, too, and its wild populations are found in different regions with an altitude up to 1200 m [6].

S. nigrum is a recognized medicinal plant, used in many folk medicines for thousands of years [1, 3, 7, 8]. Nowadays, it is the most extensively studied species of the genus *Solanum* [9], and has been associated with almost every possible pharmacological activity: antibacterial, antifungal, anticancer, antidiabetic, anti-obesity, antioxidant, anti-inflammatory, hepatoprotective, and many others [3, 9-14]. Various compounds responsible for these diverse activities have been identified in all

plant organs, among which steroidal alkaloids, saponins, flavonoids, lignins, organic acids, volatile oils, polysaccharides, and others [2, 13-16].

The species is usually considered toxic for humans and animals, due to the presence of glycoalkaloids in all plant parts, mainly solanine (95% of the alkaloid content), solamargine, solasonine, their aglycones solanidine and solasodine, etc. [3, 15, 16]. However, the content of solanine, as well as the total alkaloid content significantly decreases during plant growing and maturation [2] and the ripe berries and leaves of *S. nigrum* are edible, with rarely observed toxic and side effects if consumed in normal amounts [1, 2, 17]. Indeed, apart from its undisputed medicinal value, *S. nigrum* has been reported as an ancient famine plant of China and as one of the most important traditional leafy vegetables in several African countries (being cultivated in some of them, e.g., Nigeria) [1, 3-5, 18]. In the culinary practice, ripe berries and leaves are eaten fresh (as part of traditional salads) or more often cooked (boiled,

* To whom all correspondence should be sent:
E-mail: zhanapetkova@uni-plovdiv.net

sautéed, steam cooked), as the process is known to destroy solanine and other antinutrient compounds [3, 4, 19, 20].

Despite all this, however, the importance of *S. nigrum* in human nutrition is far less explored, compared to its medicinal properties; still, there are data about the basic macro and micronutrients in the berries, the leaves or the whole aerial parts of the plants. The fruits, in particular, have been reported to contain sufficient amounts of dietary fibers, protein, carbohydrates, minerals, vitamins, oil, and other nutrients [1, 5, 20-23]. It is well-documented that the individual plant organs and the structural parts (seeds, pulp, peels) of different berries accumulate primary and secondary metabolites to varying degrees, and, thus, they have different biological and nutrition value. On the other hand, seed-containing berries are often processed into juice or pulp (puree) and the isolated seeds and peels (skins) remain as by-products (waste), currently underutilized, but with distinct potential, both in terms of available amounts and nutrients' concentrations [24].

Based on these considerations, the aim of this study was to analyze the availability of selected phytonutrients in the fruits, and, in particular, their presence in two individual fruit structures (seeds and peels) regarded as by-products in juice production.

MATERIALS AND METHODS

The ripe fruits of black nightshade (*Solanum nigrum* L.) were hand-picked in July 2020 from wild plant populations in the region of Kapitan Dimitriev village, Peshtera municipality, Central South Bulgaria (N 42°07'26" E 24°18'52") (Fig. 1). Species identity was confirmed at the Botany Department of "Paisii Hilendarski" University of Plovdiv.



Fig. 1. Ripe fruits of *Solanum nigrum* L. (own photo)

The physical descriptors of the fresh berries – diameter and absolute weight, were determined ($n = 1000$ pcs) using a precision gauge (± 0.01 mm) and

an electronic precision balance (± 0.0001 g), respectively.

Fruit separation into structural elements (seeds and peels) was performed manually on frozen fruit (-18°C); the resulting samples were air-dried and stored until analysis. The seedcakes remaining after the extraction of seed oil, were also analysed in the study.

The moisture content was determined gravimetrically, by drying to constant weight at 105°C [25], and all results from the chemical analyses were presented on a dry weight (DW) basis.

The lipid fraction (the glyceride oil) was obtained by Soxhlet extraction of ground samples with *n*-hexane for 8 h [26]. All solvents and reagents used in the study were of analytical (p.a.) or higher grade, and were used without further purification.

Fatty acid composition of the lipids was determined by gas chromatography (GC) [27]; the respective fatty acid methyl esters (FAMES) were obtained by pre-esterification with sulfuric acid in methanol [28]. FAMES' separation was carried out on an HP 5890 instrument; capillary Supelco column, $75\text{ m} \times 0.18\text{ mm} \times 25\text{ }\mu\text{m}$, and a flame ionization detector, FID. The temperature regimen was as follows: column temperature from 140°C (held 5 min) to 240°C (held 3 min) at $4^{\circ}\text{C}/\text{min}$; injector and detector temperatures at 250°C . A standard mixture of FAMES (37 component FAME mix; Supelco, USA) subjected to GC under identical experimental conditions was used for the identification of fatty acids.

Tocopherols in the extracted oil were determined by HPLC, using a Merck-Hitachi chromatograph (Merck, Darmstadt, Germany); the column was Nucleosil Si 50-5, $250\text{ mm} \times 4\text{ mm}$; the detector – fluorescence Merck-Hitachi F 1000. The injected sample ($20\text{ }\mu\text{l}$) represented 2% crude oil solution in *n*-hexane. The mobile phase in the elution was *n*-hexane:dioxane solution, 96:4 (v/v), at a flow rate of 1 ml/min; excitation was at 295 nm, and emission at 330 nm. Tocopherol identification and quantification were achieved by comparison of retention times and peak areas, respectively, with those of a standard tocopherol solution (DL- α -, DL- β -, DL- γ - and DL- δ -tocopherol, 98% purity, purchased from Merck, Darmstadt, Germany) containing between 1 and 5 $\mu\text{g}/\text{mL}$ [29].

Unsaponifiables were determined according to the standardized method [30], after saponification of the lipid fraction and extraction with *n*-hexane.

Total sterols were separated from the unsaponifiable matter by TLC. Briefly, the unsaponifiable matter was diluted in 3 mL chloroform and 1 mL of the solution was applied to

a 20×20 cm silica gel 60 G plate. The mobile phase was hexane : diethyl ether (1:1, v/v). After that, the plate was sprayed with methanol and the line of the isolated sterols was scrapped, transferred into a column and eluted with chloroform. The solution was evaporated on a rotary evaporator and the remained sterols were determined spectrophotometrically, at a wavelength of 597 nm [31], referring to an analytical calibration curve (β -sitosterol standard solution; 0-3000 $\mu\text{g/ml}$; $R^2 = 0.9985$). Sterol composition was identified by GC, on an HP 5890 unit equipped with 25 m \times 0.25 mm DB - 5 capillary column and a flame ionization detector. The temperature gradient was from 90°C (held 3 min) to 290°C at a rate of 15°C/min and then up to 310°C at a rate of 4°C/min (held 10 min); the detector and injector temperatures were set at 320°C and 300°C, respectively; the carrier gas was hydrogen. A standard mixture of cholesterol (purity 95%, Acros Organics, New Jersey, USA), stigmasterol (purity 95%, Sigma-Aldrich, St. Louis, MO, USA) and β -sitosterol (with *ca.* 10% campesterol and *ca.* 75% β -sitosterol, Acros Organics, New Jersey, USA) was used in the comparison of the registered retention times [32]. The limit of detection in all GC and HPLC analyses of the lipid fraction was 0.05%.

Total phospholipids were determined spectrophotometrically at 700 nm after mineralization of the glyceride oil with sulfuric and perchloric acid (1:1, v/v) and reaction of the remaining phosphorus with sulfate–molybdate reagent.

The total content of soluble carbohydrates was determined by the phenol-sulfuric acid method [33], in which 100 μl of aqueous fruit extract were hydrolyzed with 1 ml of 5% phenol and 5 ml of concentrated sulfuric acid, in a water bath at 30°C for 20 min. The absorbance was read at 490 nm against a blank, and the carbohydrate content was obtained from the calibration curve built for glucose. The individual sugar contents were determined by HPLC-RID analysis of water extracts, using an Elite LaChrome Hitachi instrument with a Chromaster 5450 refractive index detector (RID) coupled with Shodex® Sugar SP0810 with Pb^{2+} (300 mm \times 8.0 mm) and Shodex SP - G (5 μm , 6 mm \times 50 mm) columns operated at 85°C; the elution was with distilled water at a flow rate of 1.0 ml/min [34]. The identification and quantification of sugars was based on their retention times and the respective peak areas, as previously described [34].

Cellulose content was determined following the procedure described by Brendel *et al.* [35], in which the acidic hydrolysis of cellulose and hemicellulose

was carried out by boiling 1 g of fruit samples with 16.5 ml of 80% CH_3COOH and 1.5 ml of concentrated HNO_3 for 1.5 h. The suspension was filtered, and the solid residue was dried at 105°C for 24 h and weighed.

Mineral elements' contents in the fruit samples were determined after mineralization at 450°C, after which the solid residue was dissolved in concentrated HCl, evaporated to dryness, and redissolved in 0.1 mol/l HNO_3 . Atomic absorption spectrophotometer Perkin Elmer/HGA 500 (Norwalk, USA) was used for the analysis of mineral elements, at the following wavelengths: Na, 589.6 nm; K, 766.5 nm; Mg, 285.2 nm; Ca, 317.0 nm; Zn, 213.9 nm; Cu, 324.7 nm; Fe, 238.3 nm; Mn, 257.6 nm; Pb, 283.3 nm; Cd, 228.8 nm; Cr, 357.9 nm. The identification of metal ions referred to a standard solution of metal salts. The respective metal contents were calculated from calibration curves for standard 1 $\mu\text{g/ml}$ solutions. The measurements were carried out in triplicate, unless stated otherwise. The results were expressed as the mean value \pm SD.

RESULTS AND DISCUSSION

The fresh berries of *S. nigrum* are matted dark blue in color, with an average diameter (measured at the widest lateral section) of 8.42 ± 0.62 mm (min 6.93 mm; max 9.62 mm). The absolute weight of the fruits was 393.75 ± 38.00 g/1000 pcs. Those basic physical characteristics of the fruit from Bulgaria did not differ from the range typical for the species [2].

As observed in previous studies for other berries [24], the seeds and, to a lesser extent, the peels are the structural elements that concentrate fruit lipids. Besides, those fruit parts, regarded as by-products in juice/pulp production, have been shown to contain sufficient amounts of valuable phytonutrients [36, 37]. Based on these grounds, and in compliance with study objectives, the air-dried seeds and peels of black nightshade fruit (with moisture content $3.25 \pm 0.03\%$) were further characterized in this study.

The total lipid fraction (glyceride oil) content in the seeds was $9.81 \pm 0.09\%$, while in the isolated peels alone its presence was practically negligible, below 1%.

The results about the content of the extracted lipid fraction were considerably below the data provided by previous studies for black nightshade seed oil; for instance, 34.5% [38], 36.5% [5], 38% [39]. This could be explained by variations in the analyzed fruit parts and the applied extraction procedures between the studies. Nevertheless, the oil content in the studied by-product was comparable with that found in maize bran (below 10%), or in some fruit by-products, such as grape seeds, date

palm seeds, guava seeds, mango seeds, and others [40].

Taking into account the results about the lipid content in the two separate waste fractions, it was considered rational to analyze and discuss further only the composition of the lipid fraction extracted from black nightshade seeds.

The fatty acid (FA) composition of the lipid fraction obtained from *S. nigrum* seeds is presented in Table 1. The data showed that three fatty acids dominated in the oil composition, linoleic (48.0%), oleic (27.8%) and palmitic (19.6%) acids. The ratio between saturated and unsaturated FAs was 1:3.27, while that between monounsaturated and polyunsaturated FAs was 1:1.72. Our results were fully consistent with previous data characterizing the seed oil of black nightshade as a rich source of polyunsaturated FAs, and, in particular, of linoleic acid. For example, the share of polyunsaturated FAs varied from 61.0% [22] to 68.4% [39] and 68.9% [38], and that of linoleic acid – from 47.9% [22] to 65.5% [5] and 67.6-67.8% [38, 39]. The numerical differences observed could readily be explained by the influence of ecological factors, fruit maturity and oil extraction methods [22, 38, 39].

Table 1. Fatty acid composition of the lipid fraction of *S. nigrum* seeds, %.

Fatty acids		Content, %
Lauric acid	C _{12:0}	0.2 ± 0.0 ^a
Palmitic acid	C _{16:0}	19.6 ± 0.15
Palmitoleic acid	C _{16:1}	0.2 ± 0.0
Margaric acid	C _{17:0}	0.1 ± 0.0
Heptadecenoic acid	C _{17:1}	0.2 ± 0.0
Stearic acid	C _{18:0}	3.3 ± 0.03
Oleic acid	C _{18:1}	27.8 ± 0.25
Linoleic acid	C _{18:2}	48.0 ± 0.40
Linolenic acid	C _{18:3}	0.2 ± 0.0
Eicosadienoic acid	C _{20:2}	0.2 ± 0.0
Behenic acid	C _{22:0}	0.2 ± 0.1
Saturated fatty acids, %		23.4
Unsaturated fatty acids, %:		76.6
Monounsaturated fatty acids, %		28.2
Polyunsaturated fatty acids, %		48.4

^a All data are presented as mean value ± standard deviation (n=3)

Table 2 presents the content of biologically active substances – unsaponifiable matter, phospholipids, sterols and tocopherols, in the extracted seed oil of *S. nigrum* fruits. The total quantity of the biologically active sterols in the unsaponifiable fraction (0.70%) was higher than that found in many common seed oils, for example, sunflower, soybean, cottonseed, saffron, and others (0.24-0.64%) [40,

41]. The phospholipid content in *S. nigrum* seed oil was also sufficiently high (6.61%), approximating that in many plant oils used in the food industry [40].

Table 2. Biologically active substances in the lipid fraction of *S. nigrum* seeds.

Compound	Content
Unsaponifiables, %	12.01 ± 0.11 ^a
Sterols, %	0.70 ± 0.0
Phospholipids, %	6.61 ± 0.06
Tocopherols, mg/kg	121.00 ± 1.11

^a All data are presented as mean value ± standard deviation (n=3)

The sterol composition of the lipid fraction from *S. nigrum* seeds is presented in Table 3. Six individual sterols were identified, among which β -sitosterol was clearly predominating (70.8%), followed by stigmasterol, cholesterol and campesterol in nearly identical shares (8.40-9.91%).

Table 3. Sterol composition of the lipid fraction of *S. nigrum* seeds.

Compound	Content, %
Cholesterol	9.50 ± 0.08 ^a
Brassicasterol	0.70 ± 0.0
Campesterol	8.40 ± 0.08
Stigmasterol	9.91 ± 0.09
Δ^7 -Campesterol	0.70 ± 0.0
β -Sitosterol	70.80 ± 0.70

^a All data are presented as mean value ± standard deviation (n=3)

With regard to oil's tocopherols, only γ -tocopherol was identified (100%; 121 mg/kg). Seed oils rich in γ -tocopherol are soybean (60-85 mg%) and corn (50-62 mg%) oils, which are the main dietary sources in the American diet, while the European diet mainly utilizes olive and sunflower oils, rich in α -tocopherol [40, 41].

The seedcakes remaining after oil extraction, as well as the peels of *S. nigrum* fruit, were further analyzed to determine other phytochemical indices. The results for the carbohydrate content in the two fruit elements are presented in Table 4.

Table 4. Carbohydrates in the by-products of *S. nigrum* fruit.

Index, %	Seedcakes	Peels
Total soluble carbohydrates	5.39 ± 0.50 ^a	8.21 ± 0.80
Sucrose	0.19 ± 0.00	0.18 ± 0.00
Glucose	2.78 ± 0.20	4.21 ± 0.40
Fructose	2.42 ± 0.20	3.82 ± 0.30
Sorbitol	nd	nd
Cellulose	14.90 ± 0.13	15.70 ± 0.17

^a All data are presented as mean value ± standard deviation (n=3); ^b Not detected.

Reasonably, the peels contained considerably higher (nearly 2-times) concentrations of total soluble carbohydrates, as well as glucose and fructose, than the seedcakes, which was observed for other berries, too [37]. The results corresponded well with the carbohydrate content of dried *S. nigrum* seeds, 5.45% [5], but, expectedly, they were significantly lower than the data achieved for dried whole berries, containing the fruit pulp sugars; 34.36% [39], 40.4% [23], 55.85% [20].

The cellulose content in the seedcakes was 14.90%, and slightly higher in the isolated peels fraction, 15.70%. Although it was not possible to make any direct comparison, as there were no previous data for *S. nigrum* fruit cellulose content, our results supported the findings by other studies suggesting that the fruit and the seeds are a good source of dietary fiber [5, 20, 23].

The data for the structure of the identified mineral elements in the studied *S. nigrum* fruit fractions, the seedcakes and the peels, are presented in Table 5.

The elemental composition revealed significant amounts of K in both by-products, with about twice as higher concentration in the isolated peels.

Table 5. Minerals in the by-products from *S. nigrum* fruit.

Minerals, mg/kg	Seedcakes	Peels
Macro minerals		
Potassium (K)	15109.34 ± 150.00 ^a	31373.32 ± 300.00
Calcium (Ca)	813.12 ± 8.00	2365.82 ± 21.11
Magnesium (Mg)	1988.07 ± 18.11	1578.53 ± 14.00
Sodium (Na)	103.18 ± 1.10	3348.46 ± 30.00
Micro minerals		
Copper (Cu)	11.93 ± 0.10	11.84 ± 0.10
Iron (Fe)	53.68 ± 0.50	88.79 ± 0.85
Zinc (Zn)	37.77 ± 0.36	27.62 ± 0.26
Manganese (Mn)	23.86 ± 0.22	19.73 ± 0.18
Lead (Pb)	< 0.01 ^b	< 0.01
Cadmium (Cd)	< 0.01	< 0,01
Chromium (Cr)	< 0.01	< 0.01

^a All data are presented as mean value ± standard deviation (n=3); ^b Not detected.

The complementary macro minerals in the seedcakes were Mg and Ca, while the content of Na was very low. The distribution of the same macro minerals was completely different in the peels; Na was the second-most abundant mineral, followed by Ca, both considerably exceeding the respective concentrations found in the seedcakes. The contents of the identified micro minerals in the two fruit structural elements were comparable, with the

exception of Fe, found at about 1.5-time higher level in the peels. The heavy metals, Pb, Cd and Cr, were practically not detected in the samples. The differences in the mineral composition of the seedcakes and the peels could be explained with the different nature of the metabolic biochemical processes during fruit maturation [21, 22]. Our results differed to some extent from previous reports, which identified Mg as the predominant mineral in the dried seeds of black nightshade fruits of different origin, followed by K, but agreed very well with the established values; Mg, 201.3 mg/100 g [20], 182.3 mg/100 g [5], 426 mg/100 g [39]. The high mineral concentrations in the analyzed fruit structures, as well as the presence of important dietary micro elements, such as Cu, Zn and Mn, support the nutritive value of the regarded by-products and the viability of seeking alternatives for their incorporation in different food and feed products.

CONCLUSIONS

The study provides new data from the determination of basic macro and micronutrients in two structural elements of black nightshade (*S. nigrum*) fruit, the seeds and the peels – glyceride oil and the profile of saturated and unsaturated fatty acids, sterols and tocopherols in the oil; carbohydrates and minerals. The results from the study contribute to a more complex appreciation of the nutritional potential of black nightshade fruits available in Bulgaria and the prospects for their processing into value-added products.

Acknowledgement: The study was supported by the Science Fund of the University of Food Technologies, Plovdiv; Project 05/20-N.

REFERENCES

1. F. Albouchi, M. Attia, M. Hanana, L. Hamrouni, *Am. J. Phytomed. Clin. Ther.*, **6**(1), 5 (2018).
2. X. Chen, X. Dai, Y. Liu, Y. Yang, L. Yuan, X. He, G. Gong, *Front. Pharmacol.*, **13**, 918071 (2022).
3. R. Jain, A. Sharma, S. Gupta, I. Sarethy, R. Gabrani, *Altern. Med. Rev.*, **16**(1), 78 (2011).
4. I. Hameed, M. Cotos, M. Hadi, *Res. J. Pharm. Technol.*, **10**(11), 4063 (2017).
5. H. Sarma, A. Sarma, *Int. Proc. Chem. Biol. Environ. Eng.*, **21**, 105 (2011).
6. V. Petkov, Contemporary Phytotherapy, Medicina i Fizkultura, Sofia, Bulgaria, 1982 (in Bulgarian).
7. I. Isaev, I. Landzhev, G. Neshev, Herbs in Bulgaria and Their Use, Zemizdat, Sofia, Bulgaria, 1977 (in Bulgarian).
8. M. Eskandari, M. Assadi, S. Shirzadian, I. Mehregan, *J. Med. Plants*, **71**(18), 75 (2019).
9. A. Azab, *Eur. Chem. Bull.*, **9**(8), 199 (2020).
10. S. Miraj, *Der Pharma Chem.*, **8**(17), 62 (2016).

11. E. H. O. Moglad, M. S. Alhassan, E. A. Abdalkareem, A. N. Abdalla, M. Kuse, *Asian J. Pharm.*, **13**(3), 246 (2019).
12. A. Alam, A. Sahar, A. Sameen, M. N. Faisal, *Food Sci. Technol*, **42**, e61822 (2022).
13. S. S. Zaghlool, A. A. Abo-Seif, M. A. Rabeh, U. R. Abdelmohsen, B. A. S. Messiha, *Antioxidants*, **8**, 512 (2019).
14. J.S. Kaunda, Y.-J. Zhang, *Nat. Prod. Bioprospect.*, **9**(2), 77 (2019).
15. A. Mohy-ud-din, Z. Khan, M. Ahmad, M. A. Kashmiri, *Pak. J. Bot.*, **42**(1), 653 (2010).
16. K. Jayakumar, K. Murugan, *J. Anal. Pharm. Res.*, **3**(6), 00075 (2016).
17. B. Yuan, D. Byrnes, D. Giurleo, T. Villani, J. E. Simon, Q. Wu, *J. Food Drug Anal.*, **26**(2), 751 (2018).
18. J. O. Odukoya, A. A. Oshodi, *Eur. J. Pure Appl. Chem.*, **5**(1), 18 (2018).
19. D. Sivakumar, A. D. T. Phan, R. M. Slabbert, Y. Sultanbawa, F. Remize, *Front. Nutr.*, **7**, 576532 (2020).
20. I. Akubugwo, N. Obasi, B. Ginika, *Pak. J. Nutr.*, **6**(4), 323 (2007).
21. A. Siddiqui, M. Hussain, M. Hameed, R. Ahmad, *Big Data Agric.*, **2**(1), 6 (2020).
22. J. Staveckienė, J. Kulaitienė, D. Levickienė, N. Vaitkevičienė, *Plants*, **12**, 268 (2023).
23. L. Jithendran, C. A. Kalpana, *Int. J. Food Nutr. Sci.*, **10**, 16 (2021).
24. M. F. Ramadan, *Food Res. Int.*, **44**, 1830 (2011).
25. The State Pharmacopoeia of the USSR, 11th edn., I. V. Tumanova (ed.), vol. 2, Medicina, Moscow, 1990 (in Russian).
26. ISO 659:2014 Oilseeds - Determination of oil content (Reference method), ISO, Geneva, Switzerland, 2014.
27. ISO 12966-1:2014 Animal and vegetable fats and oils - Gas chromatography of fatty acid methyl esters - Part 1: Guidelines on modern gas chromatography of fatty acid methyl esters, ISO, Geneva, Switzerland, 2014.
28. ISO 12966-2:2017 Animal and vegetable fats and oils - Gas chromatography of fatty acid methyl esters - Part 2: Preparation of methyl esters of fatty acids, ISO, Geneva, Switzerland, 2017.
29. ISO 9936:2016 Animal and vegetable fats and oils. Determination of tocopherol and tocotrienol contents by high-performance liquid chromatography, ISO, Geneva, Switzerland, 2014.
30. ISO 18609:2000 Animal and vegetable fats and oils - Determination of unsaponifiable matter - Method using hexane extraction, ISO, Geneva, Switzerland, 2000.
31. S. Ivanov, P. Bitcheva, B. Konova, *Rev. Franc. Corps Gras.*, **19**, 177 (1972).
32. ISO 12228-1:2014 Determination of individual and total sterols contents - Gas chromatographic method - Part 1: Animal and vegetable fats and oils, ISO, Geneva, Switzerland, 2014.
33. M. Dubois, K. Gilles, J. Hamilton, P. Rebers, F. Smith, *Anal. Chem.*, **28**(3), 350 (1956).
34. N. Petkova, R. Vrancheva, P. Denev, I. Ivanov, A. Pavlov, *Acta Sci. Nat.*, **1**, 99 (2014).
35. O. Brendel, P. P. M. Iannetta, D. Stewart, *Phytochem. Anal.*, **11**(1), 7 (2000).
36. V. Popova, Z. Petkova, T. Ivanova, M. Stoyanova, N. Panayotov, N. Mazova, A. Stoyanova, *Turkish J. Agric. For.*, **44**(6), 642 (2020).
37. V. Popova, Z. Petkova, G. Uzunova, T. Ivanova, N. Petkova, A. Stoyanova, *AIP Conf. Proceed.*, **2889**(1), 080008 (2023).
38. J. R. Dhellot, E. Matouba, M. G. Maloumbi, J. M. Nzikou, M. G. Dzondo, M. Linder, M. Parmentier, S. Desobry, *Afr. J. Biotechnol.*, **5**(10), 987 (2006).
39. J. M. Nzikou, M. Mvoula-Tsieri, L. Matos, E. Matouba, A. C. Ngakegni-Limbili, M. Linder, S. Desobry, *J. Appl. Sci.*, **7**, 1107 (2007).
40. A. Popov, P. Ilinov, *Chemistry of Lipids*, Nauka i Izkustvo, Sofia, Bulgaria, 1986 (in Bulgarian).
41. CXS 210-1999 Standard for Named Vegetable Oils, rev. 2019, FAO/WHO Codex Alimentarius Commission, Joint FAO/WHO Food Standards Programme, Rome, Italy, 1999.

Lipid composition and investigation of the physicochemical characteristics of high-oleic sunflower oil at different temperatures

V. D. Gandova¹, O. T. Teneva^{2*}, Z. Y. Petkova², I. Z. Iliev^{2,3}, A. S. Stoyanova³

¹ University of Food Technologies, Department of Analytical and Physical Chemistry, 26 Maritza Blvd., 4002 Plovdiv, Bulgaria

² University of Plovdiv "Paisii Hilendarski", Department of Chemical Technology, 24 Tzar Asen Str., 4000 Plovdiv, Bulgaria

³ University of Food Technologies, Technological Faculty, Department of Technology of Tobacco, Sugar, Vegetable and Essential oils, 26 Maritza Blvd., 4002, Plovdiv, Bulgaria

Received: November 3, 2024; Revised: April 11, 2024

High-oleic sunflower oil is characterized by high stability, and hence high quality. The aim of the present work is to determine the chemical composition of the lipid fraction (fatty acids, unsaponifiable matter, tocopherols and sterols) and some physicochemical parameters (density, surface tension, dynamic and kinematic viscosity) of high-oleic sunflower oil. The main fatty acids in the investigated oil were: oleic (77.9%), linoleic (11.5%), palmitic (5.0%), and stearic (3.3%). β -Sitosterol (79.7%) and α -tocopherol (100%) were the major components in the sterol and tocopherol fractions of the oil. The variation of the physicochemical parameters was followed at seven temperatures (20, 30, 40, 50, 60, 70, and 80 °C). With an increase in temperature, all parameters decreased and a good linear dependence was observed – density (from 0.868 g/ml to 0.847 g/ml), surface tension (from 29.775 mN/m to 12.461 mN/m), dynamic viscosity (from 44.401 mPa/s to 40.067 mPa/s), and kinematic viscosity (from 51.148 mm²/s to 47.268 mm²/s). The present results are a basis for future research on the incorporation of high-oleic sunflower oil into food products with improved functional characteristics.

Keywords: high oleic sunflower oil, fatty acids, density, surface tension

INTRODUCTION

Sunflower oil is obtained by extraction or pressing of the sunflower seeds (*Helianthus annuus* L., family Asteraceae). It is an easily mobile liquid with a light yellow color and a specific taste and odor. The main fatty acids were found to be oleic (20-40%) and linoleic acid (46-70%). The oil is mainly used in the food industry and infrequently in cosmetics, medicine and technology [1].

In recent years, through selection, new sunflower hybrids have been developed and the obtained oil is with a high content of oleic acid (60-80%) and low in linoleic acid (18-40%) [1-3]. This oil can be used in various food products [4-6] as well as for the production of biolubricants and biodiesel [4].

In the case of vegetable oils, the determination of their physicochemical parameters, such as density, viscosity and surface tension, measured at different temperatures, are important both for their production and application [7, 8].

Vegetable oils are usually used for frying and cooking of different food products. Elhefian *et al.* [9] established the physicochemical properties such as density, viscosity and acid value of four edible

vegetable oils, determined at room temperature before and after frying of potatoes, repeated five times.

The chemical, thermal and viscous characteristics of high-oleic sunflower and olive oils were determined by García-Zapateiro *et al.* [2] using different acid-catalyzed synthesis and reaction times. Maximum viscosity values were obtained for oils prepared using the sulfuric acid-catalyzed method. The temperature dependence of viscosity for all studied high-oleic oils was significantly stronger than for the original oils.

Vegetable oils are promising alternatives to mineral-based lubricants. High-oleic sunflower oil was used to develop new environmentally friendly lubricant formulations. It was blended with polymeric additives, such as ethylene vinyl acetate and styrene-butadiene-styrene copolymers at different concentrations (0.5-5% w/w). Dynamic viscosity and density measurements were performed. The viscosity of high-oleic sunflower oil increased with an increase in polymer concentration [10].

Some vegetable oils such as soybean, olive,

* To whom all correspondence should be sent:

E-mail: olga@uni-plovdiv.bg

castor, sunflower and coconut oil were investigated and it was established that the compounds present in them stimulated biosurfactant production. The results showed a decrease in surface tension of the culture medium without oil from 64.54 mN/m to 29.57 mN/m, with a critical micelle dilution CMD(-1) and CMD(-2) from 41.77 mN/m and 68.92 mN/m, respectively. Sunflower oil (with 60% content of linoleic acid) gave the best results (29.75 mN/m) with a CMD(-1) and CMD(-2) of 36.69 mN/m and 51.41 mN/m, respectively. The addition of linoleic acid decreased the surface tension from 53.70 mN/m to 28.39 mN/m, with a CMD(-1) of 29.72 mN/m and CMD(-2) of 37.97 mN/m, which suggested that the linoleic acid is responsible for the increase in biosurfactant production [11].

Density, surface tension and viscosity of five vegetable oils were also experimentally measured. The measurements were performed from 23 ± 1 °C to their respective smoke point at intervals of 20 °C. The density and surface tension linearly decreased with the increasing of temperature, whereas the viscosity decreased exponentially. It was reported that the type of oil influenced the density and viscosity, but did not affect the surface tension [8].

The aim of this study is to determine the lipid composition of sunflower oil with a high content of oleic acid and to monitor the changes in some physicochemical parameters at different temperatures.

MATERIALS AND METHODS

Sunflower oil was purchased from the commercial network of the city Plovdiv, in 2023.

Lipid composition of the oil was determined by the following analysis:

Composition of fatty acids: Gas chromatography (GC) was used for determination of the fatty acid composition of the oil. Briefly, the vegetable oil was pre-esterified with methanol in the presence of sulfuric acid in order to obtain fatty acid methyl esters (FAMES) [12]. Determination of FAMES was carried out on Agilent 8860 gas chromatograph (Santa Clara, CA 95051, US) equipped with a capillary column Supelco (SPTM-2380, Fused Silica (Bellefonte, PA, USA), 30 m × 0.25 mm × 0.25 μm (film thickness)) and a flame ionization detector (FID). For the identification of the FAMES a standard mixture Supelco, USA (FAME mix 37 components, Supelco, Bellefonte, PA USA) was used.

Content of sterols: unsaponifiables were determined according to ISO standard [13]. The sterols were isolated from the unsaponifiable matter by thin-layer chromatography (TLC) [14] and their

total content was determined spectrophotometrically at a wavelength of 597 nm. Individual sterol composition was determined on a HP 5890 gas chromatograph (Santa Clara, CA 95051, US) equipped with DB-5 capillary column (25 m × 0.25 mm) (Santa Clara, CA 95051, US) and FID. Identification was performed by comparing the retention times with those of a standard sterols mixture (Acros Organics, New Jersey, USA) [15].

Content of tocopherols: individual tocopherols were determined by high performance liquid chromatography (HPLC) on a Merck-Hitachi (Merck, Darmstadt, Germany) instrument. The column was Nucleosil Si 50-5 (250 mm × 4 mm). Fluorescence detection was used (excitement at 290 nm and emission at 330 nm). The mobile phase used was *n*-hexane:dioxane, 96:4 (v/v) and the flow rate was set at 1 ml/min [16].

The physicochemical parameters of the oil were determined at seven temperatures (20, 30, 40, 50, 60, 70, and 80 °C). Their selection was according to a diversity of technological regimes in which it's included in various food products.

The investigated parameters were as follows:

Surface tension [17] by equation (1):

$$\gamma = \frac{rg}{2} (\Delta H\rho_0 - h\rho) , \quad (1)$$

where r – radius of the capillary, m; $g = 9.8$ m/s² – the acceleration of gravity; ΔH – the maximum difference in the two gauges of the gauge, m; h – liquid level, m; ρ_0, ρ – the density of the water and the oil, g/ml.

Dynamic viscosity, by equation (2):

$$\eta = \frac{2(\rho_l - \rho_b)gr^2}{9v} \text{ (vertical fall down)}, \quad (2)$$

where g – acceleration of gravity, m/s²; ρ_l – density of the liquid, kg/m³; ρ_b – density of the ball, g/ml; r – radius of the ball, mm; v – speed with uniform movement determined by the road per unit time.

Kinematic viscosity, by equation (3):

$$\nu = \frac{\eta}{\rho} , \quad (3)$$

where η – dynamic viscosity, Pa.s; ρ – density, g/ml.

Density, by equation (4):

$$\rho = \frac{m_1 - m}{V} , \quad (4)$$

where ρ – density of the oil, g/ml; m – mass of the pycnometer, g; m_1 – mass of the pycnometer with liquid, g; V – volume, ml.

All measurements were performed in triplicate and the results were presented as the mean value of

the individual measurements with the corresponding standard deviation (SD), using Microsoft Excel.

RESULTS AND DISCUSSION

Data about fatty acid composition of the studied oil is presented in Table 1.

Table 1. Fatty acid composition of high-oleic sunflower oil.

Fatty acids		Content, %
Capric	C _{10:0}	0.2 ± 0.0
Lauric	C _{12:0}	0.1 ± 0.0
Myristic	C _{14:0}	0.1 ± 0.0
Palmitic	C _{16:0}	5.0 ± 0.01
Palmitoleic	C _{16:1}	0.2 ± 0.0
Stearic	C _{18:0}	3.3 ± 0.01
Oleic	C _{18:1 (n-9)}	77.9 ± 0.60
Linoleic	C _{18:2 (n-6)}	11.5 ± 0.09
α-Linolenic	C _{18:3 (n-3)}	0.1 ± 0.0
Arachidic	C _{20:0}	0.3 ± 0.0
Eicosenoic	C _{20:1}	0.2 ± 0.0
Behenic	C _{22:0}	0.8 ± 0.0
Lignoceric	C _{24:0}	0.3 ± 0.0
Saturated fatty acids		10.1
Unsaturated fatty acids		89.9
Monounsaturated fatty acids		78.3
Polyunsaturated fatty acids		11.6

The main fatty acids among all thirteen identified (100% of total composition) were found to be: oleic (77.9%), linoleic (11.5%), palmitic (5.0%), and stearic acid (3.3%). The results about the lipid composition were similar to the data published in the literature. The comparative analysis showed that there is variation in the amounts of some fatty acids – the content of oleic acid is lower than the data of García-Zapateiro *et al.* (81.50%) [2] and Roman *et al.* (82.33%) [3], for linoleic acid it is higher than reported by García-Zapateiro *et al.* (6.85%) [2] and Roman *et al.* (8.79%) [3], and for palmitic acid it is higher than the results of Roman *et al.* (3.59%) [3]. The differences can be explained by the different origin of the plants, which is a common tendency found for comparisons between other oils [1].

The contents of saturated, unsaturated, mono- and polyunsaturated fatty acids are given in Table 1. Sunflower oil was abundant in unsaturated fatty acids which are almost 90% of the fatty acid profile of the examined vegetable oil. Among them, monounsaturated fatty acids (78.3% of the fatty acid composition) represent about 87.1% of the content of unsaturated acids, while the amount of polyunsaturated ones was substantially low. The

results are in agreement with those reported by Roman *et al.* [3] where the content of monounsaturated fatty acids of high oleic sunflower oil is 82.41%, while the levels of polyunsaturated ones are 8.86%.

Data about the content of the main biologically active components in the investigated oil is given in Table 2.

Table 2. Content of unsaponifiable matter, sterols, and tocopherols in high-oleic sunflower oil.

Biologically active components	Content
Unsaponifiable matter, % of the oil	1.7 ± 0.01
Tocopherols, mg/kg in the oil	219 ± 2.00
α-Tocopherol, % from total tocopherols	100 ± 0.0
Sterols, % of the oil	0.6 ± 0.0
Sterol composition, % of the sterol fraction	
Cholesterol	0.7 ± 0.0
Brassicasterol	3.4 ± 0.03
Campesterol	0.9 ± 0.0
Stigmasterol	11.1 ± 0.10
Δ ⁷ -Campesterol	4.2 ± 0.04
β-Sitosterol	79.7 ± 0.70

Unsaponifiable matter of the oil mainly consists of different compounds as terpenic (sterols, tocopherols, tocotrienols, carotenoids, *etc.*) and aliphatic (fatty alcohols, saturated and unsaturated hydrocarbons) [18]. The content of unsaponifiable matter in the oil is close to that published in the literature for sunflower (1.5%), but it is lower than that for rapeseed (2.0%), maize (2.8%), and grapeseed oil (2.0%) [19].

The major part of the unsaponifiable matter in the oil consists of sterols [8]. β-Sitosterol was the main component in the sterol composition of the studied oil (79.7%) followed by stigmasterol (11.1%), Δ⁷-campesterol (4.2%), and brassicasterol (3.4%), while the rest of the identified sterols was below 1%.

In the tocopherol fraction α-tocopherol predominates, which is in agreement with data for sunflower oil [1–3].

The physicochemical parameters of high-oleic sunflower oil – density, surface tension, dynamic and kinematic viscosity were experimentally determined. All measurements were performed in the temperature range between 20 and 80°C.

Surface tension of the high-oleic sunflower oil was measured by the maximum bubble pressure method. The values of the surface tension were between 29.775 ± 0.103 mN/m and 12.461 ± 0.126 mN/m at different temperatures. In earlier studies

there were no experimentally determined results for the surface tension of high-oleic sunflower oil. According to the authors of [11] the addition of linoleic acid to the oil lowers the surface tension from 53.70 mN/m to 28.39 mN/m at room temperature (25°C). Good linear dependence was observed between surface tension and temperature according to the authors of [20]. Temperature dependence of surface tension was also observed in the investigated range of this work. With an increase in the temperature, the surface tension decreased. The results are presented in Fig. 1. After regression analysis, the linear equation was obtained ($y = 33.778 - 0.283 \cdot x$). High correlation coefficient $R^2 = 0.964$ indicates a good dependence between the two parameters.

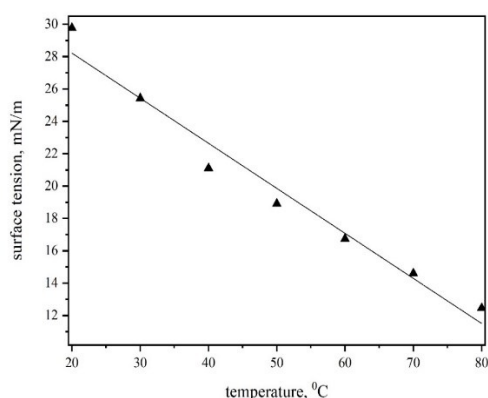


Fig. 1. Dependence between surface tension and temperature.

Experimental density was determined. Similarly to the data in the literature, a good correlation between temperature and density was observed over the same temperature range. The results are presented in Table 3. The data show that with an increase in temperature the density decreases, established by other authors [20, 21] as well.

Dynamic viscosity was determined after performing the experiment in a temperature range between 20 to 80 °C. The results are presented in Table 3. The viscosity decreases with the increase in temperature. The observed values are between 44.401 mPa.s at 20 °C and 40.067 mPa.s at 80 °C. According to other researches, the viscosity of pure sunflower oil is 39.55 mPa.s [9] and this value is comparable to the results obtained in the present study.

According to equation (3) there is a correlation between dynamic and kinematic viscosity. The kinematic viscosity is obtained by calculating while the dynamic viscosity is divided by the density (Table 3). The kinematic viscosity has values between 51.148 mm²/s and 47.268 mm²/s. The

values obtained in this study do not differ from those published by Jamil *et al.* [22] who investigated pure sunflower oil and found the dynamic viscosity to be 45.38 mPa.s and the kinematic viscosity – 49.56 mm²/s.

Table 3. Density, dynamic and kinematic viscosity of high-oleic sunflower oil.

Temperature, °C	Density, g/ml	Dynamic viscosity, mPa.s	Kinematic viscosity, mm ² /s
20	0.868 ± 0.004	44.401 ± 0.221	51.148 ± 0.156
30	0.864 ± 0.001	43.682 ± 0.162	50.519 ± 0.229
40	0.861 ± 0.007	42.963 ± 0.135	49.883 ± 0.187
50	0.857 ± 0.004	42.241 ± 0.094	49.240 ± 0.135
60	0.854 ± 0.005	41.518 ± 0.108	48.592 ± 0.242
70	0.851 ± 0.001	40.449 ± 0.184	47.527 ± 0.117
80	0.847 ± 0.007	40.067 ± 0.137	47.268 ± 0.148

CONCLUSION

The main fatty acids of the high-oleic sunflower oil were oleic, linoleic, palmitic, and stearic acid. β -Sitosterol and α -tocopherol were the major lipid – soluble biologically active components in the whole lipid fraction. For the first time some physicochemical parameters of investigated oil were calculated at seven different temperatures (20, 30, 40, 50, 60, 70, and 80 °C). The obtained values for the composition of the lipid fraction and physicochemical parameters are important for future research on the incorporation of high-oleic sunflower oil into different food products.

REFERENCES

1. R. O' Brien, W. Farr, Introduction to Fats and Oils Technology, AOCS Press, Illinois, 2000.
2. L. García-Zapateiro, J. Franco, C. Valencia, M. Delgado, C. Gallegos, M. Ruiz-Méndez, *Eur. J. Lipid Sci. Technol.*, **115**(10), 1173 (2013).
3. O. Roman, B. Heyd, B. Broyart, R. Castillo, M.-N. Maillard, *LWT-Food Sci Technol.*, **52**(1), 49 (2013).
4. R. Garcés, E. Martínez-Force, J. Salas, M. Venegas-Calderón, *Lipid Technol.*, **21**(4), 79 (2009).
5. M. Gupta, *Lipid Technol.*, **26**(11-12), 260 (2014).
6. S. González-Rámila, R. Mateos, J. García-Cordero, M. Seguido, L. Bravo-Clemente, B. Sarriá, *Foods*, **11**(15), 2186 (2022).

7. B. Esteban, J.-R. Riba, G. Baquero, A. Rius, R. Puig, *Biomass Bioenergy*, **42**, 164 (2012).
8. S. Sahasrabudhe, V. Rodriguez-Martinez, M. O'Meara, B. Farkas, *Int. J. Food Prop.*, **20**, 1965 (2017).
9. E. Elhefian, N. Alghrabli, A. Alghanoudi, *Int. J. Mod. Sci. Technol.*, **6**(10), 161 (2021).
10. L. Quinchia, M. Delgado, C. Valencia, J. Franco, C. Gallegos, *Environ. Sci. Technol.*, **43** (6), 2060 (2009).
11. C. Ferraz, A. De Araújo, G. Pastore, *Appl. Biochem. Biotechnol.*, **98**, 841 (2002).
12. ISO 12966-2:2017. Animal and vegetable fat and oils. Gas chromatography of fatty acid methyl esters – Part 2: Preparation of methyl esters of fatty acids.
13. ISO 18609:2000. Animal and vegetable fats and oils. Determination of unsaponifiable matter. Method using hexane extraction.
14. S. Ivanov, P. Bitcheva, B. Konova, *Rev. Fr. Corps. Gras.*, **19**, 177 (1972).
15. ISO 12228-1:2014. Animal and vegetable fats and oils. Determination of individual and total sterols contents. Gas chromatographic method.
16. ISO 9936:2016. Animal and vegetable fats and oils. Determination of tocopherol and tocotrienol contents by high-performance liquid chromatography.
17. R. Yankova, V. Gandova, M. Dimov, K. Dobрева, V. Prodanova-Stefanova, A. Stoyanova, *Oxid. Commun.*, **42**(3), 293 (2019).
18. D. Fontanel, *Unsaponifiable Matter in Plant Seed Oils*, Springer, London, UK, 2013.
19. Codex Stan 210. Codex standard for named vegetable oils. Revisions 2001, 2003, 2009. Amendment 2005, 2011.
20. J. Yerima, S. Solomon, A. Dikko, *Int. J. Eng. Sci.*, **4**(6), 49 (2015).
21. E. A. Melo-Espinosa, Y. Sanchez-Borroto, M. Errasti, R. Piloto-Rodriguez, R. Sierens, J. Roger-Riba, A. Christopher-Hansen, *Energy Procedia*, **57**, 886 (2014).
22. M. Jamil, Y. Uemura, K. Kusakabe, O. Ayodele, N. Osman, N. Ab Majid, S. Yusup, *Procedia Eng.*, **148**, 378 (2016).

Chemical composition of seeds from organically grown tobacco plants

L. Stoyanova^{1,2*}, M. Angelova-Romova²

¹Department of Tobacco Chemistry, Tobacco and Tobacco Products Institute, Agricultural Academy, Markovo 4108, Bulgaria

²Department of Chemical Technology, University of Plovdiv "Paisii Hilendarski", 24, Tzar Asen Str., Plovdiv 4000, Bulgaria

Received: November 3, 2024; Revised: April 11, 2024

Bulgaria is a country with agricultural traditions in terms of growing and producing tobacco. Looking for alternative uses of tobacco and trends towards ecological production of major agrarian crops from 2016, the production of tobacco under organic farming conditions has begun in Bulgaria. Oriental tobacco seeds from subgroup Basmi, variety Krumovgrad 58, grown in a certified bio-field in Bulgaria were collected, ground, and analyzed. The chemical composition and lipid biological active components of the organic tobacco seeds from two consecutive years (2020 – 2021) were studied and compared to conventionally grown tobacco seeds from the same variety. The oil content and biologically active compounds in seeds were examined. The lipid content of bio seeds was 41.7 and 38.4%, respectively. The main components in the triacylglycerol fraction were palmitic (11.20 – 14.20%), oleic (14.40 – 17.70%), and linoleic acids (64.40 – 68.20%). The iodine value of the studied tobacco oils was of the same order 134 – 138 g I₂/100 g. Tobacco seed oils are rich in linoleic acid and have beneficial properties for industrial and plant protection purposes. The ratio between unsaturated and saturated fatty acids in tobacco seed oil was 84.0:16.0 and 83.5: 16.5, respectively. The total tocopherol content was between 317 – 325 and 291 – 307 mg/kg in the first and second year, respectively, γ - and α -tocopherol predominating in the tocopherol fraction. The oxidative stability was about 10 – 13 hours. β -Sitosterol predominated in the sterol fraction and phosphatidylinositol was the main isolated phospholipid.

Keywords: organically grown tobacco, tobacco seed oil, lipid composition

INTRODUCTION

Bulgaria is a country with agricultural traditions in terms of growing and producing tobacco. Mainly, oriental varieties of tobacco are grown, with the aim of putting them into tobacco products for smoking. Looking for alternative uses of tobacco and trends towards ecological production of major agrarian crops from 2016, the production of tobacco under organic farming conditions began in Bulgaria. The Institute of Tobacco and Tobacco Products in the village of Markovo developed a „Technology for organic tobacco production“ and certified a biofield at its Experimental Tobacco Station in the town of Gotse Delchev [1]. Organic tobacco is a new industrial plant product that is processed and grown in special certified biofields, without the use of conventional plant protection products [2]. Organic farming does not allow or completely exclude the use of synthetic fertilizers, pesticides, and growth regulators. The soil is maintained by using plant residues, manure, green manure, and biological plant protection is used to control pests [3].

In the tobacco production process, seeds are known as agricultural waste. The seeds of the tobacco plant are very small, but they come in an extremely large quantity per plant. They can be preserved for a long time if they are stored in dry conditions [4]. By processing tobacco seeds, two possibly valuable products can be produced: the oil and the cake. Tobacco cultivars give a good yield of oil, ranging up to 40% of the total seed mass, and the remaining part consists of crude fiber, protein, starch, and inorganic material [5]. Oil is free of nicotine, has a low proportion of saturated fatty acids, and contains health-beneficial compounds such as tocopherols and sterols. The main fatty acids found in the tobacco oil are oleic and linoleic acids. The dominant compounds in the sterol fraction in the oriental tobacco seeds that have been reported before were β -sitosterol, stigmasterol, and campesterol [6]. Tobacco oil from seeds of oriental varieties of tobacco from the region of Bulgaria has been studied, but there are no studies on the lipid composition of seeds grown under organic farming conditions from this region.

* To whom all correspondence should be sent:
E-mail: lilyastoyanova@uni-plovdiv.bg

The aim of the study is to investigate if there are differences in the lipid composition between oil obtained from organically grown tobacco seeds the variety Krumovgrad 58, Bulgaria and oil obtained from conventional growing tobacco seeds of the same variety.

MATERIALS AND METHODS

Tobacco seeds from oriental tobacco, variety Krumovgrad 58 were used – ones grown in a special certified biofield in Goce Delchev (Institute of Tobacco and Tobacco Products) (bio) and conventionally grown tobacco (con) on a field in Kozarsko (Institute of Tobacco and Tobacco Products). All analyses were performed with seeds from two subsequent years of harvest – 2020 and 2021. The results were expressed as mean values of the two years of harvest with standard deviation.

The tobacco oil was obtained from 25 grams of ground seeds extracted with n-hexane (300 mL) using a Soxhlet extractor for 8 h at 70°C. The solvent was removed, using a rotary evaporator, at 60°C. The oil sample was weighed, closed under a nitrogen stream, and stored in a refrigerator until further analysis [7].

To determine the fatty acids of triacylglycerol's, preesterification with methanol in the presence of sulfuric acid was done [8, 9]. The obtained fatty acid methyl esters (FAMES) were identified on an Agilent 8860 gas chromatograph equipped with a capillary DB Fast FAME column, (30 m × 0.25 mm × 0.25 µm (film thickness)) and a flame ionization detector (FID). The injector and detector temperatures were set at 270°C and 300°C; nitrogen was the carrier gas. The column temperature was from 70°C (1 min), at 6°C/min to 180°C, and at 5°C/min to 250°C, and the split ratio was 50:1. A standard Supelco, USA, mixture (FAME mix 37 components, Supelco, USA) was used for the identification of FAMES.

The unsaponifiable fractions were determined according to the ISO 18609 standard [10]. Sterols were isolated from the unsaponifiable matter by thin-layer chromatography (TLC) [11] and their total content was determined spectrophotometrically at a wavelength of 597 nm. The individual sterol composition was determined on HP 5890 gas chromatograph equipped with DB 5 (25 m × 0.25 mm × 0.25 µm (film thickness)) capillary column and FID. Temperature gradient was from 90°C (3 min) up to 290°C at a rate of 15°C/min and then up to 310°C at a rate of 4°C/min (10 min); detector temperature: 320°C; injector temperature: 300°C and carrier gas was hydrogen. Identification was

performed by comparing retention times with those of a standard mixture of sterols (Acros Organics, New Jersey, USA) [12].

Individual tocopherols were determined on a Merck-Hitachi (Merck, Darmstadt, Germany) high-performance liquid chromatograph (HPLC) with fluorescence detection (excitation at 295 nm and emission at 330 nm) and Nucleosil Si 50-5 (250 mm × 4 mm) column. The mobile phase used was n-hexane:dioxane, 96:4 (v/v) and the flow rate was set at 1 mL/min [13].

Phospholipids were isolated from the seeds according to Folch *et al.* [14] using extraction with a mixture of chloroform and methanol (2:1, v/v). Two-dimensional TLC was used to determine the individual phospholipids [15]. Total phospholipid content was determined spectrophotometrically at 700 nm after mineralization of the lipid fraction with a mixture of perchloric and sulfuric acid (1:1, v/v) [16].

Oxidative stability was determined by measuring the induction period using conductometric detection of volatile compounds. Rancimat apparatus Methrom 679 (Methrom, Switzerland) was used at 100°C and air flow rate 20 L/h [17].

All measurements were performed in triplicate (n = 3) and the results were presented as mean value ± standard deviation (SD).

RESULTS AND DISCUSSION

Almost 50 % of the chemical content of the tobacco seed is reported as lipids. That is the reason tobacco seeds are rich in oil fraction. The main components of the oil fraction are fatty acids, sterols, phospholipids, and tocopherols, shown in Table 1. The data showed that there was a difference between the oils obtained from the two types of growing – 40.1 % (bio) and 39.4 % (con). It makes an impression that the seeds from harvest 2021 had lower oil yield in both variants of agrarian conditions (Table 1). The yield of oil was close to the reported values for tobacco seeds from Pakistan (40.6 %), Iraq (22 – 45%), Italy (30 – 40%) and higher from those reported from Iran (13.7%) and Serbia (27.8 – 31.3%) [18]. Zlatanov *et al.* [6] have examined Bulgarian oriental tobacco seeds and reported between 37.9 – 41.3 % yields of oil. The obtained result is typical for oriental tobacco. The yield of tobacco oil was good in comparison to other oils such as canola (37 – 41%), sunflower (25 – 47%) and safflower (38 – 48 %) [19].

Table 1. Content of bioactive compounds in tobacco seed oil

Compounds	Tobacco seed							
	<i>Krumovgrad 58 (bio)</i>				<i>Krumovgrad 58 (con)</i>			
<i>Year of harvest</i>	2020	2021	<i>AVE</i>	<i>SD</i>	2020	2021	<i>AVE</i>	<i>SD</i>
<i>Oil in the seeds, %</i>	41.7	38.4	40.1	2.3	42.3	36.5	39.4	4.2
<i>Unsaponifiable matter, %</i>	2.9	1.9	2.4	0.8	2.7	2.8	2.8	0.1
<i>Sterols, %</i>	0.8	1.2	1.0	0.3	0.8	1.2	1.0	0.2
<i>Tocopherols, mg/kg</i>	325	291	308	24	317	307	312	37
<i>Phospholipids, %</i>	1.5	1.7	1.6	0.3	1.6	1.8	1.7	0.4

Table 2. Fatty acids composition of tobacco seed oil

Fatty acids, %		Tobacco seed					
		<i>Krumovgrad 58 (bio)</i>			<i>Krumovgrad 58 (con)</i>		
<i>Year of harvest</i>		2020	2021	<i>AVE±SD</i>	2020	2021	<i>AVE±SD</i>
<i>C_{14:0}</i>	<i>Myristic</i>	0.10	0.10	0.10±0.00	0.10	0.10	0.10±0.00
<i>C_{15:1}</i>	<i>Pentadecanoic</i>	0.10	N/D*	0.10±0.00	N/D	0.30	0.30±0.00
<i>C_{16:0}</i>	<i>Palmitic</i>	14.20	12.00	13.10±1.20	13.80	11.20	12.50±1.30
<i>C_{16:1}</i>	<i>Palmitoleic</i>	0.10	0.20	0.15±0.05	0.10	0.20	0.15±0.06
<i>C_{17:0}</i>	<i>Margaric</i>	0.10	0.20	0.15±0.03	0.20	0.30	0.25±0.04
<i>C_{17:1}</i>	<i>Heptadecenoic</i>	0.30	0.40	0.35±0.05	0.20	0.30	0.25±0.08
<i>C_{18:0}</i>	<i>Stearic</i>	2.30	2.10	2.20±0.10	2.90	3.70	3.30±0.40
<i>C_{18:1}</i>	<i>Oleic</i>	17.30	17.70	17.50±0.20	17.20	14.40	15.80±1.40
<i>C_{18:2}</i>	<i>Linoleic</i>	64.40	65.90	65.20±0.80	64.70	68.20	66.50±1.70
<i>C_{18:3}</i>	<i>Linolenic</i>	0.50	0.60	0.65±0.20	0.50	0.60	0.55±0.04
<i>C_{20:0}</i>	<i>Arachidic</i>	0.10	0.20	0.15±0.05	N/D	0.20	0.20±0.00
<i>C_{20:1}</i>	<i>Gadoleic</i>	0.20	0.10	0.15±0.04	0.10	0.10	0.10±0.00
<i>C_{22:0}</i>	<i>Behenic</i>	0.20	0.40	0.30±0.05	0.20	0.30	0.25±0.03
<i>C_{22:1}</i>	<i>Erucic</i>	0.10	0.10	0.10±0.00	N/D*	0.10	0.10±0.00
<i>SFA, %</i>		17.00	15.00	16.00	17.20	15.80	16.50
<i>MUFA, %</i>		18.10	18.50	18.30	17.60	15.40	16.50
<i>PUFA, %</i>		64.90	66.50	65.70	65.20	68.80	67.00

*SFA – saturated fatty acids; MUFA – monounsaturated fatty acids; PUFA – polyunsaturated fatty acids; N/D – not detected

The amount of total sterols and tocopherols was higher than that reported by others in the ranges of 1.0% sterols and 308 – 312 mg/kg tocopherols [20]. The content of phospholipids was found to be 1.6% and 1.7% in the first and second year of analysis, respectively. These values are similar to previous studies of tobacco seeds [20].

One of the main components in oils are fatty acids (FA). Fatty acids were identified and expressed as percentage of total saturated fatty acids (SFA), monounsaturated fatty acids (MUFA) and polyunsaturated fatty acids (PUFA). The amount of PUFA was higher than the other FA – 65.70 % for *Krumovgrad 58 (bio)* seeds and 67.00 % for *Krumovgrad 58 (con)*. The average values for SFA and MUFA in the oil of bio seeds was equal to 16.00 – 18.30%, while in the conventional one SFA were

16.50 % and MUFA – 16.50%. Individual FA content was determined, shown in Table 2.

The main saturated fatty acid was palmitic 13.10 % average (bio) and 12.50 % (con). In 2020 seeds had higher content of palmitic acid for the varieties. Stearic acid was the other saturated fatty acid that had higher content – 2.20 and 3.30% in *Krumovgrad 58 (bio)* and *Krumovgrad 58 (con)* variety, respectively, during the two years of analysis. The palmitic acid in tobacco seed oil was half of that reported by Zlatanov *et al.* for Bulgarian tobacco varieties (16.40 – 27.70 %) [6]. The main fatty acid is linoleic acid which is polyunsaturated. Linoleic acid is essential in the diet, as it is incorporated into cell membranes and it is involved in the synthesis of compounds that are responsible for regulating blood pressure, as well as for inflammatory response. In addition, PUFAs are considered beneficial for health

due to their ability to reduce total cholesterol and body fat [19]. The content of linoleic acid was 64.40 – 65.90% for Krumovgrad 58 (bio) and 64.70 – 68.20% for conventional one. Oleic acid was reported as an acid with high content in tobacco seed oil. In the analyzed samples, that fatty acid was with medium value between 17.30 – 17.70% for the bio variety and 14.40 – 17.20% for the conventional tobacco seed oil.

Lipids are usually complex mixtures containing minor components that may catalyze or inhibit oxidation and because primary oxidation products are labile, they are easily converted to secondary products. Oxidation of lipids is promoted by factors such as elevated temperature, presence of light or extraneous materials such as metals or other oxidation initiators [21]. The oxidative stability is an important parameter to evaluate the storage period of vegetable oils during which they keep their nutritive quality. It depends mainly on the fatty acid composition (content of unsaturated fatty acids) and the presence of tocopherols and phenolic compounds as substantial native antioxidants. The oxidative stability of tobacco seed oils, determined by the Rancimat test, was found to be very similar to that of sunflower oil – linoleic type, with induction period at 100°C of 12.6 h and 10.1 h, for Krumovgrad 58 (bio) and Krumovgrad 58 (con), respectively. The higher oxidative stability of Krumovgrad 58 bio is a result of the lower content of linoleic acid (Table 2).

Antioxidants prevent lipid oxidation and they occur either naturally in the lipid mixture, such as vitamin E (tocopherols and tocotrienols, four species of each exist, α , β , γ , δ) or they are deliberately added synthetic compounds. There is growing interest in the natural forms of vitamin E because they are promising compounds for maintaining a healthy cardiovascular system and blood cholesterol level [22]. The natural sources of tocopherols are cereal and seeds rich in lipids [23, 24]. Tocopherol content in samples from tobacco seed oil grown under organic production conditions was 308±24 mg/kg, while in conventionally grown tobacco seeds 312±37 mg/kg as mean value of two years of harvest (Table 1). The oil from tobacco seeds Krumovgrad 58 (bio) had higher content of total tocopherols – 325 mg/kg for harvest 2020, according to results obtained from conventionally grown tobacco seeds – 317 mg/kg for harvest 2020. Krumovgrad 58 tobacco seeds showed higher total tocopherol

content compared to the data reported in the literature, regardless of the cultivation method. The individual tocopherol content was determined for the two ways of cultivation. α -Tocopherol and β -tocopherol were not determined. γ -Tocopherol was found in the oil in the range of 27.3 – 48.5% of the total tocopherol content and δ -tocopherol predominated between 51.5 – 72.7%. Krumovgrad 58 (bio) tobacco seeds oil had lower levels of γ -tocopherol than conventionally grown variety for the two years of harvest (Figure 1). Amounts of tocopherols in tobacco seed oil have been reported between 2 – 195 mg/kg [6]. Maryland tobacco seeds were reported to contain α - and γ -tocopherol with a total value between 70.636 – 217.730 μ mol/kg. The results of the study are typical for *Nicotiana spp.* from Bulgarian region reported by Popova *et al.* but in the present study δ -tocopherol predominated [18, 25]. The levels of tocopherols in the different plant oils varied over a wide range – 11 and 3468 mg/kg. The total tocopherol content from tobacco seed Krumovgrad 58 (bio) oil was close to those reported for celery oil 126.8 mg/kg, poppy oil – 123.5 mg/kg and red palm oil – 121.6 mg/kg.

Sterols are an important group of components contained in the unsaponifiable fraction of a vegetable oil. The most common plant sterols or phytosterols are: β -sitosterol, Δ^7 -campesterol, Δ^7 -stigmasterol and Δ^5 -brassicasterol [26]. The total sterol content in samples of tobacco seed oil from variety Krumovgrad 58 (bio) and (con) was near 1 % from the total lipid content. It can be compared to the sterol content in other oriental tobacco seeds varieties grown in Bulgaria, where the results showed the presence of sterols between 0.4 – 0.8% [6]. Sterols identified in high quantity in tobacco seed oils were β -sitosterol, campesterol, stigmasterol and cholesterol (Figure 2).

Figure 2 presents the levels of identified sterols in tobacco seed oil from conventionally and organically grown tobacco seeds from variety Krumovgrad 58 in two years of harvest as mean value in percentage. Harvest 2021 showed lower content of identified sterols for the two varieties and even some of them were not detected at all.

β -Sitosrerol (63.1 – 64.2%) was the main sterol in the tobacco seed oil with no significant difference between years of harvest and no matter the way of cultivation. It is near to the reported content of β -sitosrerol in tomato seed oil – 53 - 58% [27].

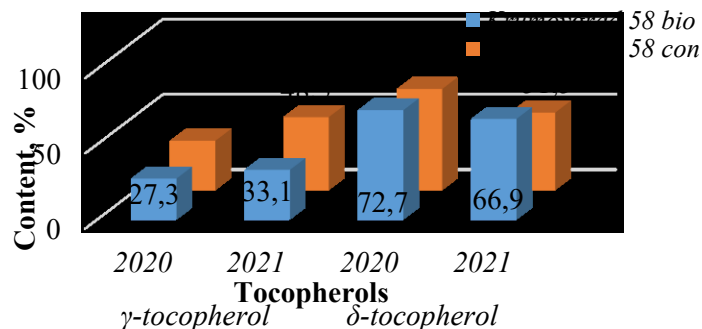


Fig. 1. Individual tocopherol content in tobacco seed oil from conventionally and organic production of tobacco seeds in two years of harvest

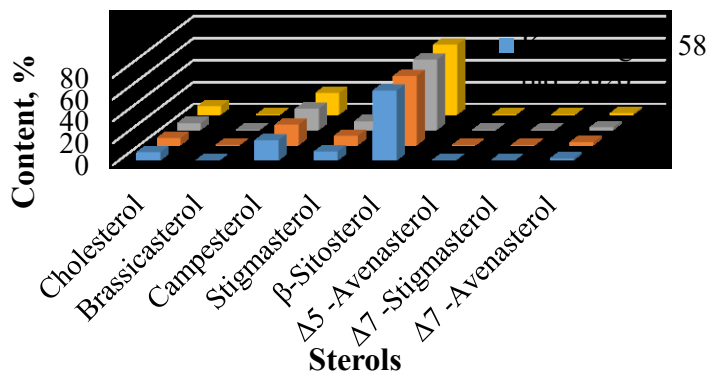


Fig. 2. Sterol content in tobacco seeds oil in two year of harvest and as mean value of the two years

Campesterol was determined as a mean value for the two years of harvest in tobacco seeds oil from Krumovgrad 58 (bio) – 18.6%, while in tobacco seed oil from Krumovgrad 58 (con) it was by 1 % higher. Stigmasterol and cholesterol were with close values – 8.3 % (bio) and 7.5% (con) for stigmasterol and 7.1% (bio) and 6.9% (con) for cholesterol, respectively. Stigmasterol was present with a higher value (7.5 – 8.3%) in a comparison to other edible vegetable oils (1.8% in blackberry seed oil; 0.3% in blueberry seed oil; 1.3% in cranberry seed oil, 1.2% in red raspberry seed oil; 2.3% in strawberry seed oil and 2.4% in kiwi seed oil) [28]. The sterol content in tobacco seeds oil of the examined variety is comparable to grape seed oil reported by Garavaglia *et al.* [29].

The other part of the lipid content in the tobacco seeds are phospholipids. Due to their wide occurrence in foods and their pro- and antioxidant effects, phospholipids have the potential as multifunctional additives in food, pharmaceutical and industrial applications [30]. They are a large group of lipid compounds reported in tobacco seeds oil between 0.2 – 1.7% [24, 31]. The oil from tobacco seeds in the current research had 1.5 – 1.8% of phospholipids. The individual phospholipid content in tobacco seed oil from the conventionally and organically grown tobacco is presented in Fig. 3.

There were no differences in the identified phospholipids. The content of phosphatidylinositol (PI) was the highest – 43.0% (bio) and 41.7 % (con),

followed by phosphatidylcholin (PC) – 27.3% (bio) and 29.9% (con) and phosphatidic acids – 10.1% (bio) and 8.6% (con). The levels of phosphatidyletanolamine, phosphatidylserine and other phospholipids were equal (from 1.0% to 2.5%).

CONCLUSION

The present study determines the seeds of the investigated tobacco variety Krumovgrad 58, grown in Bulgaria, as a potential source of glyceride oil rich in biologically active components. The chemical composition of seeds from organically grown tobacco plants from Krumovgrad 58 (bio) was examined and compared with the seeds from the same conventionally grown variety. The oil from organically grown tobacco seeds had a higher yield of oil and better oxidative stability than the conventionally grown tobacco seeds. The tobacco seeds are favorable for the production of vegetable oil whose oxidative stability is similar to that of sunflower oil – linoleic type. There was a higher tocopherol content in the tobacco seed oil from Krumovgrad 58 (bio).

The information about biologically active substances such as polyunsaturated fatty acids, tocopherols and phospholipids may be useful for determination of the nutritional value of this oil. The tobacco seed oil is a valuable source of healthy glyceride oil for human consumption and can be used in food and cosmetic industry in the future.

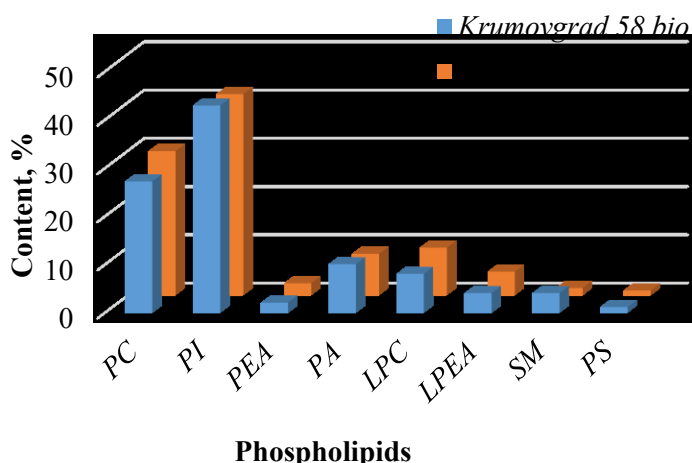


Fig. 3. Individual phospholipid content in tobacco seed oil from conventional and organic production in the two years of analysis.

*PC – Phosphatidylcholine; PI – Phosphatidylinositol; PEA – Phosphatidylethanolamine; PA – Phosphatidic acids; LPC – Lysophosphatidylcholine; LPEA – Lysophosphatidylethanolamine; SM – Sphingomyelin; PS – Phosphatidylserine.

REFERENCES

- H. Bozukov, M. Kasheva, Y. Kochev, D. Vitanova, *Bulg. J. Agric. Sci.*, **25** (4), 633 (2019).
- H. Bozukov, *Bulg. Tobac.*, **1-2**, 8 (2018).
- G. Mitev, *Tr. J. Sci.*, **17** (1), 572 (2019).
- M. Z. Ashirov, U. M. Datkhayev, D. A. Myrzakozha, H. Sato, K. S. Zhakipbekov, N. A. Rakhymbayev, B. N. Sadykov, *Sci. World J.*, **2020** (2020).
- I. T. Stanisavljević, D. T. Velić Ković, Z. B. Todorović, M. L. Lazić, V. B. Veljković, *Eur. J. Lipid Sci. Technol.*, **111** (5), 513 (2009).
- M. Zlatanov, M. Angelova, G. Antova, *Bulg. J. Agric. Sci.*, **13** (5), 539 (2007).
- ISO 659, Oilseeds. Determination of oil content (Reference method), 2014.
- ISO 12966-1, Animal and vegetable fats and oils. Gas chromatography of fatty acid methyl esters – Part 1: Guidelines on modern gas chromatography of fatty acid methyl esters, 2014.
- ISO 12966-2, Animal and vegetable fat and oils. Gas chromatography of fatty acid methyl esters – Part 2: Preparation of methyl esters of fatty acids, 2011.
- ISO 18609, Animal and vegetable fats and oils. Determination of unsaponifiable matter. Method using hexane extraction, 2000.
- S. Ivanov, P. Bitcheva, B. Konova, *Rev. Fr. Corps Gras*, **19** (3), 177 (1972).
- ISO 12228-1, Animal and vegetable fats and oils. Determination of individual and total sterols contents. Gas chromatographic method, 2014.
- ISO 9936, Animal and vegetable fats and oils. Determination of tocopherol and tocotrienol contents by high-performance liquid chromatography, 2016.
- J. Folch, M. Lees, G. H. Sloane-Stanley, *J. Biol. Chem.*, **226**, 497 (1957).
- R. Schneiter, G. Daum, Analysis of yeast lipids, Humana Press Inc., Totowa N. J., 2006.
- ISO 10540-1, Animal and vegetable fats and oils. Determination of phosphorus content. Part 1: Colorimetric method, 2014.
- ISO 6886, Animal and vegetable fat and oils. Determination of oxidation stability (Accelerated oxidation test), 1996.
- V. Popova, Z. Petkova, T. Ivanova, M. Stoyanova, L. Lazarov, A. Stoyanova, T. Hristeva, M. Docheva, V. Nikolova, N. Nikolov, V. Zheljazkov, *Ind. Crops Prod.*, **117** (3), 375 (2018).
- M. A. Ali, M. A. Sayeed, R. K. Roy, S. Yeasmin, A. M. Khan, *Asian Jour. of Biochem.*, **3**, 203 (2008).
- M. Zlatanov, M. Angelova, G. Antova, *Agric. Bohem.*, **38** (2) 69 (2007).
- F. Gunstone, J. Harwood, Occurrence and characterization of oils and fats, in: *The Lipid Handbook*, CRC Press, Boca Raton, USA, 2007, p. 37.
- M. L. Colombo, *Molecules*, **15** (4), 2103 (2010).
- A. Blanco, G. Blanco, *Med. Biochem.*, 1st edn., 2017, p. 645.
- E. Aksoz, O. Korkut, D. Aksit, C. Gokbulut, *Flavour Fragr. J.*, **35** (5), 504 (2020).
- Z. Xie, M. Whent, H. Lutterodt, Y. Niu, M. Slavin, R. Kratochvil, L. Yu, *J. Agric. Food Chem.*, **59** (18), 9877 (2011).
- A. Blanco, G. Blanco, *Med. Biochem.*, 1st edn., 2017, p. 99.
- A. M. Giuffrè, M. Capocasale, *Int. Food Res. J.*, **23** (1), 116 (2016).
- V. Van Hoed, N. De Clercq, C. Echim, M. Andjelkovic, E. Leber, K. Dewettinck, R. Verrhé, *J. Food Lipids.*, **16** (1), 33 (2009).
- J. Garavaglia, M. M. Markoski, A. Oliveira, A. Marcadenti, *Nutr. Metab. Insights*, **16** (9) 59 (2016).
- B. Y. Guo, B. Wen, X. Q. Shan, S. Z. Zhang, J. M. Lin, *J. Chromatogr. A*, **1074** (1-2), 205 (2005).
- M. Zlatanov, M. Angelova, E. Ivanova, *SP of PU – Chem.*, **34** (5) 145 (2006)

Comparative study on chemical and lipid composition of two varieties of quinoa seeds (*Chenopodium quinoa* L.)

O. T. Teneva, Zh. Y. Petkova, M. J. Angelova-Romova, G. A. Antova*

University of Plovdiv "Paisii Hilendarski", Faculty of Chemistry, Department of Chemical Technology, 24, Tzar Asen Str., Plovdiv 4000, Bulgaria

Received: November 3, 2023; Revised: April 11, 2024

The seeds of two varieties of quinoa (*Chenopodium quinoa* L.), white and black, were analysed for their chemical composition and a detailed study of their lipids was carried out as well. The chemical composition of the seeds was as follows: protein content - 15.7% and 14.5%, lipids - 5.9% and 6.6%, carbohydrates - 65.6% and 64.6%, starch - 40.2% for both varieties, water soluble sugars - 7.2% and 5.5%, and minerals - 2.4% and 2.3%, respectively. The oil content was about 6.0%, but high amounts of biologically active compounds in the seed oils of black quinoa were noted (tocopherols - 1102 mg/kg, phospholipids - 7.6% and sterols - 3.4%), while in the seed oils of white quinoa tocopherols were 365 mg/kg, phospholipids - 11.9% and sterols - 2.1%. Linoleic and oleic acids dominated in both oils, followed by palmitic and linolenic acid. Unsaturated fatty acids predominated in the lipid fraction where the content of polyunsaturated fatty acids was 53.1% (white quinoa) and 49.4% (black quinoa), followed by monounsaturated fatty acids - 30.7% and 33.5%, respectively. In the tocopherol fraction of the oils the main component was γ - tocopherol, followed by α - tocopherol. The main component of the sterol fraction was β - sitosterol (80.1% and 75.7%). Phospholipids in the seeds of the two varieties of quinoa had similar composition. Despite some differences in the chemical and lipid composition, these quinoa seeds were established to be a valuable source of proteins, carbohydrates and healthy lipid-soluble bioactive components for human nutrition.

Keywords: white and black quinoa (*Chenopodium quinoa* L.), bioactive components, proteins, lipids

INTRODUCTION

Quinoa (*Chenopodium quinoa* Willd., genus *Chenopodium*, *Chenopodiaceae* family) is widely distributed worldwide, with around 200 - 250 varieties. Quinoa is a typical crop for Andean and can be found on the territories of Colombia, Ecuador, Peru, Bolivia, Argentina and Chile [1] but high yields are seen in East Asia, Europe, Africa, and America. Nowadays, the food industry needs new gluten-free products which are beneficial for the normal metabolic processes in the human body and satisfy the psycho-physical well-being [2]. The grains of amaranth, quinoa and buckwheat pseudocereals are free of gluten and have excellent nutritional properties [3]. Quinoa seeds have a good nutritional value and they can be used in baking, as well as for replacing rice in main courses [4].

The interest in quinoa is sparked mainly by the nutritional composition. The grains are rich in macronutrients (protein and carbohydrates), biologically active compounds including dietary fibres, minerals, amino acids, phenolics, phytosterols and vitamins (ascorbic acid, thiamin, riboflavin) [5-9]. Quinoa is rich in polyphenolic compounds (mainly vanillic acid, ferulic acid and

their derivatives, as well as main flavonoids quercetin, kaempferol and their glycosides) which are good antioxidants. Some of them have anti-inflammatory properties and can reduce the risk of chronic diseases [10-13]. The quinoa seeds can be coloured in white, black and red [7] as the antioxidant activity and phenolic profiles depend by the color. The darker quinoa seeds (black quinoa) are rich of phenolic compounds and have better antioxidant activity than the white ones.

Quinoa has different composition depending by the variety of the plant. Lipid content can vary (5.94% - 10.71%) [1]. The quantity of protein is determined to be 14.2% and starch content - 47.22% - 59.72% [14]. Quinoa can be consumed as a functional food, both seeds and oil. The oil is rich of unsaturated fatty acids and they are most important for the nutritional value of the quinoa seed oil. The content of oleic acid is 33% [15]. Tocopherols are biologically active components with good protection against oxidative damage. α -Tocopherol is the major component of quinoa seed oil as the total content of tocopherol is reported to be 37.88 - 77.73 mg kg⁻¹ [16].

The color of quinoa is variable. White and black seeds are most commonly consumed but a detailed

* To whom all correspondence should be sent:

E-mail: ginant@uni-plovdiv.bg

comparative study of these two varieties of quinoa seeds is not available. The aim of this research is to examine the chemical and lipid composition, as well as biologically active composition of both white and black quinoa seeds and oils.

EXPERIMENTAL

All analyses were carried out with quinoa seeds purchased from the local market with country of origin Peru.

Proximate composition analysis

The glyceride oil was isolated from the seeds with n-hexane by Soxhlet extraction [17]. The contents of proteins, ash and moisture were analysed according to AOAC [18] and that of carbohydrates was calculated using a formula [9].

Determination of fatty acid composition

Gas chromatography was used for determination of fatty acid composition [19]. Transesterification of the oil with sulfuric acid in methanol was the way to obtain the fatty acid methyl esters (FAMES) [20]. Determination was performed on Agilent 8860 gas chromatograph. The equipment was with a capillary column DB Fast FAME (30 m x 0.25 mm x 0.25 µm (film thickness)) and a flame ionization detector (FID). The column temperature was from 70 °C (1 min), at 6 °C/min to 180 °C, and at 5 °C/min to 250 °C; the injector temperature was 270 °C and that of detector - 300 °C; nitrogen was the carrier gas. Identification was done by comparison with the retention times of a standard mixture of FAME.

Analysis of sterols

The unsaponifiable matter was extracted with n-hexane after saponification of glyceride oil [21]. Sterols were isolated from the unsaponifiable fraction by thin-layer chromatography (TLC) [22], after that they were determined spectrophotometrically at 597 nm. The composition of sterols was analysed on a HP 5890 gas chromatograph equipped with DB 5 capillary column (25 m x 0.25 mm x 0.25 µm (film thickness)) and FID. Temperature gradient was from 90 °C (3 min) up to 290 °C at a rate of 15 °C/min and then up to 310 °C at a rate of 4 °C/min (10 min); detector temperature: 320 °C; injector temperature: 300 °C and carrier gas was hydrogen. Identification was confirmed by comparison with the retention times of a standard mixture of sterols [23].

Analysis of tocopherols

The composition of tocopherols was determined in the oil by high performance liquid chromatography with Nucleosil Si 50-5 column (250

x 4 mm, particle size: 5 mm), fluorescence detection at 290 nm excitement and 330 nm emission. The operating conditions were mobile phase of hexane:dioxane = 96:4 (v/v) and flow rate of 1 mL/min [24].

Analysis of phospholipids

Phospholipids were isolated from the seeds according to Folch *et al.* [25] using extraction with a mixture of chloroform and methanol (2:1, v/v). Two-dimensional TLC was used to determine the individual phospholipids [26]. Identification was performed by comparing the Rf values with those of standards. The spots of phospholipids were scrapped and mineralized with a mixture of perchloric and sulfuric acid, 1:1 (v/v), and the quantification was performed spectrophotometrically at 700 nm [27]. The total content of phospholipids was calculated.

Statistics

All measurements were performed in triplicate (n = 3), the results were presented as mean value ± standard deviation (SD) and the significant differences were determined by one-way ANOVA (Duncan test, p < 0.05).

RESULTS AND DISCUSSION

The chemical composition of white quinoa (WQ) and black quinoa (BQ) seeds is presented in Table 1.

Table 1. Chemical composition of white and black quinoa seeds

Compounds, %	Quinoa	
	White	Black
Glyceride oil	5.9±0.4 ^a	6.6±0.3 ^a
Protein	15.7±0.2 ^a	14.5±0.1 ^b
Carbohydrates:	65.6±0.6 ^a	64.6±0.4 ^a
- starch	40.2±0.3 ^a	40.2±0.2 ^a
- water soluble sugars	7.2±0.4 ^a	5.5±0.3 ^b
Ash	2.4±0.1 ^a	2.3±0.1 ^a
Moisture	10.4±0.2 ^a	12.0±0.5 ^b

^{a,b} - Different letters mean statistical difference (Duncan test, p < 0.05).

The oil content differed among the both varieties of quinoa and it was in the range between 5.9% – 6.6%. The results were close to those reported by Nowak *et al.* [28] and Chauhan *et al.* [29]. The amount of glyceride oil was higher for BQ. Shen *et al.* [30] reported the opposite results – the content of glyceride oil in WQ was found to be 6.19% and in BQ – 5.68%. The quinoa seeds are very good sources of proteins as the quantities are close between seeds of white and black quinoa. The protein content was between 14% – 16% which is in agreement with

Diaz-Valencia *et al.* [14], while Ando *et al.* [31], Marmouzi *et al.* [32], Nowak *et al.* [28] declared about 13.0%. The content of carbohydrates was found to be 65.6% (WQ) and 64.6% (BQ) as the amount of starch was equal in both analysed types. These results are lower than reported earlier by Diaz-Valencia *et al.* [14] where the starch content was found to be 47.22% - 59.72%, but close to Ando *et al.* [31] and Marmouzi *et al.* [32] (63.7%). The quantity of water - soluble sugars was established to be 7.2% (WQ) and 5.5% (BQ). The ash content in the two analysed quinoa seeds was found to be similar (2.4%) as well as the moisture content (10.4% - WQ and 12.0% - BQ) which corresponds to the data by Przybylski *et al.* [33].

Fatty acid composition was one of the main parameters which were used for characterization of the oils in terms of their nutritional value. Fatty acid composition of white and black quinoa seed oil was established and the results are given in Table 2.

Table 2. Fatty acid composition of quinoa seed oil.

Fatty acids, %		Quinoa	
		White	Black
Lauric	C _{12:0}	0.1±0.02	-*
Myristic	C _{14:0}	0.4±0.1 ^a	0.2±0.05 ^b
Myristoleic	C _{14:1}	0.1±0.01 ^a	0.1±0.02 ^a
Pentadecanoic	C _{15:0}	0.1±0.03 ^a	0.1±0.02 ^a
Pentadecenoic	C _{15:1}	0.2±0.05	-
Palmitic	C _{16:0}	14.6±0.2 ^a	15.6±0.3 ^b
Palmitoleic	C _{16:1}	0.3±0.1 ^a	0.2±0.05 ^a
Margaric	C _{17:0}	0.1±0.01 ^a	0.1±0.02 ^a
Heptadecenoic	C _{17:1}	0.1±0.01	-
Stearic	C _{18:0}	0.2±0.05 ^a	0.9±0.1 ^b
Oleic	C _{18:1}	28.5±0.5 ^a	33.2±0.3 ^b
Linoleic	C _{18:2}	47.5±0.4 ^a	47.5±0.3 ^a
Linoleic (trans)	C _{18:2 (trans)}	0.2±0.05	-
Linolenic	C _{18:3}	5.0±0.3 ^a	1.9±0.2 ^b
Arachidic	C _{20:0}	0.3±0.05 ^a	0.2±0.03 ^a
Eicosadienoic	C _{20:2}	0.3±0.02	-
Eicosatrienoic	C _{20:3}	0.1±0.01	-
Behenic	C _{22:0}	0.4±0.1	-
Erucic	C _{22:1}	1.5±0.3	-
Saturated fatty acids		16.2	17.1
Unsaturated fatty acids		83.8	82.9
- Monounsaturated fatty acids		30.7	33.5
- Polyunsaturated fatty acids		53.1	49.4

* - Not identified; ^{a,b} - Different letters mean statistical difference (Duncan test, $p < 0.05$).

Predominating fatty acids in the oil of WQ and BQ were the unsaturated ones (UFAs). The major part of them was polyunsaturated fatty acids (PUFA) – 53.1% for the oil of WQ and 49.4% for BQ. Two essential fatty acids, linoleic acid (C18:2) and oleic

(C18:1), were in the highest quantity in both analysed quinoa seed oils. The amount of linoleic acid was determined to be the same (47.5%) in WQ and BQ while the contents of oleic acid were different. The quantity of oleic acid (C18:1) in BQ was higher (33.2%) than that in the oil from white seeds (28.5%). The results regarding the content of linoleic acid are in agreement with these reported by Shen *et al.* [30] where the content in BQ was found to be higher than in the white one – 51.75% and 43.74%, respectively, while our results regarding the content of linolenic acid (WQ – 5.0% and BQ – 1.9%) were significantly lower (WQ – 8.24% and BQ – 4.59%). The fraction of saturated fatty acids was presented by palmitic acid (C16:0) as follows – 14.6% in WQ and 15.6% in BQ. The data are higher than those reported by Shen *et al.* [30] (13.16% and 9.77%). The rest of the fatty acids were identified in minimal quantities.

The biologically active compounds in quinoa seed oil were determined and the results are presented in Table 3.

Table 3. Biologically active compounds in white and black quinoa seed oils

Compounds, %	Quinoa	
	White	Black
Unsaponifiable matter, %		
- in the oil	7.3±0.3 ^a	4.8±0.4 ^b
- in the seeds	0.4±0.0 ^a	0.3±0.0 ^b
Sterols, %		
- in the oil	2.1±0.1 ^a	3.4±0.2 ^b
- in the seeds	0.1±0.0 ^a	0.2±0.0 ^b
Tocopherols, mg/kg		
- in the oil	365±17 ^a	1102±21 ^b
- in the seeds	22±1 ^a	73±1 ^b
Phospholipids, %		
- in the oil	11.9±0.5 ^a	7.6±0.3 ^b
- in the seeds	0.7±0.0 ^a	0.5±0.0 ^b

^{a,b} - Different letters mean statistical difference (Duncan test, $p < 0.05$).

The information about the content of unsaponifiable matter of quinoa seed oil was missing in the literature. Its amount in the oil from WQ was 7.3% and in BQ – 4.8%, respectively. The results are higher than the reported in Codex Stan 19 [34] for other vegetable oils where the quantity of unsaponifiable matter is 1.0% (for peanut oil), 1.5% (soybean oil) and 2.0% (rapeseed oil). The sterols were the major part of the unsaponifiable matter. There was a difference between the contents of sterol in the oils of WQ (2.1%) and BQ (3.4%). Tocopherols (known as Vitamin E) are an excellent natural antioxidant and they are important for human health. The data about the tocopherol content of oil

from WQ and BQ were notably different. The total amount of tocopherols in the oil of BQ was 4 times higher than that of WQ. The content of phospholipids in the oils of white and black quinoa was found to be 11.9% (WQ) which is notably higher than 7.6% (BQ).

The individual composition of the sterol fraction is presented in Table 4.

Table 4. Individual sterol composition of quinoa seed oils

Sterols, %	Quinoa	
	White	Black
Campesterol	0.5±0.1 ^a	1.1±0.2 ^b
Stigmasterol	2.5±0.2 ^a	2.9±0.3 ^a
Δ ⁷ - Campesterol	1.1±0.1 ^a	1.2±0.3 ^a
β - Sitosterol	80.1±0.5 ^a	75.7±0.4 ^b
Δ ⁵ - Avenasterol	2.8±0.2 ^a	3.2±0.1 ^b
Δ ^{7,25} - Stigmastadienol	0.9±0.1 ^a	7.8±0.3 ^b
Δ ⁷ - Stigmasterol	6.9±0.2 ^a	3.6±0.2 ^b
Δ ⁷ - Avenasterol	5.2±0.1 ^a	4.5±0.3 ^b

^{a,b} - Different letters mean statistical difference (Duncan test, p < 0.05).

The individual composition of the sterol fraction of quinoa seed oils covers all major phytosterols. β – Sitosterol dominated, as its quantity in the oil of WQ is 80.1% and of BQ – 75.7%. The amounts of β – sitosterol reported by Shen *et al.* [30] are lower than our results as follows - 61.4% (WQ) and 58.0% (BQ). There were considerable differences between the amounts of Δ^{7,25} – stigmastadienol and Δ⁷ – stigmasterol. Black quinoa seed oil was rich of Δ^{7,25} – stigmastadienol (7.8%) while in the oil of WQ its quantity was minimal (under 1%). The level of Δ⁷ – stigmasterol in the oil of WQ was almost 2 times higher than in the oil of BQ. The other sterol components were in similar quantities in both varieties of quinoa. The content of stigmasterol (2.5%, WQ and 2.9%, BQ) was considerably different than the data by Shen *et al.* [30] (36.9%, WQ and 40.1%, BQ) while the content of campesterol (1.7% for WQ and 1.9% for BQ) is close to our results.

The individual composition of the tocopherol fraction of quinoa seed oil is presented in Table 5.

In the analysed quinoa seed oils α–, β– and γ– tocopherols were detected. The content of γ– tocopherol was similar (approximately 75.0%) in the oil of WQ and BQ and it was in the highest amount compared with α– and β– tocopherol. WQ seed oil had a slightly larger amount of α– tocopherol than BQ. β– Tocopherol was detected only in BQ seed oil.

Table 5. Individual tocopherol composition of quinoa seed oils

Tocopherols, %	Quinoa	
	White	Black
α- tocopherol	24.9±1.6 ^a	19.5±0.9 ^b
β- tocopherol	-*	6.0±0.5
γ- tocopherol	75.1±1.6 ^a	74.5±1.3 ^a

* - Not identified; ^{a,b} - Different letters mean statistical difference (Duncan test, p < 0.05).

The results are in agreement with other researchers who reported γ– tocopherol as the major component of the tocopherol fraction (53.7% for WQ and 67.5% for BQ) followed by a significant content of α– tocopherol (30.9% for WQ and 21.8% for BQ) [30]. The latter authors declare a total tocopherol content of 123.09 mg/kg (WQ) and 156.67 mg/kg (BQ). The results are considerably different and much lower than those presented in the current study – 365 mg/kg in the WQ and 1102 mg/kg in the BQ.

All classes of individual phospholipids were determined in the white and black quinoa seeds. The results are given in Table 6.

Table 6. Individual phospholipid composition of quinoa seeds

Phospholipids, %	Quinoa	
	White	Black
Lysophosphatidylcholine	15.6±0.2 ^a	13.5±0.5 ^b
Lysophosphatidylethanolamine	9.4±0.4 ^a	9.0±0.3 ^a
Sphingomyelin	8.8±0.3 ^a	8.4±0.2 ^a
Phosphatidylinositol	18.6±0.5 ^a	12.8±0.3 ^b
Phosphatidylcholine	10.5±0.3 ^a	9.2±0.2 ^b
Phosphatidylethanolamine	8.2±0.2 ^a	8.5±0.1 ^a
Phosphatidylserine	7.4±0.4 ^a	8.4±0.2 ^b
Monophosphatidylglycerol	-*	8.1±0.1
Diphosphatidylglycerol	8.3±0.3 ^a	9.2±0.1 ^b
Phosphatidic acids	13.2±0.2 ^a	12.9±0.4 ^a

* - Not identified; ^{a,b} - Different letters mean statistical difference (Duncan test, p < 0.05).

Lysophosphatidylcholine (LPC), phosphatidylinositol (PI), phosphatidic acids (PA) and phosphatidylcholine (PC) predominated in both quinoa seed varieties. Their quantities were similar for WQ and BQ except the phosphatidylinositol where the amount in WQ (18.6%) was notably higher than in BQ (12.8%). All other individual phospholipids (lysophosphatidylethanolamine (LPEA), sphingomyelin (SM), phosphatidylcholine (PC), phosphatidylethanolamine (PEA), phosphatidylserine (PS), monophosphatidylglycerol

(MPG) and diphosphatidylglycerol (DPG)) were observed in quantities between 7% – 11% in both quinoa seeds. The data of Przybylski *et al.* [33] are considerably different from our results: PA (1.1%), PS (4.0%), PEA (18.5%), PI (10.5%), LPEA (43.2%), PC (12.3%) and LPC (3.6%).

CONCLUSION

The comparative analysis of white and black quinoa seeds and oils shows similar lipid compositions and contents of bioactive substances. Quinoa seeds are recognised as a rich source of essential fatty acids, nutrients, high level of protein. They are free of gluten and can be considered as a food with positive effects on the human health. With that said, white and black quinoa seeds are recommended to be consumed as functional food in the human diet.

REFERENCES

1. V. Apaza, G. Caceres, R. Pinedo, Catálogo de variedades comerciales de quinua en el Perú. Ministerio de Agricultura y Riego (Perú), Instituto Nacional de Innovación Agraria Organización de las Naciones Unidas para la Agricultura y la Alimentación, 2013.
2. M. I. Hussain, M. Farooq, Q. A. Syed, A. Ishaq, A. A. Al-Ghamdi, A. A. Hatamleh, *Plants*, **10** (11), 2258 (2021).
3. L. Alvarez-Jubete, E. K. Arendt, E. Gallagher, *Int. J. Food. Sci. Nutr.*, **60**, 240 (2009).
4. R. Repo-Carrasco-Valencia, J. K. Hellström, J. M. Pihlava, P. H. Mattila, *Food Chem.*, **120** (1), 128 (2010).
5. Y. Yao, X. Yang, Z. Shi, G. Ren, *J. Food Sci.*, **79** (5), H1018 (2014).
6. E. P. Vera, J. J. Alca, G. R. Saravia, N. C. Campioni, I. J. Alpuy, *J. Cereal Sci.*, **88**, 132 (2019).
7. Y. Tang, X. Li, B. Zhang, P. X. Chen, R. Liu, R. Tsao, *Food Chem.*, **166**, 380 (2015).
8. A. Vega-Galvez, M. Miranda, J. Vergara, E. Uribe, L. Puente, E. A. Martinez, *J. Sci. Food Agric.*, **90**, 2541 (2010).
9. FAO, Food energy – methods of analysis and conversion factors, Report of a technical workshop, FAO Food and Nutrition Paper 77, Rome, 2003.
10. L. Alvarez-Jubete, H. Wijngaard, E. K. Arendt, E. Gallagher, *Food Chem.*, **119** (2), 770 (2010).
11. R. A. Carciochi, L. Galván-D'Alessandro, P. Vandendriessche, S. Chollet, *Plant Foods Hum. Nutr.*, **71** (4), 361 (2016).
12. U. Gawlik-Dziki, M. Świeca, M. Sułkowski, D. Dziki, B. Baraniak, J. Czyż, *Food Chem. Toxicol.*, **57**, 154 (2013).
13. J. Hur, T. T. H. Nguyen, N. Park, J. Kim, D. Kim, *AMB Express*, **8** (1), 143 (2018).
14. Y. K. Diaz-Valencia, J. J. Alca, M. A. Calori-Dominguez, S. J. Zanabria-Galvez, S. H. da Cruz, *Nova Biotechnol. Chim.*, **171**, 74 (2018).
15. C. Encina-Zelada, L. Barros, V. Cadavez, C. F. R. I. Ferreira, E. Pereira, U. Gonzales Barron, *Food Chem.*, **280**, 110 (2018).
16. Y. Tang, X. Li, P. X. Chen, B. Zhang, R. Liu, M. Hernandez, J. Draves, M. F. Marcone, R. Tsao, *J. Agric. Food Chem.*, **64**, 1103 (2016).
17. ISO 659, Oilseeds. Determination of oil content (Reference method), 2014.
18. AOAC. Association of Official Analytical Chemist, Official methods of analysis, 20th ed. Washington, DC, 2016.
19. ISO 12966-1, Animal and vegetable fats and oils. Gas chromatography of fatty acid methyl esters – Part 1: Guidelines on modern gas chromatography of fatty acid methyl esters, 2014.
20. ISO 12966-2, Animal and vegetable fat and oils. Gas chromatography of fatty acid methyl esters – Part 2: Preparation of methyl esters of fatty acid, 2011.
21. ISO 18609, Animal and vegetable fats and oils. Determination of unsaponifiable matter. Method using hexane extraction, 2000.
22. S. Ivanov, P. Bitcheva, B. Konova, *Rev. Fr. corps gras.*, **19** (3), 177 (1972).
23. ISO 12228-1, Part 1: Animal and vegetable fats and oils. Determination of individual and total sterols contents. Gas chromatographic method, 2014.
24. ISO 9936, Animal and vegetable fats and oils. Determination of tocopherol and tocotrienol contents by high-performance liquid chromatography, 2016.
25. J. Folch, M. Lees, G. H. Sloane-Stanley, *J. Biol. Chem.*, **226**, 497 (1957).
26. R. Schneiter, G. Daum, Analysis of yeast lipids, In: Yeast Protocol: Second Edition, Methods in Molecular Biology, W. Xiao (ed.), Humana Press Inc., Totowa N. J., 2006.
27. ISO 10540-1, Animal and vegetable fats and oils. Determination of phosphorus content. Part 1: Colorimetric method, 2014.
28. V. Nowak, J. Du, U. R. Charrondiere, *Food Chem.*, **193**, 47 (2016).
29. G. Chauhan, N. Eskin, R. Tkachuk, *Cereal Chem.*, **69** (1), 85 (1992).
30. Y. Shen, L. Zheng, Y. Peng, X. Zhu, F. Liu, X. Yang, H. Li, *Molecules*, **27** (8), 2453 (2022).
31. H. Ando, Y. C. Chen, H. J. Tang, M. Shimizu, K. Watanabe, T. Mitsunaga, *Food Sci. Technol. Res.*, **8** (1), 80 (2002).
32. I. Marmouzi, N. El Madani, Z. Charrouf, Y. Cherrah, M. E. A. Faouzi, *Phytothérapie*, **13** (2), 110 (2015).
33. R. Przybylski, G. S. Chauhan, N. A. M. Eskin, *Food Chem.*, **51** (2), 187 (1994).
34. Codex Alimentarius Commission, Codex Stan 19-1981, Standard for Edible Fats and Oils not covered by Individual Standards, 2017.

Persistent environmental contaminants in human milk samples from the northeastern region of Bulgaria

T. P. Trifonova, S. K. Georgieva*, Z. V. Peteva

Department of Chemistry, Medical University – Varna, 55 Marin Drinov Str., 9002 Varna, Bulgaria

Received: November 3, 2023 Revised: April 11, 2024

Organochlorine pesticides (OCPs) are persistent contaminants widely distributed in the environment and in the food chains. The aim of the present study was to determine the levels of 10 OCPs (DDT and its metabolites DDE and DDD, heptachlor, aldrin, heptachlor epoxide, endosulfan, endrin aldehyde, dieldrin and endrin) in human milk collected from northeastern Bulgaria. Breast milk samples from 45 first-time mothers were analyzed by capillary gas chromatography system with mass spectrometric detection (GC-MS). Important determinants such as mother's age, body mass, dietary habit and smoking were considered using a questionnaire. The inclusion criteria and the questionnaire were based on the World Health Organization's protocol. DDE (*p,p'*-dichlorodiphenyldichloroethylene), the main metabolite of DDT, was found in all breast milk samples at levels ranging from 16.89 to 94.48 ng/g lipids (mean 42.86 ng/g lipids). No concentrations of five of OCPs (heptachlor, aldrin, endosulfan, dieldrin, endrin) were detected in any of the milk samples. Heptachlor epoxide and endrin aldehyde (degradation product of endrin) were found in 18% of the milk samples only. The Sum DDTs (sum of DDE, DDD and DDT) in breast milk from Varna (54.62 ng/g lipids) was found higher than DDTs levels in milk samples from Dobrich (44.08 ng/g lipids). The levels of total DDTs in breast milk samples increased by age groups 31 – 35 and 36 – 40 years (53.47 ng/g and 69.16 ng/g lipids, respectively). Levels of OCPs in breast milk from northeastern region of Bulgaria were comparable to levels measured in other European countries.

Keywords: Organochlorine pesticides, OCPs, human breast milk, Bulgaria

INTRODUCTION

Organochlorine pesticides (OCPs) are classified as environmental organic pollutants due to their physical, chemical and toxicological properties, and their environmental and biological persistence [1]. OCPs such as DDT have been used successfully to control a number of diseases, such as malaria and typhus, and were banned or restricted in the 1970s in many parts of the world [2]. Pesticides were found as contaminants in soil, air, water and non-target organisms. Once there, they can harm plants and animals ranging from beneficial soil microorganisms and insects, non-target plants, fish, birds, and other wildlife [3]. Due to their persistence and potential immunotoxicity, carcinogenicity, neurotoxicity, reproductive toxicity and endocrine-disrupting effects, OCPs represent a significant public health problem [1]. These pollutants tend to bioaccumulate within the food chain [4]. The pesticides: DDT and its metabolites DDE and DDD, heptachlor, aldrin, heptachlor epoxide, endosulfan, endrin aldehyde, dieldrin and endrin were listed as persistent organic pollutants (POPs) in The Stockholm Convention [5].

Human exposure to OCPs can be assessed by investigation of biomarkers in body fluids such as

blood, urine, saliva, breast milk and sweat [6]. Human milk is the best matrix for biomonitoring of OCPs, due to its non-invasive collection, and its high lipid content makes the extraction of lipophilic contaminants relatively easy [7]. The contamination of human milk with environmental pollutants is of special concern due of its importance as the first food for the newborn child.

In Bulgaria, a monitoring study for OCPs in breast milk was conducted as part of 2000 – 2003 WHO/UNEP global survey of POPs in human milk from a small group of donors [7, 8]. The aim of the present study was to determine the levels of 10 OCPs (DDT and its metabolites DDE and DDD, heptachlor, aldrin, heptachlor epoxide, endosulfan, endrin aldehyde, dieldrin and endrin) in human milk collected from Northeastern Bulgaria.

EXPERIMENTAL

Sample collection

The present study was based on the voluntary participation of donors, following the World Health Organization's (WHO) protocol [7]. Breast milk samples from lactating mothers living in two regions located in northeastern Bulgaria (Varna and Dobrich regions) were collected in October 2019 – July 2021.

* To whom all correspondence should be sent:
E-mail: stgeorgieva@mu-varna.bg

Inclusion criteria for the participant mothers were: 1) age 25–40 years, 2) First-time mothers (*primiparae*), 3) breastfeeding period 30 – 40 days after childbirth; 4) resident in Varna or Dobrich for ≥ 10 years; 5) informed consent signed. Data on age, pre-pregnancy weight, height, lactation period, smoking and dietary habits were obtained from a validated "face to face" questionnaire. The study design and questionnaires were approved by the Commission for Scientific Research Ethics at the Medical University – Varna, Bulgaria (protocol № 85/2019). The collected milk samples were stored at -18°C until the laboratory analysis.

Analytical method

Preparation of milk samples was performed by a previously described analytical method [9]. Briefly, individual milk samples were defrosted, then slowly warmed up to $36\text{--}37^{\circ}\text{C}$ and carefully homogenized. Each individual milk sample (10 g) was three-step extracted with a mix of organic solvents: hexane / acetone in ratios 1:0 v/v (5 mL), 2:1 v/v (9 mL), 1:1 v/v (8 mL), respectively. The hexane layers were collected, and evaporated to near dryness in a rotary vacuum evaporator. The lipid content of the milk samples was determined gravimetrically. The cleaning-up procedure of the lipid extract was performed on a multilayer glass column filled with neutral silica and acid silica. The extract was dissolved in 2 mL of hexane and was placed in the clean-up column. The elution of OCPs was performed with 10 mL of n-hexane and 20 mL of a mix of n-hexane / dichloromethane in a ratio 9:1 (v/v). The concentrated and purified extracts from milk samples were analyzed using the gas chromatograph GC FOCUS using POLARIS Q Ion Trap mass spectrometer (IT-MS) (Thermo Electron Corporation, USA), equipped with an AI 3000

autosampler and splitless Injector. Experimental MS parameters were as follows: the Ion source and Transfer line temperatures were 220°C and 250°C , respectively. The splitless Injector temperature was 250°C . The GC oven was programmed as follows: 50°C (1 min), $30^{\circ}\text{C}/\text{min}$ to 180°C , $5^{\circ}\text{C}/\text{min}$ to 260°C , $30^{\circ}\text{C}/\text{min}$ to 290°C with a final hold for 3.0 min. A TG-5ms capillary column with a length of 30 m, 0.25 mm ID and a film thickness of $0.25\ \mu\text{m}$ was used. Helium was applied as carrier gas at a flow of 1 ml/min. Each individual sample was analyzed three times and the average of the results obtained was taken.

The detection and identification of target analytes were based on a selected precursor ion followed by application of an adequate excitation voltage for its subsequent fragmentation and the whole mass spectrum of its product ions (IT-MSn mode). GC/IT-MSn detection parameters of individual organochlorine compounds - retention times, precursor ions, voltage and product ions are present in Table 1.

Quality control

Quality control procedures included regular analysis of procedural blanks, analysis of replicate samples, and use of recovery surrogate. Pure reference standard solutions (EPA 625/CLP Pesticides Mix 2000 $\mu\text{g}/\text{ml}$ - Supelco) were used for instrument calibration, recovery determination and quantification of compounds. All solvents (acetone, dichloromethane, hexane), reagents and chromatographic silica gel used for analysis were HPLC grade from Sigma-Aldrich (St. Louis, MO, USA).

The statistical analysis of the data was based on the comparison of mean values by a t-test at a statistical significance $p < 0.05$.

Table 1. GC/IT-MSn detection parameters of individual organochlorine compounds - retention times, precursor ions, voltage and product ions.

OCPs	RT (min)	Precursor ion (m/z)	Segment start (min)	Voltage (V)	Product ions (m/z)
Heptachlor	12.50	272	12.30	2.5	235+237+239
Aldrin	13.60	263	13.40	2.0	191+227+263
Heptachlor epoxide	14.91	353	14.70	3.0	253+261+263+282
p,p'-DDE	16.94	246	16.80	3.0	269+290+323+358
Dieldrin	17.20	263	17.00	2.0	205+221+249
Endrin	17.73	263	17.60	2.0	191+227+263
Endosulfan_I	18.04	195	17.95	4.0	123+159+161
p,p'-DDD	18.37	235	18.20	2.0	165+199
Endrin aldehyde	18.69	345	18.60	2.5	243+279+281+315
p,p'-DDT	19.66	235	19.60	2.2	165+199

RESULTS AND DISCUSSION

Population characteristics

The participating women were between 25 and 40 years old, with a mean age of 30.2 years. The mean pre-pregnancy body mass index (BMI) of 21.1 kg/m² indicated a normal BMI (BMI range 18.5–24.9). The consumption of meat and eggs from 2 to 4 times per week was reported by 60% and 51% of participants, respectively. Milk and milk products were part of the daily menu of almost half of the mothers (49%). In our study group, 93% of the mothers consumed fish much less than the World Health Organization recommendations (twice a week). Seafood consumption has been suggested as a major contributor to human exposure to POPs from a number of authors [7, 10]. Less than 30% of the participants in the present study defined themselves as smokers before pregnancy. Lipid content in milk samples was in the range of 0.8% to 5.7% (mean value 3.2%).

Levels of OCPs residues in breast milk

A total of 10 organochlorine pesticides were analyzed including: 1,1,1-trichloro-2,2-bis(p-chlorophenyl) ethane (p,p'-DDT), 1,1-dichloro-2,2-bis(p-chlorophenyl)ethene (p,p'-DDE) and 1,1-dichloro-2,2-bis(p-chlorophenyl)ethane (p,p'-DDD),

heptachlor, aldrin, heptachlor epoxide, endosulfan, endrin aldehyde, dieldrin and endrin. The residues of organochlorine pesticides were determined in 45 samples from mothers living in two regions of Northeast Bulgaria – Varna and Dobrich. The summarized results regarding levels of OCPs are reported in Table 2.

The OCPs contamination profile in breast milk was dominated by p,p'-DDE, detected in 100% of samples (both Varna and Dobrich) – Table 2. The p,p'-DDT positive milk samples from Varna were found lower than the positive samples from Dobrich (25.9% and 56.0%, respectively). p,p'-DDD was present in 22.2% and 20.0% of breast milk samples from Varna and Dobrich, respectively. p,p'-DDE, the main metabolite of DDT, was found in all breast milk samples at levels ranging from 16.89 to 94.48 ng/g lipids, mean 42.86 ng/g lipids and contributed 86.6% to the Sum DDTs (sum of DDE, DDD and DDT). Mean DDT concentration in human milk from Dobrich (typical rural area) was measured higher than in samples from Varna (8.44 ng/g and 3.18 lipids, respectively). The lowest levels were found for the metabolite p,p'-DDD, for which almost 80% of the results were below the LOQ (Table 2). These results showed that residues of DDT can still be found in the human body thirty years after its ban, due to its distribution in the environment.

Table 2. Organochlorine pesticides concentrations (mean, ng/g lipid weight) in the human milk samples collected from Varna and Dobrich regions, Bulgaria

Compound	Varna region (N = 27)					Dobrich region (N = 18)			
	% of positive samples ≥ LOQ ^a	ng/g lipid weight			% of positive samples ≥ LOQ ^a	ng/g lipid weight			
		Mean	95th percentile	Range ^b		Mean	95th percentile	Range ^b	
p,p'-DDE	100	48.93	87.22	16.89 – 94.48	100	33.75	48.38	18.77 – 50.05	
p,p'-DDD	22.2	2.50	12.85	< LOQ – 13.11	20.0	1.90	11.30	< LOQ – 12.56	
p,p'-DDT	25.9	3.18	14.51	< LOQ – 16.30	56.0	8.44	15.53	< LOQ – 18.30	
Heptachlor	0	nd	–	–	0	nd	–	–	
Aldrin	0	nd	–	–	0	nd	–	–	
Heptachlor epoxide	3.7	0.04	–	< LOQ – 1.07	0	nd	–	–	
Endosulfan	0	nd	–	–	0	nd	–	–	
Endrin aldehyde	22.2	1.50	–	< LOQ – 2.06	11.1	1.63	–	< LOQ - 1.80	
Dieldrin	0	nd	–	–	0	nd	–	–	
Endrin	0	nd	–	–	0	nd	–	–	

^a LOQ – Limit of quantification; ^b Concentration ranges (min – max), nd – not detected, N – number of individual milk samples

The residual amounts of DDE found in the breast milk samples from both studied regions are due to past use of the pesticide DDT and its metabolism. A similar distribution pattern of DDTs in human milk was reported by several authors in Belgium [10], Czech Republic [11], Croatia [12], Norway [13]. The Sum DDTs in breast milk from Varna (54.62 ng/g lipids) was found higher than DDTs levels in milk samples from Dobrich (44.08 ng/g lipids).

Heptachlor, aldrin, endosulfan, dieldrin, endrin were not detected in any of the milk samples. Similar results reported Dong *et al.*, 2022 [14]. Heptachlor epoxide was found in one milk sample only. Endrin aldehyde was detected in 17.8% of all milk samples in the range from 1.25 to 10.51 ng/g lipids (from both Varna and Dobrich). The low levels of OCPs observed in breast milk samples correspond to the fact that these environmental pollutants were banned in Europe more than three decades ago.

Impact of maternal age and pre-pregnancy BMI

Because of the long biological half-lives of persistent pesticides and continuous human exposure to environmental pollutants, the concentrations of OCPs in the human body fat are expected to increase with age [13]. Maternal age has been reported as an important determinant affecting residual OCP levels in human milk [11–14]. The results in the present study were summarized by age groups and showed a positive relation between concentration of metabolites DDE and DDD and the age of mothers - Fig. 1.

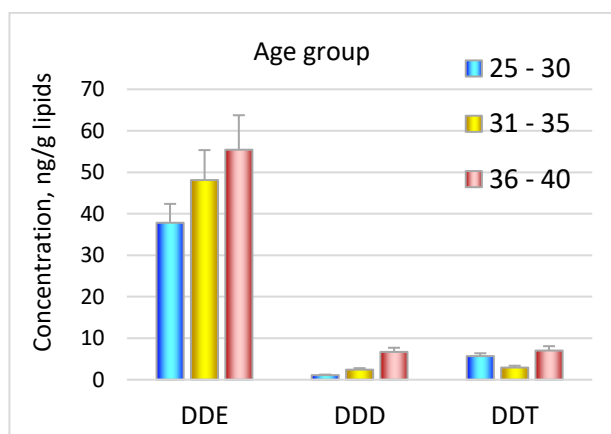


Figure 1. Distribution pattern of DDTs (ng/g lipids) in breast milk by age groups of the study population.

The mean value of the Sum DDTs in the breast milk samples was lowest in mothers aged 25-30 years (44.6 ng/g lipids), in general for both regions – Fig. 2. The levels of total DDTs in breast milk samples increased by age groups 31 – 35 and 36 – 40 years (53.47 ng/g and 69.16 ng/g lipids, respectively). The data obtained may be due to the

longer exposure to DDTs of the 36 – 40-year mothers through their diet (as the main route of exposure). The comparison of DDTs residues detected in milk samples from different age groups showed that concentrations were found significantly higher ($p < 0.05$) for mothers from Dobrich in 25-30 age than those in 31-35 age (39.33 ng/g and 61.54 ng/g lipids, respectively). Significant associations between OCPs levels in breast milk and age of *primiparae* mothers were described in a number of studies [10-13].

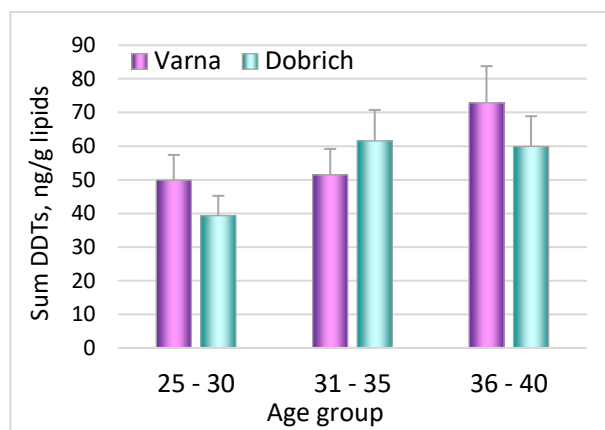


Figure 2. Comparison of Sum DDTs levels in breast milk samples from different age groups (Varna and Dobrich regions).

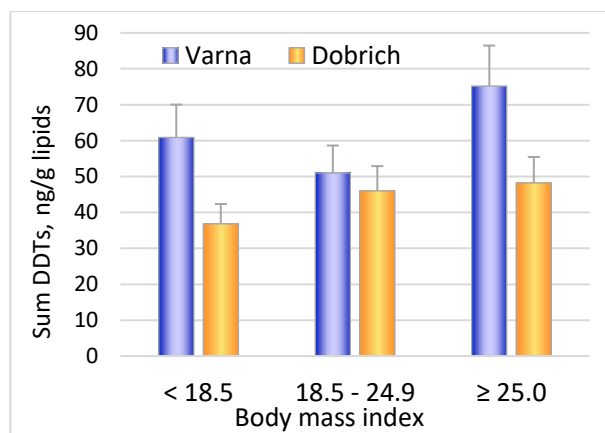


Figure 3. Comparison of Sum DDTs levels in breast milk by BMI groups (Varna and Dobrich regions).

A higher body mass index (BMI) may be associated with a higher body fat content in the human body, suggesting an accumulation of lipophilic pollutants in the adipose tissue of living organisms, including humans [4]. Several authors described a positive correlation between BMI and the serum levels of organochlorine compounds p,p'-DDE in pregnant women [4, 7]. Donors with normal BMI (18.5 – 24.9 kg/m²) were the predominant group (73% of all participants studied) with the average value of Sum DDTs in breast milk samples – 49.02 ng/g lipids (Fig. 3). The comparison of DDTs levels in milk by BMI of participants showed

statistically significant difference ($p < 0.05$) between mothers from Varna with normal and high BMI (51.0 ng/g and 75.2 ng/g lipids, respectively). The milk samples from mothers with body mass index BMI ≥ 25 showed the highest Sum DDTs (mean value 66.2 ng/g lipids). Breast milk samples from Dobrich did not show a statistically significant difference in the levels of DDT and metabolites depending on the body mass index.

Comparison with other studies

In the present study, a total median OCPs concentration was 47.07 ng/g lipids. Similar OCPs

levels were reported in Belgium by Aerts *et al.*, 2019 [10] and in Croatia by Jovanović *et al.*, 2019 [12]. Relatively higher concentrations of chlorinated pesticides were reported by Iszatt *et al.*, 2019 in Norway (mean, 88 ng/g lipids) [15] and Antignac *et al.*, 2016 in France (median, 106 ng/g lipids) [16]. The median levels of Sum DDTs (DDT, DDE and DDD) in breast milk samples from northeastern Bulgaria were comparable to the median levels reported by other studies - Table 3. Significantly higher were the levels of DDTs in India, one of the largest producers of pesticides in the world and first among the Asian countries [17].

Table 3. Comparison of median concentrations (ng/g lipid weight) of DDTs in human milk from European and Asian countries

Country	Period	N	Sum DDTs, ng/g lipids	Ref.
Bulgaria	2019 – 2021	45	46.8	Present study
Croatia	2014	79	16.8	[12]
Czech Republic	2019 – 2021	231	77	[11]
France	2011 – 2014	42	62.2	[16]
Belgium	2014	206	39.75	[10]
China	2016	60	57.4	[14]
India	2020	130	790.1	[17]

N – number of samples

CONCLUSIONS

Worldwide restrictive and preventive measures regarding persistent pollutants have resulted in a reduction in the residues of a large group of OCPs in human tissues. The pesticide DDT and its metabolites DDE and DDD are still present in traceable amounts in human milk. The residues of the main metabolite DDE indicate usage of DDT in the past. The mean level of DDTs in breast milk from Varna region was found higher than that in samples from Dobrich. Maternal age and pre-pregnancy BMI were found to be the major determinants for the pesticide residues in breast milk samples. Levels of OCPs in breast milk from the northeastern region of Bulgaria were comparable to the levels measured in other European countries. Future studies have to be focused to even further reduce human exposure to POPs and reduce *in utero* and lactation exposure of infants.

REFERENCES

1. A. S. E. Santos, J. C. Moreira, A. C. S. Rosa, V. M. Câmara, A. Azeredo, C. I. R. F. Asmus, A. Meyer, *Int. J. Env. Res. Pub. Health*, **20**(1), 778 (2022).
2. ATSDR. Toxicological Profile for DDT, DDE, and DDD, (2019).

3. S. Beduk, A. Aydin, M. Ulvi, E. Aydin, *Wat. Wastewat. Manag.*, Springer, 2022.
4. T. Fernández-Cruz, E. Martínez-Carballo, J. Simal-Gándara, *Environ. Int.* **100**, 79 (2017).
5. Stockholm Convention on persistent organic pollutants (POPs), Revised text. UNEP, 2019.
6. Human biomonitoring: facts and figures. Copenhagen: WHO Europe, 2015.
7. M. van den Berg, K., Kypke, A., Kotz, A., Tritscher, S. Y., Lee, K., Magulova, H., Fiedler, R. Malisch, *Arch. Tox.*, **91**(1), 83 (2017).
8. R. Malisch, P. Fürst, K. Šebková, *Persistent Organic Pollutants in Human Milk*. Springer. 2023.
9. S. Georgieva, T. Trifonova, Z. Peteva, *Int. J. Hyg. Env. Health.*, **251**, (2023)
10. R. Aerts, I. Van Overmeire, A. Colles, M. Andjelković, G. Malarvannan, G. Poma, E. Den Hond, E. Van de Mierop, M. C. Dewolf, F. Charlet, A. Van Nieuwenhuysse, J. Van Loco, A. Covaci, *Environ. Int.*, **131**, 104979 (2019).
11. O. Parizek, T. Gramblicka, D. Parizkova, A. Polachova, K. Bechynska, D. Dvorakova, M. Stupak, J. Dusek, J. Pavlikova, J. Topinka, R. J. Sram, J. Pulkrabova. *Sci. Tot. Environ.*, **871**, 161938 (2023).
12. G. Jovanović, S. H. Romanić, A. Stojić, D. Klinčić, M. M. Sarić, J. G. Letinić, A. Popović, *Ecotox. Environ. Safety*, **172**, 341 (2019).

13. [13] A. Polder, J. U. Skaare, E. Skjerve, K. B. Løken, M. Eggesbø, *Sci. Tot. Environ.*, **407**(16), 4584 (2009).
14. Y. Dong, S. Yin, J. Zhang, F. Guo, M. Aamir, S. Liu, K. Liu, W. Liu. *Sci. Tot. Envir.*, **830**, 154617 (2022).
15. N. Iszatt, S. Janssen, V. Lenters, C. Dahl, H. Stigum, R. Knight, S. Mandal, S. Peddada, A. González, T. Midtvedt, M. Eggesbø, *Microbiome*, **7**(1), 34 (2019).
16. [J. P. Antignac, K. M. Main, H. E. Virtanen, C. Y. Boquien, P. Marchand, A. Venisseau, I. Guiffard, E. Bichon, C. Wohlfahrt-Veje, A. Legrand, C. Boscher, N. E. Skakkebæk, J. Toppari, B. Le Bizec, *Environ. Poll.*, **218**, 728 (2016).
17. N. Dwivedi, A. A. Mahdi, S. Deo, *Environ. Research*, **221**, 115216 (2023).

Chamelea gallina from the Black Sea (Bulgaria) as a sustainable source of macronutrients and fat-soluble vitamins

A. Merdzhanova*, D. A. Dobрева, V. Panayotova, K. Peycheva, T. Hristova, R. Stancheva

Medical University of Varna, Department of Chemistry, 84 Tzar Osвoboditel Blvd., 9000 Varna, Bulgaria

Received: November 3, 2023; Revised: April 11, 2024

Marine bivalves are characterized as highly nutritional, easily digestible food, low in calories but high in proteins. Seafood nutrition data is useful for assessing the contribution to nutrient intake and for to the development of dietary guidelines. The aim of the present study is to determine the chemical composition: crude proteins, total lipids, carbohydrates, energy value and fat-soluble vitamins in white sand clam (*Chamelea gallina*). The samples were harvested from the Bulgarian coast of the Black Sea in the summer and autumn periods. Crude protein, carbohydrates and total lipids were determined using standard procedures. The fat-soluble vitamins were analysed simultaneously using high-performance liquid chromatography with ultraviolet and fluorescence detectors (HPLC-UV/FL). Analysed samples were characterised by high protein (16.4 ± 0.2 to 18.2 ± 0.1 g.100g⁻¹ ww) and low lipid content (2.26 ± 0.06 to 2.67 ± 0.13 g.100 g⁻¹ ww). Lipid levels showed greater variations compared to proteins. Carbohydrates varied between 1.72 and 2.85 g.100g⁻¹ ww and the energy values – between 99.3 and 101.3 kcal.100g⁻¹ ww. Higher amounts of all-trans retinol, cholecalciferol and vitamin K were found in the autumn samples, whereas α -tocopherol content decreased from summer to autumn. The present study reveals new data on the chemical composition of *C. gallina* harvested from the Bulgarian Black Sea coast. Despite the variations in their composition, *C. gallina* clams could be a healthy choice of low energy dense food due to high protein and fat-soluble vitamin levels and low lipid, carbohydrate and calorie contents.

Key words: *Chamelea gallina*, macronutrients, fat-soluble vitamins, Black Sea

INTRODUCTION

One of the most important resources of basic and essential nutrients for human health are marine bivalves. According to FAO [1] the seafood is easily digestible, a valuable source of dietary proteins, polyunsaturated fatty acids, fat-soluble vitamins and several biologically active components. Data on the nutritional composition of native marine species are useful for assessing their contribution to nutrient intake and for developing national dietary guidelines. Since 2012 striped venus clam *Chamelea gallina* is commercially exploited in the Bulgarian Black Sea part, maximum catches reaching 506 tonnes in 2019 [2]. It is well known that in bivalve organisms the proteins have a structural role, whereas lipids act as basic energy sources for sustaining mussel growth and development. Essential elements such as K, Na, Ca and Mg are crucial for vital physiological functions in organisms. Insufficient intake of macronutrients and essential elements can affect human health and lead to the development of different non-chronic diseases [3]. The high content of fat-soluble vitamins, especially vitamin D₃, is a specific characteristic of marine lipids and significantly increases their quality from nutritional point of view. Moreover, the differences in proximate composition and fat-

soluble vitamins content in bivalve tissues may be important not only for its optimal survival and reproductions, but for its nutritional quality. Thus, the evaluation of the chemical composition, macroelements and fat-soluble vitamins content may increase consumer's interest and predict the market feasibility of the white clam *Ch. gallina* in Bulgaria. Limited information on *Ch. gallina* nutritional quality characterized through proximate composition, macroelements (Na, K, Ca and Mg) and fat-soluble vitamins (A, E, D and K) content was found in the scientific literature. Moreover, studies of seasonal changes in the macronutrient contents of the white sand clam (*Ch. Gallina*) from the Bulgarian part of the Black Sea are lacking. The aim of the present study is to determine the chemical composition: crude proteins, total lipids, carbohydrates, energy value, macroelements and fat-soluble vitamins in white sand clam (*Ch. gallina*).

MATERIALS AND METHODS

Sample collection and preparation

Samples of white sand clam *Ch. gallina* were collected from the Northern part of Bulgarian Black Sea coast and were harvested in June and October 2021. For each specimen, the main biometric parameters were measured individually. One

* To whom all correspondence should be sent:

E-mail: a.merdzhanova@gmail.com

kilogram of white clam was brought to the laboratory. Only clams of medium size were taken for analyses. The specimens were washed, shucked and placed on a filter paper to absorb the excess moisture and then the flesh was removed.

Proximate composition analysis

The homogenized clam tissue (2.000 ± 0.005 g) was dried at $105 \pm 2^\circ\text{C}$ in an air oven for 18-20 hours to a constant weight [4]. The crude protein content was determined by Kjeldahl's method [5]. The total lipids (TL) were estimated according to the method of Bligh & Dyer [6]. The carbohydrates were determined according to BDS 13488:1976 [7]. The energy values based on fat, protein and carbohydrate contents were calculated according to WHO/FAO [8] Atwater specific coefficients (4.0 kcal.g^{-1} for proteins and carbohydrates, 9.0 kcal.g^{-1} for lipids).

Macroelements analysis

1 g wet weight (ww) of homogenized *Ch. gallina* tissue was mixed with $8 \text{ cm}^3 \text{ HNO}_3$ (65% w/v) and $2 \text{ cm}^3 \text{ H}_2\text{O}_2$ (30 %w/v), placed in Teflon vessels and digested in a microwave closed-vessel digestion system MARS 6 (CEM Corporation, USA). A 3-stage program was used according to the procedure given by Peycheva et al. [9]. The concentrations of Na, K, Ca and Mg in the samples were determined using ICP-OES spectrometer (Optima 8000, Perkin Elmer, USA).

Fat-soluble vitamin analysis

The astaxanthin, β -carotene and cholesterol contents in the edible clam tissue were evaluated. An aliquot of the homogenized sample (1.000 ± 0.005 g) was weighed and 0.3M methanolic KOH was added. Six parallel samples were prepared and subjected to saponification at 50°C for 30 min. The fat-soluble components of interest were extracted with two portions of n-hexane: dichloromethane = 2:1 solution. The combined extracts were evaporated and the dry residue was dissolved in methanol: dichloromethane and injected ($20 \mu\text{l}$) into the HPLC/UV/FL system. All fat-soluble compounds were analysed simultaneously by an HPLC system, equipped with an RP analytical column (Synergi

Hydro-RP (80 \AA , $250 \times 46 \text{ mm}$; $4 \mu\text{m}$). The results were expressed as μg per 100 g wet weight ($\mu\text{g.100 g}^{-1}\text{ww}$).

Statistical analysis

Analyses for the chemical composition, macroelements and fat-soluble vitamins were performed in six replicates and the results were expressed as mean values \pm standard deviation (SD). Mean values were compared by one-way ANOVA followed by a post-hoc Tukey's test. Statistical significance was considered at $p \leq 0.05$ (Graph Pad Prism 6).

RESULTS AND DISCUSSION

Proximate composition

The specific abiotic factors across the water basins significantly affect the proximate composition of bivalve species. According to FAO [1,8] the macronutrients proportions are species-specific and usually greater intra- and interspecies variations in chemical composition are observed. In this study considerable differences in carbohydrate and protein content in sand clam *Ch. gallina* between seasons were found. The seasonal changes of proximate composition of *Ch. gallina* tissues are presented in Table 1. It is well known that bivalves contain higher protein levels compared to fish species. Venogupal and Gopakumar [10] reported that average protein content in clams from the Indian Ocean varied between $9\text{-}14.5 \text{ g.100 g}^{-1}\text{ww}$. Significant difference in protein content was reported for *Ch. gallina* from Marmara Sea: $7.28\text{-}7.70 \text{ g.100g}^{-1} \text{ ww}$ [11], from Azov Sea: $15 \text{ g.100g}^{-1} \text{ ww}$ [12] and Adriatic Sea: $10.40 \text{ g.100g}^{-1} \text{ ww}$ [13]. Protein content of the Black Sea *Ch. gallina* was significantly higher (up to $18 \text{ g.100g}^{-1} \text{ ww}$) compared to published results. Additionally, marine proteins are classified as rich of essential amino acids and good digestibility, which increase their nutritional quality. According to FAO [8] and Regulation (EC) No 1924/2006 [14] seafood which contains protein higher than $15 \text{ g.100g}^{-1} \text{ ww}$ can be classified as "protein-rich" source and insignificant seasonal variation in protein levels described *Ch. gallina* as a sustainable natural source of proteins.

Table 1. Seasonal variations in proximate composition ($\text{g.100 g}^{-1} \text{ ww}$) and energy values ($\text{kcal.100 g}^{-1} \text{ ww}$) of edible tissues of *Ch. gallina* from Black Sea coast

Compound Month	Lipids	Proteins	Carbohydrates	Moisture	Energy values
June	2.54 ± 0.22	17.30 ± 0.54	2.40 ± 0.25	75.70 ± 1.50	101.62 ± 3.50
July	2.67 ± 0.30	16.40 ± 0.37	2.80 ± 0.50	74.80 ± 0.95	100.83 ± 3.15
October	$2.26^{a,b} \pm 0.25$	$18.10^{a,b} \pm 0.95$	$1.85^{a,b} \pm 0.20$	76.10 ± 2.05	$99.82^{a,b} \pm 2.80$

Values with ^{a,b} are significantly different ($p < 0.05$) ^a-June vs. October; ^b-July vs. October

Total lipid (TL) content showed an opposite pattern compared to proteins, with the highest values in summer (July - 2.67g.100g⁻¹ ww) and lowest in October (2.26 g.100g⁻¹ ww). One possible reason is the accumulation of energy reserve prior to gametogenesis (June-July) in this clam species. Generally, no significant variation was observed for TL values in *Ch. Gallina*. The average TL content during the analysed months was below 3 g.100g⁻¹ ww, thus white clam can be classified as “low lipid” species [14]. Significantly lower amounts for TL content were reported for Marmara Sea striped venus clam – 0.59 (June) to 1.06 g.100g⁻¹ ww (October) (Özden et al., 2009) [11], for Azov Sea clam – 0.9 g.100g⁻¹ ww (Bityutskaya et al., 2021) [12], whereas Adriatic Sea white clam showed a similar pattern-decrease of TL in summer: 1.55 g.100g⁻¹ ww (June) to two-fold decrease in autumn: 0.73 g.100g⁻¹ ww (September) (Orban et al., 2007) [13].

According to Venogupal and Gopakumar [10] the carbohydrate content in shellfish is low. In the present study, a seasonal pattern in the carbohydrate contents is observed and decrease in autumn period (up to 1.84 g.100g⁻¹ ww), compared to summer months was found. One possible explanation is that the carbohydrate levels (as energy reserves) can vary- utilise or accumulate in response to changes in environmental conditions [13]. Similar seasonal decrease of carbohydrate content in autumn samples was reported for Adriatic Sea *Ch. gallina* [13], whereas Özden et al. [11] showed significantly higher levels for carbohydrates in the range of 4.44 (June) to 3.40 g.100g⁻¹ ww (October). Bityutskaya et al. [12] reported a higher level of carbohydrates in samples collected in Azov Sea (3.4 g.100g⁻¹ ww). There is no comparable data for proximate composition of white clam *Ch. Gallina* from Bulgarian Black Sea coast in the scientific literature. The analysed venus clam demonstrated constant seasonal levels of the energy values which depend on primary metabolites content and showed a minor change mainly related to a decrease in lipid and

carbohydrate amounts. The calculated energy levels of *Ch. gallina* edible tissues are in the range of 99.82 – 101.83 kcal.100g⁻¹ ww. Based on the results obtained throughout the study period, the clam presented a low energy content. Significantly lower energy values are reported for Marmara Sea *Ch. gallina* – average 66.5 kcal.100⁻¹ g ww [11] and for Azov Sea white clam – 58 kcal.100⁻¹ g ww [12]. This difference is due to the significantly lower amounts of total lipids and proteins found for this species.

Macroelement contents

Macroelements play an important role in various metabolic processes. Their deficiency can lead to a number of chronic diseases; therefore, it is necessary to maintain an adequate intake through a balanced diet rich in these elements. Potassium is a very important, osmotically active inside cell element, acting together with sodium in regulation of body's water balance. The recommended from EFSA sodium RDI is safe and can reduce risks of CVD development in adult population. In addition, magnesium and calcium can prevent CVD, osteoporosis and certain cancer forms. Bivalve species usually accumulate the physiologically active macroelements in their edible tissues [11,13]. This statement is well illustrated in the present study since the analyzed clam species is a good source of sodium and potassium, especially in the autumn months. The seasonal changes of macroelements content of *Ch. gallina* edible tissues are presented in Table 2. Significant seasonal differences (p<0.05) in macroelement contents were observed. The highest concentration of all analysed elements were found in autumn months. It is well known that sodium is naturally present in foods of animal origin such as white clams. This statement is confirmed by the obtained results, where, sodium has the highest levels (over 4000 mg.kg⁻¹ ww), among all elements while magnesium has the lowest concentration. K, Ca and Mg have stable levels during the summer months, while the largest fluctuations (p<0.05) are determined for sodium.

Table 2. Seasonal variations in macroelements content (mg.kg⁻¹ ww) of edible tissues of *Ch. gallina* from Black Sea coast

	K	Na	Ca	Mg
June	1605.20±180.16	2968.70±136.6	786.4±178.8	573.5±25.0
July	1527.30±112.47	1988.40±115.63	749.5±108.42	546.72±13.77
October	2171.5±229.40 ^{a,b}	4037.20±281.95 ^{a,b}	1759.40±190.50 ^{a,b}	958.5±85.50 ^{a,b}

Values with ^{a,b} are significantly different (p < 0.05) ^a-June vs. October; ^b-July vs. October

Table 3. Seasonal variations in fat-soluble vitamin content ($\mu\text{g}\cdot 100^{-1}\text{g ww}$) of edible tissues of *Ch. gallina* from Black Sea coast

	Vit A	Vit E	Vit D ₃	Vit K
June	35.60±5.52	7673.00±350.50	40.10±5.20	52.00±6.50
July	40.50±8.35	8200.00±410.10	39.65±3.45	55.84±5.30
October	38.60±10.15	6377.00±280.24 ^b	41.70±6.10 ^b	56.30±5.27 ^a

It can be summarised that the macroelements show the following pattern of distribution during the study period: Na > K > Ca > Mg. The EFSA has developed the recommended daily intake (RDI) for these macroelements: for potassium 3500 mg.d⁻¹ (2016)[15]; for sodium 2000 mg.d⁻¹ (2019)[16]; for magnesium (2015)[17] 350 mg.d⁻¹ and for calcium (2015)[18] 750 mg.d⁻¹ for men and 700 mg.d⁻¹ for women. The presented results show that a 100 g portion of the white clam edible tissues (autumn samples) can provide over 200% of the RDI for Na, Ca and Mg, while up to 62% of RDI for K. Significantly higher contents for all analysed macroelements were reported for Marmara Sea *Ch. gallina* [11], for Adriatic Sea [13] and Azov Sea [12] white clams. As filter-feeding species bivalves can intake macroelements through seawater and food. Observed differences compared to presented results may be due to specific abiotic environmental factors as salinity, temperature, available foods and other.

Fat – soluble vitamins

Fat-soluble vitamins are essential metabolites for the optimal homeostasis, reproductive cycle and growth of bivalves. Mussels are among marine animal species that are characterized as good sources of vitamins. In their edible tissues, these substances significantly vary depending on the season of catch, the size of the individuals, the reproductive period, the nutrients received through their food intake, etc. In this study fat soluble vitamins are expressed as an average and standard deviation (mean ±SD) and the results are shown as microgram per 100 grams wet weight ($\mu\text{g}\cdot 100^{-1}\text{g ww}$) in Table 3.

The average content of the three analysed vitamins over the studied months for white clam species showed insignificant seasonal changes in the levels of vitamins A, D₃ and K.

The analysed fat-soluble component with high antioxidant activity is vitamin E (α -tocopherol). Among studied vitamins α -tocopherol was found in highest amount – average 7417 $\mu\text{g}\cdot 100^{-1}\text{g ww}$, with peak determined in July (8200 $\mu\text{g}\cdot 100^{-1}\text{g ww}$, $p < 0.05$). According to EFSA [19] and Ordinance No. 1/22.01.2018 of the Ministry of Health [20] the established amounts in 100 g of edible tissue of white clam *Ch. gallina* provide significantly good

amounts of vitamin E compared to the recommended daily intake (RDI) - average 57% of RDI.

In this study vitamin A was detected in lowest values - average 38.20 $\mu\text{g}\cdot 100^{-1}\text{g ww}$, which confirms that the analysed species is not a good source of this vitamin. The RDI recommendations [19] for vitamin A are between 490 $\mu\text{g}\cdot \text{d}^{-1}\text{g}$ (for women) and 570 $\mu\text{g}\cdot \text{d}^{-1}\text{g}$ (for men). Based on the average amounts determined, consumption of 100 g portion in this species provides up to 6-8% of the RDI for vitamin A. Venogupal and Gopakumar [10] reported higher values for vitamin A in the mussel species (54 $\mu\text{g}\cdot 100^{-1}\text{g ww}$), but significantly lower amount for vitamin E (750 $\mu\text{g}\cdot 100^{-1}\text{g ww}$) compared to our results. MacDonald [21] reported similar results for vitamin A (38.7 $\mu\text{g}\cdot 100^{-1}\text{g ww}$) and lower for vitamin E (790 $\mu\text{g}\cdot 100^{-1}\text{g ww}$) for the New Zealand green-lipped mussel tissues. There is limited information on *Ch. gallina* fat-soluble vitamin content. Orban *et al.*[13] reported lower vitamin E values (920 $\mu\text{g}\cdot 100^{-1}\text{g ww}$) for Adriatic Sea white clam whereas vitamin A was detected in trace amounts.

Vitamin D₃ is essential for various physiological processes and has a vital role for maintenance of normal blood levels of calcium and phosphorus. This vitamin is usually presented in high concentrations in marine lipids. In this study high content of vitamin D₃ was found – average 40.46 $\mu\text{g}\cdot 100^{-1}\text{g ww}$, which supplies over 200 % of RDI [18]. Merdzhanova *et al.* [22] reported significantly lower levels (3.10 $\mu\text{g}\cdot 100^{-1}\text{g ww}$) for vitamin D₃ in black mussel *M. galloprovincialis* from Bulgarian Black Sea coast.

Vitamin K has anti-inflammatory activity, and can act as a vital component against various chronic aging diseases. In addition, this vitamin affects age-associated diseases due to its antioxidant and anti-inflammatory effects. Popa *et al.* [23] supposed that vitamin K, along with magnesium supplementations, can affect bone fractures especially in elderly population. In the present study insignificant seasonal variations were found in vitamin K content. Average level in *Ch. gallina* edible tissue is 54.6 $\mu\text{g}\cdot 100^{-1}\text{g ww}$, supplying 78% of RDI for this vitamin [18]. There is not comparable information for Black Sea *Ch. gallina* vitamins content.

CONCLUSION

Wild striped venus clam *Ch. gallina* from the Bulgarian Black Sea coast may be classified as a food with high nutritional quality due to its proximate composition, macroelements and fat-soluble vitamin content. Regardless of the observed variations in the chemical composition, the white clam is rich in protein (average 17.30 g.100⁻¹g ww), lipid (average 2.5 g.100⁻¹g ww) and carbohydrate (average 2.35 g.100⁻¹g ww). High amounts of Na, K, Ca and Mg were determined in white clam edible tissues, which make it a valuable source of macroelements in human food. There is no available information for the seasonal changes in fat-soluble vitamin contents in striped venus clam *Ch. gallina* from the Bulgarian Black Sea coast. This species can supply over 270 % of RDI for vitamin D₃, 78 % of RDI for vitamin K and over 50% for vitamin E. Significant quantities of Ca (average 1100 mg.kg⁻¹ ww) and Mg (average 690 mg.kg⁻¹ ww) along with high levels of both vitamin D₃ and K demonstrated its promising potential in prevention osteoporosis and several non-chronic diseases.

Acknowledgement: *This study is financially supported by the National Science Fund of Bulgaria: Project # KII-06-OIIP03/11 from 18 Dec 2018.*

REFERENCES

1. FAO, The state of mediterranean and black sea fisheries, General fisheries commission for the Mediterranean, Rome, p. 172, 2018.
2. M. R. Gumus, V. R. Todorova, M. Panayotova, *Ecologia balcanica*, **3**, 63 (2020).
3. F. Biantolino, A. D. Leo, I. Parlapiano, L. Papa, S. Giandomenico, L. Spada, E. Prato, *Polish Journal of Food and Nutrition Sciences*, **69** (1), 71 (2019). <https://doi.org/10.31883/pjfn-2019-0001>.
4. AOAC 950.46. 2000, Moisture in meat and meat products, Air drying method, AOAC official methods of analysis, 17th ed., Association of official analytical chemists, Gaithersburg, MD, USA, p. 2200, 2000.
5. BDS 9374:1982, Meat and meat quality, Determination of crude protein in meat (in Bulgarian), 1982, p. 25.
6. E. Bligh, W. J. Dyer, *Canadian Journal of Biochemistry and Physiology*. **37** (8), 911 (1959).
7. BDS 13488:1976, Method for determination of starch content (in Bulgarian), 4, 1976.
8. FAO, Nutrition elements of fish, The state of fisheries and aquaculture, Rome, 2010.
9. K. Peycheva, V. Panayotova, R. Stancheva, L. Makedonski, A. Merdzhanova, N. Cicero, G. Camilleri, F. Fazio, *Human Health Risk. Natural Product Research*, (2021). Doi: 10.1080/14786419.2021.1921770.
10. V. Venugopal K. Gopakumar, *Comprehensive Reviews in Food Science and Food Safety*, **16** (6), 1219 (2017).
11. Ö. Özden, N. Erkan, Ş. Ulusoy, *International Journal of Food Sciences and Nutrition*, **60** (5), 4022 (2009).
12. O. E. Bityutskaya, L. V. Donchenko, K. I. Moshenec, Analysis of technical and chemical characteristics as well as the nutritional value of clams from the sea of Azov, *IOP Conference Series: Earth And Environmental Science*, **640**, 032045 (2021).
13. E. Orban, G. Di Lena, T. Nevigato, I. Casini, R. Caproni, G. Santaroni, G. Giulini, *Food Chemistry*, **101** (3), 1063 (2007). ISSN 0308-8146.
14. Regulation (EC) No 1924/2006 of the European Parliament and of the Council of 20 December 2006 on nutrition and health claims made on foods. OJEU. L404, 9 (2006).
15. EFSA NDA panel, Scientific opinion on dietary reference values for potassium, *EFSA Journal*, **14**, 10, 4592, 56 (2016). Doi:10.2903/j.efsa.2016.4592.
16. EFSA, Dietary reference values for sodium (2019). Doi: 10.2903/j.efsa.2019.5778.
17. EFSA NDA panel, Scientific opinion on dietary reference values for magnesium. *EFSA Journal*, **13** (7), 4186 (2015). Doi:10.2903/j.efsa.2015.4186.
18. EFSA, Dietary reference values for nutrients: summary report, *EFSA Supporting Publication*, 15121, 92 (2017). Doi:10.2903/sp.efsa.2017.e15121.
19. EFSA NDA panel, Scientific opinion on dietary reference values for calcium, *EFSA Journal*, **13**, 5, 4101, 82 (2015). Doi:10.2903/j.efsa.2015.4101.
20. Ordinance №1/22.01.2018 on the physiological feeding of population, ministry of health, Bulgaria, , 2018, (in Bulgarian).
21. G. McDonald, Identification of health and nutritional benefits of new Zealand aquaculture seafood's, Report for aquaculture New Zealand, Nelson, 2010, p. 41.
22. A. Merdzhanova, D. A. Dobрева, V. Panayotova, *Biological Resources of Water*, 181 (2018).
23. D. S. Popa, G. Bigman, M. E. Rusu, *Antioxidants*, **10** (4), 566 (2021). <https://doi.org/10.3390/antiox10040566>.

Characterization of by-products from industrial processing of the essential oil crops rose, hyssop and thyme

A. M. Slavov, G. I. Marovska*

University of Food Technologies, Department of Organic Chemistry and Inorganic Chemistry,
26 Maritsa Blvd., 4000 Plovdiv, Bulgaria

Received: November 3, 2023; Revised: April 11, 2024

Bulgaria is rich in medicinal and aromatic plants and has very well developed essential oil industry. Processing of the essential oil-bearing plants results in obtaining several main products: essential oil, water, absolute, concrete and different extracts, having applications in perfumery, cosmetics, medicine, wellness, tourism, etc. The low content of essential oil in the plants is a prerequisite for generation of large volumes of by-products. The aim of the present study is to investigate three by-products: from rose (*Rosa damascena* Mill.) – provided by Old Rose Distillery, Strelcha, Plovdiv, Bulgaria, 2020; hyssop (*Hyssopus officinalis*) – provided by Galen-N Ltd., Zelenikovo, Brezovo, Bulgaria, 2020; and thyme (*Thymus serpyllum*) – provided by EKOMAAT Ltd., Mirkovo, Sofia, Bulgaria, 2020. The three solid by-products resulted from industrial steam distillation of the raw materials. It was found that the residues were rich sources of dietary fibers: $66.77 \pm 1.08\%$, $62.28 \pm 1.15\%$, and $79.94 \pm 1.11\%$ for rose, hyssop and thyme, respectively. The by-products were subjected to extraction with hot 70% ethanol and ethanolic extracts and alcohol-insoluble parts (AIP) were obtained. The polyuronide content (PU) of the AIP by-products was in the $4.03 \pm 0.24 - 8.89 \pm 0.14\%$ range and the degree of esterification: $59.41 \pm 2.52 - 86.05 \pm 1.25\%$. The AIPs were extracted employing hot 0.1M HCl and pectic polysaccharides with $12.45 \pm 0.14\%$, $7.19 \pm 0.19\%$, and $7.31 \pm 0.23\%$ yield were obtained for the rose, hyssop and thyme, respectively. The results from the present study suggest that the by-products from the essential oil industry, namely rose, hyssop and thyme, could be successfully valorized and serve as a source of dietary fibers and pectic polysaccharides.

Keywords: *Rosa Damascena* Mill., *Hyssopus officinalis*, *Thymus serpyllum*, dietary fibers, pectic polysaccharides

INTRODUCTION

Bulgaria is among the countries rich in essential oil-bearing medicinal, edible and aromatic plants, having wide application in cosmetic, perfumery, food industry, tourism, medicine, as well as in culinary technology. Among the most famous are rose and lavender, for which the country holds one of the first places in terms of production and quality of the obtained products [1]. Moreover, a large number of other essential oil-bearing and medicinal plants, herbs and spices, such as: melissa, basil, chamomile, hyssop, thyme, lemon balm, yellow horned poppy, yarrow, etc., although industrially processed in a smaller scale, are recently gaining popularity.

The rose has been among the flowering plants most appreciated by humankind since ancient time. Its significance lies in socio-cultural life, decorative usage, symbol of appreciation, but roses are also a rich source of biologically active substances, and they are widely used by the essential oil industry. Important products obtained industrially from oil-bearing roses are aroma products: essential oil, water, absolute, etc. The most traditional processing

of roses is steam-water distillation (about 90% of the plant material processed), followed by production of rose concrete and absolute through non-polar solvent extraction (5-6%), and use of the remaining 3-4% for making rose water [1]. A relatively new treatment is supercritical CO₂ extraction [2]. On average, the essential oil amount in fresh *Rosa damascena* flowers is in the 0.030-0.045 % range [1]. For the *Rosa centifolia* and *Rosa alba*, these amounts are even lower: 0.02 % [3] and 0.015-0.030 % [4], respectively. About 3500-4000 kg of fresh *Rosa damascena* flowers are needed for every kilogram of rose oil, and approximately 2 kg of wet wastes are generated from 1 kg of the initial rose mass [5]. The residues generated are usually discarded but they could serve as a starting material for obtaining valuable substances, such as dietary polyphenols, polysaccharides, etc.

Thyme (wild thyme, *Thymus serpyllum*) is well known as a medicinal plant - for making syrups, tinctures, infusions, etc. Besides, the thyme is used for production of essential oil [6]. The main biologically active substances are thymol and carvacrol, but the plant is also rich in 1,8-cineole,

* To whom all correspondence should be sent:

E-mail: gerij_vlaseva@abv.bg

myrcene, β -caryophyllene, germacrene, etc. [7]. It has been found to possess antiseptic, antimicrobial, antitumor and cytotoxic properties, and well-expressed antioxidant activity [8, 9].

Medicinal hyssop (*Hyssopus officinalis*) is a subshrub native to the Mediterranean, North Africa, Middle East, Europe, and North America. The plant is used as a seasoning for salads, meats, soups, and sauces. Hyssop is a component in the production of some liqueurs and absinthe [10]. The plant and its essential oil has pronounced antifungal [11], antimicrobial [12], and antioxidant activity [13].

The economic growth and the increase in the areas of new or forgotten essential oil crops and production of essential oils is also accompanied by an increase in the amount of distilled plant biomass. Essential oil manufacturers are constantly looking for different technological solutions for reduction and utilization of generated plant production waste from the essential oil industry. The aim is, on the one hand, to reduce the cost of the main products of the essential oil industry. Another ecological point of view aims to reduce the impact on the environment by reducing the amount of landfill generated biodegradable waste. This can be achieved by using the distilled biomass as a raw material for obtaining secondary products.

MATERIALS AND METHODS

The solid by-products from essential oil industry were kindly provided by:

1). Old Rose Distillery, Strelcha, Plovdiv, Bulgaria, 2020 harvest; resulting from steam-water distillation of rose (*Rosa damascena* Mill.) – abbreviated as 20RD_SD_S;

2). Galen-N Ltd., Zelenikovo, Brezovo, Bulgaria, 2020 harvest; from steam distillation of hyssop (*Hyssopus officinalis*) – abbreviated as 20HO_SD_Z;

3). ECOMAAT Ltd., Mirkovo, Sofia, Bulgaria, 2020 harvest; from steam distillation of thyme (*Thymus serpyllum*) – abbreviated as 20TS_SD_M.

Immediately after the end of distillation and the distillation stills were opened, the solid residues were cooled down, checked for impurities (weeds, insects, minerals, etc.) and collected. The biomass was dried in a laboratory drier at 50°C and stored at ambient temperature until further treatment.

All the reagents used for the analyses were of analytical grade and were provided by the local suppliers.

Water-ethanolic extracts of the solid residues were prepared according to [14]. The alcohol-insoluble parts (AIP) from the extraction were further used for extraction of pectic polysaccharides.

The acidic extraction of AIP was performed as follows: 70 g of AIP was extracted with 1.4 L of 0.1 M HCl (pH 1.2) at 90°C for 1 h with constant stirring (100 rpm); the mass was filtered through nylon cloth (250 mesh) and the residue was subjected to a second extraction with 1 L of 0.1 M HCl at 90°C for 1 h. The mass was filtered and both filtrates were combined. The filtrate was precipitated with 3 volumes of 96% ethanol for 24 h at 4°C, and the precipitate was filtered through nylon cloth (250 mesh) and dried. The obtained polysaccharides were dissolved in 100 mL of distilled water and dialyzed (Spectra/Por 1, Breda, the Netherlands, Mr. cut-off 6–8 kDa) for 72 h against deionized water. The remaining solution in the dialysis membrane was freeze-dried and denoted as acid extractable polysaccharides.

The moisture content of the by-products was determined with a Kern MLB50-3 moisture analyzer (Kern&Sohn, Germany). The amount of crude protein in the by-products was determined by the Kjeldahl method with an automatic nitrogen analyzer UDK152 (Velp Scientifica, Italy) with a correction factor of 6.25. The ash content was estimated after incineration of the by-products at 605°C in a muffle furnace (MLW 212.11, MLW, Germany) to a constant weight. The degree of esterification (DE, %) and the polyuronide content (PU, %) were determined according to [15].

The amount of total, insoluble and soluble dietary fibers in the by-products were determined using K-TDFR-100A (Megazyme, Ireland), according to AOAC method 991.43 "Total, soluble and insoluble dietary fibers in foods" (First action 1991) and AACC method 32-07.01 "Determination of soluble, insoluble and total dietary fibers in foods and food products" (Final approval 10-16-91) [16].

The polysaccharides' protein content, amount of neutral sugars, and anhydrogalacturonic acid content were determined spectrophotometrically, employing the Bradford method using AMRESCO E535-KIT (AMRESCO, Solon, Ohio, USA) with bovine gammaglobulin as standard, by the phenol-sulfuric acid method with D-galactose as standard, and by the m-hydroxydiphenyl method using D-galacturonic acid as standard, respectively, as described by Slavov *et al.* [17]. The molecular weight of the isolated polysaccharides was determined using an ELITE LaChrome (Hitachi) HPLC system with a VWR Hitachi Chromaster 5450 refractive index detector, and an OHPak SB-806M (Shodex ®) column. The samples and standards were eluted with 0.1 M NaNO₃ at an elution rate of 0.8 mL/min, column temperature 30°C, and detector temperature 35°C. The column was equilibrated with Shodex pullulan (Showa DENKO, Japan) standards (2

mg/mL) with molecular weights of 6.2×10^3 , 10.0×10^3 , 21.7×10^3 , 48.8×10^3 , 113.0×10^3 , 200.0×10^3 , 366.0×10^3 , and 805.8×10^3 Da.

The degree of methylesterification (DM) and the degree of acetylation (DAc) of the isolated polysaccharides were determined as described by Slavov *et al.* [17].

The thermal properties of the polysaccharides were investigated employing differential thermal analysis-thermogravimetry (DTA-TG) with TGA Q50 (TA Instruments, Alzenau, Germany). The pectin sample (9.1480 mg, 9.5150 mg and 11.0040 mg for 20RD_SD_S, 20HO_SD_Z and 20TS_SD_M, respectively) was heated in air (air speed 20 mL/min) in a corundum crucible over the 30–550°C range with a rate of 5°C/min. The cooling was performed with 20°C/min rate from 550°C to 30°C.

Statistical analysis. The values were expressed as mean of three replicates \pm SD. Statistical significance was detected by analysis of variance (ANOVA, Tukey’s test; value of $p < 0.05$ indicated statistical difference).

RESULTS AND DISCUSSION

The general characteristics of the by-products are presented in Table 1. The analyses

were carried out to determine the main physicochemical parameters of the by-products (Table 1) suggested that rose had almost twice as high content of mineral substances (similar data were also obtained in the study of other by-products, for example, for lemon balm [18]) in comparison with thyme and hyssop. Wild thyme (20TS_SD_M) had the lowest protein content: $6.82 \pm 0.46\%$, twice

less than the other two by-products. The polyuronide content in 20HO_SD_Z and 20TS_SD_M was of the same order: around 5%, and 20RD_SD_S was distinctive with the highest content ($8.89 \pm 0.14\%$). In the following analyses, the dietary fibers content was investigated. Separate analyzes were performed to determine total and soluble and insoluble dietary fibers. From the results it could be concluded (Table 1) that the amounts of insoluble dietary fibers predominated (thyme showed the highest content with $75.79 \pm 1.12\%$), and the soluble dietary fibers amount was comparable with the data for PU (Table 1), which corresponded roughly to the amount of polyuronides (pectin-type polysaccharides). The total dietary fibers content suggested that these by-products from the essential oil industry, also taking into account their polyphenol content [19, 20], could be used to enrich food products (various types of pasta, crackers, snacks, also meat products) with dietary fibers, while also increasing the antioxidant capacity and potentially their shelf life [18].

In the following experiments, the by-products were subjected to extraction with 70% ethanol. This extractant was chosen in order to ensure maximum extractability of the low-molecular substances, such as: phenolic acids, polyphenolic compounds, terpenes, pigments, sugars, etc., depending on the selectivity of the respective extractant, but also to ensure the preservation of biopolymers (polysaccharides, proteins) in the residue after extraction – the alcohol-insoluble parts (AIP). This methodology has been previously tested with other plant materials and adapted to current by-products [21].

Table 1. General characteristics of rose, hyssop and thyme by-products

By-product Parameter, %	20RD_SD_S	20HO_SD_Z	20TS_SD_M
Moisture	8.99 ± 0.31^a	9.56 ± 0.24^a	8.95 ± 0.58^a
Ash	8.74 ± 0.36^a	5.12 ± 0.86^b	4.47 ± 0.25^b
Crude protein	13.05 ± 0.38^a	12.28 ± 0.62^a	6.82 ± 0.46^b
PU	8.89 ± 0.14^a	5.85 ± 0.12^b	4.03 ± 0.24^c
DE	62.59 ± 1.28^b	59.41 ± 2.52^b	86.05 ± 1.25^a
SDF	6.98 ± 0.76^a	$5.21 \pm 0.80^{a,b}$	4.15 ± 0.69^b
IDF	59.79 ± 1.08^b	57.07 ± 1.15^c	75.79 ± 1.12^a
TDF	66.77 ± 1.08^b	62.28 ± 1.15^c	79.94 ± 1.11^a

PU - polyuronide content; DE – degree of esterification; SDF – soluble dietary fibers; IDF – insoluble dietary fibers; TDF – total dietary fibers; The results were expressed as mean \pm SD ($n = 3$). ^{a,b,c}Different letters mean statistical difference (Tukey’s HSD test, $p < 0.05$).

Table 2. Yield and physico-chemical parameters of pectic polysaccharides extracted by 0.1 M HCl from AIPs of 20RD_SD_S, 20HO_SD_Z and 20TS_SD_M

	Yield, %	AUAC, µg/mg	DM, %	DAC, %	Neutral sugars, µg/mg	Molecular weight, × 10 ⁴ , Da	Proteins, µg/mg
20RD_SD_S	12.45±0.14 ^a	760.67±6.33 ^a	56.14±1.51 ^a	1.02±0.41 ^c	881.11±24.87 ^a	2.31±0.12 ^b	61.15±0.92 ^c
20HO_SD_Z	7.19±0.19 ^b	729.83±6.98 ^b	39.25±1.32 ^c	1.83±0.42 ^b	853.90±25.10 ^a	2.79±0.15 ^a	121.65±0.95 ^a
20TS_SD_M	7.31±0.23 ^b	667.50±5.28 ^c	48.93±2.51 ^b	2.32±0.11 ^a	791.98±19.17 ^b	2.55±0.11 ^b	71.19±0.81 ^b

AUAC – Anhydrouronic acids content; DM – degree of methoxylation; DAC – degree of acetylation; The results were expressed as mean ± SD (n = 3). ^{a,b,c}Different letters in a column mean statistical difference (Tuckey's HSD test, p < 0.05).

Table 3. Uronic acids and monosaccharides composition of pectic polysaccharides extracted by 0.1 M HCl from AIPs of 20RD_SD_S, 20HO_SD_Z and 20TS_SD_M

	GlcA	GalA	Gal	Rha	Ara	Fuc	Xyl	Man
	(µg/mg polysaccharide)							
20RD_SD_S	25.13±2.14 ^a	742.44±5.89 ^a	191.24±8.37 ^a	54.78±3.47 ^a	51.47±6.31 ^a	1.17±0.10 ^c	1.24±0.47 ^c	33.56±1.23 ^a
20HO_SD_Z	9.34±0.11 ^c	710.06±3.15 ^b	110.31±1.54 ^b	39.70±2.04 ^b	43.56±1.59 ^b	1.57±0.10 ^b	11.26±0.87 ^b	25.14±1.56 ^b
20TS_SD_M	12.01±0.11 ^b	639.18±4.13 ^c	181.20±1.25 ^a	51.13±1.58 ^a	36.85±1.04 ^c	1.79±0.15 ^a	15.36±0.80 ^a	31.81±1.17 ^a

GlcA – D-Glucuronic acid; GalA – D-Galacturonic acid; Gal – D-Galactose; Rha – L-Rhamnose; Ara – D-Arabinose; Fuc – L-Fucose; Xyl – D-Xylose; Man – D-Manose. The results were expressed as mean ± SD (n = 3). ^{a,b,c}Different letters in a column mean statistical difference (Tuckey's HSD test, p < 0.05).

Furthermore, the AIPs were subjected to acid extraction employing 0.1 M HCl for one hour at 85°C. This extraction resembles the industrial process for extraction of pectin from citrus and apple pulp (by-products from the fruit juice manufacturing) and serves as rough estimation for the amount of pectic polysaccharides which could be obtained following the industrial protocols [22]. The yield and the physico-chemical characteristics of the obtained pectic polysaccharides are presented in Table 2.

AIPs of rose by-products (20RD_SD_S): 12.45±0.14% showed the highest yield of acid-soluble pectic polysaccharides. The other two by-products yielded approximately two times lower amounts of polysaccharides. The galacturonic acid content was above 650 µg/mg polysaccharide which suggested that these polysaccharides could be regarded from industrial point of view as pectins (Table 3). The DM values suggested that the isolated pectins are middle-esterified and only the 20RD_SD_S polysaccharide had DM above 50% (56.14±1.51%). The degree of acetylation is relatively low (below 2.5%) for all pectins. The molecular weights of the polysaccharides were similar and the highest value had the 20HO_SD_Z pectin (2.79±0.15 × 10⁴ Da).

In the next experiments, the monosacchride composition of the pectins was assessed after hydrolysis with 2M trifluoroacetic acid and the data are presented in Table 3. The monosacchride present

in the highest concentration was galacturonic acid: 742.44±5.89, 710.06±3.15, and 639.18±4.13 µg/mg in 20RD_SD_S, 20HO_SD_Z, and 20TS_SD_M polysaccharide, respectively. These results are in accordance with the determination of anhydrogalacturonic content (Table 2). The galactose was the next more abundant monosacchride, followed by rhamnose and arabinose. The ratio of GalA to Rha was 13.6, 17.9, and 12.5 for 20RD_SD_S, 20HO_SD_Z and 20TS_SD_M polysaccharide, respectively. These values suggested that this treatment extracted pectic polysaccharides rich in rhamnagalacturonan I macromolecules [23].

Pectic polysaccharides are widely used in the food industry as jellifying agents, stabilizers and thickeners [17, 22]. This application is influenced by the temperature at which different food systems could be subjected to treatments. For this reason, in the next experiments the extracted polysaccharides were investigated for their thermal stability by DTA-TG. The change in the weight of the 20RD_SD_S polysaccharide in the 25–550°C range took place in three stages. When heated from 25°C to 125°C, the weight decreases by 7.5%, which is probably due to the release of bound water. Similar observations were reported by Einhorn-Stoll *et al.* [24]. The degradation of the material started after 128°C and proceeded in two stages: 128–367°C and 369–500°C. In the first stage, when the temperature rose to 367°C, the sample lost 52.1% of its weight.

Thermal destruction took place in the temperature range 128–367°C, and the maximum speed of the process was at 276.5°C. In the last stage of the process with an increase of temperature to 500°C, the weight was reduced by 30.3%. This stage was

associated with oxidative destruction of carbon residues. The peak maximum was observed at 436.2°C (Figure 1). The solid residue above 500°C was 10.1% (by weight).

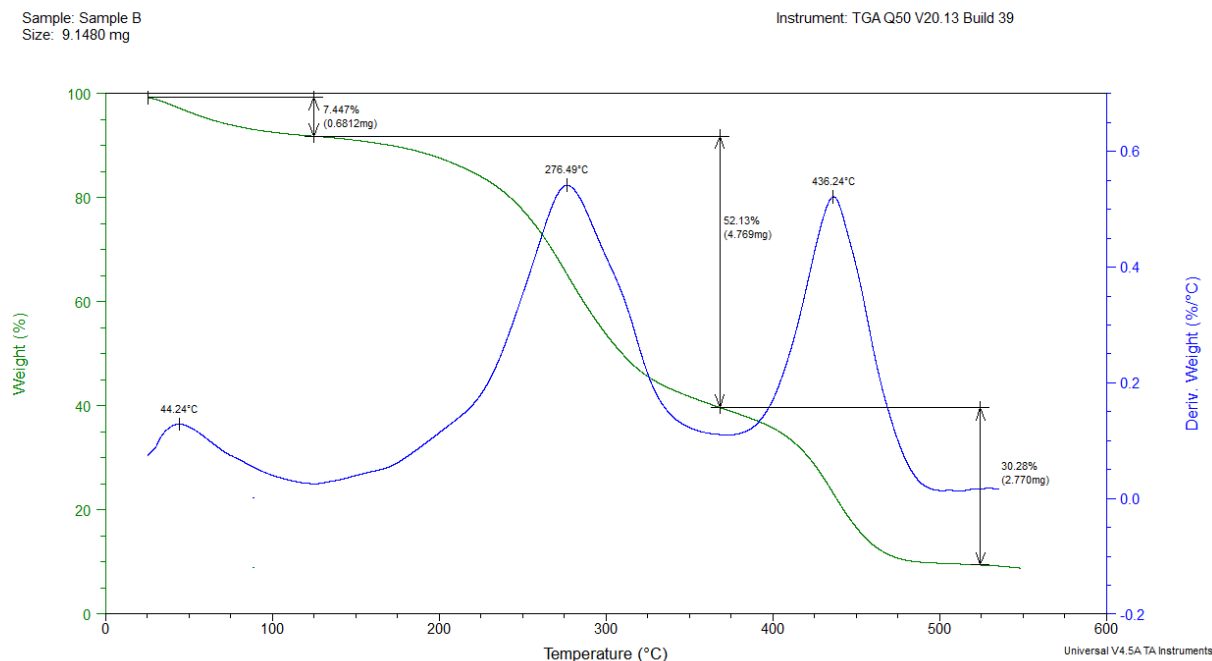


Figure 1. Thermogram of 20RD_SD_S polysaccharide

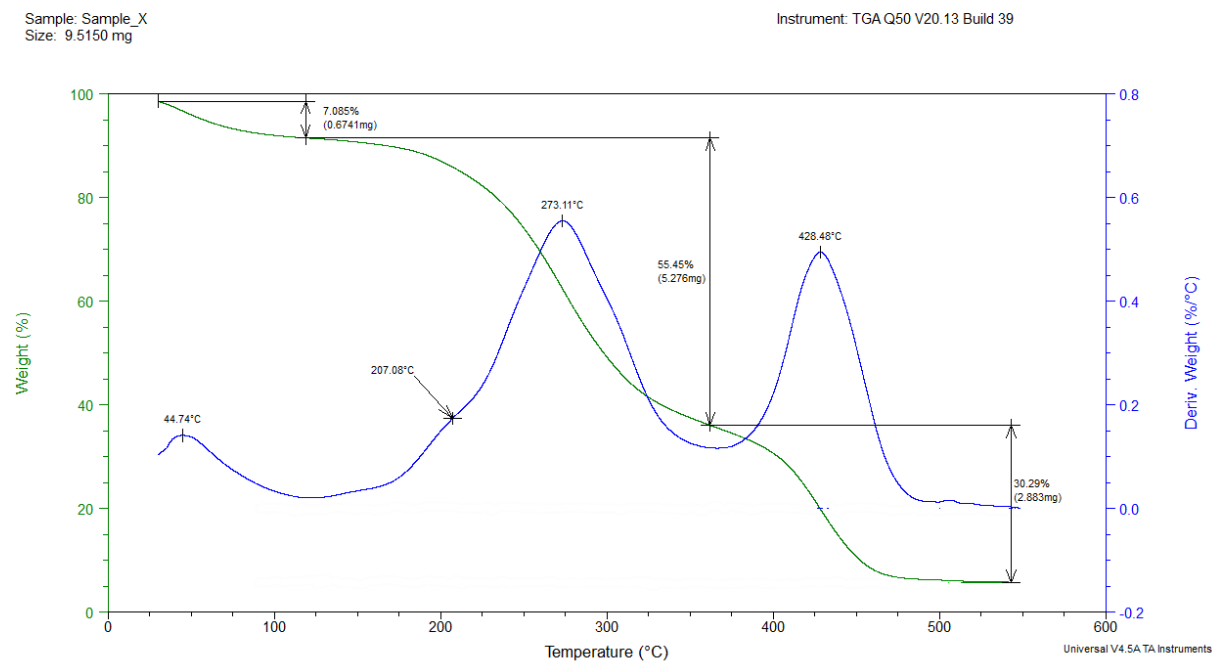


Figure 2. Thermogram of 20HO_SD_Z polysaccharide

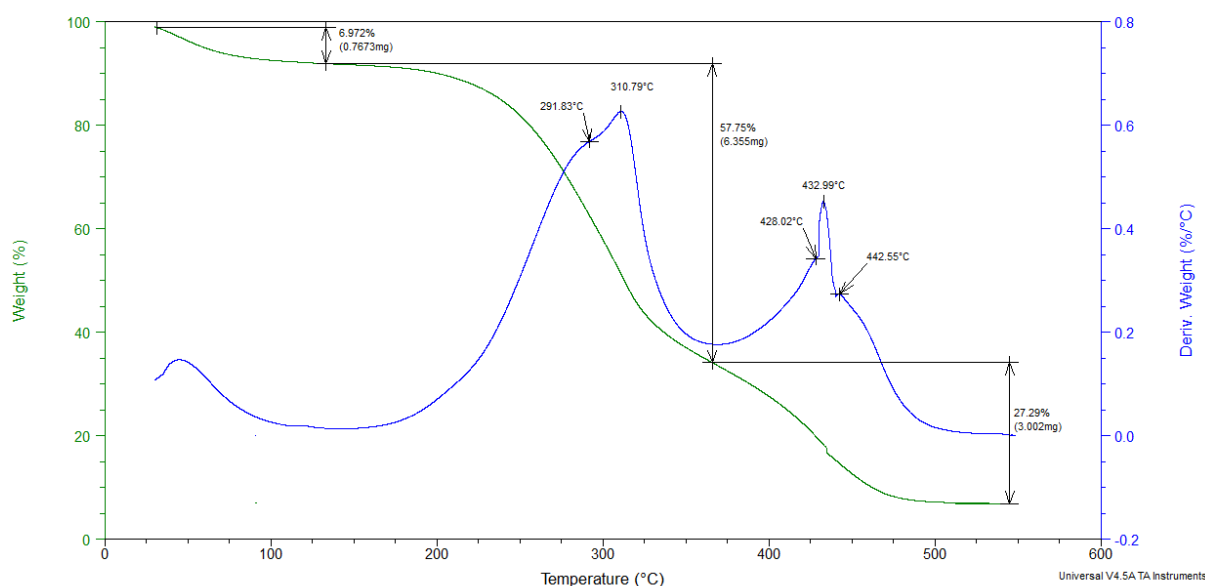


Figure 3. Thermogram of 20TS_SD_M polysaccharide

The change in the weight of the 20HO_SD_Z polysaccharide in the temperature range of 25–550°C, took place in three stages. When heated from 25°C to 119°C, the weight decreased by 7.1%, which tentatively was due to the release of water. Degradation of the material began after 124°C and proceeded in two stages: first stage in the temperature range 153–362°C and second stage 370–550°C. In the first stage, the highest rate of degradation was observed at 273.1°C, the sample lost 55.5% of its weight, and probably as a result of breaking of chemical bonds with close energy, products with a mass different from that of the main ones for the stage were released, expressed by the appearance of a second peak with a maximum at 207.1°C, which overlaps with the main one. In this stage, thermal destruction of the material took place. In the third stage of the process, with a rise in temperature to 550°C, the weight was reduced by 30.3%, with a maximum rate of decomposition at 433°C. Two secondary peaks appeared with maxima at 428 and 442.5°C, which were due to the release of oxidative degradation products of different masses (Figure 3). Einhorn-Stoll *et al.* [25] investigated the thermal stability of native and modified citrus pectins and concluded that they started to significantly decompose after 200°C. The solid residue at 550°C was 7.7% (by weight).

The change in the weight of the sample 20TS_SD_M in the temperature range of 25–550°C took place in three stages. When heated from 25°C to 133°C, the weight decreased by 7.0%, which was probably due to the release of water. The degradation of the material started after 152°C and took place in two stages: first stage in the temperature interval 153–366°C in which the sample lost 57.7% where the maximum speed of the process was at 310.8°C and second stage 370–550°C, with a weight loss of 27.6% and a maximum speed at 310.8°C. In the first

stage of degradation, probably as a result of the breaking of chemical bonds with close energy, products with a mass different from that of the main ones for the stage were released, expressed by the appearance of a second peak with a maximum at 291.2°C, which overlaps with the main one. In this stage, thermal destruction of the material took place. In the third stage of the process with a rise in temperature to 550°C, the weight was reduced by 27.6%, with a maximum rate of decomposition at 433°C. Two secondary peaks appeared with maxima at 428 and 442.5°C, which were due to the release of oxidative degradation products of different masses (Figure 3). Einhorn-Stoll *et al.* [25] investigated the thermal stability of native and modified citrus pectins and concluded that they started to significantly decompose after 200°C. The solid residue at 550°C was 7.7% (by weight).

The DTA-TG analyses suggested that the pectins isolated by acid extraction from 20RD_SD_S, 20HO_SD_Z and 20TS_SD_M had thermal stability up to 200–220°C and above these temperatures substantial degradation of polysaccharide chains was detected. Similar results for marigold pectic polysaccharides were reported by Slavov *et al.* [12].

CONCLUSION

Three solid by-products resulting from industrial steam distillation of rose (20RD_SD_S), hyssop (20HO_SD_Z) and wild thyme (20TS_SD_M) were investigated aiming at their potential valorization. It was found that the residues were rich sources of dietary fibers: 66.77±1.08%, 62.28±1.15%, and 79.94±1.11% for rose, hyssop and thyme,

respectively. The by-products were subjected to extraction with hot 70% ethanol by obtaining ethanolic extracts and alcohol-insoluble parts (AIPs). The polyuronic content of the AIP by-products was in the 4.03 ± 0.24 – $8.89 \pm 0.14\%$ range and the degree of esterification: $59.41 \pm 2.52\%$ – $86.05 \pm 1.24\%$. The AIPs were extracted by employing 0.1 M HCl and pectic polysaccharides with $12.45 \pm 0.14\%$, $7.19 \pm 0.19\%$, and $7.31 \pm 0.23\%$ yield were obtained for rose, hyssop and thyme, respectively. The DTA-TG analyses suggested that the pectins isolated by acid extraction from 20RD_SD_S, 20HO_SD_Z and 20TS_SD_M had thermal stability up to 200-220°C and above these temperatures substantial degradation of polysaccharide chains was detected. The results from the present study suggested that the by-products from the rose, hyssop and thyme essential oil industry, could be successfully valorized and serve as a source of dietary fibers and pectic polysaccharides.

Acknowledgement: We acknowledge the financial support from the National Science Fund (Ministry of Education and Science) of Bulgaria, project KII-06-Austria/4. The authors would like to thank Associate Professor Ivelina Vasileva, PhD (Department of Organic and Inorganic Chemistry, University of Food Technologies – Plovdiv, Bulgaria) for the technical support.

REFERENCES

1. E. Georgiev, A. Stoyanova, The Aromatic Industry Specialist's Guide. University of Food Technologies, Academic Publishing, Plovdiv, Bulgaria, 2006 (in Bulgarian).
2. P. B. Gomes, V. G. Mata, A. E. Rodrigues, *J. Supercrit. Fluids*, **41**, 50 (2007).
3. M. A. Khan, S. Rehman, *Int. J. Agric. Biol.*, **7**, 973(2005).
4. A. Dobreva, F. Tinchev, V. Heinz, H. Schulz, S. Toepfl, *Zeitschrift für Arznei- & Gewürzpflanzen*, **15(3)**, 127 (2010).
5. S. Erbaş, H. Baydar, *Rec. Nat. Prod.*, **10(5)**, 555 (2016).
6. A. Kowalczyk, M. Przychodna, S. Sopata, A. Bodalska, I. Fecka, *Molecules*, **25**, 4125 (2020).
7. K. Ložienė, J. Vaičiūnienė, P. Venskutonis, *Planta Med.*, **64**, 772 (1998).
8. S. Jarić, M. Mitrović, P. Pavlović, *eCAM*, **101978**, 1 (2015).
9. I. Rasooli, P. Owlia, *Phytochem.*, **66**, 2851 (2005).
10. Absinthe. Encyclopædia Britannica, vol. 1, 11th edn., H. Chisholm (ed.) Cambridge University Press, 1911, p. 75.
11. M. Letessier, K. Svoboda, D. Walters, *J. Phytopath.*, **149**, 673 (2001).
12. G. Mazzanti, L. Battinelli, G. Salvatore, *Flavour Frag. J.*, **13**, 2894 (1998).
13. A. Džamić, M. Soković, M. Novaković, M. Jadranin, M. Ristić, V. Tešević, P. Marin, *Ind. Crops Prod.*, **51**, 401 (2013).
14. G. Marovska, I. Hambarliyska, N. Petkova, I. Ivanov, I. Vasileva, A. Slavov, *Philipp. J. Sci.*, **152(3)**, 861 (2023).
15. M. Kratchanova, A. Slavov, C. Kratchanov, *Food Hydrocoll.*, **18(4)**, 677 (2004).
16. S. C. Lee, L. Prosky, J. W. DeVries, *J. Assoc. Off. Anal. Chem.*, **75**, 395 (1992).
17. A. Slavov, M. Ognyanov, I. Vasileva, *Food Hydrocoll.*, **101**, 105545 (2020).
18. I. Vasileva, R. Denkova, R. Chochkov, D. Teneva, Z. Denkova, T. Dessev, P. Denev, A. Slavov, *Food Chem.*, **253**, 13 (2018).
19. G. Marovska, I. Vasileva, A. Slavov, *Proceed. 11th Intern. Congress "Nutrition science with evaluation of the present and look to the future"*, 26-29 May 2022, Varna, Bulgaria, 2022.
20. R. Chochkov, R. Denkova, Z. Denkova, P. Denev, I. Vasileva, T. Dessev, A. Simitchiev, V. Nenov, A. Slavov, *Period. Polytech. Chem. Eng.*, **66(1)**, 157 (2022).
21. A. Slavov, P. Denev, I. Panchev, V. Shikov, N. Nenov, N. Yantcheva, I. Vasileva, *Ind. Crops Prod.*, **100**, 85 (2017).
22. C. D. May, *Carbohydr. Polym.*, **12**, 79 (1990).
23. M.-C. Ralet, J.-F. Thibault, in: H. A. Schols, R. G. F. Visser, A. G. J. Voragen (eds.), *Pectins and Pectinases*. Wageningen Academic Publishers, 2009, p. 35.
24. U. Einhorn-Stoll, H. Kunzek, G. Dongowski, *Food Hydrocoll.*, **21**, 1101 (2007).
25. U. Einhorn-Stoll, H. Kunzek, *Food Hydrocoll.*, **23**, 40 (2009).

Degradation of pyrene by laccase from *Trametes versicolor*

M. S. Brazkova^{1*}, R. Y. Koleva², G. V. Angelova¹, A. I. Krastanov¹

¹Department of Biotechnology, University of Food Technologies, 26 Maritza Blvd., Plovdiv, Bulgaria

²Department of Chemical Technologies, Burgas 'Asen Zlatarov' University, 1 Prof. Yakim Yakimov Blvd., Burgas, Bulgaria

Received: November 3, 2023; Revised: April 11, 2024

In recent years the development of eco-friendly remediation technologies with economical advantage is based on the incorporation of microorganisms or their enzyme systems in the degradation processes. In the present study purified laccase with specific activity 105.8 U/mg, obtained after submerged cultivation of the basidiomycete *Trametes versicolor*, was used in free and immobilized form for pyrene degradation. The alginate gel entrapment method and the encapsulation in amphiphilic dendritic-linear-dendritic block copolymers were applied as immobilization techniques. The free form of the enzyme was able to reduce the concentration of pyrene by 15 ppm to a final concentration of 185 ppm at the 20th day. The application of the enzyme, encapsulated in amphiphilic dendritic-linear-dendritic block copolymers, resulted in a decrease of the concentration of pyrene ranging from 4 ppm to 28 ppm for the different preparations. The degradation of pyrene with laccase immobilized in Ca-alginate gel led to a decrease in the concentration of the compound by 26 ppm for 20 days.

Keywords: Laccase, pyrene, immobilization, encapsulation, amphiphilic polymers

INTRODUCTION

The processes of vast industrialization and urbanization in recent years are tightly connected with the increasing concentrations of xenobiotic compounds in the environment. These compounds are used as intermediates in various industrial processes including the production of pesticides, personal care products, disinfectants, polycyclic aromatic hydrocarbons (PAHs), pharmaceutically active compounds, phenolic compounds and other chemicals [1]. Because of their high toxicity, they could be related to many health conditions, such as infections of the respiratory tract, disruption of the endocrine system, development disorders, and carcinogenic and mutagenic effects [2, 3]. On the other hand, they can cause harmful effects towards the ecosystems as well, due to their ability to accumulate in the food chain.

Polycyclic aromatic hydrocarbons are a group of over a hundred organic compounds widely spread in the environment. The level of their toxicity is strongly related to their structure and mostly to the number of fused benzene rings in their molecules. The persistence of these compounds makes them a serious threat to animal and human health and also leads to environmental pollution. Pyrene is a polycyclic aromatic hydrocarbon which has 4 fused benzene rings in its molecule thus making it

extremely resistant to microbial degradation. It is one of the model compounds used in PAHs degradation studies because it is abundantly found in the contaminated environment [4]. This compound enters the environment mostly through the combustion of diesel fuel, but it also is a result of the production of bleaching agents and dyes. Pyrene and its derivatives have many applications due to their unique properties such as blue emission, high chemical stability and charge-carrier mobility in diverse scientific fields like organic light-emitting diodes (OLEDs), organic field-effect transistors (OFETs) and organic photovoltaic cells (OPVs) [5]. Having in mind these factors it is easy to suppose that xenobiotics represent serious environmental problems and the urge to develop a successful detoxification technique is exigent.

Many conventional techniques used for the treatment of xenobiotic contamination failed in the research process mainly because of problems like waste disposal and high costs, but mostly because the obtained degradation products are in some cases even more toxic than the initial compound. This hazardous stage is supposed to be avoided by the implementation of biological agents in the degradation processes leading to economically advantageous and eco-friendly technology. Several bacterial representatives have proven their ability to use pyrene as a sole source of carbon and energy

* To whom all correspondence should be sent:

E-mail: mbrazkova@ufti-plovdiv.bg

© 2024 Bulgarian Academy of Sciences, Union of Chemists in Bulgaria

but this capability is presented only in laboratory-scale studies. Some white-rot fungi (WRF), macromycetes and ectomycorrhizal fungi amongst all species in the fungal kingdom are also able to fully mineralize PAHs [6]. *Trametes versicolor*, a WRF, is known for its ability to degrade various aromatic compounds, due to the synthesis of a unique enzymatic complex, containing ligninases, oxidases and laccases [7–10]. The enzymes of the lignin-degrading enzymatic system could be applied in the degradation process in native or purified form. The application of immobilized microbial enzymes in the degradation of PAHs is one of the prospective approaches because the immobilized enzymes can stay stable longer in unfavorable conditions in terms of temperature and pH. Also, these biocatalysts can be easily separated from the reaction mixtures and reused multiple times. Immobilized preparations obtained by entrapment, encapsulation, adsorption and covalent binding have been studied for their degradation capacity towards PAHs [11]. On the other hand, laccases have broad substrate specificity but only for water-soluble substrates. By the encapsulation of the enzyme in dendritic-linear-dendritic (DLD) block copolymers its substrate specificity could be extended because these polymers can selectively adhere to various surfaces and bound hydrophobic substances in aqueous medium.

The aim of this study is the evaluation of the effectiveness of purified free and immobilized laccase from *Trametes versicolor* to degrade pyrene in an aqueous medium.

MATERIALS AND METHODS

All reagents used in the experiments were of analytical grade unless otherwise stated. Pyrene (CAS Number 129-00 0,98%), acetonitrile (HPLC grade), sodium alginate and n-hexane were purchased from Merck KGaA (Germany). The DLD block copolymers were generously provided by the Department of Chemistry of SUNY College of Environmental Science & Forestry, Syracuse, NY, USA.

Microorganism and cultivation conditions

The basidiomycete *Trametes versicolor* NBIMCC 8939 is maintained on Chapek-Dox agar medium with the following composition (g/L): sucrose – 30.0; yeast extract – 5.0; NaNO₃ – 2.0; K₂HPO₄ – 1.0; MgSO₄·7H₂O – 0.5; KCl -0.5; FeSO₄·7H₂O – 0.01 and agar – 15.0 with pH 6.5 and stored in tubes at 4°C.

Liquid Chapek-Dox medium with the addition of 6mM 2-methoxyphenol was used for the enzyme

synthesis. After 144 h of cultivation on a rotary shaker at 220 rpm and 28°C the cultural broth was separated from the biomass by centrifugation at 6000 rpm for 10 minutes and the protein content and laccase activity were determined in the broth, as well as the concentration of dry biomass.

Enzyme activity and protein determination

Syringaldazine was used as a substrate for the evaluation of the laccase activity where the change of the absorption at 530 nm was monitored for 5 minutes at 37°C. The reaction mixture with a total volume of 300 µL consists of 220 µL potassium-phosphate buffer (50 mM, pH 4.5), 30 µL substrate solution (0.216 mM in methanol) and enzyme solution. One unit of enzyme activity corresponds to 0.001 change in OD at the reaction conditions and is expressed as units per mL. The total protein concentration was evaluated according to the “Bradford” method [12].

Isolation and purification of laccase

After the cultural broth was collected laccase was isolated as previously reported [7]. Briefly, the cultural broth was separated from the biomass by filtration through a glass-fibre filter followed by ultrafiltration through a 30 000 Da membrane on Millipore Prep/Scale-TFF unit and 400 mL pressure cell. After size-exclusion chromatography on Sephacryl 200-HR the blue fractions were collected and concentrated again for obtaining of a homogeneous enzyme preparation.

Immobilization

The obtained enzyme was immobilized by two methods – by gel entrapment and by encapsulation. For the gel entrapment method, a 2% sodium alginate solution was prepared with constant stirring and heating. The obtained alginate solution was cooled and the enzyme in a final concentration of 2 mg/mL was added and mixed well. The mixture was added dropwise with a syringe and a G21 needle into cooled (4°C) 0.5% solution of CaCl₂ with constant gentle stirring which continued for 1 h after the last drop was introduced to the solution. Afterwards, the formed Ca-alginate beads were separated from the solution through filtration and washed twice with distilled water. The loading efficiency and immobilization effectiveness were calculated according to Daasi *et al.* [13].

For the encapsulation of the enzyme dendritic-linear-dendritic copolymers were used. Those polymers were synthesized from reactive poly (benzyl ether)monodendrons of the second [G-2], third [G-3] and fourth [G-4] generation by coupling

with poly(ethylene glycol)s with a molecular weight of 5 kDa or 10.8 kDa [14]. Laccase aqueous solution with a concentration of 2mg/mL was mixed with 0.007 g of each DLD polymer in a final volume of 10 mL. The mixtures were placed on a rotary shaker for 12 h at 4 °C followed by 8 h at room temperature [7].

Pyrene removal by free and immobilized laccase

An aqueous solution of purified laccase with a final concentration of 2 mg/mL was used as a medium for the degradation of pyrene. The PAH was added to the aqueous mixture to reach a final concentration of 200 ppm. The control samples contained 200 ppm pyrene in aqueous medium. The experimental tubes were placed on a rotary mixer at 25°C in absence of light for 20 days. Samples were taken daily for spectral and HPLC analysis.

Deionized water was used for the degradation of pyrene by the Ca-alginate laccase preparation. Each test tube contained 200 ppm pyrene and 1 g immobilized preparation. The control samples contained 200 ppm pyrene and 1 g Ca-alginate beads without enzyme. The tubes were placed on a rotary shaker at 25°C in darkness for 20 days and samples were taken daily for further examinations.

Pyrene in a final concentration of 200 ppm was added to the enzyme-copolymer complex and the experimental tubes were placed on a rotary shaker at 25°C in the absence of light. The control samples contained DLD polymers in aqueous medium and 200 ppm pyrene. Samples were taken daily for spectral and HPLC analysis.

Spectral analysis

The spectral analysis was conducted on UV-VIS spectrophotometer SpectroStar NANO (BMG Labtech, Germany). Samples were taken daily until the 20th day of the experiment. 200 µL aliquot of each test tube was placed in a 96-well UV plate and the spectrum was recorded in the range of 220-400 nm with a resolution of 2 nm.

Extraction of pyrene

The samples were extracted threefold with hexane for the determination of the residual pyrene concentration. Anhydrous Na₂SO₄ was then added to the collected fractions to remove residual water from the samples. Afterwards, they were transferred into a flask with appropriate volume and evaporated under vacuum until completely dry. Acetonitrile (5 mL) was used for dissolution of the dry residue. The samples were then filtered through

a syringe filter (0.45 µm) and used for determination of pyrene concentration.

HPLC analysis

Residual pyrene concentration was determined on Agilent Infinity 1220 HPLC system equipped with UV-VIS detector and Agilent Zorbax Eclipse PAH (5 µm, 4.6×150 mm) column. Acetonitrile was used as mobile phase with a flow of 1 mL/min, injection volume was 20 µL, and detection was made at 220 nm wavelength. The retention time for pyrene at these conditions was 2,73 min.

RESULTS AND DISCUSSION

The evaluation of the ability of laccase to degrade pyrene in aqueous medium was made by the comparison of the data obtained after implementation of free enzyme, enzyme entrapped in Ca-alginate gel and enzyme encapsulated in DLD polymers. To our knowledge to date, there is no other study exploring the degradation of pyrene in aqueous medium by immobilized laccase entrapped in amphiphilic polymers.

As a result of the cultivation process, cultural broth with laccase activity of 6545 U/mL was obtained. After the purification procedures, the enzyme preparation had a specific activity of 105.8 U/mg protein and a protein content of 56 mg/mL. After appropriate dosage, the enzyme was used in free form or immobilized form for the degradation of pyrene.

A summary of the data obtained during the spectral analysis is presented in Fig. 1. The differences between the different samples are visible. When the free purified enzyme was introduced to the reaction mixture there were almost no visible changes in the spectra during the whole experiment (Fig. 1A). On the other hand, the sample with the entrapped in Ca-alginate laccase demonstrated significant changes in the spectra (Fig. 1B). Samples taken on the 10th, 15th and 20th day show lower absorbance values in the monitored range. These changes in the spectra must be due to oxidation processes of pyrene during the experiment. The formed new intermediates are the reason for the decrease in the absorbance values. Many studies discuss the ability of bacteria immobilized in alginate [15] and fungal mycelium [16] to degrade PAHs, but the information regarding the sole application of laccase in such process is very scarce. Fig. 1C presents the spectral data obtained with laccase encapsulated in [G-2] polymer.

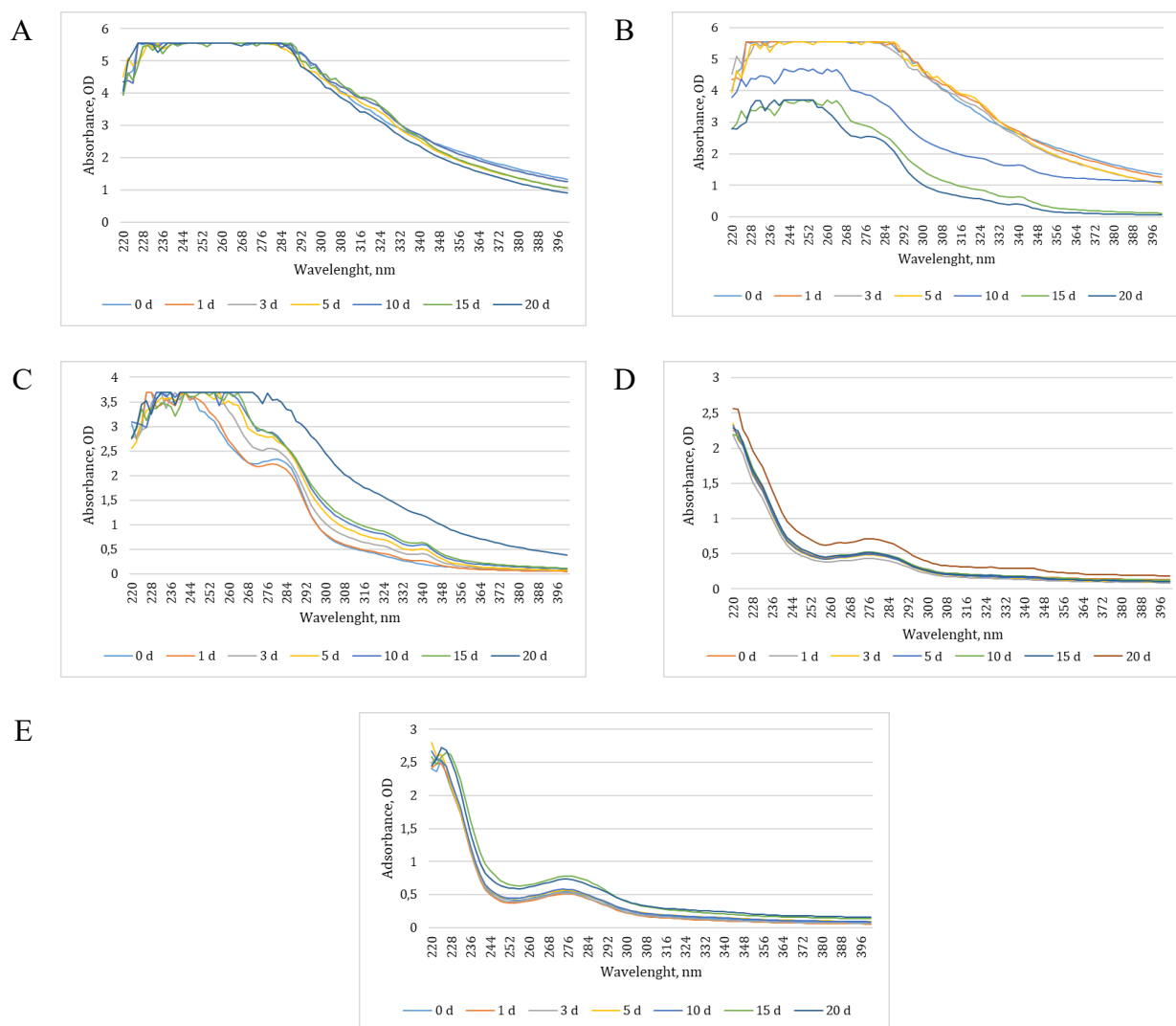


Fig. 1. Spectral data of the reaction mixture between A) Purified laccase and pyrene; B) Entrapped laccase and pyrene; C) Laccase, modified with [G-2] block copolymer and pyrene; D) Laccase, modified with [G-3] block copolymer and pyrene; E) Laccase, modified with [G-4] block copolymer and pyrene.

The changes in the graph are visible, but yet not as intensive as the ones in Fig. 1B. A slight increase of the absorbance values was recorded during the experiment and the highest values were observed on the 20th day. With laccase encapsulated in [G-3] and [G-4] polymers, the spectral changes occurred around the 15th day of the experiment and represented a minor increase in the spectral curves, most likely because of the oxidation processes that took place in the degradation system. It is important to state that when encapsulated in these polymers the enzyme is located in the central part, whilst the polymer envelops it, creating a hydrophobic surrounding. The monomers in the DLD polymers are different which explains the differences in the spectral data, and proves that in fact the polymer is based on poly(benzyl ether)s monodendrons of second generation and poly(ethylene glycol) with molecular weight 5000 Da ([G-2]). Since the water solubility of PAHs is very low it could be assumed

that the polymer acts as a mediator for the pyrene oxidation resulting in higher transformation rates. The usage of amphiphilic block copolymers for laccase encapsulation is a relatively new but promising approach for the removal of persistent organic pollutants [7, 17]. Yet there is no other study in the available literature discussing their effectivity regarding pyrene transformation.

The changes in the spectra of the samples correspond to the data obtained by the quantitative analysis. Figure 2 shows the residual pyrene concentration after 20 days of incubation with the used laccase preparations. When free purified enzyme was applied to the reaction mixture for 20 days the pyrene concentration was by 15 ppm lower than the initial. The application of entrapped in Calcium alginate gel led to higher degradation values, reaching 174 ppm residual pyrene on the 20th day. The application of the enzyme encapsulated in DLD polymers of second generation was the most

promising, where the obtained pyrene removal was 14% or 172 ppm of pyrene were present in the sample at the end of the process. With the preparations based on polymers of third and fourth generation, the degradation rates were 2 and 10%, respectively.

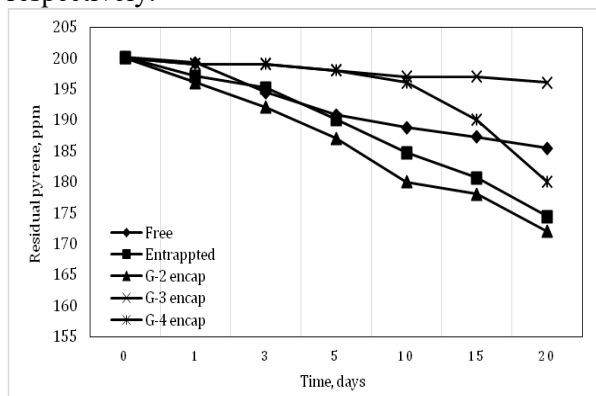


Fig. 2. Residual pyrene concentration

Compared to other studies, the obtained results initiate that with the implementation of some optimization of the process, higher degradation rates could be achieved. Laccase from *Lenzites betulinus* was immobilized for pyrene and benzo(a)pyrene degradation where over 80% and 40% degradation was achieved, respectively. The enzyme had a high degradation capacity which could be intensified by variation of the process parameters [18]. Deng *et al.* [19] applied immobilization of laccase on ferromagnetic nanoparticles for degradation of anthracene (3-ring PAH) and benzo(a)pyrene – a 5-ring PAH. The effects of time, pH, temperature, initial concentration of PAH and absence or presence of mediators were investigated. It was proven that the degradation efficiency could be significantly improved with the introduction of mediators into the reaction mixture. The immobilized preparation itself demonstrated a degradation rate of 39% for benzo(a)pyrene and in the presence of HBT, the degradation rate increased to 99.1%. In another study, laccase from *T. versicolor* was employed in the oxidation of 14 PAHs. The introduction of mediators in the degradation system led to a significant increase in the oxidation of pyrene to 48% whereas the degradation rate without a mediator was only 6% [20].

CONCLUSION

In the present study, the ability of free and immobilized laccase for the degradation of pyrene in aqueous medium was evaluated. The spectral data demonstrated changes in the absorbance values with time in the UV range, caused by structural changes in the pyrene molecule. For the first time,

amphiphilic polymers were used for degradation of pyrene. The results indicated a potential for the development of a eco-friendly detoxifying technology. The application of DLD-based polymers for the degradation of water-insoluble xenobiotics in aqueous medium is a prospective field for new experiments. Further experiments are needed for the optimization of the degradation process regarding pH, temperature, duration of the process, presence of mediators, illumination, etc.

Acknowledgement: This work was supported by the Bulgarian Ministry of Education and Science under the National Research Programme “Young scientists and postdoctoral students”, approved by DCM # 577 / 17.08.2018”. This study would not be possible without the generous contribution of Prof. Ivan Gitsov from the Department of Chemistry at SUNY College of Environmental Science & Forestry, Syracuse, NY, USA.

REFERENCES

1. S. Mishra, Z. Lin, S. Pang, W. Zhang, P. Bhatt, S. Chen, *Front. Bioeng. Biotechnol.*, **9**, 632059 (2021).
2. V. K. Mishra, G. Singh, R. Shukla, *Clim. Change Agri. Ecosys.*, **2**, 133 (2019).
3. L. B. Bertotto, T. R. Catron, T. Tal, *Neuro. Toxicol.*, **76**, 235 (2020).
4. N. Agrawal, P. Verma, S. K. Shahi, *Bioresour. Bioprocess.*, **5**, 11 (2018).
5. J. Merz, M. Dietz, Y. Vonhausen, F. Wöber, A. Friedrich, D. Sieh, I. Krummanacher, H. Braunschweig, M. Moos, M. Holzapfel, C. Lambert, T. Marder, *Chem. Eur. J.*, **26**, 438 (2020).
6. A. Saraswathy, R. Hallberg, *FEMS Microbiol. Lett.*, **210**, 227 (2002).
7. M. Brazkova, G. Angelova, A. Krastanov, *Proc. Of the Fourth Intl. Conf. On Adv. Appl. Sci. Environ. Tech. – ASET* (2016).
8. A. Krastanov, R. Koleva, Z. Aleksieva, I. Stoilova, *Biotechnol. Biotechnol. Equip.*, **27**, 4263 (2013).
9. H. Yemendzhiev, Z. Aleksieva, A. Krastanov, *Biotechnol. Biotechnol. Equip.*, **23**, 1337 (2009).
10. I. Stoilova, G. Dimitrova, G. Angelova, A. Krastanov, *Bulg. J. Agric. Sci.*, **23**, 988 (2017).
11. M. Fernandez, M. Sanroman, D. Moldes, *Biotechnol. Adv.*, **31**, 1808 (2013).
12. M. Bradford, *Anal. Biochem.*, **72**, 248 (1976).
13. D. Daasi, S. Rodriguez-Couto, M. Nasri, T. Mechichi, *Int. Biodeterior. Biodegrad.*, **90**, 71 (2014).
14. I. Gitzov, K. L. Wooley, J. M. J. Fréchet, *Angew. Chem., Int. Ed. Engl.*, **31**, 1200 (1992).
15. Z. You, H. Xu, K. J. Shah, J. Tao, D. Cai, *Chem. Eng. Trans.*, **81**, 19 (2020).
16. J. Low, N. Abdullah, S. Vikineswary, *Res. J. Environ. Sci.*, **3**, 357 (2009).
17. M. Brazkova, M. Gerginova, I. Gitsov, A. Krastanov, in: *Microbes in the Spotlight: Recent*

- Progress in the Understanding of Beneficial and Harmful Microorganisms, Mendez-Vilas (ed.), Brown Walker Press, 2016, p. 45.
18. X. Wang, S. Sun, Z. Ni, Z. Li, J. Bao, *J. Serb. Chem. Soc.*, **83**, 549 (2018).
 19. J. Deng, H. Wang, H. Zhan, C. Wu, Y. Huang, B. Yang, A. Mosa, W. Ling, *Chemosphere*, **301**, 134753 (2022).
 20. A. Majcherczyk, C. Johannes, A. Huttermann, *Enzyme Microb. Technol.*, **22**, 335 (1998).

Potential toxicity, physicochemical properties and environmental behavior of L-carvone

Y. K. Koleva¹, I. Z. Iliev^{2,3*}, V. D. Gandova⁴, A. S. Stoyanova³

¹ Department of Chemistry, University "Prof. Assen Zlatarov", 1 Prof. Yakimov Str., 8010 Burgas, Bulgaria

² University of Plovdiv "Paisii Hilendarski", Department of Chemical Technology, 24 Tzar Asen Str., 4000 Plovdiv, Bulgaria

³ University of Food Technologies, Department Technology of Tobacco, Sugar, Vegetable and Essential oils, Technological Faculty, 26 Maritza Blvd., 4002, Plovdiv, Bulgaria

⁴ University of Food Technologies, Department of Analytical and Physical Chemistry, 26 Maritza Blvd., 4002 Plovdiv, Bulgaria

Received: November 3, 2024; Revised: April 11, 2024

The monoterpene ketone carvone [6,8(9)-p-pentadien-2-one; 1-methyl-4-isopropenyl-6-cyclohexene-2-one] is a colorless to pale yellowish liquid with a characteristic cumin-spiced odor and a sharp, warm, sweet taste. It is found as a main component in essential oils of cumin, fennel, spearmint, *etc.*, from which it is isolated, but for industrial purposes it is synthesized. It is stable in soaps, detergents and cosmetics. Its uses include the preparation of perfume compositions with spicy and fantasy notes, fern, clove, chypre, *etc.*, aromatic compositions for the food industry - mainly mint-carvone type, spices, liqueurs, *etc.* It is used in significant quantities in gums and oral hygiene preparations (toothpastes, mouthwashes, *etc.*). The goal of the present work is to predict the physical, toxicological properties and environmental fate of L-carvone by the CompTox Chemistry Dashboard.

Keywords: L-carvone, toxicity, physicochemical properties, environmental behavior

INTRODUCTION

The volatile monocyclic ketone carvone [6,8(9)-p-pentadien-2-one; 1-methyl-4-isopropenyl-6-cyclohexene-2-one] is a colorless to pale yellowish liquid. Two enantiomers of carvone, (R)-(-)-carvone (L-carvone) and (S)-(+)-carvone (D-carvone), are found in various essential oils. Both enantiomers are with different properties: (S)-(+)-carvone has an optical activity of $\alpha_D^{20} +64.3^\circ$ and is the main constituent of caraway (*ca.* 60%) and dill essential oils (*ca.* 50%). (S)-(+)-carvone possesses the typical caraway aroma., Therefore, D-carvone and the essential oils that contain it are mainly used as a taste enhancer for the food industry (in aromatic compositions - mainly mint-carvone type, spices, liqueurs, *etc.*), and fragrance industry (in perfume compositions with spicy and fantasy notes, fern, clove, chypre, *etc.*) (R)-(-)-carvone has an optical activity $\alpha_D^{20} -62.5^\circ$, occurs in spearmint oil at a concentration of 70-80%. L-carvone and the essential oils that contain it are frequently added to toothpastes, mouth washes, chewing gums, *etc.* [1-3].

Both enantiomers are isolated by fractional distillation of essential oils, but for industrial purposes they are synthesized [1].

Some physicochemical (density, surface tension and refractive index), kinetic and thermodynamic parameters (surface energy, surface heat capacity, reaction rate constant) of carvone were measured at a temperature range between 6 and 30 °C [4].

It has been found that treating cedar wood with carvone affects its physicochemical properties, which may allow to reduce or inhibit the adhesion of microorganisms responsible for its biodegradation [5].

Carvone also exhibits a variety of biological properties, e.g., antimicrobial [4, 6-12], antioxidant [13, 14], antidiabetic [15, 16], anti-inflammatory [17-19], neurological [20-22], *etc.* [23, 24].

Carvone is among the 80 aromatic substances, described in Regulation 2023/1554 [25] that can cause hypersensitivity of skin and allergy contact dermatitis [26-30]. Its presence in the essential oils used in perfumery and cosmetic preparations should be defined on the label at a concentration above 0.01% in rinse-off products for skin and hair (shampoos, shower gels, masks, *etc.*) and over 0.001%, in those that remain in contact with skin (creams, toilet milks, lotions, *etc.*).

The goal of the present work is to predict the physical, toxicological properties and environmental fate of L-carvone by the CompTox Chemistry Dashboard.

* To whom all correspondence should be sent:

E-mail: ivanz.iliev@uni-plovdiv.bg

MATERIALS AND METHODS

CompTox Chemistry Dashboard

The free and accessible web-based application Dashboard was used, which has access to nine databases of chemical compounds [31, 32].

Environmental fate and transport

The data were obtained from online databases or predicted using different models such as: EPI Suite, NICEATM, TEST and OPERA. Various properties were included in the study, for example the adsorption coefficient, atmospheric hydroxylation rate, biodegradation half-life, fish biotransformation half-life, as well as parameters to assess bioaccumulation potential, such as bioaccumulation factors and bioconcentration factors. The obtained predicted values were derived using different models [31, 32].

Chemical properties

Experimental and predicted physical and chemical properties, such as log octanol-water partition coefficient (logP), water solubility (S), melting point (MP) and others, were used. The data is presented in two separate tables, as experimental and predicted [31, 32].

RESULTS AND DISCUSSION

Knowledge of the physicochemical properties of potential chemical alternatives is a requirement of the alternatives assessment process for two reasons. First, the inherent hazard of a chemical, such as its

capacity to interfere with normal biological processes, and its physical hazards and environmental fate (degradation, persistence) are determined by its intrinsic physicochemical properties and the system with which it is interacting. Second, physicochemical properties can be used to eliminate from consideration chemicals that are likely to exhibit particular physical or toxicological hazards. As important as this data is, obtaining it is relatively fast and inexpensive, and can be readily done at the initial stages of the alternatives assessment [33].

Physical properties include freezing point, boiling point, melting point, infrared spectrum, electronic parameters, viscosity, and density. Some of them (e.g., electronic parameters, molecular weight, boiling/freezing point) are directly associated with environmental fate and health effects. A number of different software packages and algorithms are available for predicting physicochemical properties, and predictions are often in excellent agreement with experimentally-derived values [33].

In the present work, the CompTox Chemistry Dashboard was used to predict the physicochemical properties (environmental fate) of L-carvone.

Data of prediction environmental fate (Bioconcentration factor, Atmospheric hydroxylation rate, Biodegradation half-life, Fish biotransformation half-life (Km) and Soil adsorption coefficient (Koc) and physicochemical properties) of L-carvone are presented in Table 1.

Table 1. Predicted properties for L-carvone.

Property	Experimental average	Predicted average	Experimental median	Predicted median	Experimental range	Predicted range
Bioconcentration factor, L/kg	-	7.55	-	7.55	-	4.62 to 10.5
Atmospheric hydroxylation rate, ml/molecule.s	-	1.66 e-10	-	1.66 e-10	-	1.66 e-10
Biodegradation half-life, days	-	3.47	-	3.47	-	3.47
Fish biotrans formation half-life (Km), days	-	9.12e-2	-	9.12e-2	-	9.12e-2 to 0.237
Soil adsorption coefficient (Koc), L/kg	-	214	-	214	-	214
Polarizability, Å ³	-	18.0	-	18.0	-	18.0
Henry's law, atm-m ³ /mol	-	3.31e-4	-	3.31e-4	-	3.31e-4
ReadyBiodeg, Binary 0/1	-	0.00	-	0.00	-	0.00
Boiling point, °C	230	227	230	227	229 to 230	224 to 231
Flash point, °C	-	86.5	-	86.5	-	84.1 to 88.9
Melting point, °C	-	18.1	-	9.86	-	9.00 to 35.4

Molar refractivity, ml	-	45.5	-	45.5	-	45.5
Molar volume, ml	-	160	-	160	-	160
Surface tension, dyn/ml	-	32.0	-	32.0	-	29.8 to 34.2
Density, g/ml	-	0.947	-	0.947	-	0.940 to 0.954
logD5.5, Log10 unitless	-	2.36	-	2.36	-	2.36
logD7.4, Log10 unitless	-	2.36	-	2.36	-	2.36
Liquid chromatography Ret., min	-	9.34	-	9.34	-	9.34
Vapor pressure, mm Hg	0.103	9.86e-2	0.103	0.102	0.103	6.56e-2 to 0.1...
Water solubility, mol/L	8.70e-3	6.75e-3	8.71e-3	6.79e-3	8.67e-3 to 8.71e-3	2.44e-3 to 1.10e-2
Index of refraction,	-	1.48	-	1.48	-	1.48
LogKoa: Octanol-Air	-	5.06	-	5.06	-	5.06
LogKow: Octanol-Water	2.71	2.62	2.71	2.58	2.71	2.27 to 3.07

Table 2. Predicted results of physicochemical properties for L-carvone using software TEST.

Properties	Experimental value	Consensus	Hierarchical clustering	Single model	Group contribution	Nearest neighbor
Normal boiling point, °C	231.0	224.3	230.7		213.0	229.3
Melting point, °C		35.4	46.7		9.4	50.0
Flash point, °C	88.9	83.1	89.0		73.6	86.8
Vapor pressure, mm Hg	0.103	0.156	0.122		0.175	0.177
Density, g/ml	0.940	0.954	0.957		0.957	0.948
Surface tension, dyn/ml	34.239	34.201	34.301		35.331	32.970
Water solubility, mg/L	1299.528	731.267	1272.750		216.953	1416.181

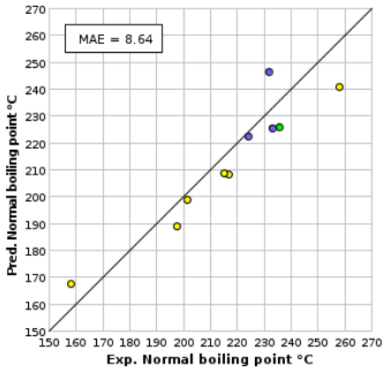
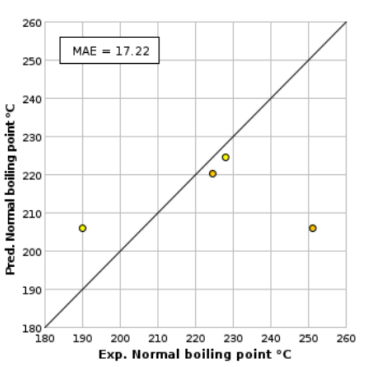
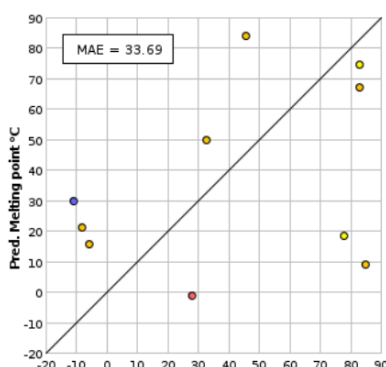
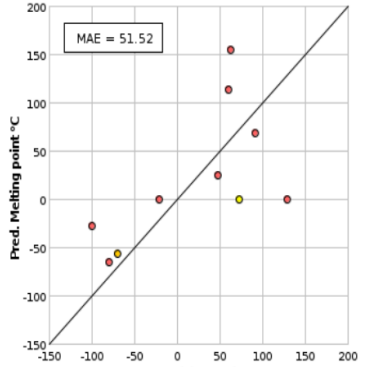
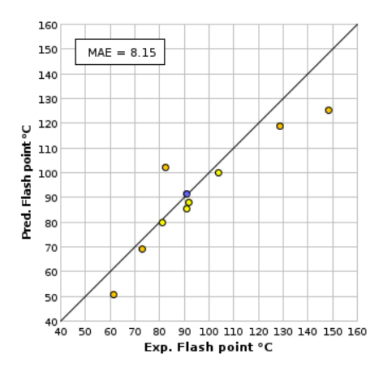
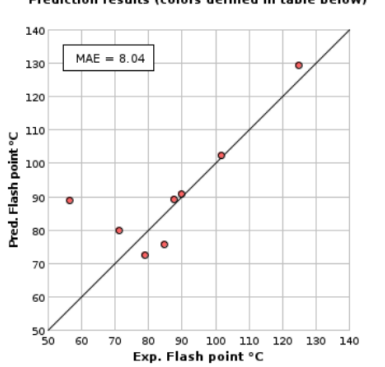
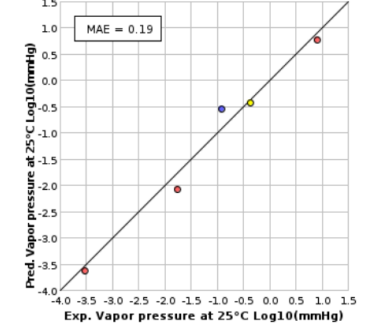
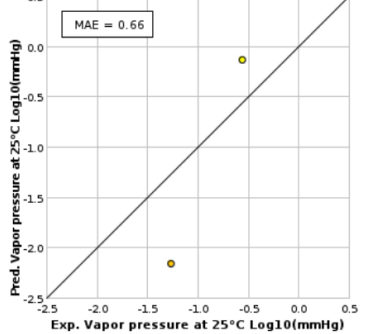
There are four experimental data values of L-carvone. The physicochemical properties are estimated by OPERA.

An EPA software application (the Toxicity Evaluation Software Tool (TEST)) was implemented for evaluating the physicochemical properties of L-carvone using quantitative structure-activity relationship (QSAR) methodologies. Data predicting the properties of L-carvone by the software TEST (CompTox Chemistry Dashboard) is presented in Table 2.

There are six experimental values of L-carvone – normal boiling point, flash point, vapor pressure, density, surface tension and water solubility. Prediction results (Consensus method) for all properties are obtained of individual predictions with the following methods (Hierarchical clustering, Single model, Group contribution, Nearest neighbor).

For each property a training and external test set are defined. Predictions for the test chemical and for the most similar chemicals in the sets have been made (Table 3).

Table 3. Predicted physicochemical properties of L-carvone by Consensus method.

Physical and chemical properties	Predictions for the test chemical and for the most similar chemicals in the training set	MAE*	Predictions for the test chemical and for the most similar chemicals in the external test set	MAE*
Normal boiling point, °C	<p>Prediction results (colors defined in table below)</p> 	<p>Entire set-10.36 Similarity coefficient ≥ 0.5 (8.64)</p>	<p>Prediction results (colors defined in table below)</p> 	<p>Entire set-11.46 Similarity coefficient ≥ 0.5 (17.22)</p>
Melting point, °C	<p>Prediction results (colors defined in table below)</p> 	<p>Entire set-26.64 Similarity coefficient ≥ 0.5 (33.69)</p>	<p>Prediction results (colors defined in table below)</p> 	<p>Entire set-30.21 Similarity coefficient ≥ 0.5 (51.52)</p>
Flash point, °C	<p>Prediction results (colors defined in table below)</p> 	<p>Entire set-14.53 Similarity coefficient ≥ 0.5 (8.15)</p>	<p>Prediction results (colors defined in table below)</p> 	<p>Entire set-16.91 Similarity coefficient ≥ 0.5 (8.04)</p>
Vapor pressure, mm Hg	<p>Prediction results (colors defined in table below)</p> 	<p>Entire set-0.40 Similarity coefficient ≥ 0.5 (0.19)</p>	<p>Prediction results (colors defined in table below)</p> 	<p>Entire set-0.47 Similarity coefficient ≥ 0.5 (0.66)</p>

Density, g/ml	<p>Prediction results (colors defined in table below)</p> <p>MAE = 0.01</p>	Entire set-0.04 Similarity coefficient ≥ 0.5 (0.01)	<p>Prediction results (colors defined in table below)</p> <p>MAE = 0.03</p>	Entire set-0.04 Similarity coefficient ≥ 0.5 (0.03)
Surface tension, dyn/ml	<p>Prediction results (colors defined in table below)</p> <p>MAE = 0.50</p>	Entire set-1.16 Similarity coefficient ≥ 0.5 (0.50)	No chemicals in the test set exceed a minimum similarity coefficient of 0.5 for comparison purposes	Entire set-1.32 Similarity coefficient ≥ 0.5 (1.38)
Water solubility, mg/L;	<p>Prediction results (colors defined in table below)</p> <p>MAE = 0.33</p>	Entire set-0.50; Similarity coefficient ≥ 0.5 (0.33)	<p>Prediction results (colors defined in table below)</p> <p>MAE = 0.24</p>	Entire set-0.58 Similarity coefficient ≥ 0.5 (0.24)

*Mean absolute error in g/ml

A toxic endpoint is the result of a study conducted to determine how dangerous a substance is. The data collected from such studies are used to report the relative toxicity of the compound to various regulatory agencies and environmental compliance groups. Toxic endpoints can include mortality, behavior, reproductive status or physiological and biochemical changes [34].

Toxic endpoints are acute or chronic. Acute studies generally last no longer than a week and examine endpoints such as mortality and behavior. With acute studies, a common endpoint is an LD₅₀, which is the dose of a compound required to kill half the organisms in the study. Chronic studies are longer in duration (more than a week) and include endpoints such as reproduction, long-term survival and growth. Chronic studies are valuable because

they examine the effects of extremely low concentrations of compounds that may persist in the environment for long periods of time [34].

There are two experimental values (toxicological endpoints) for L-carvone – Ames mutagenicity and oral rat LD₅₀. Prediction results (Consensus method) for all toxicological endpoints for L-carvone are obtained of individual predictions with the following methods (Hierarchical clustering, Single model, Group contribution, Nearest neighbor).

Data predicting the toxicological endpoints of L-carvone by the CompTox Chemistry Dashboard are presented in Table 4.

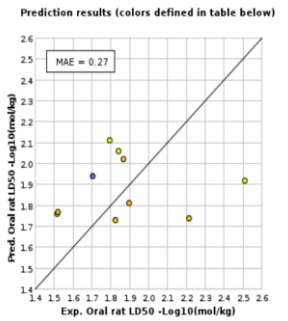
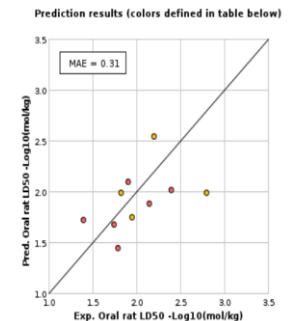
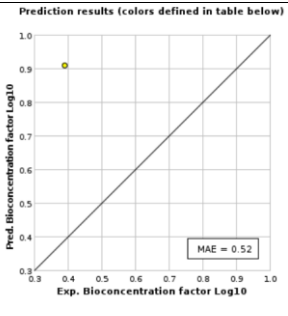
For each toxicological endpoint a training and an external test set are defined. Predictions for the test chemical and for the most similar chemicals in the sets were made (Table 5).

Table 4. Predicted results of toxicological endpoints for L-carvone.

Properties	Experimental value	Consensus	Hierarchical clustering	Single model	Group contribution	Nearest neighbor
96 h fathead minnow LC ₅₀ , mg/L		5.573	10.113	5.630	5.157	3.284
48 h <i>Daphnia magna</i> LC ₅₀ , mg/L		1.802	1.768	1.768	1.870	
48 h <i>Tetrahymena pyriformis</i> IGC ₅₀ , mg/L					1.857	
Oral rat LD50, mk/kg	1639.780	1635.355	2039.099			1311.552
Bioconcentration factor		4.628	2.120	24.353	1.920	
Developmental toxicity		true	true	false		true
Ames mutagenicity	false	false	false			false
Estrogen Receptor RBA						1.289×10 ⁻⁴
Estrogen Receptor Binding		false	false	false	false	true

Table 5. Predicted toxicological properties of L-carvone from Consensus method.

Toxicological properties	Predictions for the test chemical and for the most similar chemicals in the training set	MAE*	Predictions for the test chemical and for the most similar chemicals in the external test set	MAE*
96 h fathead minnow LC ₅₀ , mg/L		Entire set-0.48 Similarity coefficient ≥ 0.5 (0.47)		Entire set-0.55 Similarity coefficient ≥ 0.5 (0.41)
48 h <i>Daphnia magna</i> LC ₅₀ , mg/L		Entire set-0.50 Similarity coefficient ≥ 0.5 (0.63)		Entire set-0.74 Similarity coefficient ≥ 0.5 (0.40)
48 h <i>Tetrahymena pyriformis</i> IGC ₅₀ , mg/L	No similar chemicals could be predicted		No similar chemicals could be predicted	

Oral rat LD ₅₀ , mk/kg		Entire set- 0.34 Similarity coefficient \geq 0.5 (0.27)		Entire set-0.43 Similarity coefficient \geq 0.5 (0.31)
Bioconcentration factor		Entire set- 0.42 Similarity coefficient \geq 0.5 (0.52)	No chemicals in the test set exceed a minimum similarity coefficient of 0.5 for comparison purposes	Entire set-0.51 Similarity coefficient \geq 0.5 (0.80)
Developmental toxicity		Concordance -1.00 Sensitivity- 1.00 Specificity- 1.00		Concordance-0.80 Sensitivity-0.75 Specificity-1.00
Ames Mutageni-city		Concordance -0.90 Sensitivity-0 Specificity-1		Concordance-0.80 Sensitivity-N/A Specificity-0.80
Estrogen Receptor RBA	No similar chemicals could be predicted		No similar chemicals could be predicted	
Estrogen Receptor Binding		Concordance -N/A Sensitivity- N/A Specificity- N/A		Concordance-0.75 Sensitivity-1.00 Specificity-0.50

*Mean absolute error in g/ml

CONCLUSION

Prediction and investigation of the physicochemical properties of L-carvone can be used as a screening for its potential to cause human and environmental toxicity. Experimental data is limited, forcing decisions about the potential of a compound now and in the future to be made on the basis of limited data and information. Therefore, alternative *in silico* methods, such as the CompTox Chemistry Dashboard, are used to assess their behavior (potential toxicity, physicochemical properties and environmental fate and transport).

REFERENCES

1. K. Bauer, D. Garbe, H. Surburg, Common Fragrance and Flavour Materials. Preparation, Properties and Uses. IV Compl. Revised Edition, Wiley-VCH Verlag GmbH, Weinheim, Germany, 2001.
2. K. Baser, G. Buchbauer, Handbook of Essential Oils: Science, Technology, and Applications, Taylor and Francis Group, LLC CRC Press an imprint of Taylor and Francis Group, an Informa business, 2010.
3. A. Stoyanova, Guide for the Specialist in the Aromatic Industry, Plovdiv, BNAEOPC, 2022.
4. I. Iliev, H. Fidan, V. Gandova, S. Stankov, Y. Koleva, A. Stoyanova, *Oxid. Commun.*, **45**, 655 (2022).
5. B. Hassan, S. Moulay, El A. Soumya, El H. El Hassan, B. Saïd, I. Saad, *Int. J. Sci. Eng. Res.*, **6**, 767 (2015).

6. K. Aggarwal, S. Khanuja, A. Ahmad, T. Santha Kumar, V. Gupta, S. Kumar, *Flavour Fragr. J.*, **17**, 59 (2002).
7. Y. Chan, K. Siow, P. Ng, U. Gires, B. Majlis, *Mater. Sci. Eng. C*, **68**, 861 (2016).
8. F. Demirci, Y. Noma, N. Kirimer, K. H. C. Başer, *Z. Nat. C*, **59**, 389 (2004).
9. M. Esfandyari-Manesh, Z. Ghaedi, M. Asemi, M. Khanavi, A. Manayi, H. Jamalifar, F. Atyabi, H. Jamalifar, R. Dinarvand, *J. Pharm. Res.*, **7**, 290 (2013).
10. C. Giovana, N. de Simone, L. de Priscilla, C. Paula, F. Marcelo, M. Marcelle, P. Janaina, R. de Thais, F. Jose, *Afr. J. Plant Sci.*, **10**, 203 (2016).
11. C. Morcia, M. Malnati, V. Terzi, *Food Addit. Contam. Part A*, **29**, 415 (2011).
12. I. Moro, G. Gondo, E. Pierri, R. Pietro, C. Soares, D. de Sousa, A. dos Santos, *Braz. J. Pharm. Sci.*, **53** (2018).
13. S.-H. Mun, O.-H. Kang, D.-K. Joung, S.-B. Kim, J.-G. Choi, D.-W. Shin, D.-Y. Kwon, *Exp. Ther. Med.*, **7**, 891 (2014).
14. M. Elmastas, I. Dermirtas, O. Isildak, H. Aboul-Enein, *J. Liq. Chromatogr. Relat. Technol.*, **29**, 1465 (2006).
15. S. Sabir, D. Singh, J. Rocha, *Pharm. Chem. J.*, **49**, 187 (2015).
16. U. Muruganathan, S. Srinivasan, D. Indumathi, *J. Acute Dis.*, **2**, 310 (2013).
17. U. Muruganathan, S. Srinivasan, *Biomed. Pharmacother.*, **84**, 1558 (2016).
18. M. da Rocha, L. Oliveira, C. Santos, D. de Sousa, R. de Almeida, D. Araújo, *J. Nat. Med.*, **67**, 743 (2013).
19. T. Marques, M. Marques, J.-V. Medeiros, R. Silva, A. dos Reis Barbosa, T. Lima, D. de Sousa, R. de Freitas, *Inflammation*, **37**, 966 (2014).
20. C. Sousa, B. Neves, A. Leitão, A. Mendes, *Biomedicines*, **9**, 777 (2021).
21. D. de Sousa, F. de Farias Nóbrega, R. de Almeida, *Chirality*, **19**, 264 (2007).
22. L. Faliagkas, D. Vokou, G. Theophilidis, *Planta Med. Lett.*, **2**, e6 (2015).
23. M. Sánchez-Borzone, L. Delgado-Marín, D. García, *Chirality*, **26**, 368 (2014).
24. A. Bouyahya, H. Mechchate, T. Benali, R. Ghchime, S. Charfi, A. Balahbib, P. Burkov, M. Shariati, J. Lorenzo, N. Omari, *Biomolecules*, **11**, 1803 (2021).
25. Regulation (EC) 2023/1545 of the European Parliament and of the Council, of 26 July 2023, on Cosmetic Products; Official Journal of the European Union, 2023.
26. C. Ahlgren, T. Axéll, H. Möller, M. Isaksson, R. Liedholm, M. Bruze, *Clin. Oral Investig.*, **18**, 227 (2014).
27. M. Corazza, A. Levratti, A. Virgili, *Contact Dermat.*, **46**, 366 (2002).
28. C. Hansson, O. Bergendorff, J. Wallengren, *Contact Dermat.*, **65**, 362 (2011).
29. B. Hausen, *Dtsch. Med. Wochenschr.*, **109**, 300 (1984).
30. L. Kroona, G. Warfvinge, M. Isaksson, C. Ahlgren, J. Dahlin, Ö. Sörensen, M. Bruze, *Contact Dermat.*, **77**, 224 (2017).
31. USA EPA; CompTox Chemistry Dashboard: <https://comptox.epa.gov/dashboard/>.
32. A. Williams, C. Grulke, J. Edwards, A. McEachran, K. Mansouri, N. Baker, G. Patlewicz, I. Shah, J. Wambaugh, R. Judson, A. Richard, *J. Cheminformatics*, **9**, 61 (2017).
33. NIH, A Framework to Guide Selection of Chemical Alternatives: <https://www.ncbi.nlm.nih.gov/books/NBK253956/>.
34. SCIENCING: <https://sciencing.com/definition-toxic-endpoint-6603458.html>.

Predicting the potential absorption, distribution, metabolism and excretion of the aldehyde citral

Y. K. Koleva¹, I. Z. Iliev^{2,3*}, V. D. Gandova⁴, A. S. Stoyanova³

¹ Department of Chemistry, University "Prof. Assen Zlatarov", 1 Prof. Yakimov Street, 8010 Burgas, Bulgaria

² University of Plovdiv "Paisii Hilendarski", Department of Chemical Technology, 24 Tzar Asen Str., 4000 Plovdiv, Bulgaria

³ University of Food Technologies, Department Technology of Tobacco, Sugar, Vegetable and Essential oils, Technological Faculty, 26 Maritza Blvd., 4002, Plovdiv, Bulgaria

⁴ University of Food Technologies, Department of Analytical and Physical Chemistry, 26 Maritza Blvd., 4002 Plovdiv, Bulgaria

Received: November 3, 2023; Revised: April 11, 2024

Citral is an acyclic monoterpene aldehyde that occurs in natural products in two forms: α -form (*trans*-3,7-dimethyl-2,6-octadiene-1-al) and β -form (*cis*-3,7-dimethyl-2,7-octadiene-1-al). The *trans*-form is also called geranial (citral a) and the *cis*-form neral (citral b). This aromatic substance is found in many essential oils - eucalyptus, lemongrass, citronella, lyceum, lemon wormwood, verbena, *etc.* It is mainly isolated from eucalyptus, lychee, lemongrass and other essential oils. For industrial purposes, however, it is synthesized. It has poor resistance to light, air and heat. Technical citral is more stable in soaps. It is used in perfumery and cosmetics, to flavor various food products and it is also used as a raw material for the synthesis of many other aromatic substances. The aim of the present study is to predict the biological effects of citral by applying an *in silico* approach.

Keywords: citral, absorption, distribution, metabolism, excretion

INTRODUCTION

Citral [CAS 106-26-3] is an acyclic monoterpene aldehyde that occurs in natural products as an isomeric mixture of geranial (*E*-3,7-dimethyl-2,6-octadienal) and neral (*Z*-3,7-dimethyl-2,6-octadienal). The *trans*-form is also called (citral a) and the *cis*-form (citral b). In the isomeric mixtures, geranial is usually the predominant one. It is usually isolated from different essential oils [1–3], for industrial purposes, however, it is synthesized from various other compounds, such as isoprene, methylheptenone, β -pinene, linalool or geraniol [1].

As an oxygen derivative, it exhibits antimicrobial properties against various test microorganisms, such as Gram-positive and Gram-negative bacteria, yeasts, molds [4–9], with pronounced antioxidant [5, 7, 8] and other biological properties [4, 7].

Technical citral is more stable in soaps. It is used in perfumery (with citrus, verbena, floral and fantasy notes) and cosmetics, to flavor various food products (with a citrus smell, as a substitute for lemon oil). Citral is also used as a raw material for the synthesis of many other aromatic substances [1, 3]. It is often encapsulated and, in combination with various polysaccharides, is used on one hand as a flavoring agent and preservative [6, 10–12], and on the other as a component of edible food coatings [10, 11, 13].

Findings have shown that for people with sensitive skin, it can cause allergies, resulting in skin redness, as well as breathing disorders [14–16]. Therefore, it is included in the list of 80 allergens of Regulation 2023/1554 of EC [17]. Its amount should be labeled on perfumery or cosmetic products when the content is more than 0.01% in rinse-off products for skin and hair (shampoos, shower gels, masks, *etc.*) and more than 0.001% in those that remain in contact with skin (creams, toilet milks, lotions, *etc.*).

The aim of the present study is to predict the biological effects of citral by applying an *in silico* approach, such as lipophilicity, water solubility, pharmacokinetics and other characteristic medicinal formulations.

MATERIALS AND METHODS

Compound data

Citral has been shown to exhibit apoptotic, anti-nociceptive and anti-inflammatory functions. These are compounds containing a chain of two isoprene units [18].

SwissADME. This web tool grants free access to data regarding various properties and predictive models necessary in determining the physico-chemical parameters and for evaluating pharmacokinetics of various compounds [19].

* To whom all correspondence should be sent:

E-mail: ivanz.iliev@uni-plovdiv.bg

According to the "Rule of Five", a given molecule is orally active/absorbed when it does not violate any two or more of the rules. However, some complicated natural products are not suited to the rules. For that, a variety of other rules and filters regarding drug-likeness that are equal to the "Rule of Five" have been proposed [20–22].

Hopkins in 2012 developed the QED (quantitative estimate of drug-likeness) concept [23] which generated eight physicochemical properties, which include four of the five (MW, iLOGP, HBAs and HBDs) and four other parameters such as topological polar surface area (TPSA), number of

rotatable bonds (ROTBs), number of aromatic rings (nAROMs), and number of alerts for undesirable substructures (ALERTs i.e. PAINS #alert and Brenk #alert) using 771 marketed oral drugs [23]. The concept of QED is the most flexible and adopted compared to ordinary drug-likeness rules [19].

RESULTS AND DISCUSSION

Some physicochemical parameters of citral are given in Table 1.

Lipophilic characteristics of citral are presented in Table 2.

Table 1. Physicochemical properties of citral

Molecular weight (g/mol)	Number of heavy atoms	Number of aromatic heavy atoms	Fraction Csp ³	Number of rotatable bonds	Number of H-bond acceptors	Number of H-bond donors	Molar refractivity	TPSA (Å ²)
152.23	11	0	0.50	4	1	0	49.44	17.07

Table 2. Lipophilic characteristics of citral.

iLOGP	XLOGP3	WLOGP	MLOGP	SILICOS-IT	Consensus Log P _{o/w}
2.47	3.03	2.88	2.49	2.65	2.71

* XLOGP3, an atomistic accost including corrective factors and knowledge based library; WLOGP, application of purely atomistic method stationed on fragmental system; MLOGP, an archetype of topological method suggested on a linear relationship with implemented 13 molecular descriptors; SILICOS-IT, an mongrel method entrust on 27 fragments and 7 topological descriptors; iLOGP, a physics-based method lean on free energies of solvation in n-octanol and water calculated by the generalized-born and solvent accessible surface area (GB/SA) model [19].

Table 3. Water solubility characteristics of citral

ESOL			Ali <i>et al.</i> [24]				SILICOS-IT				
Log S (ESOL)	Solubility		Log S	Solubility		Class	Log S SILICOS-IT	Solubility		Class	
	mg/ml	mol/L		mg/ml	mol/L			mg/ml	mol/L		
-2.43	5.67e-01	3.73e-03	S	-3.05	1.34e-01	8.83e-04	S	-1.96	1.66e+00	1.09e-02	S

*I – insoluble; PS – poorly soluble; S – soluble; VS – very soluble.

Table 4. Pharmacokinetic parameters of citral

GI absorption	BBB permeant	P-gp substrate	CYP1A2 inhibitor	CYP2C19 inhibitor	CYP2C9 inhibitor	CYP2D6 inhibitor	CYP3A4 inhibitor	Log K _p (Skin permeation) (cm/s)
High	Yes	No	No	No	No	No	No	-5.08

Table 5. Drug-likeness rules and bioavailability score of citral

Lipinski <i>et al.</i> [20]	Ghose <i>et al.</i> [21]	Veber <i>et al.</i> [28]	Egan <i>et al.</i> [29]	Muegge <i>et al.</i> [30]	Bioavailability score
Yes; 0 violation	No; 1 violation MW < 160	Yes	Yes	No; 2 violation: MW < 200; Heteroatoms < 2	0.55

Table 6. Medicinal chemistry properties of the compound citral

Pains	Brenk <i>et al.</i> [32]	Leadlikeness	Synthetic accessibility (SA)
0 alert	3 alerts: aldehyde, isolated alkene, michael acceptor 1	No; 1 violation: MW < 250	2.49

Log P data define citral as lipophilic. Two different topological approaches predicting water solubility are included in SwissADME, with the first one applying an ESOL model. (Solubility class: Log S Scale: Insoluble & lt; -10 weakly & lt; -6, moderately & lt; -4 soluble & lt; -2 very & lt; 0 & lt; high), and the second was adapted by Ali *et al.* [24]. A third predictor of SwissADME has been developed from SILICOS-IT (Solubility class: Log S Scale: Insoluble & lt; -10 weakly & lt; -6, moderately & lt; -4 soluble & lt; -2 very & lt; 0 & lt; high), the linear coefficient being corrected by molecular weight ($R^2 = 0.75$).

Water solubility characteristics of citral are presented in Table 3. Citral has high water solubility. For the prediction of passive absorption in the gastrointestinal tract, as well as in drug development, the BOILED-Egg model is used, which is very rapid, spontaneous and effective [25]. The space of molecules with a greater degree of absorption from the gastrointestinal tract is colored white, and this is most likely to penetrate the brain – in yellow [19]. It is known that between 50 and 90% of molecules with therapeutic properties from the five main isoforms of citral are biotransformed from cytochrome P450 (CYP) isoenzymes [26, 27].

Pharmacokinetics parameters of citral are presented in Table 4. The data indicate a high level of absorption of the gastrointestinal tract and a high BBB, i.e. citral is not the substrate for P-gp. The data show that citral cannot be a substrate of P-gp, it is also a non-inhibitor of the cytochrome P450 isozymes. Citral is weak in permeability which is determined by the skin permeability coefficient (Log Kp) [27]. Access to five different filters, which are based on rules with different ranges of properties, and define the molecule as a drug, is given by section SwissADME. The Lipinski *et al.* [20] (Pfizer) filter

is the pioneer for rule-of-five along with Ghose *et al.* [21] (Amgen), Veber *et al.* [28] (GSK), Egan *et al.* [29] (Pharmacia) and Muegge *et al.* [30] (Bayer) methods. The specific needs of the end-user with respect to the chemical space are formed by different evaluations which allow a choice of diverse methods. A description of each rule violation appears in the output panel [19].

Drug-likeness rules and bioavailability score of citral are presented in Table 5.

Citral expressed and followed the rule invoked in SwissADME, the violation shown by it is minimal [31]. In the model of Brenk *et al.* [32] components, which are smaller and less hydrophobic, are considered rather than those defined by "Lipinski's rule of 5" to extend the possibilities of optimization of lead. For example, lead optimization was developed by a method where molecular weight between 100 and 350 Da, ClogP between 1 and 3.0 is taken [33]. A fingerprint-based approach was used to estimate Synthetic accessibility (SA) [34].

The medically important properties of citral are presented in Table 6. No reaction alerts were observed for PAIN alert, but were observed for Brenk *et al.* [32]. Therefore, there is some deviation of citral in terms of its drug similarity. It is seen that the molecule is at the prediction site, i.e. in the yolk (high brain penetration) of BOILED-Egg (Fig. 1). The molecule of citral is depicted as red indicating non-substrate of P-gp (PGP-).

Citral was evaluated for drug-likeness by bioavailability radar (Figure 2).

Six physicochemical properties: lipophilicity (from -0.7 to +5.0), molecular mass (from 150 to 500 g/mol), polarity (of 20 and 130Å), insolubility (log S not higher than 6), insaturation (the fraction of carbons in sp^3 hybridization not less than 0.25)

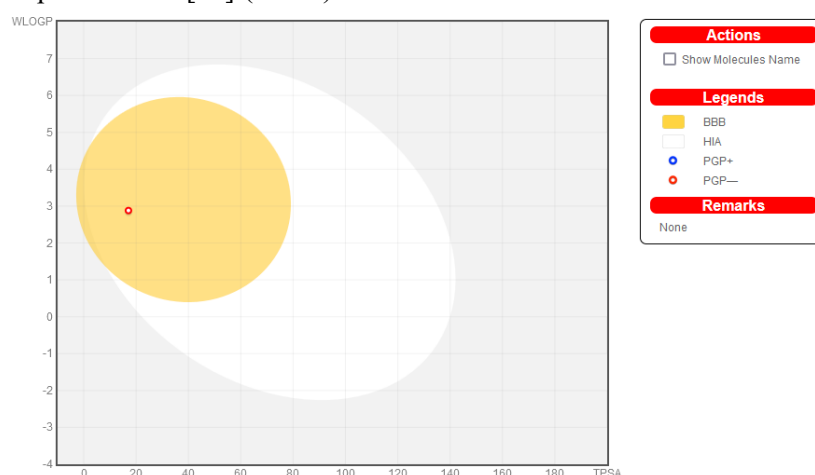


Fig 1. Schematic representation of perceptive evaluation of passive gastrointestinal absorption (HIA) and brain penetration (BBB) with the three molecules using BOILED-Egg (WLOGP vs. TPSA).

and flexibility (no more than 9 rotating connections) outline an optimum space (pink area) which predict its bioavailability when consumed orally [19].

Bioavailability radar gives the most general idea of the drug-likeness of a molecule. The compound is in the optimal range of the pink zone with small deviations in some parameters (Fig. 2).

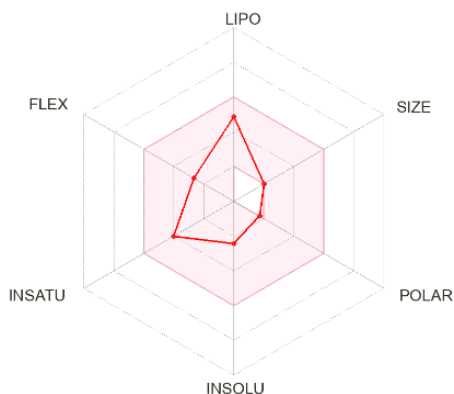


Fig. 2. Schematic diagram of bioavailability radar for drug likeness of citral.

CONCLUSIONS

In order to act as a drug, citral must meet certain requirements that will allow the relevant biological events to take place. The SwissADME tool makes it possible to calculate medically important physicochemical, pharmacokinetic and other parameters of flavoring substances.

REFERENCES

1. K. Bauer, D. Garbe, H. Surburg, Common Fragrance and Flavor Materials. Preparation, Properties and Uses. 4th Completely Revised Edition, Wiley – VCH Weinheim, New York, Chichester, Brisbane, Singapore, Toronto, 2001.
2. K. Baser, G. Buchbauer, Handbook of Essential Oils: Science, Technology, and Applications, Taylor and Francis Group, LLC CRC Press an imprint of Taylor and Francis Group, an Informa Business, 2010.
3. A. Stoyanova, Guide for the Specialist in the Aromatic Industry. Bulgarian National Association of Essential Oils, Perfumery and Cosmetics, Plovdiv, 2022.
4. E. Adukwu, M. Bowles, V. Edwards-Jones, H. Bone, *Appl. Microbiol. Biotechnol.*, **100**, 9619 (2016).
5. O. Celebi, H. Fidan, I. Iliev, N. Petkova, I. Dincheva, V. Gandova, S. Stankov, A. Stoyanova, *Turkish J. Agr. Fores.*, **47**, 67 (2023).
6. D.-H. Huang, C.-C. Wang, C.-H. Yeh, J.-C. Tsai, Y.-T. Huang, P.-H. Li, *J. Food Drug Anal.*, **26**, 82 (2018).
7. C. Shi, X. Zhao, Z. Liu, R. Meng, X. Chen, N. Guo, *Food Nutr. Res.*, **60**, 1 (2016).
8. L. Guimarães, M. Cardoso, P. de Sousa, J. de Andrade, S. Vieira, *Rev. Ciênc. Agron.*, **42**, 464 (2011).

9. E. Wuryatmo, A. Klieber, E. Scott, *J. Agric. Food Chem.*, **51**, 2637 (2003).
10. G. Marci, E. Rabea, M. Badawy, *Appl. Food Biotechnol.*, **5**, 69 (2018).
11. W.-C. Lu, D.-H. Huang, C.-C. Wang, C.-H. Yeh, J.-C. Tsai, Y.-T. Huang, P.-H. Li, *J. Food Drug Anal.*, **26**, 82 (2018).
12. A. Samusenko, *Oxid. Commun.*, **31**, 511 (2008).
13. I. Yoplac, L. Vargas, P. Robert, A. Hidalgo, *Heliyon*, **7**, e06737 (2021).
14. L. Hagvall, J. Christensson, *Contact Dermat.*, **71**, 280 (2014).
15. P. de Mozzi, G. Johnston, *Contact Dermat.*, **70**, 377 (2014).
16. A. Sarkic, I. Stappen, *Cosmetics*, **5**, 11 (2018).
17. Regulation (EC) 2023/1545 of the European Parliament and of the Council, of 26 July 2023, on Cosmetic Products; Official Journal of the European Union, 2023.
18. National Library of Medicine PubChem, <https://pubchem.ncbi.nlm.nih.gov/compound/643779>.
19. A. Daina, O. Michielin, V. Zoete, *Sci. Rep.*, **7**, 42717 (2017).
20. C. Lipinski, F. Lombardo, B. Dominy, P. Feeney, *Adv. Drug Delivery Rev.*, **23** (1-3), 3 (1997).
21. A. Ghose, V. Viswanadhan, J. Wendoloski, *J. Combin. Chem.*, **1** (1), 55 (1999).
22. S. Bhal, K. Kassam, I. Peirson, G. Pearl, *Mol. Pharm.*, **4** (4), 556 (2007).
23. G. Bickerton, G. Paolini, J. Besnard, S. Muresan, A. Hopkins, *Nat. Chem.*, **4** (2), 90 (2012).
24. R. Ali, A. Marella, T. Alam, R. Naz, M. Akhter, M. Shaquiquzzaman, R. Saha, O. Tanwar, M. Alam, J. Hooda, *Indones. J. Pharm.*, **23** (4), 193 (2012).
25. L. Di, P. Artursson, A. Avdeef, G. Ecker, B. Faller, H. Fischer, J. Houston. M. Kamsy, E. Kerns, S. Kramer, H. Lennernas, K. Sugano, *Drug Discov. Today*, **17**, 905 (2012).
26. C. Ogu, J. Maxa, *Bayl. Univ. Med. Cent.*, **13** (4), 421 (2000).
27. D. Ranjith, C. Ravikumar, *Res. J. Pharmacogn. Phytochem.*, **8** (5), 2063 (2019).
28. D. Veber, S. Johnson, H.-Y. Cheng, B. Smith, K. Ward, K. Kopple, *J. Med. Chem.*, **45** (12), 2615 (2002).
29. W. Egan, K. Merz, J. Baldwin, *J. Med. Chem.*, **43** (21) 3867 (2000).
30. I. Muegge, S. Heald, D. Brittelli, *J. Med. Chem.*, **44** (12) 1841 (2001).
31. J. Baell, G. Holloway, *J. Med. Chem.*, **53**, 2719 (2010).
32. R. Brenk, A. Schipani, D. James, A. Krasowski, I. Gilbert, J. Frearson, P. Wyatt, *Chem. Med. Chem.*, **3** (3), 435 (2008).
33. M. Hann, G. Keseru, *Nature Rev. Drug Discov.*, **11**, 355 (2012).
34. P. Ertl, A. Schuffenhauer, *J. Cheminform.*, **1** (8), 96 (2009).

Non-polar phytochemical compounds from dandelion (*Taraxacum officinale* Weber ex F.H. Wigg.) flowers

I. Ivanov^{1*}, M. Todorova², N. Petkova¹, I. Dincheva³

¹ Department of Organic Chemistry and Inorganic Chemistry, University of Food Technologies, 26 Maritza Blvd., 4002 Plovdiv, Bulgaria

² Faculty of Chemistry, Department of Organic chemistry, 24, Tzar Assen Str., 4000 Plovdiv, Bulgaria

³ Agro Bio Institute, 8 Dragan Tsankov Blvd., 1164 Sofia, Bulgaria

Received: November 3, 2023; Revised: April 11, 2024

Dandelion is a well-known edible and medicinal plant with numerous studies of its health benefits. Interest presents its polyphenolic and carbohydrate composition and its non-polar components in the aerial parts and roots have been identified. There are no studies about the composition of the fatty acid phytochemicals in the flowers of the dandelion. The main purpose of the present study is a comparative investigation of n-hexane, ethanol, and n-hexane/ethanol (1:1 v/v) soluble compounds from dandelion flowers (*Taraxacum officinale* Weber ex F.H. Wigg.) collected during the flowering period. The GC-MS analysis of the non-polar (lipid) fractions showed the presence of 30 biologically active phytochemicals. The fatty acids predominated in the investigated extracts [(50-60 % of total ion current (TIC)], followed by triterpenes (9-11 % of TIC) and phytosterols (7-8 % of TIC). Polyunsaturated fatty acids - linoleic acid and α -linolenic acid (10 – 15 % of TIC) were identified as the major components. Phytosterols were mainly represented by β -sitosterol (3-4 % of TIC) and stigmasterol (above 2% of TIC), while pentacyclic triterpenes from cycloartenol 3-acetate (3-4% of TIC) and β -amyrin (above 2% of TIC) were found. Based on the fatty acid profile, the nutritional indices directly correlated with the lipid metabolites profile responsible for human health were calculated: Index of atherogenicity (IA) – 1.2-1.6; Index of thrombogenicity (IT) – 0.6-0.7; Hypocholesterolemic/hypercholesterolemic (HH) ratio – 1.0-1.3; Health-promoting index (HPI) – 0.6-0.8; Unsaturation index (UI) – 72 and linoleic acid/ α -linolenic acid (LA/ALA) ratio – 1.1. The current results reveal the nutritional potential and health benefits of edible dandelion flowers.

Key words: dandelion, edible flowers, lipid profile.

INTRODUCTION

Dandelion *Taraxacum officinale* (L.) Weber ex F.H. Wigg. is a medicinal plant member of Asteraceae family, subfamily Cichorioideae, tribe Lactuceae. It is widely distributed in the warmer temperate zones of the Northern Hemisphere as a perennial weed [1]. The dandelion roots and herbs have been utilized for the treatment of various ailments such as kidney disease, dyspepsia, heartburn, spleen, liver complaints, and anorexia, in cases of poor digestion, water retention and against liver diseases including hepatitis (due to its hepatoprotective effect) [1-3]. In Bulgarian traditional herbal medicine, this plant is used for treatment of digestive diseases, prevention of renal gravel and loss of appetite [4, 5]. The main suppliers of dandelion are: Bulgaria, followed by former Yugoslavia, Romania, Hungary and Poland [6]. Dandelion active ingredients were found in both the roots and leaves [7]. Its roots and leaves contain sesquiterpenes, triterpenes, phytosterols (taraxasterols, their acetates and 16-hydroxy derivatives, α - and β -amyrin, β -sitosterol and stigmasterol), several

phenolic compounds (chicoric acid, monocaffeoyl-tartaric, 4-caffeoylquinic, chlorogenic, caffeic, p-coumaric, ferulic, p-hydroxybenzoic, protocatechuic, vanillic, syringic and p-hydroxyphenylacetic acids), as well as three coumarins (umbelliferone, esculetin and scopoletin) [1, 8]. Apart from above mentioned secondary metabolites, the dandelion roots are a rich source of polysaccharides, mainly inulin-type fructans and smaller amounts of pectin, resin, and mucilage [1, 7, 9].

Edible flowers have been used in the form of food (syrups, jellies, sauces and various desserts) and fine spices for their medicinal properties and nutritional value. The fresh flowers have been consumed for years in many cultures (Ancient Greeks, Romans and Chinese) and have also been used to treat certain ailments [10].

On this basis, in the present study we investigated the non-polar content of 95 % ethanol, n-hexane and 95% ethanol/n-hexane (1:1 v/v) extracts derived from dandelion flowers. The lipid nutritional indices were calculated.

* To whom all correspondence should be sent:
E-mail: ivanov_ivan.1979@yahoo.com

EXPERIMENTAL

Plant material and extractions

Aerial parts (flowers) of a wild-growing population of dandelion (*T. officinale* Weber ex F.H. Wigg.) in Plovdiv region, Bulgaria were randomly collected during flowering stages. The samples were dried in the shadow at room temperature and finely ground in a laboratory homogenizer. Twenty-five grams of the dried and ground material was extracted three times (250 ml) with three different solvents ethanol, n-hexane and a mixture of ethanol, and n-hexane ratio (1:1) for 24 hours under maceration. The combined extracts were evaporated on a vacuum evaporator and used for subsequent experiments.

Gas Chromatography-Mass Spectrometry (GC-MS) analysis

The dry extracts obtained from dandelion flowers were saponified with an ethanolic solution of 2 M KOH under reflux for 1.5 h. After cooling, the obtained extracts were separated by triple liquid-liquid extraction with n-hexane. GC-MS analysis was conducted on a gas chromatograph Agilent Technology Hewlett Packard 7890 A, connected with mass detector Agilent Technology 5975 C inert XL EI/CI MSD at 70 eV, under conditions as previously described [11, 12]. The obtained mass spectra were examined using 2.64 AMDIS (Automated Mass Spectral Deconvolution and Identification System), National Institute of Standardization and Technology, USA.

Nutritional Indices Calculation

A polyunsaturated-to-saturated fatty acids (PUFA/SFA) ratio, an index of atherogenicity (IA), an index of thrombogenicity (IT), a hypocholesterolemic/hypercholesterolemic ratio (h/H), a health-promoting index (HPI), and a linoleic acid/linolenic acid (LA/ALA, n-6:n-3) ratio were calculated from the GC-MS composition data following the formulas described by Chen and Liu [13].

RESULTS AND DISCUSSION

The resulting hexane, ethanol, and hexane-ethanol (1:1) extracts were hydrolyzed and the yield of the extract was calculated. Among them, the hexane extract was obtained with the highest yield (5.1 %), while the ethanol fraction (3.7 %) and a mixture of hexane and ethanol (1:1, v/v) (4.4 %) were obtained with significantly lower yields. As a next step, we performed GC-MS analysis of the three extracts obtained. The results are summarized in Table 1. Twenty-eight compounds were detected in

different investigated fractions (fatty acids, fatty alcohols, alkanes, phytosterols and triterpenes).

Fatty acids (52 – 62 % of TIC) dominate the three extracts obtained from dandelion flowers. All three extracts contain phytosterols (6 – 7 % of TIC) and triterpenes (9 – 11 % of TIC) in relatively equal amounts. Fatty alcohols were in relatively lower concentrations about 2 % of TIC. The highest content of saturated fatty acids (SFA) was found in the hexane fraction – 32 % of TIC, with 50 % due to palmitic acid C_{16:0}. Another interesting finding of the study is that the major unsaturated fatty acid is linoleic acid C_{18:2} and α -linolenic acid C_{18:3} dominate the fractions as linoleic acid C_{18:2} represent more than 50 %.

Comparative phytochemical screening shows that in the non-polar fraction obtained from dandelion flowers, fatty acids predominate over 60 % of TIC, while in similar extracts obtained from dandelion leaves, the relative content of fatty acids is only about 2 % of TIC [11].

A difference was also observed in the lipid profile of the fatty acids and fatty alcohols present in dandelion leaves and flowers. Shorter chain fatty acids from C₅ to C₈ were found in flowers, while in leaves they are from C₁₆ to C₂₆, respectively [11]. A similar phenomenon was also observed in the profile of fatty alcohols in the leaves, they ranged from C₁₈ to C₃₀ [11], while only four fatty alcohols – myristyl alcohol (C₁₄), cetyl alcohol (C₁₆), stearyl alcohol (C₁₈) and diterpene alcohol phytol (C₂₀) were identified in the flowers. About 6 times lower amount of phytosterols (about 7 % of TIC) was also observed in the flowers, compared to about 46 % of the TIC in the leaves. Both plant parts contain β -sitosterol and stigmasterol, but campesterol (about 1 % of TIC) was found only in the flowers (Table 1).

The amounts of pentacyclic triterpenes in the two plant organs were relatively similar (17% of TIC in the leaves and 11% of TIC in the flowers), but no taraxasteryl acetate was identified in the flowers.

The main and predominant components in the extracts obtained from dandelion flowers are fatty acids. The ratio Σ PUFA/ Σ SFA, the indices IA, IT, HH, HPI and LA/ALA were calculated, which are indicators of the potential health effect of the flowers (Table 2). The potential health benefits of the various lipid components can be evaluated and compared with those obtained from other raw materials and foods. Due to the relatively similar content of PUFA and SFA, extracts containing hexane (n-hexane and n-hexane/ethanol (1:1) were characterized by the highest Σ PUFA/ Σ SFA ratio (\approx 1.0) compared to the ethanol extract (0.7) (Table 2).

Table 1. Relative percentage of phytochemical compounds in the non-polar [n-hexane, ethanol (EtOH) and n-hexane-ethanol (1:1)] fraction of the dandelion flowers identified by GC-MS. Results are presented as a percentage (%) of the total ion current (TIC).

Retention time	Retention index	Compounds	EtOH	n-Hexane	EtOH/n-Hexane
		<i>Fatty acids</i>			
7.91	980	Valeric acid C _{5:0}	0.14	3.01	0.15
12.03	1168	Enanthic acid C _{7:0}	0.64	0.69	0.59
7.15	926	Caproic acid C _{6:0}	0.17	0.48	0.14
10.84	1124	Caprylic acid C _{8:0}	0.44	0.40	0.30
15.60	1324	Capric acid C _{10:0}	ND*	0.06	0.04
19.27	1523	Lauric acid C _{12:0}	2.69	2.49	2.53
22.50	1724	Myristic acid C _{14:0}	4.57	4.92	4.83
29.70	1922	Palmitic acid C _{16:0}	16.45	13.00	16.67
32.65	2095	Linoleic acid C _{18:2}	14.98	10.29	15.54
32.70	2101	Oleic acid C _{18:1}	2.05	1.87	1.96
32.77	2104	Linolenic acid C _{18:3}	13.53	9.37	13.21
32.84	2126	Stearic acid C _{18:0}	4.71	3.67	3.80
36.47	2328	Arachidic acid C _{20:0}	2.14	2.43	2.54
		<i>Alkanes</i>			
12.36	1200	Dodecane	0.04	0.05	0.03
20.45	1600	Hexadecane	0.03	ND	ND
		<i>Fatty alcohols</i>			
22.95	1758	Myristyl alcohol C ₁₄	ND	0.18	0.16
25.16	1801	Cetyl alcohol C ₁₆	0.20	0.25	0.14
30.71	1943	Phytol C ₂₀	1.54	1.61	1.03
31.46	1990	Stearyl alcohol C ₁₈	0.61	0.42	0.35
		<i>Tocopherols</i>			
43.23	2885	α -Tocopherol	1.00	2.71	0.93
		<i>Phytosterols</i>			
47.51	3187	Campesterol	0.88	1.12	1.03
47.83	3206	Stigmasterol	2.34	2.22	2.04
48.57	3264	β -Sitosterol	4.31	3.92	3.57
		<i>Triterpenes</i>			
48.81	3275	α -Amyrin	1.71	1.43	1.15
49.30	3313	β -Amyrin	2.30	2.17	1.98
50.41	3321	Lupeol acetate	1.88	1.55	1.69
50.57	3343	Lanosterol	1.83	2.06	1.63
51.46	3402	Cycloartenol 3-acetate	3.42	3.87	2.68
		<i>Total identified</i>	84.60	76.24	80.67
		Fatty acids	62.51	52.67	62.28
		Fatty alcohols	2.35	2.46	1.68
		Phytosterols	7.53	7.27	6.63
		Triterpenes	11.14	11.09	9.13

*ND – not detected.

The type of fatty acids has a greater influence on the risk of cardiovascular disease than the total amount of fat. There is some evidence that AI and TI

can be used as indicators of risk factors or predictors of cardiovascular disease, with AI and TI values higher than 1.0 indicating a greater risk of disease.

As a result, it is important to maintain a low level of these indices in a healthy diet on a daily basis [13, 14].

If a food's IA and IT are lower than 1.0, it has a lower atherogenic and thrombogenic potential [13, 14]. Our results showed variability between the samples as regards both the atherogenic index and the thrombogenic index. The obtained results from dandelion flower show that the IA is near up to 1.0 while the IT is below 1.0 (Table 2).

Also, studies have found that oils with (h/H) ratio (hypocholesterolemic/ hypercholesterolemic) relatively high over 1.0, and with low IA and IT indices, contribute to reducing the incidence of cardiovascular disease and cholesterol levels [15]. Based on the fatty acid composition of the oils obtained from dandelion flowers, it was found that the (h/H) ratio) was above 1.0. The polyunsaturated fatty acids in the extracts are in a very well-balanced ratio of n-6/n-3 (1:1) (Table 2), which is highly recommended for the normal functioning of various physiological processes. The optimal n-6/n-3 PUFA ratio should be in the range of 1:1 to 2:1 for normal physiological functions in the body due to the competitiveness of n-6 and n-3 PUFA [16].

These results for lipid indices define fresh dandelion flowers as a suitable component of rational nutrition in humans. Their consumption can lead to a reduction in the risk of cardiovascular diseases [13, 14].

Table 2. Nutritional health indices of lipid compounds obtained from dandelion flowers.

Nutritional indices	EtOH	n-Hexane	EtOH/n-Hexane
Saturated fatty acid (SFA)	31.95	31.14	31.59
Unsaturated fatty acid (UFA)	30.56	21.53	30.69
UFA/SFA	0.96	0.69	0.97
Index of atherogenicity (IA)	1.22	1.63	1.26
Index of thrombogenicity (IT)	0.61	0.72	0.61
Hypocholesterolemic/hypercholesterolemic (h/H) ratio	1.29	1.06	1.28
Health-promoting index (HPI)	0.82	0.61	0.80
Unsaturation index (UI)	72.6	50.6	72.6
Linoleic acid/ α -linolenic acid (n-6/n-3) ratio	1.11	1.10	1.17

CONCLUSION

The lipid composition of dandelion flowers has been determined. Fatty acids above 62 % are mainly identified, the ratio of saturated and unsaturated fatty acids is in a balanced ratio of 1:1; in addition, dandelion flowers are a source of short-chain fatty acids C₅-C₈ as well. The lipid fraction is also rich in triterpenes (over 11 %) and phytosterols (over 7 %) which have a beneficial effect on the lipid profile of the humans, reduce and balance blood cholesterol levels [14, 15]. Lipid indices such as atherogenicity and thrombogenicity, h/H ratio, n-6/n-3 ratio were calculated and they are all in their optimal values for human health [13-16]. All these results show that edible dandelion flowers are a suitable nutritional resource for rational human nutrition.

REFERENCES

1. K. Schütz, R. Carle, A. Schieber, *J. Ethnopharmacol.*, **107**, 313 (2006).
2. B. Sweeney, M. Vora, C. Ulbricht, E. Basch, *J. Herb. Pharmacother.*, **5**, 79 (2005).
3. I. Z. Sohail, M. Afzal, A. Afzal, I. Ur Rahman, S. Shad, B. Ahmed, N. Anjum, K. Qureshi, A. Bibi, *J. Pharmacogn. Phytochem.*, **3(2)**, 15 (2014).
4. P. Pamukov, H. Ahtardjiev, *Prirodna apteka, Zemizdat, Sofia*, 1990 (in Bulgarian).
5. I. Landjev, *Encyclopedia of medicinal plants in Bulgaria*, Publishing house Trud, Sofia, 2010 (in Bulgarian).
6. G. Bisset, D. Phillipson, F. C. Czygan, D. Frohne, D. Holtze, A. Nagell, H. J. Pfander, G. Willuhn, W. Buff (eds.), *Herbal Drugs and Phytopharmaceuticals: A Handbook for Practice on a Scientific Basis*. CRC Press, Boca Raton, Ann Arbor, London, Tokyo, 1994, p. 486.
7. M. Amin, S. Sawhney, M. Jassal, *Pharmaceut. Anal. Acta*, **4**, 221 (2013).
8. I. G. Ivanov, *Int. J. Pharmacognosy and Phytochem. Res.*, **6(4)**, 889 (2014).
9. N. Petkova, I. Ivanov, S. Topchieva, P. Denev, A. Pavlov, *Sci. Bulletin. Ser. F Biotechnol.*, **19**, 190 (2015).
10. I. Petrova, N. Petkova, I. Ivanov, *Int. J. Pharmacognosy and Phytochem. Res.*, **8(4)**, 604 (2016).
11. I. Ivanov, N. Petkova, J. Tumbarski, I. Dincheva, I. Badjakov, P. Denev, A. Pavlov, *Z Naturforsch. C. J. Biosci.*, **73**, 41 (2018).
12. I. Ivanov, I. Dincheva, I. Badjakov, N. Petkova, P. Denev, A. Pavlov, *Int. Food Res. J.*, **25**, 282 (2018).
13. J. Chen, H. Liu, *Int. J. Mol. Sci.*, **21**, 5695 (2020).
14. S. K. Tilami, L. Kouřimská, *Nutrients*, **14(18)**, 3795 (2022).
15. N. D. Lorenzo, O. V. Santos, S. C. S. Lannes, *Food Sci. Technol. (Campinas)*, **41(2)**, 524 (2021).
16. S. Park, J. J. Lee, J. Lee, J. K. Lee, J. Byun, I. Kim, J. H. Ha, *Int. J. Mol. Sci.*, **23(12)**, 6384 (2022).

Application of “Green chemistry” principles to the modification of carbohydrates from natural sources for bio-additives in plastics

D. Vassilev^{1*}, N. Petkova², D. Yaneva¹, P. Denev²

¹Technical University of Gabrovo, Department of Mathematic, Informatic and Natural Sciences, 4, H. Dimitar Str., 5300 Gabrovo, Bulgaria

²University of Food Technologies, Department of Organic Chemistry and Inorganic Chemistry, 26 Maritsa Blvd., 4002 Plovdiv, Bulgaria

Received: November 3, 2023 Revised: April 11, 2024

Interest in sucrose esters which are surfactants and environmental products, attracts the attention of researchers and manufacturers, due to the fact that renewable, easily available raw materials are used for their production. Sucrose esters are non-toxic, biocompatible and biodegradable products that are widely used in food technology, cosmetics and medicine. Many industrial technologies generate waste that poses a risk of environmental pollution. The research activity in recent years is aimed at the search for new technological solutions to intensify the processes, by applying the principles of "green chemistry". For reactions taking place in solution, the use of ultrasound is effective. Ultrasound has been found to affect the rate of chemical reactions in solution through the phenomenon of cavitation. In the synthesis and modification of organic compounds, research related to the application of ultrasound in the preparation of esters is promising, as is the aim of the present work - reduction of reaction time, increase of yields, use of safe raw materials, reduction of energy consumption. The intensifying effect of ultrasound effect in the transesterification of methylcaprate with sucrose, catalyst K_2CO_3 at room temperature was demonstrated, sucrose caprate being obtained with a significant minimization of reaction time. The characterization of the obtained ester was carried out by FT-IR, 1H and ^{13}C spectroscopy. The potential plasticizing effect of the synthesized ester was evaluated. Polyvinyl chloride was used, with different amounts of the synthesized ester added. PVC polymer films with different ester concentrations were prepared and analyzed by differential scanning calorimetry and mechanical tests (modulus of elasticity).

With the use of ultrasound energy during the process, a reduction in reaction time, use of safe raw materials, and a reduction in energy consumption were achieved. From the data obtained on the glass transition temperature and mechanical tests, we can expect an application of the ester as a biodegradable additive with plasticizing properties.

Keywords: green chemistry, sucrose ester, bio-plasticizer, bio-additives

INTRODUCTION

Polyvinyl chloride (PVC) is one of the polymers with extensive application. PVC has specific properties attributed to the chlorine atoms in its molecule. Its advantages are high strength, corrosion resistance and accessibility, and this leads to widespread application both in building materials, domestic and industrial products. However, the fragility of PVC limits its use [1-8].

Plasticizers are important additives in the industrial production of plastics, including PVC. Plasticizers contribute to uniform mixing and compatibility by effectively weakening the intramolecular bonds of polymer chains. This improves the plasticity of the material, making it more flexible and plastic while improving the characteristics of the product. Different types of plasticizers are available, with phthalate plasticizers being widely used [9-12].

Plasticizers are major additives in the processing of polyvinyl chloride (PVC), phthalates being exten-

sively utilized. However, they have been proven harmful to human health and the environment, necessitating the use of bio-alternatives.

Phthalate plasticizers, including dioctyl phthalate, dibutyl phthalate, di-(2-ethylhexyl phthalate) and diisononyl phthalate, are the most common plasticizers in PVC processing [13, 14]. Dioctyl phthalate (DOP) has excellent compatibility with PVC due to its low molecular weight, allowing it to be easily inserted between polymer molecules and providing high plasticization efficiency, and it is very popular for modifying PVC materials [15, 16]. However, the application of DOP in the food and pharmaceutical industry is limited by the hazard to human health and the environment [17]. Therefore, there is a growing need for the development and study of new plasticizers that are non-toxic and environmentally safe. Of the esters of aliphatic acids, the most commonly used as plasticizers are stearates and oleates, especially for compositions with plasticity at low temperatures. This group also includes sebacinates and adipinates, but their

* To whom all correspondence should be sent:
E-mail: dvasilev@tugab.bg

production is limited by their high cost and high volatility [4-6].

The present study uses the bio-resource sucrose to obtain suitable alternatives to conventional plasticizers, using ultrasonic synthesis to obtain an ester of sucrose with the higher fatty acid – capric acid.

EXPERIMENTAL

For the synthesis, an ultrasonic bath DimoffA-2/2, with generator power of 100W, and frequency of 44 kHz was used. Chimtex® AR reagents were used – sucrose, capric acid, sodium sulfate anhydrous (Na₂SO₄), sodium, methanol, hexane.

Thin-layer chromatography (TLC) for monitoring the progress of the reaction

Thin-layer chromatography was performed on silica gel Kieselgel 60 F254 plates (Merck, Germany). Two variants of elution were used with different mobile phases.

Variant A: The TLC plate was developed in three different types of mobile phases as follows: 1. Chloroform: methanol: water 85/13.5/1.5 v/v/v; 2. Chloroform/methanol/acetic acid 98.5/1.5/1.4 v/v/v and 3. n-hexane/diethyl ether/acetic acid 70/30/1 v/v/v.

Variant B: The TLC plate was developed in a mobile phase consisting of ethyl acetate/methanol/water 17:2:1 v/v/v. TLC spots were visualized by spraying with 10% sulfuric acid in methanol and heating at 120°C for 5 min.

FTIR spectroscopy

FTIR spectra were recorded on a Nicolet Avatar spectrometer (Thermo Scientific, USA, ZnSe crystal) on KBr pellets in the frequency range from 4000 to 500 cm⁻¹ with a resolution of 4 cm⁻¹ and 132 scans. The absorption was reported in wavenumbers (cm⁻¹).

¹H and ¹³C NMR spectroscopy.

The ¹H and ¹³C NMR spectra were recorded on a Bruker spectrometer (500 MHz frequency) in CDCl₃ with tetramethylsilane (TMS) as a standard. The chemical shifts (δ) were expressed in ppm.

Synthesis of methyl caprate

In a round-bottom flask with a ground glass joint, the appropriate 0.0035 moles of capric acid were weighed out. Then, 250 ml of hexane and 1 dm³ of 1% H₂SO₄ in CH₃OH were added. The flask was connected to a water-cooled reflux condenser and heated in a water bath at a temperature of 68-70°C. After 120 min the reaction was interrupted, and the reaction mixture was cooled to room temperature.

100 ml of distilled water was added and neutralized with 10% Na₂CO₃. The sample was extracted three times with hexane. The collected extracts were dried over anhydrous Na₂SO₄. The solvent was distilled to yield methyl caprate.

Synthesis of sucrose caprate

In an Erlenmeyer flask, 50 ml of methanol was placed and appropriate amounts of methyl caprate, sucrose, and the catalyst sodium methylate were weighed in their respective molar ratios (1:1). The mixture was sonicated at 40°C. After the reaction stopped, the synthesis was stopped, and the solvent was distilled. The residue was dissolved in 25% NaCl / n-butanol 1:1 and partitioned with a separatory funnel. After separation of the phases, the organic phase was dried over anhydrous Na₂SO₄. Then, the solvent was distilled, and the resulting sucrose caprate was obtained.

Investigation of the applicability of the obtained ester as a bio-plasticizer

For the purposes of the experiment, commercial polyvinyl chloride (PVC) without colorants, stabilizers, and fillers (EMKA®), was used. As a bio-plasticizer of polyvinyl chloride, the ultrasound-synthesized sucrose caprate was used at a concentration of 10, 20, 30, 40%. The experimental studies were carried out with samples in the form of polymer films prepared by casting from a solution in tetrahydrofuran using the following methodology: the amount of polyvinyl chloride weighed on an analytical scale was placed in a beaker and 100 cm³ of tetrahydrofuran was added to it. The mixture was heated in a water bath at 40°C until the polyvinyl chloride was completely dissolved, then the weighed amount of sucrose caprate was added. The resulting solution was homogenized for 2 h, then poured into a Petri dish and left at room temperature until the solvent had completely evaporated. The film was dried at room temperature in a vacuum dryer [3].

The thermal properties of the resulting films were investigated by differential scanning calorimetry (DSC). The measurements were carried out on a scanning calorimeter DSC 204 F1 Phoenix (NETZSCH Gerätebau GmbH) in argon medium, with a heating flow rate of 20 cm³/min at the following temperature modes:

- Heating from 20°C to 200 °C at a speed of 10 K/min (first scan);
- Isothermal mode at 200 °C for 3 min;
- Cooling in liquid nitrogen from 200 °C to –50 °C, with a cooling rate of 10 K/min;
- Isothermal mode at -50 °C for 5 min;

- Heating from -50 °C to 200 °C at a speed of 10 K/min (second scan).

The weight of a single sample of each specimen was 2.5-4.2 g. The glass transition temperature T_g was determined on the second scan as the inflection point of the thermogram. The processing was carried out with specialized software PROTEUS for DSC 204 F1.

Strength indicators were determined with *Lloyd LSI* tensiometer, in uniaxial tensile deformation at a speed of 100 mm/min at room temperature, on samples with a width of 10 mm. Using the specialized dynamometer software, the values of the breaking voltage (MPa) and the modulus of elasticity (MPa) were calculated for each sample. For each content of sucrose caprate, 9-12 samples were examined, and the results were averaged.

RESULTS AND DISCUSSION

In the IR spectra, several areas characteristic of carbohydrates stand out - about 3300 cm^{-1} there is a wide asymmetrical band due to the valence oscillations of -OH. The strong interaction between the structural elements of the macromolecules in the modified sucrose is the reason in the spectrum considered, bands arise due to complex vibrations, which can be defined as oscillations of both the furanose ring and the macromolecule as a whole. Stretching vibrations (C-C), (C-O), (C-O-C) of the furanose structure are observed between 1000 and 1200 cm^{-1} . Depending on the degree of substitution, the maximum of this band is shifted and at the same time the half-width changes. This is due to the hydroxyl groups that form the hydrogen bonds, as well as to the esterification of some of them.

In the ^1H NMR spectrum of sucrose caprate, two regions can be distinguished - in the range 0-3 ppm characteristic of methyl and methylene protons from the acid and 3.0-5.0 ppm characteristic of protons from the carbohydrate part, which are shown in Table 1. The chemical shift for methyl group protons in sucrose caprate is observed at 0.96~0.99 ppm. The signals for protons from the methylene groups are in the range of 1.31~2.36 ppm. Glucose protons of glucopyranose are observed in the range of 3.39~5.40 ppm and glucose protons of fructofuranose - 3.62~4.52 ppm.

In the ^{13}C NMR spectrum, signals that are typical of the carbonyl carbon atom at 174.36 ppm are observed. Signals for methyl carbon atoms are observed in the range of 14.02 ppm. The signals of the carbon atoms of the pyranose, respectively, of the furanose ring, are observed in the range 62.26-108.18 ppm, with carbon atoms from the pyranose ring being at the lower frequencies and for the

furanose at the higher frequency range. In order to investigate the applicability of sucrose caprate as bio-plasticizer for PVC, the data from the DSC analysis of the tested samples (Table 2) were analyzed.

Table 1. Chemical shift (δ , ppm) in the ^1H NMR spectrum

Group	Chemical shift (δ , ppm) for sucrose caprate
CH_3-	0.96~0.99
$-(\text{CH}_2)_n-$	1.31~1.68
$-(\text{CH}_2)_n-\text{CH}_2-\text{O}$	2,34~2,36
$-\text{O}-\text{C}-\text{H}-\text{O}$	5.39~5.40
H-Glc	3.39~5.40
H-Fru	3.62~4.52

Table 2. Dependence of the glass transition temperature T_g on the ester content of the sample.

Content of sucrose caprate in PVC, %	Glass transition temperature T_g , °C
0	80.5
10	59.3
20	60.9
30	62.8
40	64.6

The results obtained from the thermograms show the presence of only one inflection point (one glass transition temperature) in the thermograms of the studied films, which points to the good mixability between the esters and PVC. The glass transition temperatures of the test specimens depending on the content of the esters are presented in Table 2. There is a significant decrease in T_g with increasing ester content, which is a confirmation of its plasticizing effect on PVC. When the content of the esters increases, there is a sharp decrease in the glass transition temperature. For a more detailed study of the mechanical and strength characteristics and the change of the elastic properties, tensile deformation tests were conducted, calculating the parameters: stress at break, Young's modulus, elongation at break.

The results (Table 3) show that as the content of sucrose caprate increases, the modulus of elasticity decreases and the elongation at break of the sample increases. The change in tensile strength (breaking tension) of the sample depending on the sucrose caprate content indicates that the tensile strength decreases. Data from DSC and mechanical tests show a plasticizing effect of sucrose caprate in the polyvinylchloride film as it reduces the glass transition temperature, the modulus of elasticity and the breaking tension and increases the relative elongation at break.

Table 3. Mechanical properties of PVC containing sucrose caprate.

Ester content, %	Stress at break, MPa	Young's Modulus, MPa	Elongation at break, %
0%	52.4	1483.0	5.5
10%	24.5	746.3	80.5
20%	17.8	634.8	99.6
30%	16.9	540.6	124.3
40%	15.8	506.3	143.8

CONCLUSION

In response to the requirements for plasticized PVC in terms of environmental friendliness and health considerations, traditional plasticizers can be replaced with bio-based and environmentally friendly plasticizers derived from renewable resources, thus expanding the scope of application of PVC and its products.

The tested applicability of ultrasound-derived sucrose caprate as a bio-additive with a plasticizing effect in polyvinyl chloride was confirmed by differential scanning calorimetry, determining the effect of the ester on the glass transition temperature T_g . It was found out that the increase of its quantity results in decrease of polymer T_g , i.e. the flexibility of macromolecules increases, which is a prerequisite for higher deformability. This supports the conclusion that the ester mixture has a plasticizing effect. This is also confirmed by the mechanical properties of the PVC films used with different ester contents.

The results obtained at this stage of the study allow to conclude that sucrose caprate can be applied as a bio-additive with a plasticizing effect in polyvinyl chloride.

Acknowledgement: We acknowledge the financial support from the Fund for Scientific Research of the Technical University of Gabrovo, project #2202C/2023.

REFERENCES

- G. Wypych, Handbook of plasticizers, ChemTec Publishing, 2004.
- V. Hristova-Baghdasarian, T. Vrabcheva, J. Tishkova, *Bulgarian Journal of Public Health*, **6** (2), (2014)
- B. Yin, N. Aminlashgari, X. Yang, M. Hakkarainen, *European Polymer Journal*, **58**, 34 (2014).
- I. Baker, R. Willing, D. Furlong, F. Grieser, C. Drummond, *Journal of Surfactants and Detergents*, **3** ((1), 13 (2000).
- W. He, G. Zhu, Y. Gao, H. Wu, Z. Fang, K. Guo, *Chemical Engineering Journal*, **380**, 122532 (2020).
- Y. Ma, S. Liao, Q. Li, Q. Guan, P. Jia, Y. Zhou, *Reactive and Functional Polymers*, **147**, 104458 (2020).
- W. Li, J. Qin, S. Wang, D. Han, M. Xiao, Y. Meng, *ACS Sustainable Chemistry & Engineering*, **6**(7), 8476 (2018).
- T. Deng, S. Li, X. Yang, L. Xu, H. Ding, M. Li, *RSC Advances*, **12**(40), 26297 (2022).
- M. Li, S. Li, J. Xia, C. Ding, M. Wang, L. Xu, X. Yang, K. Huang, *Materials & Design*, **122**, 366 (2017)
- H. Zhu, J. Yang, M. Wu, Q. Wu, J. Liu, J. Zhang, *ACS Sustainable Chemistry & Engineering*, **9**(45), 15322 (2021)..
- G. Feng, L. Hu, Y. Ma, P. Jia, Y. Hu, M. Zhang, C. Liu, Y. Zhou, *Journal of Cleaner Production*, **189**, 334 (2018)..
- P. Jia, Y. Ma, F. Song, C. Liu, L. Hu, Y. Zhou, *Materials Today Chemistry*, **21**, 100518 (2021).
- M. S. Qureshi, A. R. bin Yusoff, M. Wirzal, M. D. H. Sirajuddin, J. Barek, H. I. Afridi, Z. Üstündag, *Critical Reviews in Analytical Chemistry*, **46**(2), 146 (2016).
- S. Lee, M. S. Park, J. Shin, Y.-W. Kim, *Polymer Degradation and Stability*, **147**, 1 (2018).
- F. Song, C. Huang, X. Zhu, C. Liu, Y. Zhou, P. Jia, *Journal of Applied Polymer Science*, **138**(33), 50809 (2021).
- V. A. Pereira, A. C. Fonseca, C. S. M. F. Costa, A. Ramalho, J. F. J. Coelho, A. C. Serra, *Polymer Testing*, **85**, 106406 (2020).
- J. Tan, T. Zhang, F. Wang, N. Huang, M. Yu, L. Wei, P. Jia, X. Zhu, *Journal of Cleaner Production*, **375**, 133943 (2022).

Type 2 diabetes mellitus and vascular complications

K. V. Petkova- Parlapanska¹, E. D. Georgieva², Y. D. Karamalakova¹, P. I. Goycheva³,
G. D. Nikolova^{1*}

¹Medical Chemistry and Biochemistry Department, Medical Faculty, Trakia University, Stara Zagora, 6000, 11 Armeiska Str., Bulgaria

²Department of General and Clinical Pathology, Forensic Medicine, Deontology and Dermatovenereology, Medical Faculty, Trakia University, 11 Armeiska Str., 6000 Stara Zagora, Bulgaria

³Propaedeutic of Internal Diseases Department, Medical Faculty, Trakia University Hospital, Stara Zagora, Bulgaria

Received: November 3, 2023; Revised: April 11, 2024

Diabetes mellitus and its complications have imposed a significant burden on public health. High death rates in type 2 diabetes are linked to vascular complications, with the risk of myocardial infarction and stroke tripling in patients with this illness. Oxidative stress can lead to the dysfunction of the advanced glycation end products and the receptor for advanced glycation end products. This study aims to examine potential biomarkers for the early development of vascular complications in type 2 diabetes mellitus. The study included 67 patients with type 2 diabetes mellitus (T2DM) with a male-to-female ratio of 1:1.3. They were divided into two groups based on the presence or absence of macroangiopathic vascular complications. To evaluate the oxidative stress in the studied groups, nitric oxide (NO•) radicals were investigated by electron paramagnetic resonance (EPR) spectroscopy and GPx, eNOS, TNF- α , and TGF- β with ELISA kits following the manufacturer's instructions. All studied parameters were compared with 35 healthy controls.

In summary, the presented results show that high levels of ROS in T2DM and diabetic patients with vascular complications lead to increased levels of NO radicals, depletion of antioxidant enzymes, and increased levels of pro-inflammatory cytokines (TNF- α , TGF- β) which interfere with induced migratory responses and contribute to dysfunction.

Keywords: diabetes mellitus, vascular complications, GPx, eNOS, TNF- α , TGF- β

INTRODUCTION

Diabetes mellitus is still being researched, along with its associated pathologies and complications, as it continues to be the eleventh most common cause of death [1]. About 90% of patients with diabetes have type 2 diabetes mellitus (T2DM), and it affects the economically active population between the ages of 35 - 64 the most. High death rates in T2DM are linked to vascular complications, with the risk of myocardial infarction and stroke tripling in patients with this illness [2]. Diabetes mellitus is also the most frequent cause of acquired blindness, renal failure, and amputation of limbs. Despite significant progress and outstanding achievements in the study of the mechanisms of the development of T2DM and the success of new medicinal products to control glycemia, the complications associated with the disease continue to increase [3]. Therefore, current research is focused on investigating the possible mechanisms for the development of T2DM, such as oxidative advanced glycation of end products (AGE) and of the receptor for advanced glycation end products (RAGE). Levels of AGE and RAGE can

cause inflammation and tissue damage by promoting the expression of vascular cell adhesion molecules, monocyte chemoattractant protein-1, endothelin-1, and plasminogen activator inhibitor-1 (PAI-1), and are involved in damage to vessels and tissues [4]. Superoxide anion, hydroxyl radicals, and hydrogen peroxide are examples of reactive oxygen species (ROS) that mediate oxidative reactions in the development of diabetic cardiovascular complications. The heart contains endogenous antioxidant enzymes that protect against ROS toxicity, including SOD, CAT, GPx, GST, and glucose-6-phosphate dehydrogenase. Primary pathological features of diabetic cardiomyopathy include increased levels of malondialdehyde and markers of oxidative stress, as well as necrosis factor- α (TNF- α) and tumor growth factor (TGF)- β [5 -8]. An increased level of 3-nitro-tyrosine is another indicator of oxidative stress in T2DM [9]. Peroxynitrite (ONOO⁻) and nitrogen dioxide (NO₂) react to form peroxynitrite, which reacts with free tyrosine or proteins to produce 3-nitrotyrosine. This impairs mitochondrial function in the myocardium.

* To whom all correspondence should be sent:

E-mail: galina.nikolova@trakia-uni.bg

It should be noted that protein nitration and lipoproteins may also play a direct pathophysiological role in the development of atherosclerosis.

Sirtuin-1 (SIRT1) has a major role in regulating the response to oxidative stress by influencing DNA repair and cell survival. Recent studies suggest that it also regulates cellular glycolytic stress by controlling the glyoxalase system [10]. This is particularly relevant in T2DM, where oxidative stress is one of the primary pathophysiological processes associated with complications. These complications can continue even after carbohydrate metabolism indicators are normalized, leading to vascular complications.

This study aims to examine potential biomarkers for the early development of vascular complications in T2DM.

EXPERIMENTAL

Ethics statement

This work was conducted according to the Declaration of Helsinki, and approved by the Ethics Board, "Clinic for Endocrinology and Metabolic Diseases", UMHAT "Prof. St. Kirkovich" in Stara Zagora, Bulgaria. Written informed consent (2021/2023 MF, TrU, Stara Zagora) was obtained from the patients after hospitalization between January 2021 and August 2023.

Study design and subjects

All reagents were purchased from Merck KGaA, Darmstadt, Germany. The study included T2DM 67 patients, in ratio 1:1.3 male - to - female, and based on the presence or absence of macroangiopathic vascular complications they were divided into two groups (Table 1).

To assess macroangiopathic complications, patients were defined as having experienced a cardiovascular event if they had been diagnosed with coronary heart disease, cerebrovascular disease, and/or peripheral arterial disease. At the time of study entry, 45 (58%) T2DM patients had poor disease compensation. Venous blood was collected at the Clinic for Endocrinology and Metabolic Diseases on the day of the study by venipuncture from a peripheral venous source between 8:00 a.m. and 10:00 a.m. in a vacutainer for serum with a clot activator - 4 mL. The samples collected for the electron paramagnetic resonance (EPR) study were immediately imaged and then frozen at - 80°C for the ELISA assay. About half of the patients with diabetes (58.1 %) were obese. The proportion of patients suffering from ischemic heart disease was 37.6 %. Eleven of the patients (11.8 %) had a history

of cerebrovascular disease. None of the diabetics presented symptomatic lower extremity arterial disease. At study entry (58 %) of T2DM patients with vascular disease had poor disease compensation, defined as HbA1c > 7 % and fasting blood glucose values > 6.1 mmol/L. In terms of therapy, diabetics with good glycemic control (22 patients) took oral hypoglycemic agents (sulfonylureas and biguanides), and in 6 patients biguanides were combined with insulin; 7 patients were on insulin monotherapy. In the subgroup of diabetics with poor glycemic control (n = 45), 15 were treated with oral hypoglycemic agents (sulfonylureas and biguanides); 10 were on insulin therapy, in 20 of whom it was combined with oral medication (insulin plus biguanides). The comparison was made with 35 healthy volunteers, 14 males, and 21 females, with a mean age of 43.32 ± 9.28 years. Only 7 (7.4 %) of the controls had slightly increased body weight (BMI 31- 33). Participants were matched for gender. Patients with and without vascular disease were balanced/matched for gender and age. Table 1 presents the key characteristics of diabetics with concomitant vascular disease and healthy controls.

Electron paramagnetic resonance (EPR) study

All EPR measurements were performed at room temperature on a Bruker BioSpin GmbH, Ettlingen, Germany, equipped with a standard resonator. The EPR experiments were carried out in triplicate. Spectral processing was performed using Bruker WIN-EPR and Sinfonia software, 2009. Based on the methods published by Yoshioka *et al.* [12] and Yokoyama *et al.* [13], the EPR method was developed and adapted for the •NO radical levels estimation.

Enzyme-linked immunosorbent assay

All markers of oxidative stress were measured with ELISA kits following the manufacturer's instructions. The ELISA kits were as follows: Human eNOS (ab241149); Human TNF- α ELISA Kit (ab181421); Human TGF- β ELISA Kit (ab100647).

Statistical analysis

Statistical analysis was performed with Statistica 8, StaSoft, Inc. (Madrid, Spain), and the results were expressed as means ± SE. All data were expressed as means ± SE and obtained by one-way ANOVA, and in the LSD post hoc test, $p > 0.05$ was considered statistically significant. To define which groups were different from each other, LSD post hoc tests were used.

Table 1. Clinical and laboratory data of the studied patients

Variables	Controls ($n = 35$)	DMT2 ($n = 22$)	DMVC ($n = 45$)
Age	43.32 ± 6.45	52.13 ± 4.85	55.75 ± 7.04
Sex (M/F)	14 M/21 F	11 M/11 F	22M/23 F
Disease duration (years)	-	10.7 ± 7.3	12.7 ± 8.6
BMI (kg/m ²), mean ± SD	26.07 ± 3.52	32.11 ± 5.44	33.56 ± 6.21
Blood sugar (mmol/L), mean ± SD	4.98 ± 0.32	8.05 ± 5.11	9.55 ± 4.89
HbA1c%	5.69 ± 0.44	6.37 ± 0.85	9.87 ± 1.27
GFR (mL/min/1.73 m ²)	110.08 ± 9.32	96.39 ± 4.25	89.91 ± 3.01
UAE (mg/day)	1.20 ± 0.35	21.80 ± 1.	24.57 ± 6.85
FBC (mmol/L)	5.31 ± 0.28	6.43 ± 0.89	12.72 ± 5.15
Cholesterol (mmol/L)	4.17 ± 0.3	5.01 ± 0.7	5.47 ± 0.6
Triglycerides (mmol/L)	1.31 ± 0.15	2.13 ± 0.2	2.65 ± 0.2
HDL (mmol/L)	0.91 ± 0.019	1.19 ± 0.04	1.32 ± 0.05
LDL (mmol/L)	2.03 ± 0.11	2.72 ± 0.24	2.96 ± 0.2
CRP (pg/mL)	14.14 ± 0.42	26.68 ± 0.95	51.86 ± 2.79

RESULTS AND DISCUSSION

Clinical and laboratory data for healthy volunteers (controls) diabetes mellitus (T2DM) and diabetes mellitus with vascular complications (DMVC) are presented in Table 1.

GPx antioxidant enzymes' activity in patients with T2DM and controls

Investigation of the intracellular oxidative status involves measurement of antioxidant enzyme activity, which includes GPx activity. The results indicated a statistically significant difference in GPx activity (Fig. 1) in the diabetic group, T2DM compared to healthy controls ($p = 0.0001$) and diabetic patients with vascular complications T2DMVC ($p = 0.003$).

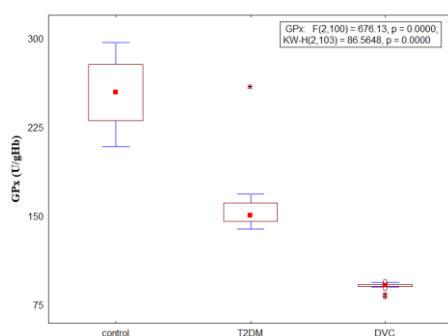


Fig. 1. Activity of antioxidant enzyme GPx in serum samples of diabetic mellitus patients compare to controls and patients with complications. LSD post hoc test, * $p < 0.05$ vs. control; ** $p < 0.05$ vs. DMT2.

Figure 1 presents the reduced activity of the antioxidant enzyme glutathione peroxidase (GPx) in patients with T2DM and vascular complications compared to a control group ($p < 0.05$). The results are consistent with the findings of other studies [14]. The GPx reduced activity was attributed to the

exhaustion of the antioxidant defense system after radical over generation. The autoxidation of glucose in diabetic patients leads to the formation of hydrogen peroxide (H_2O_2). Additionally, H_2O_2 inactivates the antioxidant defense system. The accumulation of H_2O_2 is suggested as a potential explanation for the decreased activity of GPx. Severe oxidative stress, possibly induced by radical over generation, is implicated in the inactivation of GPx. It is interesting to note that GPx, which is usually stable, may become inactivated under conditions of significant oxidative stress. High glucose conditions are mentioned as a factor that can cause the inactivation of GPx through glycation.

The pro-inflammatory cytokine TNF- α and TGF- β levels

The mean value for the tumor necrosis factor (Fig. 2A) in a group with complications of the TNF- α was statistically significantly higher compared to the control groups ($p < 0.05$) and T2DM ($p < 0.05$). Transforming growth factor- β (TGF- β ; Fig. 2B) was statistically significantly higher in the group with vascular complications compared to healthy volunteers ($p < 0.05$) and T2DM ($p < 0.05$). Monocyte-associated inflammatory mediators such as TNF α (Fig. 2A) and CRP (Table 1) have a key role in reducing the risk of cardiovascular diseases in type 2 diabetic conditions [15]. The pathophysiological mechanisms show that the altered monocyte profile precedes the exacerbated secretion of tumor necrosis factor-alpha (TNF- α). The obtained results confirm data reported in the literature [16] that TGF- β is involved and is directly related to diabetic cardiomyopathy which increases the risk of functional and structural abnormalities of the heart. These indicators can be used for the prevention, diagnosis and treatment of diabetes-

related cardiomyopathy [17-19]. Endothelial nitric oxide synthase (eNOS) is regulated by SIRT1. Previous studies have shown that SIRT1 can deacetylate endothelial nitric oxide synthase (eNOS) [20]. Since impaired NO production and vasodilation are associated with diabetes - accelerated endothelial dysfunction, it has been suggested that by regulating SIRT1-mediated eNOS, the vasodilator effects may be controlled [18]. Therefore, information on the levels of NO and eNOS in serum samples of patients with diabetes mellitus is of utmost importance (Fig. 3.).

NO and eNOS levels in serum

NO has been implicated as a major mediator of endothelium-dependent relaxation and together with EDRF (endothelium-dependent relaxing factor), EDCF (endothelium-dependent contracting factor) and EDHF (endothelium-dependent hyperpolarizing factor) plays an important role in the regulation of vascular tone and vasoreactivity, especially in resistance blood vessels where a small change in membrane potential causes a significant change in diameter [21, 22]. A possible mechanism of impaired vasodilation by TNF- α may be through epoxyeicosatrienoic acids (EETs) are synthesized in endothelial cells from arachidonic acid through cytochrome P450 oxygenase [23]. There are various ways in which TNF- α activates NOS. Essentially, it leads to a significant decrease in mRNA levels. Furthermore, the activation of eNOS by TNF- α necessitates the activation of protein kinase B, which is done through the activation of the sphingosine-1-phosphate receptor [24]. The activation of eNOS by TNF- α is associated with an increased production of NO, which provides protective effects against dendritic cell adhesion to the endothelium that TNF- α triggers. Increased TNF- α expression induces ROS production, leading to endothelial dysfunction in type 2 diabetes. TNF- α -related endothelial dysfunction in patho-physiological conditions is associated with excess ROS production and reduced NO bioavailability [25].

Vascular dysfunction or damage induced by aging, smoking, inflammation, trauma, hyperlipidemia, and hyperglycemia are among the myriad risk factors that may contribute to the pathogenesis of many cardiovascular diseases, such as hypertension, diabetes, and atherosclerosis [26]. However, the exact mechanisms underlying the impaired vascular activity remain unclear. The available evidence suggests that inflammatory cytokines play a major role in disrupting both macrovascular and microvascular circulation in vivo and in vitro. Additionally, the AGE/RAGE and NF- κ B signaling pathways are instrumental in promoting TNF- α expression, thereby increasing the production of circulating and local vascular TNF- α . This increase in TNF- α expression leads to the production of ROS, which in turn leads to endothelial dysfunction.

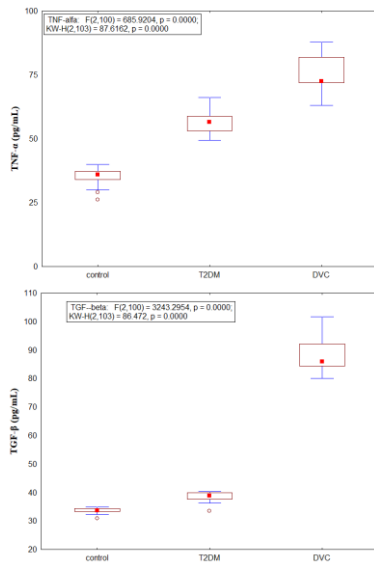


Fig. 2. Pro-inflammatory cytokine levels: (A) TNF- α ; (B) TGF- β in serum samples of diabetic mellitus patients compare to controls and patients with complications; LSD post hoc test, * $p < 0.05$ vs. control; ** $p < 0.05$ vs. T2DM.

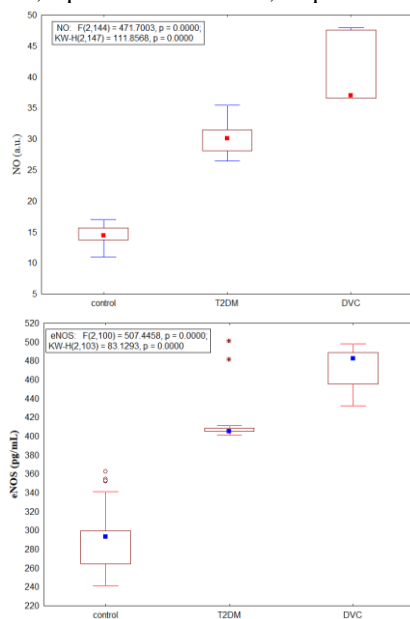


Fig. 3. NO and eNOS levels in serum samples of diabetic mellitus patients compare to controls and patients with complications; LSD post hoc test, * $p < 0.05$ vs. control; ** $p < 0.05$ vs. T2DM.

CONCLUSIONS

In summary, the presented results show that high levels of ROS in T2DM and diabetic patients with vascular complications lead to increased levels of NO radicals, depletion of antioxidant enzymes, and increased levels of pro-inflammatory cytokines (TNF- α , TGF- β) which interfere with monocyte-induced migratory responses and contribute to monocyte dysfunction.

Acknowledgement: This study was funded by scientific project №15/2023 of the Medical Faculty, Trakia University, Stara Zagora, Bulgaria, and the Ministry of Education and Science BG-RRP-2.004-0006” Development of research and innovation at Trakia University in service of health and sustainable well-being”.

REFERENCES

1. A. Schmidt, *Arteriosclerosis, Thrombosis, and Vascular Biology*, **38**, (9), e159 (2018).
2. C. González-Juanatey, M. Anguita-Sánchez, V. Barrios, I. Núñez-Gil, J. Gómez-Doblas, X. García-Moll, *J. Clin. Med.*, **12**, 5218 (2023).
3. J. Johnson, R. Jagers, S. Gopalkrishna, A. Dahdah, A. Murphy, N. Hanssen, P. Nagareddy, *ARS*, **36**, 652 (2022).
4. J. Lee, J. Yun, S. Ko, *Nutrients*, **14**, 3086, (2022).
5. Y. Tan, Z. Zhang, C. Zheng, K. Wintergerst, B. Keller, L. Cai, *Nat. Rev. Cardiol.*, **17**, 585 (2020).
6. M. Panayotova, K. Peeva, P. Chakarova, *Pediatrics*, **55** (3), 22 (2018).
7. O. Akpoveso, E. Ubah, G. Obasanmi, *Antioxidants*, **12**, 123 (2023).
8. N. Byrne, N. Rajasekaran, E. Abel, H. Bugger, *Free Radic. Biol. Med.*, **169**, 317 (2021).
9. G. Jakubiak, G. Ciešlar, A. Stanek, *Antioxidants*, **11**, 856 (2022).
10. N. Syed, A. Bhatti, P. John, *Antioxidants*, **12**, 1663 (2023).
11. D. Yoshioka, M. Hamada, T. Okamoto, Y. Kobori, Y. Kobayashi, *Photochem. Photobiol. Sci.*, **21**, 1781 (2022).
12. Y. Horizumi, S. Goto, M. Takatsuka, H. Yokoyama, *Mol. Pharmaceutics*, **20**, 2911 (2023).
13. V. Pouresmaeil, A. Al Abudi, A. Mahimid, M. Sarafraz Yazdi, A. Es-Haghi, *Biol. Trace Elem. Res.*, **201**, 617 (2023).
14. S. Ngcobo, B. Nkambule, T. Nyambuya, K. Mokgalaboni, A. Ntsethe, V. Mxinwa, P. Dlodla, *Biomed. Pharmacother.*, **146**, 112579 (2022).
15. S. Kimball, A. Joshi, W. Carson, A. Boniakowski, M. Schaller, R. Allen, J. Bermick, F. Davis, P. Henke, C. Burant, S. Kunkel, *Immunity*, **66**, 2459 (2017).
16. S. Seksaria, S. Mehan, B. Dutta, G. Gupta, S. Ganti, A. Singh, *J. Biochem. Mol. Toxicol.*, **37**, 23330 (2023).
17. M. Panayotova, M. Muhtarov, P. Dragomirova, V. Bangyozov, V. Boeva-Bangyozova, *Gen. Med.*, **20** (3), 47 (2018).
18. T. Meng, W. Qin, B. Liu, *Front. Endocrinol.*, **11**, 568861 (2020).
19. M. Su, W. Zhao, S. Xu, J. Weng, *Antioxidants*, **11**, 108 (2022).
20. M. Muhtarov, V. Boeva-Bangyozova, M. Panayotova, D. Popov, *Gen. Med.*, **21** (1), 64 (2019).
21. F. Nappi, A. Fiore, J. Masiglat, T. Cavuoti, M. Romandini, P. Nappi, S. Avtaar Singh, J. Couetil, *Biomedicines*, **10**(11), 2884 (2022).
22. M. Razan, S. Amissi, R. Islam, J. Graham, K. Stanhope, P. Havel, R. Rahimian, *Biomedicines*, **11**, 1129 (2023).
23. F. Isse, A. El-Sherbeni, A. El-Kadi, *Drug Metab. Rev.*, **54**, 141 (2022).
24. Q. Xiao, D. Wang, D. Li, J. Huang, F. Ma, H. Zhang, X. Ha, *JDC*, 108565 (2023).
25. M. Thomas, M. Coughlan, M. Cooper, *Cell Metabolism*, **35**, 253 (2023).
26. W. Frąk, A. Wojtasińska, W. Lisińska, E. Młynarska, B. Franczyk, J. Rysz, *Biomedicines*, **10**, 1938 (2022).

Silybum marianum reduces acute kidneys injury by modifying biochemical changes and oxidative stress levels in glycerol-induced CRUSH syndrome

Y. D. Karamalakova^{1*}, E. D. Georgieva², K. V. Petkova-Parlapanska¹, V. B. Slavova³,
K.V. Ivanova⁴, V. A. Ivanov³, G. D. Nikolova¹

¹Department of Chemistry and Biochemistry, Medical Faculty, Trakia University, 11 Armeiska Str., 6000 Stara Zagora, Bulgaria

²Department of General and Clinical Pathology, Forensic Medicine, Deontology and Dermatovenerology, Medical Faculty, Trakia University, 11 Armeiska Str., 6000 Stara Zagora, Bulgaria

³Department of Social medicine, Health Management and Disaster Medicine, Medical Faculty, Trakia University, 11 Armeiska Str., 6000 Stara Zagora, Bulgaria

⁴ General and Clinical Pathology, Forensic Medicine and Deontology, Medical Faculty, Trakia University, 11 Armeiska Str., 6000 Stara Zagora, Bulgaria

Received: November 3, 2023; Revised: April 11, 2024

Crush syndrome (CS), also known as traumatic rhabdomyolysis, is a condition that can occur as a result of various incidents such as traffic accidents, earthquakes, and long-term crushing of muscle-rich parts. This condition arises due to the destruction of striated muscle cells. When the compressive pressure is suddenly removed, the damaged cells and myoglobin (Mb), which is nephrotoxic, are carried by oxygenated blood, leading to myoglobinuria, acute kidney injury (AKI), metabolic disorders, hypovolemic shock, and multiple organ dysfunction syndrome (MODS). This study aims to investigate the protective effects of *Silybum marianum* (*S. marianum*, *SM*) against induced toxicity resulting from glycerol (Gly) intramuscular injection (50 % glycerol: 0.9 % saline), which can lead to CS. The study involved 24 rats, which were randomly divided into four groups: (1) controls; (2) *S. marianum* treated (oral, 5 g/1 kg per day, 18 days); (3) Gly (8 mg/kg b.wt.: 50 % saline, intramuscular (i.m.), once, only on day 16); and (4) *S. marianum* (oral, 5 g/1 kg per day, 18 days) administered for 18 days, once per day, and Gly (8 mg/kg body weight: 50% saline, i.m., once, only on day 16). By the end of the 19 experimental days of Gly administration, no mortality was observed in rats. After euthanasia, histopathological, biochemical and oxidative stress studies were performed on right kidney tissues and blood samples. All parameters of groups 1 and 2 were similar. The Gly-administered group showed significant weight loss ($p < 0.003$) compared to the control and *S. marianum* groups. On the other hand, the combined treatment Gly + *S. marianum* demonstrated a significant increase in antioxidant defense ($p < 0.005$). This can be attributed to the suppression of oxidative stress and reduced reactive oxygen/nitrogen production observed in the kidney and blood. Additionally, treatment with *S. marianum* provided protection against acute tubular necrosis, medullary congestion, and apoptotic indices recorded in the Gly group. Combination therapy of Gly and *S. marianum* improves tubular necrosis, activates antioxidant enzyme defense, and reduces free radicals. Longer treatment with this therapy can prevent CS (rhabdomyolysis).

Keywords: Crush syndrome, AKI, *S.marianum*, oxidative stress, protection

INTRODUCTION

Crush syndrome (CS) or traumatic rhabdomyolysis (RM) is a medical condition that results from direct injury to the body and is characterized by ischemic necrosis of muscle tissue due to prolonged limb compression or body swelling. This condition can cause electrolyte disturbance, dark urine (myoglobinuria), and elevated creatine kinase levels. These factors can lead to various clinical complications such as myoglobinuria, acute kidney injury (AKI), hypovolemic shock (HSc), and multiple organ dysfunction (MODS) [1, 2]. CS is a medical condition that frequently occurs in the aftermath of natural disasters like earthquakes, volcanic eruptions

and traffic accidents, as well as during wars and stampedes. The syndrome is commonly seen in the aftermath of large-scale disasters that result in significant material losses and casualties. Although CS can affect all vital organs of the body, AKI is the most prominent complication.

AKI is a common consequence after CS, which leads to a decrease in renal function, electrolyte metabolism disturbances, and hypovolemic shock following the release of compression. The pathogenesis of CS-induced AKI is multifactorial and may involve renal ischemia-reperfusion (I/R) injury, systemic inflammation, and excessive deposition of myoglobin structures (Mb) in renal tubules released from damaged muscle tissue [2-4]. During CS, the breakdown of muscle cells leads

* To whom all correspondence should be sent:
E-mail: * yanka.karamalakova@trakia-uni.bg

to the release of large Mb amounts. After glomerular infiltration, Mb directly enters the renal tubules where it precipitates and promotes the formation of tubule-blocking casts. As a result, the damaged tubular epithelial cells lead to AKI. AKI clinically refers to an increase in serum creatinine by more than 0.3 mg/dl and a decrease in urine output by less than 0.5 mL/kg/h for six hours. Regrettably, even with the administration of dialysis or kidney transplantation, most CS individuals succumb to multiple organ failure due to a systemic inflammatory response [4, 5].

After the kidneys experience prolonged oxidative stress (OS), their blood flow is significantly reduced. Although the blood supply is restored after debridement, the subsequent I/R process triggers an accelerated production of reactive oxygen and nitrogen species (ROS/RNS), as well as an enhanced systematic inflammatory response [4]. Recent research has pointed towards ferroptosis (which involves iron retention, reduced glutathione (GSH), accumulation of ferro-dependent lipid peroxidation, and ROS) as a potential therapeutic target for reducing AKI following cardiac surgery [4, 6]. On the other hand, in renal tubules, Mb binds to uromodulin and uric acid, which promotes acute CS-AKI [7], and is phagocytosed by lysosomes to produce iron and Fe^{2+} [8, 9]. Excessive filtration of Mb causes the activation of iron overload, which releases free divalent Fe^{2+} ions. These ions produce hydroxyl radicals ($\bullet OH$) via Fenton synthesis, leading to OS damage and lipid peroxidation in the affected cells. This can make it difficult to redox-modulate oxidative damage to the kidney [4, 10, 11]. In cases of AKI, ROS- and RNS-induced OS can cause significant damage to renal tubules, leading to prolonged lipid peroxidation and activation of cytoprotective mechanisms [12]. To counteract this, antioxidants such as vitamins E and C, N-acetylcysteine, dimethyl thiourea, melatonin, and selenium have been used in experimental animal models affected by glycerol-induced CS-AKI [12]. Additionally, natural plants have been found to protect kidney cells by reducing ROS and RNS levels, which are directly associated with oxidative stress in the kidneys. This helps modulate the oxidation of proteins, lipids, and nucleic acids while also restoring antioxidant enzyme inhibition [13].

The mechanism of action after CS-induced AKI and anti-inflammatory treatments highlight the importance of early intervention with antioxidant therapy to improve kidney function and treat AKI. This is crucial in preventing the progression of chronic nephropathy. The most commonly used

method to induce CS/RM in rats and lead to AKI is through intramuscular injection of glycerol [14].

Silybum marianum L (*S. marianum*) is a potent extract from milk thistle known for its anti-inflammatory, antioxidant, and AKI-protective properties. It is a cell permeability regulator and membrane stabilizer that boosts protein and nucleic acid synthesis in kidney cells, modulates immune-stimulatory cytokines and increases cell replication. *S. marianum* is effective in preventing premature death and is a must-have in any health professional's arsenal [14, 18, 19]. This research aimed to evaluate the protective potential of *S. marianum* against Gly-induced AKI by assessing the performance of key antioxidant enzymes (GSH, SOD, and CAT), along with intracellular $\cdot NO$ radicals and ROS production in the Wistar rats kidneys.

EXPERIMENTAL

Gly-induced kidneys AKI and S. marianum co-treatment

Twenty-four female Wistar rats were housed in a controlled environment with a room temperature of 23°C and a 12-hour light/dark cycle. The rats (6 weeks old; 200-305 g), were kept at the Medical Faculty, Trakia University, Stara Zagora. The Research Ethics Committee/Medical Faculty (project code: MF7/2019; MF6/2022; BFSA 266/20), Trakia University and the European Directive 210/63/EU-22.09.2010 were strictly followed during the experiment. To prepare for the experiment, the female rats were deprived of water for 24 hours and then injected intramuscularly (i.m.) with a calculated dose of 50% v/v Gly/saline. The injection was divided equally into the right/ left hind limb (8 mg/kg body weight) and was given once on the 16th day of the experiment [20]. The experiment involved administering *S. marianum* (92% purity) orally at a concentration of 0.5 %, v/v (5 g/1 kg body weight) for 18 days, daily. Control animals were treated i.m. with physiological solution. After the treatment, each rat was allowed to recover for 3 days under laboratory conditions. On day 19, the rats were sacrificed under anesthesia using xylazine (270 mg/kg) and ketamine (30 mg/kg) administered i.p.

Blood (2 cm³) was collected through cardiac puncture and centrifuged at 4000 rpm at 4 °C for 10 min and 200 μL of serum from each group was stored at -4°C until further use.

The kidneys were immediately collected, and washed with ice-cold saline. The left kidney from each animal was stored in 10% formalin for histological examination, while the right kidney was homogenized and, after the addition of solvents, centrifuged at 4000 rpm at 4 °C for 10 min.

Supernatants (300 μ L) were prepared for biochemical analysis.

The study was performed with 4 groups, 6 animals per group: (1) normal diet; (2) *S. marianum* treated (oral, 5 g/ 1 kg per day for 18 days); (3) Gly (8 mg/kg b.wt.: 50 % saline, i.m., once, only at day 16th); and (4) *S. marianum* (oral, 5g/ 1 kg per day, 18 days) administered for 18 days, one per day and Gly (8 mg/kg b.wt.: 50 % saline, i.m., once, only at day 16th). By the end of the 19th day after Gly administration, no mortality was observed.

Biochemical, enzyme-linked and oxidative stress markers evaluation

Blood samples were centrifuged at 3000 rpm at 4 °C for 10 min until serum was separated, and blood urea nitrogen (BUN), creatinine (Cre), potassium (K⁺), and sodium (Na⁺) concentrations were determined spectrophotometrically (Sigma Aldrich, USA).

Kidney homogenates were centrifuged at 5000 rpm for 10 min and the supernatants were collected for the thiobarbituric acid- based method described by Ohkawa *et al.*, 1979 [21], in μ mole MDA/g tissue. Superoxide dismutase (SOD) and catalase (CAT) were measured using methods described by Sun *et al.*, [22] and by Aebi *et al.*, [23], respectively. The pro-inflammatory markers tumor necrosis factor (TNF- α) and interleukin-6 (IL-6) were evaluated in serum using commercially available ELISA kits (Sigma Aldrich, USA) according to the manufacturer's instructions. Kidney homogenates of 100 mg were homogenized with 900 μ L 50 mM spin-trap N-tert-butyl-alpha-phenylnitron (PBN) dissolved in dimethyl sulfoxide (DMSO) using one-cycle sonication (2 min). After 5 min of ice incubation, the suspension was centrifuged at 4000 rpm for 10 min at 4 °C, transferred into a cold Eppendorf tube and immediately analyzed by EPR spectroscopy [24] for ROS production. NO• radicals were studied by adapted EPR estimation of the spin-adduct formed between carboxy- PTIO K and generated radicals, by [25, 26].

Histopathological examination

Left kidneys were washed with saline, fixed in 10 % neutral formalin for 24 h, dehydrated in a series of increasing alcohol concentrations, and deparaffinized. Then, the sections were rehydrated and stained with hematoxylin/ eosin to quantify the extent of tubular injury, dilatation, vacuolization, and necrosis in kidney tissues [27].

Statistical analysis

Statistical analysis was performed with Statistica

8.0, Stasoft, Inc., one-way ANOVA, using Student's t-test and Tukey-Kramer post hoc tests, to determine significant differences among data groups. EPR spectral processing was performed using Bruker Win-EPR and Sinfonia software. The results were expressed as means \pm standard error of mean (SEM, n=6). p-Values less than 0.05 were considered as statistically significant.

RESULTS AND DISCUSSION

AKI due to CS is a serious condition that can lead to a loss of renal filtration rate and accumulation of protein residues in renal tissues. The Gly-induced CS-AKI model is used in animal research to understand the mechanisms causing this injury. This model displays a myoglobinuric state and a significant decrease in filtration rate, which is caused by the accumulation of ROS/ RNS resulting in inflammation [1, 2, 14]. Understanding AKI's pathophysiology is crucial to develop effective treatments.

Plant antioxidants act as protectors and therapeutic agents against Mb-induced OS, preventing lipid peroxidation and ameliorating inflammatory response, ultimately preventing AKI damage. These findings demonstrate the potential for developing new treatments for this condition [4, 14, 28]. The study reported that administration of *S. marianum* significantly inhibited blood and renal inflammation in an AKI model/ferroptosis and reduced lipid peroxidation, OS and ROS/RNS formations.

S. marianum regulates biochemical parameters, electrolytes and lipid peroxidation in CS-induced AKI

The Gly-induction caused a significant increase in serum Cre ($p < 0.05$), BUN ($p < 0.004$), K⁺ ($p < 0.05$) in the AKI group compared to controls, indicating acute renal dysfunction associated with toxic renal Mb levels. In contrast, significant decrease in Na⁺ concentration in controls was not observed in the AKI group (Fig. 1).

In addition, *S. marianum* was significantly ameliorating Gly-induced AKI and directly regulating BUN, in comparison to animals receiving Gly alone. Interestingly, *S. marianum* administration in Gly-induced AKI animals insignificantly decreased Cre, K⁺, and Na⁺, but effectively ameliorated the renal injury (seen by histopathology). It significantly decreased lipid peroxidation levels to values almost comparable to healthy controls (300.9 \pm 1.12 μ mol vs. 274.4 \pm 2.66 μ mol, respectively), (Fig. 2).

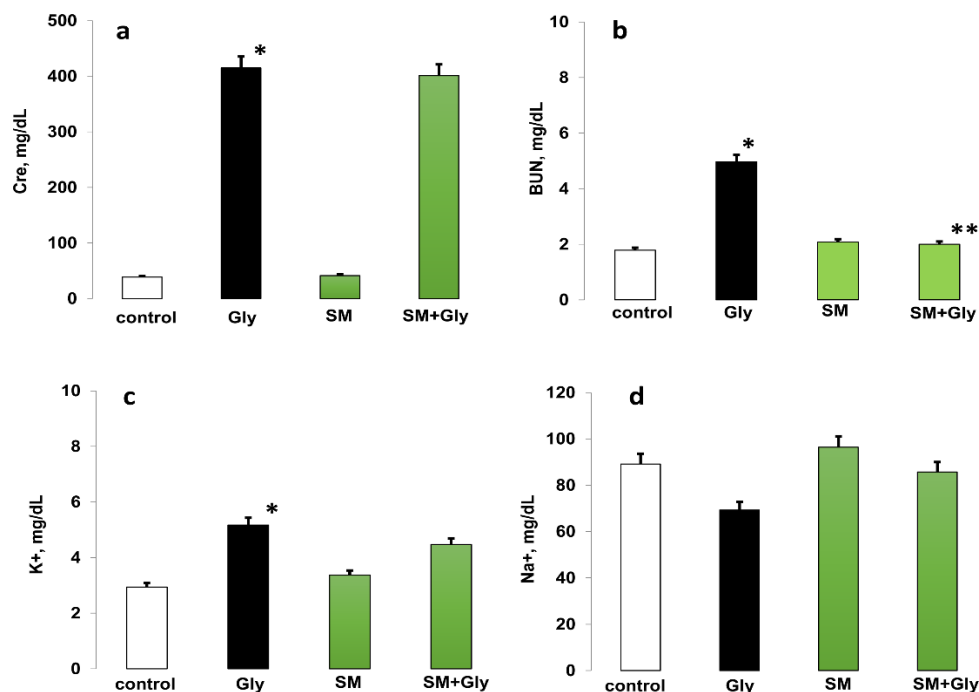


Figure 1. Effects of *S. marianum* and combination on biochemical parameters represented as mean ± SEM (n=6) for each group. To define difference per groups have used the Student t-tests; *p < 0.05 vs. the control group; **p < 0.05 vs. the Gly group. .

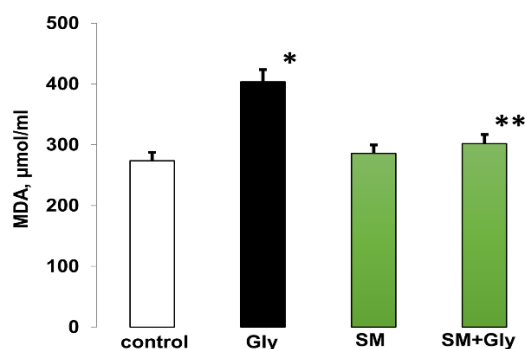


Figure 2. Effects of *S. marianum* and combination on MDA levels in kidneys homogenates To define difference per groups have used the Student t-tests (n=6); *p < 0.05 vs. the control group; **p < 0.05 vs. the Gly group.

Administration of *S. marianum* (0.5 %) after Gly-induced AKI can alleviate signs of AKI, normalize BUN, and reduce renal edema. In addition, the administration of *S. marianum* lowers OS and reduces the accumulation of tissue lipids, which is probably due to the normalization of the relative gene expression of antioxidant enzymes [4, 14]. The presented results are in agreement with the studies of other researchers, according to which pretreatment with *S. marianum* reduces lipid peroxidation and lowers Gly-induced AKI, decreased myoglobinuric nephrotoxicity and renal ischemia [14, 29]. On the other side, at the cellular level, *S. marianum*, 0.5% administrated, is not sufficient to completely normalize the Gly-induced elevation in electrolytes

(K⁺, Na⁺), biochemical (Cre) concentrations and oxidative changes, i.e. additional stimulation is needed to restore normal blood cells in the renal tubules with minimal protein deposition.

S. marianum regulates endogenous antioxidants, ROS production and nitric oxide (•NO) in CS-induced AKI

In CS-AKI rats, the heme and free ferro accumulation in the cytoplasm and mitochondria of kidney cells is remarkably increased, which causes a ferro-dependent lipid peroxidation and ROS/RNS increase [30]. In addition, Liu *et al.*, [31] found increased concentrations of hydrogen peroxide (H₂O₂), myeloperoxidase, and nitric oxide (•NO) in the serum and muscle of rats with experimentally induced CS-AKI. Moreover, CS-AKI is due to OS and free-radical processes, and treatment with antioxidants or radical scavengers suggests a beneficial therapeutic effect (Fig. 3.).

Gly-induction resulted in a significant decrease in SOD and CAT activity (p<0.05; Figs. 3A, 3B) and a significant increase in ROS production and •NO concentration in the kidney (p < 0.003; Figs. 3C, 3D), compared to controls. Treatment with 0.5 % *S. marianum* significantly ameliorated Gly-induced AKI, restored renal endogenous enzymes, and protectively reduced renal OS by modulating ROS/•NO concentrations compared to the Gly group (p<0.001).

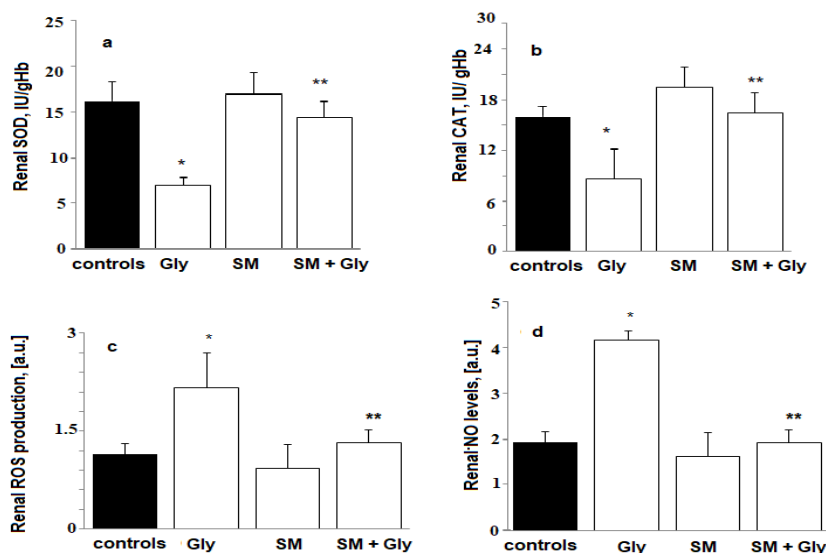


Figure 3. Effects of *S. marianum* and combination on antioxidant enzymes and ROS/RNS concentrations represented as mean ± SEM (n=6) for each group. To define difference per groups the Student t-tests were used; *p < 0.05 vs. the control group; **p < 0.05 vs. the Gly group.

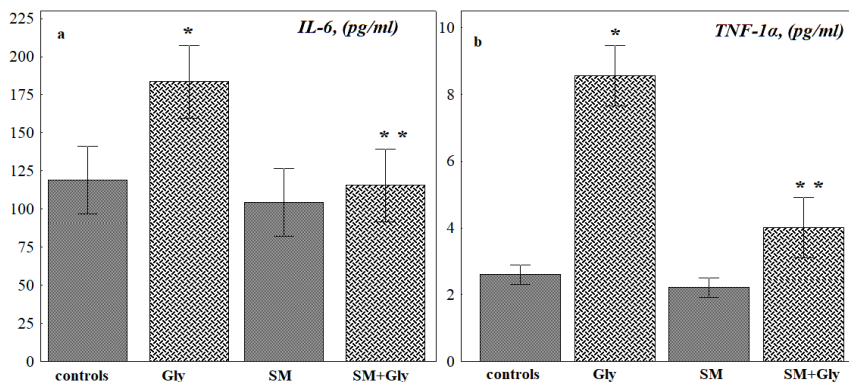


Figure 4. Effects of *S. marianum* and combination on proinflammatory cytokines (IL-6; TNF-α) represented as mean ± SEM (n=6) for each group. To define difference per groups the Student t-tests were used; *p < 0.05 vs. the control group; **p < 0.05 vs. the Gly group.

Table 1. Comparative histopathological appearances/ changes in tested groups. Legend: 0-no changes; 1-weak changes; 2-moderate changes; 3-strong changes.

	Controls	Gly	<i>S. marianum</i>	<i>S. marianum</i> + Gly
Kidney tubule cavity expansion	0	3	0	1
Glomerular hypertrophy	0	3	1	0
Renal tubular epithelial cell edema	0	2	0	0
Interstitial inflammatory infiltration	0	1	0	0
Inflammation	0	2	0	0
Necrosis	0	2	0	1
	0	2	0	0

Recent studies have reported that antioxidant molecules are able to protect against Mb-induced OS through ROS/RNS scavenging mechanisms, endogenous enzyme restoration, and alleviation of acute mitochondrial ROS production/lipid peroxidation in renal tubular cells [16-18]. *S. marianum*, 0.5 % may reduce ROS/RNS, following activation of the reperfusion injury salvage kinase

(RISK) pathway, by inducing AKI/endothelial NO synthase (eNOS) activation and subsequent reduction of •NO radical mediated cytoprotective signaling [32, 33]. Reduced ROS/RNS generation suppresses the pro-inflammatory response and leads to full recovery of Gly-induced AKI, thereby reducing renal damage and increasing survival rate [32, 33]. In response to OS, proinflammatory

cytokines, IL-6 and TNF- α , are released, activating macrophages and T-lymphocytes at the site of inflammation. Released IL-6, TNF- α , and c-Jun N-terminal kinase (JNK) are directly involved in the pathophysiological progression of CS-induced AKI [14, 34]. Rats exposed to Gly treatment revealed a significant increase in renal IL-6 and TNF- α circulation, compared to control ($p < 0.05$) (Figs. 4A, 4B).

In conclusion, this work presents *S. marianum* (0.5 %) as a stable antioxidant that can be potentially used to ameliorate the devastating Gly-induced signs of acute kidney injuries (remodeling the severe degenerative changes in renal corpuscles; accumulation of protein casts in the mesangial tissue; degeneration of renal tubules; severe congestion of the renal blood vessels) (Table 1), normalized BUN and alleviated renal OS and pro-inflammation, indirectly by preventing fibrotic processes, by long lasting Crush syndrome.

Acknowledgement: This research was funded by the scientific project No.6/2022-Medical Faculty, Trakia University, Bulgaria; and Ministry of Education and Science BG-RRP-2.004-0006" Development of research and innovation at Trakia University in service of health and sustainable well-being". The team extends special thanks to Prof. Anna Tolekova, MD, PhD for the assistance given during the experiment.

REFERENCES

1. Y. Liu, M. Yu, L. Chen, J. Li, X. Liu, C. Zhang, X. Xiang, X. Li, Q. Lv, *Laboratory and Clinical Approaches*, **57**, 469 (2022).
2. H. Jin, X. Lin, Z. Liu, J. Wang, J. Wang, Y. Zhang, C. Cao, Y. Chai, S. Shou, *Eur. J. Trauma Emerg. Surg.*, **48**, 4585 (2022).
3. N. Li, J. Chen, C. Geng, X. Wang, Y. WangSun, N. Wang, P. Han, Z. Li, H. Fan, S. Hou, *Cell Death Discovery*, **8**, 90 (2022).
4. O. Qiao, X. Wang, Y. Wang, N. Li, Y. Gong, *J. Adv. Res.*, (2023).
5. Q. Lv, M. Long, X. Wang, J. Shi, P. Wang, X. Guo, J. Song, A.C. Midgley, H. Fan, S. Hou, *Shock: Injury, Inflammation, and Sepsis: Laboratory and Clinical Approaches*, **56**, 1028 (2021).
6. M. Guerrero-Hue, C. García-Caballero, A. Palomino-Antolín, A. Rubio-Navarro, C. Vázquez-Carballo, C. Herencia, D. Martín-Sánchez, V. Farré-Alins, J. Egea, P. Cannata, M. Praga, *The FASEB Journal*, **33**, 8961 (2019).
7. N. Panizo, A. Rubio-Navarro, J.B.M. Amaro-Villalobos, J. Egido, J.A. Moreno, *Kidney and Blood Pressure Research*, **40**, 520 (2015).
8. Z. Ke, Y. Bai, H. Zhu, X. Xiang, S. Liu, X. Zhou, Y. Ding, *Food Chemistry*, **389**, 132972 (2022).
9. M. P. Richards, *Antioxidants & Redox Signaling*, **18**, 2342 (2013).
10. H. Min, Y. Qi, Y. Zhang, X. Han, K. Cheng, Y. Liu, H. Liu, J. Hu, G. Nie, Y. Li, *Advanced Materials*, **32**, 2000038 (2020).
11. S. Song, S. Kim, S. Lee, J. Moon, H. Hwang, J. Kim, S. Park, K. Jeong, Y. Kim, *Int. J. Mol. Sci.*, **21**, 8564 (2020).
12. R. Ranasinghe, M. Mathai, A. Zulli, *Life Sciences*, **138**, 121466 (2023).
13. M. Gyurászová, R. Gurecká, J. Bábíčková, L. Tóthová, *Oxidative Medicine and Cellular Longevity*, (2020).
14. H. Eltahir, H. Elbadawy, A. Alalawi, A. Aldhafiri, S. Ibrahim, G. Mohamed, A.G.S. Shalkami, M. Almikhlafi, M. Albadrani, Y. Alahmadi, M. Abouzied, *Acta Biochim. Pol.*, **70**, 277 (2023).
15. S. Mukhtar, Z. Xiaoxiong, W. Khalid, A. Moreno, J. Lorenzo, *Food Anal. Methods*, **1** (2023).
16. M. Ghodousi, H. Karbasforooshan, L. Arabi, S. Elyasi, *Eur. J. Clin. Pharmacol.*, **79**, 15 (2023).
17. M. Bahmani, H. Shirzad, S. Rafeian, M. Rafeian-Kopaei, *eCAM*, **20**, 292 (2015).
18. S. Brantley, N. Oberlies, D. Kroll, M. Paine, *J. Pharmacol. Exp. Ther.*, **332**, 1081 (2010).
19. M. Fallahzadeh, B. Dormanesh, M. Sagheb, *Am. J. Kidney Dis.*, **60**, 896 (2012).
20. M. Hareedy, L. Abdelzaher, D. Badary, S. Mohammed Alnasser, A. Abd-Eldayem, *Nephrol. Ther.*, **17**, 160 (2021).
21. H. Ohkawa, N. Ohishi, K. Yagi, *Anal. Biochem.*, **95**, 351 (1979).
22. Y. Sun, L.W. Oberley, Y. Li., *Clin. Chem.*, **34**, 3 (1988).
23. H. Aebi, *Meth Enzymol.*, **105** (1984).
24. H. Shi, Y. Sui, X. Wang, Y. Luo, L. Ji, *Comp. Biochem. Physiol. C Toxicol. Pharmacol.*, **140**, 1 (2005).
25. K. Yokoyama, K. Hashiba, H. Wakabayashi, et al., *Anticancer Res.*, **24**, 6 (2004).
26. T. Yoshioka, N. Iwamoto, K. Ito, *J. Am. Soc. Nephrol.*, **7**, 6 (1996).
27. J. Wu, X. Pan, H. Fu, Y. Zheng, Y. Dai, Y. Yin, Q. Chen, Q. Hao, D. Bao, D. Hou, *Sci Rep.*, **7**, 10114, (2017).
28. H. Lee, S. Kim, G. Lee, M. Choi, H. Chung, Y. Lee, H. Kim, H. Kwon, H. Chae, *Sci. Rep.*, **7**, 6513 (2017).
29. R. Parekh, D. Care, C. Tainter, *Emerg. Med. Pract.*, **14**, 1 (2012).
30. L. Zorova, I. Pevzner, A. Chupyrkina, S. Zorov, D. Silachev, E. Plotnikov, D. Zorov, *Chem. Biol. Interact.*, **25**, 256 (2016).
31. S. Liu, Y. Yu, B. Luo, X. Liao, Z. Tan, *Heart Lung Circ.*, **22**, 284 (2013).
32. J. Kobayashi, I. Murata, *Physiol. Rep.*, **6**, 13633 (2018).
33. I. Murata, Y. Abe, Y. Yaginuma, K. Yodo, Y. Kamakari, Y. Miyazaki, D. Baba, Y. Shinoda, T. Iwasaki, K. Takahashi, J. Kobayashi, Y. Inoue, I. Kanamoto, *Ann. Intensive Care*, **4**, 90 (2017).

34. B. Zhang, P. Wang, Y. Cong, J. Lei, H. Wang, H. Huang, S. Han, Y. Zhuang, *J. Orthop. Surg. Res.*, **12**, 110 (2017).
35. X. Zhao, H. Wang, Y. Yang, Y. Gou, Z. Wang, D. Yang, C. Li, *Drug Des. Devel Ther.*, **4**, 1903 (2021).
36. H. Senturk, S. Kabay, G. Bayramoglu, *World J Urol.*, **26**, 401 (2008).

Neuroprotective effect of *Silybum marianum* in brain regions after experimental ochratoxicosis

Y. D. Karamalakova^{1*}, E. D. Georgieva², K. V. Petkova-Parlapanska¹, V. A. Ivanov³,
G. D. Nikolova¹

¹ Department of Chemistry and Biochemistry, Medical Faculty, Trakia University, 11 Armeiska Str.,
6000 Stara Zagora, Bulgaria

² Department of General and Clinical pathology, Forensic medicine, Deontology and Dermatovenereology,
Medical Faculty, Trakia University, 11 Armeiska Str., 6000 Stara Zagora, Bulgaria

³ Department of Social medicine, Health management and Disaster medicine, Medical Faculty, Trakia University,
11 Armeiska Str., 6000 Stara Zagora, Bulgaria

Received: November 3, 2023; Revised: April 11, 2024

Silybum marianum L. (SM) was investigated for its possible protective effect against ochratoxin A-induced (OTA) toxicity in mice brain. OTA instigates oxidative changes leading to reactive oxygen/ nitrogen species (ROS/RNS) overproduction. SM oral administration prevents the physiological abnormalities and improves the oxidative stress parameters in the cerebral cortex (CX) and cerebellum (CB). Moreover, analysis showed that SM administration decreased ROS production and DNA genotoxicity in the brain regions, even in the OTA group. The significantly increased SOD and CAT activities in SM and SM + OTA groups confirm the positive neuroprotective effect of SM on the cellular antioxidant system. The results suggested that SM protects against OTA-induced brain oxidative disorders and other abnormalities.

Keywords: SM, OTA, CB, CX, oxidative stress

INTRODUCTION

Ochratoxin, a mycotoxin produced by various toxigenic fungal species (*Aspergillus ochraceus* and *Penicillium verrucosum*), as a secondary metabolite, is a common food contaminant [1, 2] with a long half-life. In relation to the three isoforms (ochratoxin A, B, and C), ochratoxin A (OTA) is the most potent toxin [1]. OTA has been implicated in hepatotoxicity, teratotoxicity, immunotoxicity, enzymuria, and neurotoxicity [3, 4]. The chronic and acute mechanisms of OTA-induced neurotoxicity are still unknown. Hayes et al. [5] and Wangikar et al. [6] suggest that the deleterious OTA effects on neural tissue are expressed in its accumulation in the adrenal medulla, substantia nigra, striatum, cortex, and hippocampus. Other studies, suggested the OTA involvement in mitochondrial damage, inhibition of protein synthesis, single-stranded DNA breaks, and oxidative stress (OS) damage [2, 8]. OTA crosses the blood-brain barrier (BBB), accumulates in the central nervous system, and induces neuronal apoptosis [9-11]. Sava et al. [12] commented that acute OTA administration produced higher levels of reactive oxygen/nitrogen species (ROS/RNS) in six brain regions and induced redox malformations. Acute OTA exposure also suggests depletion of striatal dopamine and associated metabolites, as well

as decreased tyrosine hydroxylase immune-reactivity [12] in the brain. Bhat et al. [13] concluded that OTA treatment alters various biological pathways mobilized by OS and increases ROS/RNS productions. Chronic, low-dose OTA exposure increases lipid peroxidation, causes Parkinsonism in mouse models [12, 14] and simultaneously involved in neurodegenerative disorders [15].

Plant antioxidants are possible reducers of the progression of neurotoxic/ neurodegenerative diseases in animal models [16-17]. *Silybum marianum* L. (SM) as a potent milk thistle extract has possessed antioxidant, cyto-protective, anti-inflammatory, and anticancer properties [18]. The flavonolignan and polyphenolic constituents due to the ability to antioxidant-scavenging ROS/RNS, inhibit lipid peroxidation [18, 19], and act in protein synthesis [20]. The SM ability to cross the blood-brain barrier and improve psychomotor and cognitive impairment in animal models defines the extract as a possible neuroprotective agent [17, 21].

The main objectives of the study were to elucidate the neuroprotective effect of SM by determining: 1) the SM and OTA pharmacokinetics; 2) the SM protective effects on OS parameters and enzymatic cerebral defensive system in mouse brain regions after OTA-induced neurotoxicity.

* To whom all correspondence should be sent:

E-mail: * yanka.karamalakova@trakia-uni.bg

EXPERIMENTAL

2-3 mg/g OTA isolated from *Aspergillus Ochraceus* strain (Isolate D2306; 80°C / 1 h) was described previously [22]. The *SM* powder and other reagents were purchased from Sigma Aldrich, USA.

Experimental design

The animal protocol was approved by the Directive 2010/63/EU and by the Ethical Committee for Animals and Trakia University, Stara Zagora, Bulgaria (131/ 6000-0333/ 09.12.2015).

Male, BALB/c mice (n = 24; 36 ± 2.0 g, 7-weeks old; 7 days acclimatized) were used. Neurotoxicity was induced chronically using OTA administration at 1.32 mg/kg body weight (b.w.), orally for 28 days (~18.5 mg OTA/ kg). The mice were divided into 4 groups (n=6) as follows: (1) Controls with basic diet; (2) *SM* group - administered orally with *SM* (200 mg/kg b.w.) every day for 28 days; (3) The OTA group- mice were fed with OTA (ED₅₀;1,32 mg/kg) per day, orally given for 28 days; (4) *SM* + OTA group, the mice were given both *SM* extract (200 mg/kg per day for 28 days, orally) and OTA (1,32 mg/kg per day for 28 days, orally, 2 hrs after *SM* administration). The defined quantities of *SM* and OTA were mixed with virgin olive oil (Mikroo, Greece) before treatment, respectively. Additionally, the physiological status and changes in spontaneous behavior were monitored on the 7th, 14th and 28 day until euthanasia.

Brain regions isolation

The mice were weighed, and observed for changes in spontaneous behavior daily until euthanasia (50 mg/kg Nembutal, i.p.), on day - 29. The both brains sections: cerebral cortex (CX) and cerebellum (CB) were separated, fixed in cold PBS (pH = 7.5) under ice (-4°C), homogenized and estimated for OS injuries.

Biodistribution

100 mg of CX and CB regions were sonicated in cold PBS (10% w/v), centrifuged (2000×g 15 min, 4°C) and evaluated directly for *SM* and OTA biodistribution, by X-band EPR spectrometer (Bruker), by method previously described [23].

ROS production

100 mg CX and CB regions were added to 900 µl (50 mM) N-t-butyl-alpha-phenylnitron (PBN) dissolved in dimethyl sulfoxide (DMSO) (2:1 w/v), centrifuged (4000 rpm, 10 min, 4°C) and studied according to Shi *et al.* [24].

The biodistribution and ROS production studies were performed with an Electron Paramagnetic Spectroscopy (X-Band EPR, Bruker, Germany) analyzer, in fivefold spectral measurement in: 3503 – 3515 G center field, 6.42-20.00 mW microwave power, 5 – 10 G modulation, 5 scans per sample, and the results are presented in arbitrary units (a.u.).

Oxidative DNA damage and enzymatic defense

The 8-hydroxydeoxyguanosine (8-OHdG), superoxide dismutase (SOD) and catalase (CAT) measurements were carried out using CellBiolabs Ins - ELISA kits (Germany), following manufacturer's instructions.

Statistical analysis

Statistical analysis was performed with Statistica 8.0, Stasoft, Inc., two-way ANOVA. EPR processing was performed using Bruker Win-EPR and Sim-fonia Software. The results were expressed as means ± standard error, mean (SEM, n = 6). The differences between groups were analyzed by Student's t-test, and p < 0.05 was considered as significant.

RESULTS AND DISCUSSION

SM possesses protective effects on delayed neuronal cell death in the rat hippocampus [18], on dopaminergic neuron [21], on prophylactic capabilities in acetaminophen-induced injuries on CX [25].

The present study reports the *SM*-neuroprotective efficacy against OTA-induced neurotoxicity in brain regions, is in terms of OS lesions. OTA neurotoxic potential has been observed in Neuro-2a cells in a dose-dependent manner [13] and its known that induce changes in the cells might be mediated by OS pathways, producing ROS/ RNS oxidants, which was effectively reversed by natural antioxidants [13]. In contrast, Kaur *et al.* [26] reported that *SM* effectively reducing dopaminergic neurons damages against induced neurotoxicity in brains, acting as ROS/ RNS scavenger. The chronic OTA exposure registered weak depression, weakness, and spontaneous locomotor activity, well expressed on 19th day (Table 1).

Notably, *SM* (p < 0.003) significantly restored food consumption to animals receiving OTA, vs. OTA group. This was evident after the first 19 days when food intake was reduced >17%. In contrast, no changes in physiological status and behavior in the *SM* group and *SM* + OTA were detected.

Table 1. SM and OTA results of the mean body weight values (BW) and behavior in experimental ochratoxicosis in male BALB/c mice. In group ± SEM (n = 6); (0): none, (1): mild, (2): moderate.

Treatment (n = 6)	BW(g)		Weak depression	Weakness locomotor activity
	19 th day	28 th day		
SM	204.7 ± 1.4	258.2 ± 4.9	-	-
OTA	205.9 ± 0.8	230.2 ± 3.8	++	62
SM +OTA	208.1 ± 1.03	241.2 ± 2.51	++	++
Controls	207.7 ± 3.45	251.8 ± 4.12	-	-

Several evidences indicated the flavonoid-containing *SM* as potent immune-modulatory and anti-inflammatory action and suppression of oxidative immune-toxicity [26] against mycotoxins. In addition, *SM* probably acts as a potent cognitive enhancer and neuro-inflammator without affecting cerebellar neurons, regulates oxidative stress oxidation and improves memory processes [26, 27]. Favorable changes in BW, food intake, and normalizing of appetite were observed in *SM* and *SM* + OTA combination.

Although *SM* is a large molecule for absorption by simple diffusion, Bosch-Barrera *et al.* comment on notable improvements in central nervous system and brain metastases in patients receiving an oral nutraceutical product containing *SM* [28]. The *SM* and OTA biodistribution in brain regions, were investigated and are presented on Fig. 1.

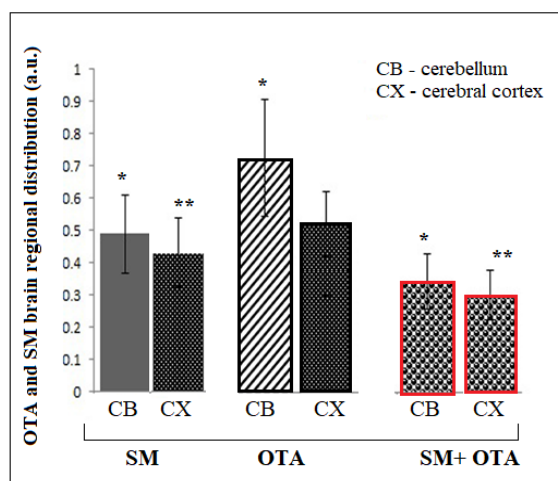


Figure 1. EPR analyses of *SM* and OTA biodistribution in brain regions.

At the 29th day, the EPR results showed highest *SM* and OTA localization in CB, followed by the CX. A relatively almost 2.3-fold OTA accumulation found in the CB and CX, compared to *SM* localization in the same regions, was a prerequisite for a high OTA neurotoxicity in the brain regions. Increased OTA accumulation found in the CB and CX is consistent with the findings of

other investigators [14]. Sava *et al.* [14] reported that OTA, as an inhibitor of mitochondrial oxidative metabolism, is stably delayed in the CB, but despite the highest OTA accumulation, this area remains the least regionally vulnerable. Moreover, OTA exposure contributed to impaired hippocampal neurogenesis *in vivo*, leading to cognitive deficits and depression also observed in our groups [29].

Deficient repair processes and the uneven distribution of oxidative DNA damage across brain regions caused by endo- and exogenous factors have been associated with many neurodegenerative diseases [14, 29]. Our report on the brain region effects of OTA, were focused on DNA damages, the augmented ROS generation (including $\bullet\text{O}_2^-$, $\text{HOO}\bullet$, and $\text{OH}\bullet$), and on *SM* cerebral OS and enzymatic protection, alone and in combination [30]. According to the data in Table 2, significantly higher DNA damages ($p < 0.05$) and ROS levels ($p < 0.001$) and significantly lower SOD ($p < 0.001$) and CAT levels ($p < 0.001$) were detected in the CB vs CX regions, after OTA treatment. *SM* administration resulted in a significant decrease in oxidative DNA damages and ROS concentrations, a significant restoration in enzymatic protection, and decreases in OS injuries, in both regions.

Acute/ chronic OTA administration previously has been reported to cause OS cascades in mouse brain, evidenced by significant increases in ROS/RNS, lipid peroxidation and oxidative DNA malformations across 6 brain regions [14, 29]. Our findings suggest that chronic OTA administration provoke strong inflammatory responses in CB and CX, as well as increase in the DNA breaks, ROS/RNS accumulation and depletes CB/CX enzymatic defense. In addition, Aktas and Sevimli [31] comment that *SM* has protective properties against oxidative insults by potentially modulating the $\bullet\text{O}_2^-$, $\text{HOO}\bullet$, and $\text{OH}\bullet$ formation, along with protein oxidation products in the cortices of the elderly rodent brain. In another experiment, *SM* increased the enzyme activities which neutralized lipid peroxidation and normalized ROS production [32].

Table 2. SM and OTA results of the DNA damages, ROS production (a.u.), SOD and CAT defenses in experimental ochratoxicosis in male BALB/c mice. Data are presented as the means ± SEM (n = 6). *Significant difference towards controls (p < 0.05); **Significant difference towards OTA group (p < 0.001).

Parameters	Controls (n =6)	SM (n =6)	OTA (n =6)	SM + OTA (n=6)
Cerebellum (CB)				
DNA (ng/ml)	6.3 ± 1.02	5.91 ± 1.62**	15.91 ± 5.02*	8.33 ± 2.82**
ROS (a.u.)	1.45 ± 0.12	0.74 ± 0.007*/**	2.44 ± 0.63	0.95 ± 0.06*/**
SOD (IU/gHb)	1673 ± 12.02	1599 ± 9.09**	658 ± 3.92*	1422 ± 14.78**
CAT (IU/gHb)	17.9 ± 1.66	18.03 ± 2.56**	7.55 ± 2.11	15.95 ± 3.72**
Cerebral cortex (CX)				
DNA (ng/ml)	4.35 ± 1.09	4.99 ± 0.72**	12.87 ± 3.02*	9.04 ± 2.00**
ROS (a.u.)	1.1 ± 0.004	0.57 ± 0.002*/**	2.07 ± 0.07	1.23 ± 0.05**
SOD (IU/gHb)	1351 ± 11.02	1287 ± 8.08**	611 ± 7.14*	833 ± 11.7*/**
CAT (IU/gHb)	16.82 ± 3.8	17.05 ± 3.01	8.38 ± 4.13*	14.03 ± 3.6**

In the OTA toxicity, inhibited ROS/ lipid peroxidation and restarting of SOD and CAT antioxidants in the neurons of the cerebellum and cerebral cortex after SM protection are signs of brain tissues reduction and antioxidant protective mechanism. In consistent to our results, SM has been reported to act as an antioxidant, to stimulate respiratory activity, and inhibit ROS/ lipid peroxidation in brain mitochondria by increasing the concentrations of endogenous antioxidant enzymes [31, 33]. Moreover, SM is able to alleviate cognitive impairment and through redox modulatory reactions to improve cellular antioxidant status, which protects the cerebellum better vs. cerebral cortex in SM, and in SM + OTA treated rodents [27].

CONCLUSION

In conclusion, our results indicate a neuroprotective effect of SM on OTA-induced brain toxicity. The protective properties of SM are strongly related to its antioxidant potential against OS and could find application as protector against OTA-induced experimental ochratoxicosis.

Acknowledgement: This research was funded by the scientific project No.6/2022-Medical Faculty, Trakia University, Bulgaria; and Ministry of Education and Science BG-RRP-2.004-0006" Development of research and innovation at Trakia University in service of health and sustainable well-being".

REFERENCES

1. L. A. Haighton, B. S. Lynch, B. A. Magnuson, E. R. Nestmann, *Crit. Rev. Toxicol.*, **42**, 147 (2012).
2. A. Pfohl-Leszkowicz, R.A. Manderville, *Mol. Nutr. Food Res.*, **51**, 61 (2007).
3. M. Castegnaro, D. Canadas, T. Vrabcheva, T. Petkova-Bocharova, I.N. Chernozemsky, A. Pfohl-Leszkowicz, *Mol. Nutr. Food Res.*, **50**, 519 (2006).
4. A. Mally, G. C. Hard, W. Dekant, *Food Chem. Toxicol.*, **45**, 2254 (2007).
5. A.W. Hayes, R. D. Hood, H. L. Lee, *Teratol.*, **9**, 93 (1974).
6. P. B. Wangikar, P. Dwivedi, A. K. Sharma, N. Sinha, *Birth Defects Res. Part B Dev. Reproductive Toxicol.*, **71**, 352 (2004).
7. J. C. Gautier, D. Holzhaeuser, J. Markovic, E. Gremaud, B. Schilter, R.J. Turesky, *Free Radic. Biol. Med.*, **30**, 1089 (2001).
8. P. Jennings, C. Weiland, A. Limonciel, K. M. Bloch, R. Radford, L. Aschauer, *Arch. Toxicol.*, **86**, 571 (2012).
9. A. Ose, H. Kusuhara, C. Endo, K. Tohyama, M. Miyajima, S. Kitamura, et al., *Drug Metab. Dispos.*, **38**, 168 (2010).
10. A. Belmadani, G. Tramu, A. M. Betbeder, E. E. Creppy, *Hum. Exp. Toxicol.*, **17**, 380 (1998).
11. X. Zhang, C. Boesch-Saadatmandi, Y. Lou, S. Wolfram, P. Huebbe, G. Rimbach, *Genes. Nutr.*, **4**, 41 (2009).
12. V. Sava, O. Reunova, A. Velasquez, R. Harbison, J. Sanchez-Ramos, *Neurotoxicol.*, **27**, 82 (2006).
13. P. V. Pandareesh Bhat, F. Khanum, A.Tamatam, *Front. Microbiol.*, **7**, 1142 (2016).
14. V. Sava, O. Reunova, A. Velasquez, J. Sanchez-Ramos, *J. Neurol. Sci.*, **249**, 68 (2006).
15. R. Sharma, S. M. Gettings, G. Hazell, N. Bourbia. *Toxicol.*, **483**, 153376 (2023).
16. M. Rasool, A. Malik, M.S. Qureshi, A. Manan, P.N. Pushparaj, M. Asif, M. H. Qazi, A. M. Qazi, M. A. Kamal, S. H. Gan, I. A. Sheikh, *Evid. Based Complement. Alternat. Med.*, **17**, 979730 (2014).
17. S. Mehri, Q. Dadesh, J. Tabeshpour, F. V. Hassani, G. Karimi, H. Hosseinzadeh, *Jundishapur J. Nat. Pharm. Prod.*, e37644.

18. C. Nencini, G. Giorgi, L. Micheli, *Phytomed.*, **14**, 129 (2007).
19. P. Kosina, V. Kren, R. Gebhardt, F. Grambal, J. Ulrichová, D. Walterová, *Phytother. Res.*, **16**, S33 (2002).
20. K. Hirayama, H. Oshima, A. Yamashita, K. Sakatani, A. Yoshino, Y. Katayama, *Brain Res.*, **1646**, 297 (2016).
21. M.J. Wang, W.W. Lin, H. L. Chen, Y. H. Chang, H. C. Ou, J. S. Kuo, J. S. Hong, K. C. Jeng, *Eur. J. Neurosci.*, **16**, 2103 (2002).
22. S. Stoev, H. Daskalov, B. Radicc, A. M. Domijanc, M. Peraicac, *Vet. Res.*, **33**, 83 (2002).
23. V. Gadzheva, R. Koldamova, *Anti-cancer Drug Design.*, **16**, 247 (2001).
24. H. H. Shi, Y. X. Sui, X.R. Wang, Y. Luo, L. Ji, *Comp. Biochem. Physiol. C Toxicol. Pharmacol.*, **140**, 115 (2005).
25. O. J. Onaolapo, M.A. Adekola, T. O. Azeez, K. S. Adejoke, Y. Onaolapo, *Biomed. Pharmacoth.*, **85**, 323 (2017).
26. A. K. Kaur, A. Wahi, K. Brijesh, A. Bhandari, N. Prasad, *IJPRD*, **3**, 1 (2011).
27. R. Haddadi, Z. Shahidi, S. Eyvari-Brooshghalan, *Phytomed.*, **79**, 153320 (2020).
28. J. Bosch-Barrera, E. Sais, N. Cañete, J. Marruecos, E. Cuyàs, A. Izquierdo, R. Porta, M. Haro, J. Brunet, S. Pedraza, et al., *Oncotarget.*, **7**, 32006 (2016).
29. Sava V, Velasquez A, Song S, Sanchez-Ramos, *J. Toxicol. Sci.*, **98**, 187 (2007).
30. M. Więckowska, R. Szelenberger, M. Niemcewicz, P. Harmata, T. Poplawski, M. Bijak, *Molec.*, **28** (18), 6617 (2023).
31. I. Aktas, M. Sevimli, *Van Vet. J.*, **31** (2), 87 (2020).
32. S.Y. Zhu, Y. Dong, J. Tu, Y. Zhou, X. H. Zhou, B. Xu, *Pharmacogn Mag.*, **10**, 92 (2014).
33. C. R. de Avelar, E. M. Pereira, P. R. de Farias Costa, R. P. de Jesus, L. P. M. de Oliveira, *World J Gastroenterol.*, **23** (27), 5004 (2017).

Green methods for inulin extraction from common salsify (*Tragopogon porrifolius* L.) roots and its application in metal nanoparticle synthesis

I. Hambarliyska^{1*}, N. Petkova¹, P. Georgieva¹, A. Slavov¹, M. Ognyanov², D. Karashanova³, B. Georgieva³, Y. Tumbarski⁴

¹Department of Organic Chemistry and Inorganic Chemistry, University of Food Technologies, 26 Maritza Blvd., 4002 Plovdiv, Bulgaria

²Laboratory of Biologically Active Substances-Plovdiv, Institute of Organic Chemistry with Centre of Phytochemistry, Bulgarian Academy of Sciences, 139 Ruski Blvd., 4000 Plovdiv, Bulgaria

³Institute of Optical Materials and Technologies "Acad. J. Malinowski", Bulgarian Academy of Sciences, Acad. G. Bonchev Str., Bl. 109, 1113 Sofia, Bulgaria

⁴Department of Microbiology, Technological Faculty, University of Food Technologies, 4002 Plovdiv, Bulgaria

Received: November 3, 2023; Revised: April 11, 2024

The aim of the current research is the isolation and chemical characterization of inulin from common salsify (*Tragopogon porrifolius* L.) roots using green extraction technique (microwave- and ultrasound-assisted irradiation) and its further application in the metal nanoparticle synthesis. Functional properties and color characteristics of isolated inulin were also evaluated. The highest yield was obtained for inulin isolated by microwave-assisted extraction (23 %). The degree of polymerization of inulin was 22-23 with average molecular mass of 3.4 kDa. The structure of inulin-type fructan was confirmed by FT-IR and NMR spectroscopy, where the presence of β (2 \rightarrow 1) bonds was found. Inulin from common salsify showed better oil-holding capacity than water-holding one, high cohesiveness and good to fair flowability. The possibility of synthesis of gold and nickel nanoparticles was investigated by the reduction reaction of 0.001M H₂AuCl₄ and 0.01M Ni(NO₃)₂, respectively, and the effect of temperature on the production of metal nanoparticles was followed. Promising results for synthesis of golden nanoparticles using inulin from common salsify were obtained. Moreover, golden nanoparticles synthesized with common salsify showed potent anti-*Candida* activity and antifungal activity, especially against *Aspergillus*. The obtained results demonstrated the potential application of common salsify inulin in the pharmaceutical industry as a food supplement due to its functional properties and antimicrobial potential of golden nanoparticles synthesized by reduction of H₂AuCl₄ with common salsify inulin solution.

Keywords: *Tragopogon porrifolius*, inulin, nanoparticles, antimicrobial activity.

INTRODUCTION

Inulin and fructooligosaccharides (FOS) are part of the fructans family, widely distributed in various medicinal plants, fruits and vegetables as storage carbohydrates [1]. They are used as dietary fibers or nutritional ingredients in numerous food products. Moreover, the application of inulin in pharmacy as a drug carrier, encapsulating agent, and vaccine adjuvant constantly increases [2-6]. Therefore, the search for new valuable sources of inulin, except traditionally used chicory, dahlia, and Jerusalem artichoke [1-3], gain more and more attention during the last decade. The interest in current research is provoked by one vegetable, common salsify (*Tragopogon porrifolius* L.), as a promising source of inulin with potential use in culinary practice.

Common salsify (*Tragopogon porrifolius* L.) is an annual or biennial plant, used as a root vegetable with excellent nutritional and dietary properties, that belongs to the *Asteraceae* family [7-10]. It has three subspecies, namely: *T. porrifolius* subsp. *australis*,

T. porrifolius subsp. *cupani* and *T. porrifolius* subsp. *porrifolius* [8]. It can reach 50–110 cm in height and possesses a cylindrical taproot (15–30 cm long and 2.5–3 cm wide, brownish-yellow outer skin and white skin). The root has a very mild and slightly sweet flavor similar to oysters, hence the designation "oyster plant". Its older roots have a milky sap and a slightly distally branched, glabrous stem. Leaves are basal and stalked, alternate, sessile, sheathing lamina linear to linear-lanceolate (grass-like), 20–40 cm long [7-9]. It is rarely cultivated, mainly in the Mediterranean region, but deserves wider attention and use in the human diet. Various parts of the plant are consumed in Southern and Central Europe, North America, and the United Kingdom; it is also used to treat cancer in Lebanese folk medicine. Phytochemical investigations on this plant revealed that it contains carbohydrates, proteins, lipids (mainly monounsaturated fatty acids, essential fatty acids, vitamins, and polyphenol components) [7-11]. Common salsify root is low in calories but rich in protein, small amounts of vitamin A, B1, B2, C, PP,

* To whom all correspondence should be sent:

E-mail: vanya.hambarliyska@gmail.com

B6, fibers, minerals, such as Ca, Fe, Mg, K, P, Fe, and 4-18 % fructans (inulin and/or fructooligosaccharides, dry matter) [8, 11]. However, the most valuable component is inulin – a fructan with prebiotic properties, which has a positive effect on the functions of the human digestive tract [3, 6, 12]. The average content of inulin in its roots is 15.17 % (fresh matter). Inulin concentrations are similar in both roots and spring plowing (15.19%) [8-10]. In Portugal and Poland, common salsify (*Tragopogon porrifolius* L.), is alternative inulin source plant, and is also cultivated due to its utilization in culinary practices [8, 9]. From the above mentioned data, it can be concluded that roots of common salsify (*Tragopogon porrifolius* L.) are a promising source of inulin. However, detailed data about inulin characteristics and functional properties are still missing. The aim of the current research is the isolation, chemical characterization and evaluation of the functional properties of inulin from common salsify (*Tragopogon porrifolius* L.) roots using green extraction techniques (microwave and ultrasound-assisted irradiation) and its further application for metal nanoparticles (NPs) synthesis.

MATERIALS AND METHODS

All solvents and reagents were of analytical grade.

Plant material

The plant material used for the analysis was *Tragopogon porrifolius* 'Fiore Blu'. The seeds were planted during March 2021 in vegetable gardens in Kostievo village and Rakovski town (Plovdiv region, Bulgaria). The roots were harvested during the second year of cultivation in July-September.

Isolation of inulin from common salsify (Tragopogon porrifolius L.)

The dried and finely ground roots from common salsify were extracted using deionized water as a solvent (1:10 w/v) by three methods:

1. Conventional extraction under a reflux at 100 °C for 60 min under constant stirring.

2. Ultrasound-assisted extraction in the ultrasonic bath IsoLab (Wertheim, Germany) at a frequency of 40 kHz, 120 W power, at 80 °C for 20 min.

3. Microwave-assisted extraction in a microwave device (Daewoo KOR, with microwave power 700 W and frequency of 2450 MHz) for 5 min [14].

The extraction procedure was performed in triplicate. The water extracts were obtained through a Buchner funnel filtration. The combined extracts were precipitated with the addition of four volumes of acetone, then cooled down to -18 °C, kept for 24 h and filtered. The crude polysaccharide was dried

and dissolved in hot water, precipitated, and washed with acetone [14].

Characterisation of inulin from common salsify

The melting point of inulin was measured on a Kofler melting point apparatus. The reducing groups were determined spectrophotometrically by the PAHBAH method at 410 nm, while total fructose content – using resorcinol-thiourea reagent at 480 nm [14]. The purity of the polysaccharide was analyzed by HPLC instrument Elite LaChrome Hitachi (Tokyo, Japan) with a Shodex® Sugar SP0810 (300 × 8.0 mm i.d.) at 85 °C, coupled to a refractive index detector (VWR Hitachi Chromaster, 5450, Tokyo, Japan). Homogeneity and molecular weights were evaluated by high-performance size-exclusion chromatography (HPLC-SEC) performed on ELITE LaChrome (Hitachi, Japan), equipped with column Shodex OH-pack 806 M (i.d. 8 mm) [15]. Polydispersity index (X) of inulin was calculated as the ratio of the two molecular weights (Mw/Mn) [14]. The IR spectra (2 mg) were collected on a Fourier transform infrared (FT-IR) spectrophotometer VERTEX 70v (Bruker, Bremen, Germany) in KBr pellets. The spectra were recorded in the 4000–400 cm⁻¹ range at 120 scans and resolution of 2 cm⁻¹. ¹H and ¹³C NMR spectra of polysaccharide samples (20 mg/0.6 mL 99.95 % D₂O) were recorded using a Bruker AVIII 500 MHz spectrometer.

Functional properties

Color measurement of inulin was performed with a portable colorimeter Model WR-10QC D 65 lighting, following the CIELAB (L*, a*, b*) system, as previously described [16]. Functional properties of inulin, such as swelling properties, water- and oil-holding capacity were analysed according to Robertson *et al.* [17]. Angle of repose, densities (true, bulk, and tapped), flowability and wettability were determined as previously described [18].

Synthesis and characterization of metal NPs with inulin from common salsify

Aqueous solution of inulin from common salsify with degree of polymerization (DP) 22, obtained after microwave-assisted extraction, with concentrations (0.2 % and 0.5 %), 0.001 M HAuCl₄ and 0.01 M Ni(NO₃)₂ water solutions (Sigma-Aldrich, Germany) were used for synthesis of metal NPs. In a 2 mL Eppendorf tube 1 mL of inulin solution (0.2 or 0.5 %) and 0.5 mL of chlorauric acid or nickel nitrate solution were mixed. The test tube was shaken and incubated at 85°C (Diterm, Robotics, Velingrad). The synthesized metal NPs (the synthesis time was determined by preliminary

visual and UV-Vis observations) were characterized by transmission electron microscopy (TEM) after placing a drop of the solution onto a standard copper grid coated with amorphous carbon layer and dried for 24 h. Observations were done and photomicrographs were obtained using a JEOL JEM 2100 high-resolution transmission electron microscope (JEOL Ltd., Tokyo, Japan) at an accelerating voltage of 200 kV in conventional mode and high-resolution mode for TEM and HRTEM (high-resolution TEM) images, respectively. Statistical analysis of the nanoparticle size distribution was performed using Image J software. Phase composition identification was performed using the International Center for Diffraction Data (ICDD) PDF-2 Database [19].

Antimicrobial activity of obtained nanoparticles with inulin from common salsify

Eighteen microorganisms (Gram-positive and

Gram-negative bacteria, yeasts, and fungi) were used from the collection of the Department of Microbiology (University of Food Technologies, Plovdiv, Bulgaria) for the investigation of antimicrobial activity. The antimicrobial activity of obtained nanoparticles was determined by the conventional agar well diffusion method as described previously by Tumbarski et al. [20].

Statistical analysis

All experimental measurements were carried out in triplicate and the values were expressed as average of the three analyses ± standard deviation.

RESULTS AND DISCUSSION

Characterisation of inulin from common salsify

Physicochemical characteristics of inulin from common salsify (*Tragopogon porrifolius* L.) roots are presented in Table 1.

Table 1. Physicochemical characteristics of inulin from common salsify (*Tragopogon porrifolius* L.) roots

Characteristics	Classical extraction	Ultrasound-assisted extraction	Microwave-assisted extraction
Yield, %	19	15	23
Purity, %	67	74	64
Melting point, °C	158-162.5	191-194	170-174.5
Fructose content, %	59	75	74
Reducing groups, %	2.3	3.8	3.3
Molecular weight (Mw), Da	3471	3325 2713	3345
Mn, Da	3310	3183 2602	3192
Polydispersity index (PD)	1.05	1.05	1.05
Degree of polymerization	21	22	22
Degree of polymerization (by NMR)	23	15-16	20-21
<i>Color characteristics</i>			
L	87.41±3.24	85.43±2.14	83.92±1.14
a	3.91±0.30	4.05±0.32	4.16±0.42
b	9.91±1.25	9.92±0.51	9.93±0.53
C	10.65±1.24	10.06±0.72	9.96±0.63
h	68.16±0.99	68.12±1.13	66.10±2.39
ΔE	14.89±0.15	15.08±0.20	19.27±0.61
<i>Functional properties</i>			
Swelling index, g/cm ³	3.70	4.79	5.45
Water holding capacity, g water/ g	1.02	1.34	2.36
Oil holding capacity, g oil/g	6.20	6.52	6.95
Wettability, s	90	112	116
True density (g/ cm ³)	0.73	0.81	0.81
Bulk density (g/ cm ³)	0.20	0.22	0.22
Tapped density (g/ cm ³)	0.20	0.30	0.38
Carr's index	32	34	34
Hausner ratio	1.47	1.49	1.49
Flowability	high	high	high
Cohesiveness	intermediate	intermediate	intermediate

Table 2. Electron diffraction indexing of gold NPs prepared with inulin from common salsify roots

d [Å]	hkl	COD* Entry
2.3925	111	Au cubic S.G. Fm-3m Cell parameter: 4,14500 Å #96-901-3045
2.0720	200	
1.4651	202	
1.2495	311	

Commented [a1]: Таблица 2 не трябва да е тук. Тя всъщност се повтаря по-долу нъдето и е мястото... Моля, от тук да се изтрие!

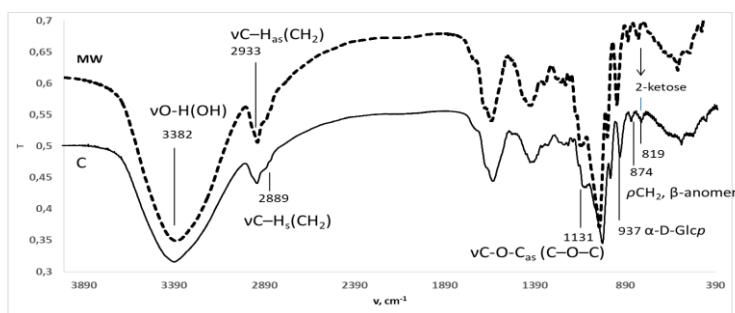


Figure 1. FT-IR spectra of inulin isolated from common salsify (*Tragopogon porrifolius* L.) roots, where C- classical extraction (-), MW – microwave-assisted extraction (- -).

The highest inulin yield was observed for microwave-assisted extraction – 23 %, together with the highest degree of polymerization 20-22. The highest purity (74 %) and fructose content (75 %) were obtained employing ultrasound-assisted extraction (74 %), however the cavitation process reflects on degree of polymerization (15-16) which is lower than the degree of polymerization of inulin extracted using microwave-assisted extraction. There are no significant differences in the color characteristics of isolated inulins by the different extraction methods. Our data for the lightness of inulin were comparable with data for other inulins isolated from different plant sources such as echinacea, chicory, Jerusalem and globe artichoke [16]. The obtained values for water- and oil-holding capacities of common salsify inulin were close to previously reported data for long-chained chicory (1.59 g water/g sample and 3.4 g oil/g sample, respectively) [16], and black salsify (0.5±0.1 water/g sample and 6.1±0.5 oil/g sample, respectively) [15]. However, our results on the oil-holding capacity of inulin were more than five times higher than commercial chicory inulin and globe artichoke inulin (1.37 and 1.38 g oil/g sample, respectively) [15, 21], and Jerusalem artichoke – 1.02 g oil/g sample [22]. The obtained inulin demonstrated high flowability and intermediate cohesiveness, based on Carr's index and Hausner ratio. The highest swelling properties, water and oil-holding capacity were found for inulin from microwave-assisted extraction. This could be explained by the highest molecular

weight and degree of polymerization. Common salsify (*Tragopogon porrifolius* L.) inulin yield coincided with reported data in the literature: 15 – 20 % [8, 9]. Its content is three times higher than this in roots of meadow salsify (*Tragopogon pratensis* L.) (5-9 % dw) [23]. In general, microwave-assisted extraction significantly reduced the time for extraction to 15 min, while the yield, molecular weight were similar to the inulin extracted by conventional long time (3 hours) extraction.

FT-IR spectroscopy

The FT-IR spectra of inulin isolated from common salsify (*Tragopogon porrifolius* L.) roots by classical extraction and microwave-assisted extraction are shown in Figure 1. The spectra contain all typical bands for inulin-type fructans [24], as follows: a broad band at 3300 cm⁻¹ due to O-H stretching vibrations associated with inter- and intramolecular hydrogen bonds in the inulin structure. The bands at 2930–2932 cm⁻¹ are due to C-H asymmetric stretching vibrations. The bands at 2882 cm⁻¹ are characteristics for the symmetric stretching vibrations of C-H. The bands in the region from 1200 to 970 cm⁻¹ are mainly due to C-C and C-O stretching in the pyranosyl ring and C-O-C stretching vibrations of glycosidic bonds. The bands at 1120 cm⁻¹ were characteristic of C-O-C ring stretching vibrations from glycoside linkage. The bands at 1028–1029 cm⁻¹ were assigned to C-O stretching vibrations, together with bands at 987 cm⁻¹. In the fingerprint region typical bands for

inulin and inulin-type fructans are observed. The presence of α -D-glucopyranosyl residue in the polymer chain is observed at 934 cm^{-1} . The band for β -anomer bendings in C1-H was found at 873 cm^{-1} and the occurrence of band at 817 cm^{-1} confirmed the presence of 2-ketofuranose or 2-ketopyranose. Similar bands in the FT-IR spectra were reported earlier for inulin type fructan, especially the bands at 935 , 873 , and 818 cm^{-1} , typical for inulin from different plant sources such as echinacea, dahlia, chicory [14, 16] and black salsify [15].

NMR spectroscopy

This is the first detailed research on the structural characteristics of inulin from common salsify roots. The chemical shifts in ^1H NMR and ^{13}C NMR spectra are shown in Figure 2 and Figure 3.

In the ^1H NMR spectrum (Figure 2) of common salsify inulin typical chemical shifts for glucose and fructose units were found: ^1H NMR (500 MHz, D_2O); δ 5.45, 5.44, 4.30, 4.27, 4.26, 4.21, 4.19, 4.12, 4.11, 4.09, 3.94, 3.92, 3.87, 3.84, 3.78, 3.72, 3.70, and 3.68 ppm. This inulin spectrum contains an isolated resonance for the single anomeric α -glucose proton, observed at 5.45 ppm (Figure 2). In the range from 3.68 to 4.30 ppm all protons for fructose units were found. Anomeric glucose signal H-1 showed low intensity in comparison with the high intensity of fructose units. The integration of the H-1 signal of the glucose unit at δ 5.4 ppm and the H-3 and/or H-4 signals of the fructosyl units between δ 3.6 and 4.30 ppm gave a mean DPn. The DPn distribution of inulin obtained by spectrophotometry analysis ranged from 16 to 23.

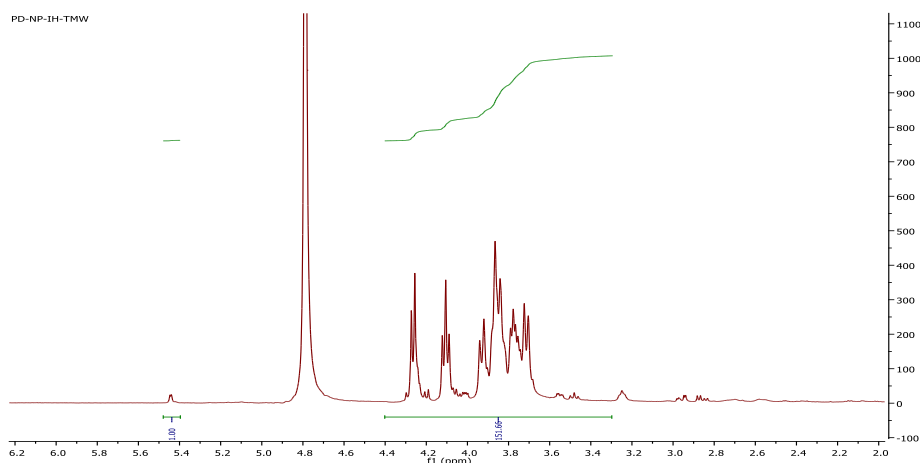


Figure 2. ^1H NMR spectrum of inulin isolated from common salsify (*Tragopogon porrifolius* L.) roots (500 MHz, D_2O); δ 5.45, 5.44, 4.30, 4.27, 4.26, 4.21, 4.19, 4.12, 4.11, 4.09, 3.94, 3.92, 3.87, 3.84, 3.78, 3.72, 3.70, 3.68.

In the ^{13}C NMR spectrum of inulin from common salsify roots chemical shifts typical only for fructose units were observed (Figure 3): ^{13}C NMR (126 MHz, D_2O); δ 103.20, 81.03, 76.93, 74.22, 62.09, and 60.85 ppm. The spectrum contains prominent shifts for C1–C6 carbons (C1 60.85 ppm, C2 103.20 ppm, C3 76.93 ppm, C4 74.22 ppm, C5 ~81 ppm, and C6 ~60.85 ppm) of fructosyl residue due to fructose repeated units. Similar shifts in the ^{13}C NMR spectrum were reported for inulin which contained bonds $\rightarrow 1$ -Fruf-(2 \rightarrow and Fruf-(2 \rightarrow [14, 16]. However, ^{13}C shifts due to glucose were not observed (Figure 3). This superposition of glucose

shifts was observed in other studies and was reported for inulin from echinacea, dahlia, and stevia [14, 16].

Metal nanoparticle synthesis using inulin from common salsify roots

Inulin coated NPs were used in drug delivery [4, 6]. It was reported that inulin coated plasmonic gold NPs were used as a tumor-selective tool for cancer therapy [4, 5]. Therefore, the synthesis of nanoparticles with inulin is prospective field of application for both inulin from common salsify roots and the synthesized gold NPs.

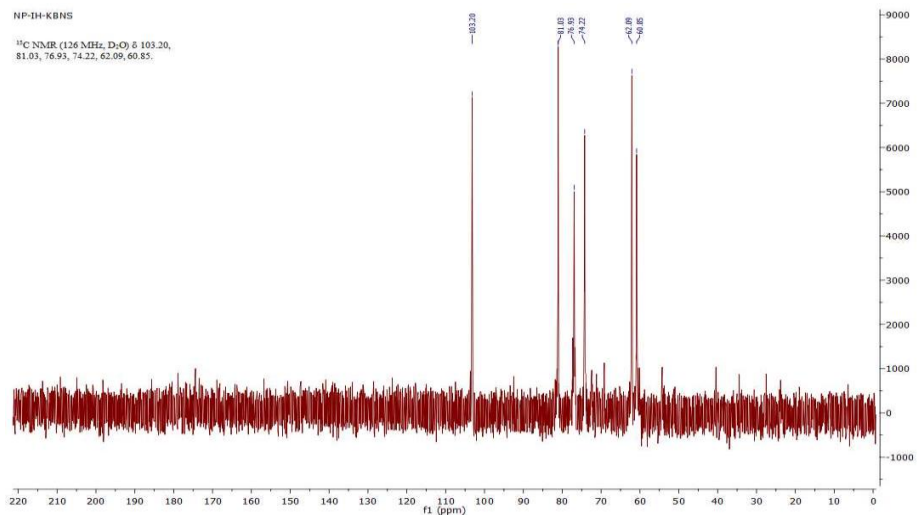


Figure 3. ^{13}C NMR spectrum of inulin from common salsify (*Tragopogon porrifolius* L.) isolated by ultrasound-assisted irradiation 40 kHz (^{13}C NMR (126 MHz, D_2O); δ 103.20, 81.03, 76.93, 74.22, 62.09, 60.85).

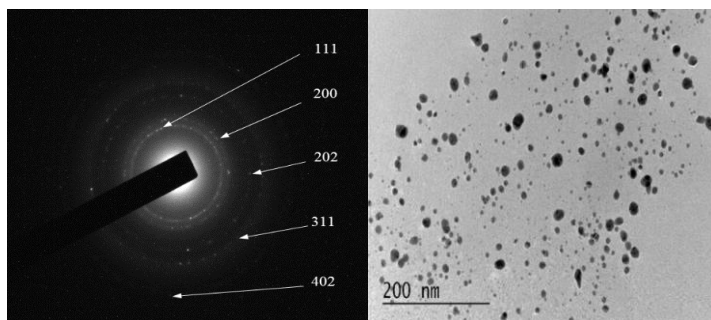


Figure 4. TEM (Transmission electron microscopy) microphotographs and electron diffraction of Au NPs 2:1 with inulin from common salsify roots in concentration 0.5 %

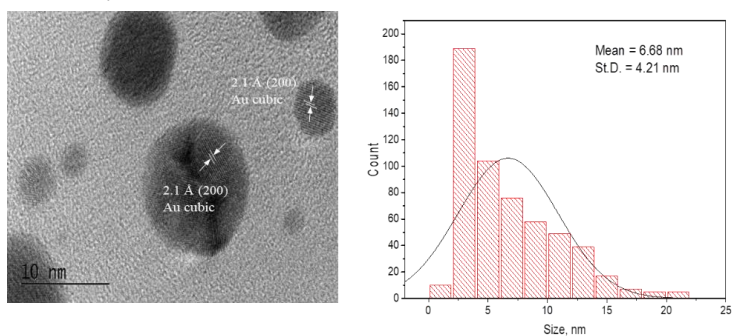


Figure 5. High-resolution TEM microphotograph and particle size distribution (Au NPs 2:1 with inulin from common salsify roots in concentration 0.5 %)

Table 3. Antimicrobial activity of golden and nickel nitrate NPs

Test microorganism	Common salsify inulin Au NPs	Common salsify inulin Ni
<i>Bacillus subtilis</i> ATCC 6633	-	-
<i>Bacillus amyloliquefaciens</i> 4BCL-YT	-	-
<i>Staphylococcus aureus</i> ATCC 25923	-	-
<i>Listeria monocytogenes</i> ATCC 8632	-	-
<i>Enterococcus faecalis</i> ATCC 29212	-	12
<i>Salmonella enteritidis</i>	-	-
<i>Klebsiella</i> sp.	-	-
<i>Escherichia coli</i> ATCC 25922	-	-
<i>Proteus vulgaris</i> ATCC 6380	-	-
<i>Pseudomonas aeruginosa</i> ATCC 9027	-	-
<i>Candida albicans</i> NBIMCC 74	9	-
<i>Saccharomyces cerevisiae</i>	-	-
<i>Aspergillus niger</i> ATCC 1015	9	-
<i>Aspergillus flavus</i>	9	-
<i>Penicillium</i> sp.	-	-
<i>Rhizopus</i> sp.	-	-
<i>Fusarium moniliforme</i> ATCC 38932	-	-
<i>Mucor</i> sp.	-	-

Commented [a2]: NPs

The gold NPs were predominantly spherical in shape, but irregularly shaped as could be seen from Figure 4. The size distribution was from 0 to 20 nm, the predominant size being from 2-4 nm (Figure 5). The phase has cubic gold NPs (Table 2) and the information was obtained from the electron diffraction and high resolution imaging. In addition, inulin from common salsify roots successfully supported and coated the gold NPs. Nickel NPs were not observed visually or using TEM and one possible explanation was that inulin did not possess enough reducing power to reduce Ni^{2+} to Ni^0 . The antimicrobial potential of synthesized golden NPs and mixture of inulin and $\text{Ni}(\text{NO}_3)_2$ were evaluated for the first time. The results are summarized in Table 3.

It was found that gold NPs prepared with inulin from common salsify roots showed moderate antimicrobial activity only against yeasts and fungi, especially *Candida albicans* NBIMCC 74, *Aspergillus niger* ATCC 1015 *Aspergillus flavus*. However, common salsify inulin and $\text{Ni}(\text{NO}_3)_2$ showed moderate activity only against Gram-negative bacteria *Enterococcus faecalis* ATCC 29212. Both, gold NPs and inulin and $\text{Ni}(\text{NO}_3)_2$ mixture, were inactive against Gram-positive bacteria.

CONCLUSION

To the best of our knowledge this is the first detailed study on the isolation, structural elucidation,

and evaluation of the functional properties of inulin from common salsify roots. The study revealed that common salsify contains linear inulin composed of fructose units linked with β -(2→1) bonds and a terminal glucose unit linked α -(1→2), having DP of 20-22 and molecular-weight similar to the chicory inulin. Microwave-assisted extraction was evaluated as a prospective green method for obtaining high-molecular inulin in high yield. The common salsify inulin showed better oil-holding capacities, than water-holding properties, high fowability and intermediate cohesiveness. All these properties revealed the potential of this inulin to be used as a functional ingredient, as taste and structure modifier of formulated food systems. An interesting and promising application of polysaccharides (particularly inulin from common salsify roots) is the synthesis of metal NPs by reduction of their salts. By this way, Au NPs were successfully synthesized and they were characterized by TEM. The antimicrobial potential of golden NPs with common salsify inulin permits its further application in food and pharmacy.

Acknowledgement: Research equipment of Distributed Research Infrastructure INFRAMAT, part of Bulgarian National Roadmap for Research Infrastructures, supported by Bulgarian Ministry of Education and Science was used in this investigation.

REFERENCES

1. J. Van Loo, P. Coussement, L. Leenheer, H. Hoebregs, G. Smits, *Crit. Rev. Food Sci. Nutr.*, **35**, 525 (1995).
2. E. Dobrange, D. Peshev, B. Loedolff, W. Van den Ende, *Biomolecules*, **9**, 615 (2019).
3. T. Barclay, M. Ginic-Markovic, M. Johnston, P. Cooper, N. Petrovsky, *Carbohydr. Res.*, **352**, 117 (2012).
4. Li A. Volsi, D. Jimenez de Aberasturi, M. Henriksen-Lacey, G. Giammona, M. Licciardi, L. Liz-Marzán, *J. Mater. Chem.B*, **4**, 1150 (2016).
5. F. Afinjuomo, S. Abdella, S. Youssef, Y. Song, S. Garg, *Pharmaceuticals*, **14**, 855 (2021).
6. M. Wang, K. Cheong, *Molecules*, **28**, 1613 (2023).
7. N. Eruygur, E. Ucar, M. Ataş, M. Ergul, M. Ergul, F. Sozmen, *Toxicol. Rep.*, **7**, 59 (2020).
8. M. Konopinski, *Acta Sci. Pol-Hortorum Cultus*, **8**, 27 (2009).
9. M. Beirão-da-Costa, M. Janeiro, F. Simão, A. Leitão, *Alimentos E Nutrição Araraquara*, **16**, 221 (2009).
10. E. Patkowska, M. Konopinski, *Acta Sci. Pol-Hortorum Cultus.*, **10**, 2 (2011).
11. T. K. Lim, *Edible Medicinal and Non Medicinal Plants: Vol. 9, Modified Stems, Roots, Bulbs*, Springer Science+Business Media Dordrecht, 2016.
12. N. Zeeni, C. Daher, L. Saab, M. Mroueh, *Appetite*, **72**, 1 (2014).
13. P. Kheoane, C. Tarirai, T. Gadaga, L. Carmen, R. Nyanzi, *J. Food Res.*, **6**, 17 (2016).
14. N. Petkova, G. Sherova, P. Denev, *Int. Food Res. J.*, **25**(5) (2018).
15. N. Petkova, *Asian J. Pharm. Clin. Res.*, **11**, 221 (2018).
16. N. Petkova, A. Petrova, I. Ivanov, I. Hambarlyiska, Y. Tumbarski, I. Dincheva, M. Ognyanov, P. Denev, *ChemEng.*, **7**, 94 (2023).
17. F. Robertson, D. de Monredon, P. Dysseleer, F. Guillon, R. Amado, J.-F. Thibault, *LWT*, **33**, 72 (2000).
18. R. Jirayucharoensak, K. Khuenpet, W. Jittanit, S. Sirisansaneeyakul, *Dry. Technol.*, **37**, 1215 (2019).
19. K. Lazarova, D. Christova, D. Karashanova, B. Georgieva, G. Marovska, A. Slavov, T. Babeva, *Sensors*, **23**, 2941 (2023).
20. Y. Tumbarski, I. Deseva, D. Mihaylova, M. Stoyanova, L. Krastev, R. Nikolova, V. Yanakieva, I. Ivanov, *Food Technol. Biotechnol.*, **56**, 546 (2018).
21. W. El-Kholy, G. Bisar, R. Aamer, *Food Nutr. Sci.*, **14**, 70 (2023).
22. S. Rashid, A. Rakha, M. Butt, M. Asghar, *Progr. Nutr.*, **20**, 191 (2018).
23. N. Petkova, E. Ehlmanov, I. Ivanov, P. Denev, International Scientific-Practical Conference "Food, Technologies & Health", 2013, Proceedings Book, 142, (2013).
24. M. Grube, M. Bekers, D. Upite, E. Kaminska, *Spectroscopy*, **16**, 289 (2002).

Investigation of the effect of ultrasound-assisted extraction on the yield and tannin content of white oregano extracts

V. V. Paskova, K. Z. Dobрева*, I. T. Dimitrova

Trakia University, Department of Food Technology, 38 Graf Ignatiev Str., 8600 Yambol, Bulgaria

Received: November 3, 2023; Revised: April 11, 2024

Oregano and its extracts are rich in a variety of biologically active substances, which makes them suitable for use in food industry, pharmacy, *etc.* The influence of the technological parameters – solvent concentration, temperature and duration of ultrasound-assisted extraction on the yield and tannin content of extracts of white oregano (*Origanum heracleoticum* L.) was studied. The data were compared with those obtained with conventional extraction methods. The resulting ethanol extracts are highly viscous liquids with a dark brown color, characteristic of the plant spice smell and a specific burning taste. The highest yield and highest tannin content in ultrasound-assisted extraction of cultured white oregano was obtained with 70% ethanol at a temperature of 60°C during the process, hydromodule 1:10 and duration 60 min. The use of ultrasound-assisted impact to extract tannins from cultured white oregano allows to achieve higher yields and reduce the duration of the process, compared to conventional extraction methods.

Keywords: white oregano, ultrasound-assisted extraction, ethanol extracts, tannins.

INTRODUCTION

The plants produce diverse groups of secondary metabolites that may find application as additives or antioxidants in food production and in the pharmaceutical industry [1]. The extraction and purification of these metabolites from plant-based raw materials is a challenge for scientists to propose suitable methods that are relatively simple, safe and inexpensive [2].

In recent years, unconventional techniques have been used to obtain enriched plant extracts, such as ultrasound-assisted extraction, enzyme extraction and microwave extraction [3]. According to Michalaki *et al.* [4], the interest in ultrasound-assisted extraction is due to its positive impact on the extraction process of biologically active compounds (high yield of extract, low costs and short duration of the process). Ultrasound-assisted extraction has been used to extract valuable compounds such as proteins [5], carbohydrates [6], polysaccharide-protein complex [7], oils [8, 9], polyphenolic compounds [10], isoflavones [11], lycopene [12] and others.

White oregano (*Origanum heracleoticum* L.) is a herbaceous perennial of *Lamiaceae* family. In natural habitats in Bulgaria, it is widespread in the eastern rocky slopes of the Rhodopes, as well as in Belasitsa, Struma Valley and Kresna Gorge; the cultivated oregano is grown in Ruse, Pleven, Momchilgrad and Plovdiv regions [13]. White oregano and the extracts derived from it have proven

antioxidant and antimicrobial properties due to the biologically active substances contained in them. The purpose of the study is to investigate the effect of ultrasound on the yield and composition of extracts of white oregano (*Origanum heracleoticum* L.), as well as to establish the most appropriate parameters of the process, namely temperature and duration, affecting the degree of extraction of tanning agents [14–18].

The purpose of this study is to investigate the effect of ultrasound on the yield and content of tannins in extracts of white oregano (*Origanum heracleoticum* L.), as well as to establish the most appropriate parameters of the process - temperature and duration, affecting the degree of extraction of tannins.

EXPERIMENTAL

Plant material

The above-ground mass of Bulgarian cultivated white oregano (*Origanum heracleoticum* L.), purchased from the commercial network, 2021 harvest accompanied by a certificate for the main physical, chemical and microbiological indicators, ensuring the quality of the raw material, was used. Prior to analysis, the raw material was milled on a laboratory mill with a particle size of the 0.006 m predominant fraction, determined by sieve analysis [19].

Methods

The moisture content of the raw material (%) was determined by azeotropic distillation in a Dean and

* To whom all correspondence should be sent:
E-mail: krasimira.dobрева@trakia-uni.bg

Stark laboratory apparatus [19]. The content of tanning agents in the raw material was determined by exhaustive extraction with hot water at boiling and titration of the extract obtained with 0.1 N KMnO₄ with an indigo carmine indicator, % [20]. Ethanol with concentrations of 50 and 70% was used as a solvent.

The extraction was carried out in an ultrasonic bath of model ELMA, Elmasonic P30H - Germany, with a frequency of 37 kHz at a hydromodule of 1:10, at temperatures of 30, 40, 50 and 60 °C and duration of 15, 30 and 60 min. After filtration, the solvent was separated from the solutions by its evaporation on a rotary vacuum evaporator at a water bath temperature of 60-65°C. Extracts were stored at 4 - 6°C until analysis.

To compare the yields and the content of tannins, an exhaustive extraction of the raw material without stirring was carried out with 70% ethanol at a temperature of 60°C (52.23 ± 0.48%). At an interval of 60 min the raw material was treated with pure solvent, the extracts were collected and the solvent was separated on a rotary vacuum evaporator. The content of tannin substances was determined in the extracts according to the methodology described above. The values of the studied technological parameters were chosen based on literature data and preliminary studies. All experiments were performed in triplicate, and the values in the tables and graphs are the arithmetic means presented with their standard deviation. The data obtained from the measurements and calculations were processed in MS Excel 2016 (Microsoft Corp.) at significance level α = 0.05.

RESULTS AND DISCUSSION

The analyzed raw material contains 12.7 ± 0.10 % moisture and 17.12 ± 0.12 % tanning agents. The data point out that the amount of tannins is by about 4% higher than the data published by Baycheva *et al.* [21] (13.84%), which can be explained with the different climatic conditions in different harvest years. The content of tannin substances in cultivated white oregano is lower than the data in the literature for wild white oregano of 20.6 to 22.5 % [21, 22], due to different origins.

The scheme of the experiments and obtained results is presented in Table. 1.

It is seen from the data that the extract yield increases by increase in the duration and temperature of the extraction with both solvents. Its amounts are higher when extracted with 70% ethanol (42.28 ÷ 64.25%).

Table 1. Extract yield of Bulgarian cultivated white oregano.

Duration, min	Temperature, °C	Yield relative to exhaustive extraction, %	
		50% ethanol	70% ethanol
30	15	34.41 ± 0.27	42.28 ± 0.39
	30	42.66 ± 0.36	44.08 ± 0.38
	60	44.32 ± 0.42	45.16 ± 0.33
40	15	40.49 ± 0.35	47.25 ± 0.42
	30	41.99 ± 0.33	47.84 ± 0.43
	60	44.41 ± 0.34	48.94 ± 0.41
50	15	40.14 ± 0.38	46.32 ± 0.43
	30	41.05 ± 0.39	51.48 ± 0.50
	60	43.61 ± 0.35	52.56 ± 0.50
60	15	45.21 ± 0.36	51.94 ± 0.50
	30	48.06 ± 0.42	58.62 ± 0.54
	60	50.01 ± 0.43	64.25 ± 0.61

The conducted studies revealed that lower yields of extract are obtained at different temperatures with duration of the process of 15 min; relatively higher values are found when the temperature is increased to 60 °C and the duration is extended to 60 min. A greater influence on the extract yield has the temperature of the process rather than its duration, confirmed in the literature [21]. According to literature data, the ethanol concentration also affects the extraction of ethanol [23]. Higher concentrations of ethanol (over 70%) get the extraction of biologically active substances (phenols) from oregano more complicated.

The content of tanning agents in the extracts of cultivated white oregano is presented in Table 2, and the degree of their extraction compared to the raw material is presented in Figs. 3 and 4. The content of tanning agents in the extract obtained during exhaustive extraction of cultivated white oregano (14.43 ± 0.01%) was determined - 85.5% compared to that in the initial material.

Table 2. Content of tannins in extracts of cultivated white oregano

No.	Temperature, °C	Duration, min	Tannins, %	
			50% ethanol	70% ethanol
1	30	15	5.4 ± 0.05	6.2 ± 0.05
2	30	30	6.4 ± 0.06	6.8 ± 0.06
3	30	60	7.5 ± 0.07	7.4 ± 0.07
4	40	15	5.9 ± 0.05	7.2 ± 0.06
5	40	30	6.7 ± 0.06	6.3 ± 0.06
6	40	60	7.2 ± 0.06	6.8 ± 0.06
7	50	15	7.4 ± 0.07	7.5 ± 0.07
8	50	30	7.5 ± 0.07	7.6 ± 0.07
9	50	60	8.8 ± 0.08	8.0 ± 0.07
10	60	15	8.3 ± 0.08	8.3 ± 0.08
11	60	30	9.2 ± 0.09	8.9 ± 0.08
12	60	60	9.4 ± 0.09	10.2 ± 0.09

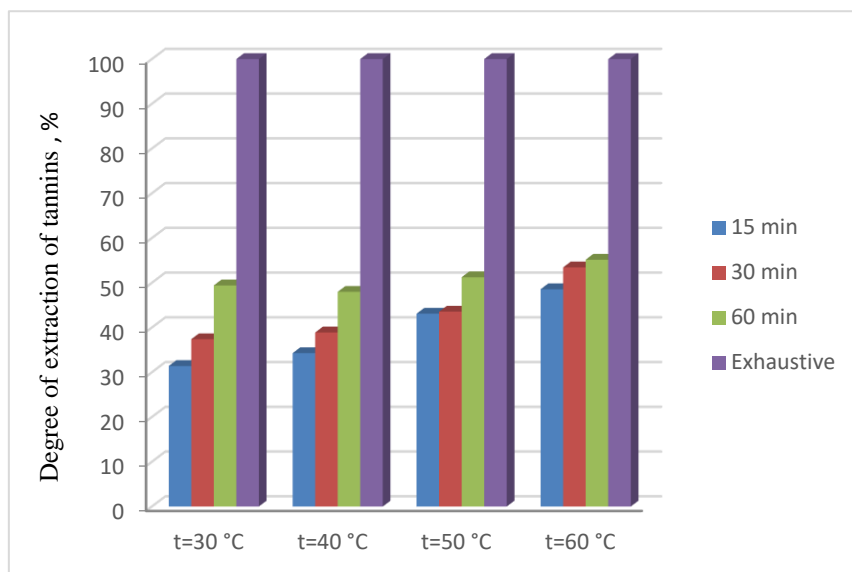


Fig. 1. Extraction rate of tannins at 50% ethanol extraction.

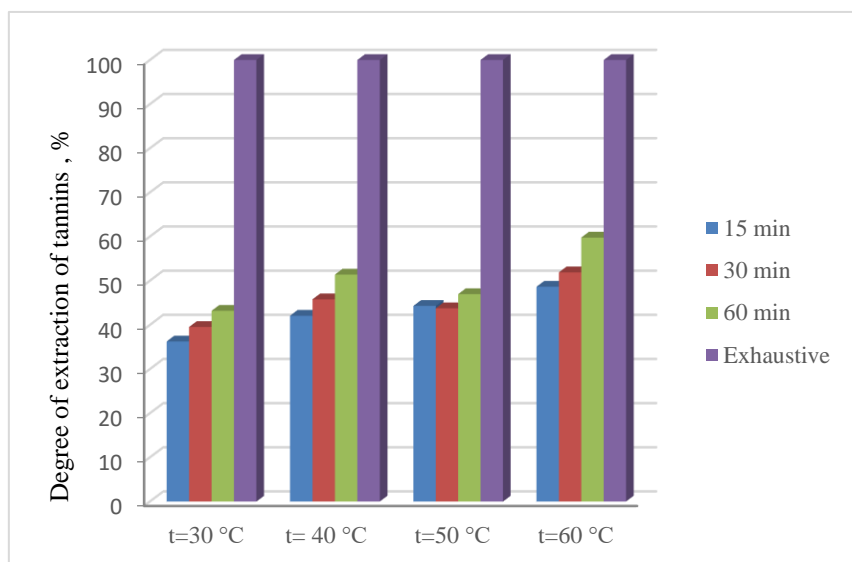


Fig. 2. Extraction rate of tannins at 70% ethanol extraction.

The data show that the content of tannins in the extracts obtained at 30°C and 40°C is relatively low: 5.4 ÷ 7.5% at 50% ethanol and 6.2 ÷ 7.5% at 70% ethanol. Higher values were reported at a temperature of 60°C (8.3 ÷ 9.4% at 50% ethanol and 8.3 ÷ 10.2% at 70% ethanol). The influence of the duration of the process on the content of tannins maintains the same trend as for extract yield. The amount of tannins in the extract obtained for 15 min was significantly lower compared to that at 60 min extraction. Similar values were reported for the content of tannins in the extracts obtained for 30 and 60 min extraction.

From the data presented in Figs. 3 and 4 is evident that at a temperature of 30°C, the degree of

extraction of tannin substances from the output raw material is comparatively low (31.4 – 37.4% at 50% ethanol and 36.3 ÷ 43.02% at 70% ethanol). At 60°C, extraction of tannins over 50% was observed, and the highest values are accounted for extraction at 70% ethanol and 60 min process duration (52.1 %).

Similar results were obtained by Baicheva *et al.* [21] with extraction without ultrasound, hydromodule 1:10, temperature 60°C and duration of 6 h (57.88 %).

Similar dependencies for the influence of the temperature and duration of the process on the content of tannins in liquid extracts have also been found with other essential oil raw materials: cape

gooseberry leaves [24], thyme herb [25], rosemary herb [26], sage herb [27].

As a consequence of the cavitation in the ultrasound-assisted extraction, a greater dispersion of the solid phase in the liquid is achieved, resulting in a larger contact surface. In this way, higher yields are obtained in a shorter time with small amounts of solvent [28].

A comparison of the yields and tannin contents in ethanol extracts obtained by conventional extraction (without stirring) [29] and ultrasound-assisted extraction, under the same conditions: solvent concentration, duration, temperature and hydromodulus, indicates 30 – 35 % higher values at ultrasound-assisted extraction.

CONCLUSION

Highest ultrasound-assisted extraction yield of cultivated white oregano with 70% ethanol with the highest content of tannins is obtained at temperature of 60°C during the process, hydro module 1:10 and duration 60 min. The use of ultrasound to extract tannins from cultivated white oregano (*Origanum heracleoticum* L.) allows to achieve higher yields and reduce the process duration.

Acknowledgement: 3 FTT/2021 "Ultrasound-assisted extraction of fennel (*Anethum graveolens* L.) and white oregano (*Origanum vulgare* L.)".

REFERENCES

1. F. Bourgaud, A. Grivot, S. Milesi, E. Gontierq, *Plant Science*, **161**, 839 (2001).
2. H. F. Zhang, X. H. Yang, Y. Wang, *Trends Food Sci. and Technol.*, **22**, 672 (2011).
3. J. Azmir., I. S. M. Zaidul, M. M. Rahman, K. M. Sharif, A. Mohamed, F. Sahena, A. K. M. Omar, *J. Food Eng.*, **117**, 426 (2013).
4. A. Michalaki, H. C. Karantonis, A. S. Kritikou, N. S. Thomaidis, M. E. Dasenaki, *J. Molecules*, **28** (5), 2033 (2023).
5. W. Qu, H. Ma, J. Jia, R. He, L. Luo, Z. Pan, *Ultrason. Sonochem.*, **19** (5), 1021 (2012).
6. B. Karki , B.P. Lamsal, S. Jung, J. Van Leeuwen , A. Pometto , D. Grewell , S. Khanal, *J. Food Eng.*, **96**, 270 (2010).
7. Y. C. Cheung, K. C. Siu, Y. S. Liu, J. Y. Wu, *Process. Biochem.*, **47**(5), 892 (2012).
8. J. Ruiz-Jiménez, M. D. L. de Castro, *Anal. Chim. Acta*, **502** (1), 75 (2004).
9. F. Adam, M. A. Vian, G. Peltier, F. Chemat, *Bioresour. Technol.*, **114**, 457 (2012).
10. T. Jerman, P. Trebse, B. Vodopivec, *Food Chem.*, **123**, 175 (2010).
11. M. A. Rostagno, M. Palma, C. G. Barroso, *J. Chromatogr. A.*, **1012**, 119 (2003).
12. Z. Lianfu, L. Zelong, *Ultrason. Sonochem.*, **15**, 731 (2008).
13. M. Anchev, Flora of the People's Republic of Bulgaria, Publishing House of BAS, Sofia (Bg), 1989.
14. W. Zheng, S. Wang., *J. Agric. Food Chem.*, **49** (11), 5165 (2001).
15. H. Hotta, S. Nagano, M. Ueda, Y. Tsujino, J. Koyama, T. Osakai, *Biochim. Biophys. Acta*, **1572**, 123 (2002).
16. V. Exarchou, N. Nenadis, M. Tsimidou, I. Gerathanassis, A. Troganis, D. Boskou, *J. Agric. Food Chem.*, **50**, 5294 (2002).
17. M. Hossain, N. Brunton, C. Barry-Ryan, A. Martin-Diana, M. Wilkinson, *Rasayan J. Chem.*, **1**, 751 (2008).
18. C. Timothy, V. Priya, R. Gayathri, *Drug Invent. Today*, **10**, 1903 (2018).
19. A. Stoyanova, E. Georgiev, T. Atanasova, T. Manual for laboratory exercises on essential oils, Academic Ed. UFT, 2007.
20. State Pharmacopoeia of the USSR, XI, Publishing house "Medicine", 1990, p.286.
21. S. Baycheva, K. Dobрева, G. Mihaylova, *ARTTE*, **7**(3), 206 (2019).
22. Sh. Goyal, G. Tewari, K. Pandey, A. Kumari, *J. Chem.*, **2021** (2021).
23. A. Oreopoulou, G. Goussias, D Tsimogiannis, V. Oreopoulou, *Food Bioprod. Process.*, **123**, 378 (2020).
24. T. Ivanova, V. Popova, N. Mazova, A. Stoyanova, S. Damianova, *DOAJ*, **8** (1), 34 (2019).
25. S. Damianova, S. Tasheva, A. Stoyanova, D. Damianov, *J. Essent. Oil Bear. Plants*, **11** (5), 443 (2008).
26. S. Damianova, S. Tasheva, A. Stoyanova, D. Damianov, *J. Essent. Oil Bear. Plants*, **13** (1), 1 (2010).
27. S. Mollova, S. Tasheva, S. Damyanova, M. Stoyanova, A. Stoyanova, *J. Food Packag. Sci. Techn. and Technol.*, **8** (6), 40 (2016).
28. C. Carrera, A. Ruiz-Rodríguez, M. Palma, C. G. Barroso, *Anal. Chim. Acta*, **732**, 100 (2012).
29. V. Paskova, I. Taneva, K. Dobрева, *Appl. Res. Tech. Technol. Educ.*, **11** (4), (2023).

Phytochemical characterization of different varieties of thyme

Ts. S. Valev, K. Zh. Dobrev^{*}, M. D. Dimov

Trakia University, Faculty of Engineering and Technology, 38 Graf Ignatiev Street, 8600 Yambol, Bulgaria

Received: November 3, 2024; Revised: April 11, 2024

For centuries, thyme has been used as a spice and medicinal plant. Of the more than 350 established species of plants of *Thymus* genus, garden thyme (*Thymus vulgaris* L.) and common thyme (*Thymus serpyllum* L.) have economic importance. Three chemotypes of thyme are the object of this study - thymol, citral and geraniol. The main physical and chemical characteristics of the studied thymes are determined - humidity, proteins, fibers, lipids, essential oil and mineral composition. The chemical composition of organic substances in the essential oils of the different chemotypes was determined by GC – MS analysis. The distribution of the components by groups has been established. The yield of essential oil is highest in "French" and "Pagane" varieties. "French" and "German Winter" thyme oils are characterized by a high thymol content (36.98 % and 55.49 %, respectively), which determines their classification as thymol chemotype. In the essential oil of "Slava" variety, the main components are geraniol (28.89%), nerol (3.84%) and geranyl acetate (34.35%), which define it as a citral chemotype. Main components in "Pagane" thyme oil are geraniol (55.56%) and geranyl acetate (27.72%), defining it as a geraniol chemotype. The determination of the phytochemical characteristics of thyme aims to provide information on its condition, its suitability for storage and processing, as well as to determine the type and technological parameters for its processing.

Keywords: *Thymus vulgaris* L., chemical composition, essential oil, GC/MS.

INTRODUCTION

Today, about 250 species of thyme are known, 214 of which are species and 36 are subspecies divided into eight sections: *Mikantes*, *Mastihcina*, *Piperella*, *Teucroides*, *Pseudothymbra*, *Thymus*, *Hyphodromy* and *Serpyllum* [1–4]. It is distributed mainly in the Mediterranean, where it originates. Today it is cultivated in Spain, France, Italy, Portugal, Germany, Algeria, Egypt, England, the Caribbean, the USA [5, 6]. The composition of essential oil in thyme is influenced by many factors such as: genotype (species, genus, family, order, class), agrometeorological (geographical origin, climatic conditions, soil composition, etc.) and technological factors (cultivation, species - collection, storage, processing technology, etc.) [4, 7–11].

In Bulgaria, thyme can be found in diverse soil and climatic conditions, semi-mountainous terrains at different altitudes, along roads, meadows and sunny places, together with other heat-loving plants. Likes sandy, stony and drained soils: brown forest, cinnamon forest, neutral and slightly alkaline soils [10, 12].

The varieties grown in our country: "German Winter", (*Thymus vulgaris* sv "German"), "French" (*Thymus vulgaris* cv. 'French'), "Slava" (*Thymus marshallianus*) and "Pagane" (*Thymus siptorpii* L.) differ in both morphological and aroma-flavor characteristics, as well as in the composition of essential oil [12].

"Pagane" variety was selected from the population of *Thymus marshallianus*. It has upright, highly branched tufts and a subtle, fresh, pleasant rose fragrance. The yield of essential oil is 0.55-0.85%, which is rich in geraniol – 74-76% and nerol 15-17%.

"Slava" variety was created from species *Thymus siptorpii* L. The plants have upright stems, the variety is suitable for mechanized cultivation, high yield. It contains essential oil in the fresh aerial mass 0.5-0.7%, with the main ingredient citral - up to 23%, citronellol - up to 10% and geraniol - up to 36%. The aroma is fresh, subtle with a citral note, reminiscent of lemon balm, suitable for the food industry. Both varieties are product of Bulgarian selection [12].

The variety "German Winter" was introduced from Germany and belongs to the species *Thymus vulgaris* L. The tufts are more compact, with erect flower-bearing stems, equal in height. The variety successfully winters under our conditions. The content of essential oil is 0.28% with the main ingredient thymol – 39.71% - 61.44%, carvacrol – up to 6.04% [12, 13].

The purpose of the research is to determine the phytochemical characteristics of different types and chemotypes of thyme grown in Bulgaria, which provides information on its condition, its suitability for storage and processing, the method and technological parameters of its processing, and the possibilities for the application of aromatic products, obtained from it as well.

EXPERIMENTALS

Plant material

The aerial part of thyme from "French", "German Winter", "Slava" and "Pagane" varieties was used, delivered from the experimental field of the Institute of Roses, Essential and Medical Cultures - Kazanlak, Bulgaria during the months of May-June 2023.

In order to reduce a significant part of the humidity

^{*} To whom all correspondence should be sent:

E-mail: krasimira.dobrev@trakia-uni.bg

and improve the storage of the raw material, the aerial part of the plant was dried in a dry, shaded and ventilated place for 20 days, immediately after harvesting. It was packed in paper bags and stored in a dark, dry and cool place.

Chemical analyses

The raw materials (air-dried) were analyzed for moisture content by azeotropic distillation using a Dien – Stark laboratory device, % [14]; for protein content, by Kjeldahl, results are expressed as % w/w (BDS - ISO 5983-1: 2006); for fat content, by Soxhlet, results are expressed as % w/w (BDS - ISO 6492: 2007); for fiber content, by Henberg and Stoman, results are expressed as % w/w (BDS - AOAC, 2007) and for ash content, by incineration in a muffle furnace at 650 °C, results are expressed as % w/w (BDS - ISO 5984: 2007).

Mineral analysis

The mineral composition (except for phosphorus) was determined by flame AAS on a Perkin Elmer spectrometer according to BDS EN 15510: 2017. The sample was dried in a dry or wet manner and dissolved in acid to obtain a solution with an optimum concentration of the elements. It was atomized in air-acetylene flame at a temperature of 2000 - 3000°C. The absorption (optical density) was determined and the concentration was calculated using a standard curve.

The phosphorus content was determined as the air-dry sample was burned at 500 - 550 °C until gray-white ash was obtained. Phosphorus was determined by the method of Gerike and Kurmis, measuring the optical density at a wavelength of 470 nm [15].

Essential oil extraction

Prior to the technological processing the raw material has been cut into pieces measuring 1.5 - 2 cm.

The essential oil was extracted by hydrodistillation in a Clevenger-type laboratory apparatus, % w/v. The distillation begins with the separation of the first drop of distillate into a container. Distillation is complete when two consecutive measurements in 30 min do not mark an

increase in the amount of essential oil [14]. The obtained essential oils were dehydrated over anhydrous Na₂SO₄ and stored in glass vials at 4 - 6 °C until analysed. The yields of the essential oils were converted to absolutely dry mass.

Gas chromatography (GC) and gas chromatography/mass spectrometry (GC/MS) analyses

The chemical composition of the essential oils was determined by gas chromatography (GC) and gas chromatography-mass spectrometry (GC/MS) by direct headspace analysis according to ISO standards (ISO 11024-1: 1998, ISO 11024-2: 1998).

GC analysis: Agilent 7890 A device with flame ionization detector; HP-INNOWax polyethylene glycol column (60 m × 0.25 mm; 0.25 µm film thickness); temperature conditions: 70 °C for 10 min, 70 - 240 °C at 5 °C/min, 240 °C for 5 min; 240-250 °C at 10 °C/min, 250 °C for 15 min; helium carrier gas, 1 cm³/min constant velocity; injector: split, 250 °C, split ratio 50:1.

GC-MS analysis: Agilent 5975 C device, helium carrier gas, column and temperature conditions as in the GC assay; detectors: FID, 280 °C, MSD, 280 °C transfer line.

The flavor components were identified by comparison with the witness retention index and mass spectra (MS), stacked at retention time, the amount was given in percentage.

All experiments were performed in triplicate, with averaged values in the tables and graphs, and represented with their mean and standard deviation. The measurements and calculations were processed in MS Excel 2016 (Microsoft Corporation Inc.) at a level of significance α=0.05.

RESULTS AND DISCUSSION

The studied plants have low humidity, which is an indicator of good storage of the raw material. The composition of the dried above-ground part of the raw material is shown in Table 1, and the mineral composition in Table 2.

Table 1. Physical and chemical characteristics of various varieties thyme

Components	French	German Winter	Slava	Pagane
Moisture, %	6.74	6.46	6.47	6.38
Proteins, %	12.96	8	8.09	8.91
Fats, %	1.93	1.99	1.23	1.75
Ash, %	7.31	10.01	8.75	9.75
Fibers, %	22	26.47	26.3	19.06
Essential oil, % w/v	0.18	0.1	0.1	0.18

Table 2. Mineral composition of various varieties of thyme

№	Ca %	P %	K mg/kg	Mg mg/kg	Mn mg/kg	Zn mg/kg	Cu mg/kg	Fe mg/kg
German Winter	0.52	0.27	8 942.92	2 515.27	81.30	39.95	11.99	3703.66
Slava	0.66	0.10	9 791.58	2 156.78	59.28	49.10	13.71	1996.44
Pagane	0.41	0.13	10 551.06	2 393.39	67.75	48.83	11.86	1853.57
French	0.55	0.14	9 908.12	1 949.56	40.02	31.93	8.82	993.67

The amount of proteins in the studied raw materials is comparable to the data on the content of proteins in other herbaceous plants of the *Lamiaceae* family - common oregano, mint, sage, savory, rosemary, basil (4.88 - 22.98%). The fat and fiber content is lower compared to the raw materials (from 4.07 to 15.22% for fat and from 37.00 to 45.70% for fiber) due to their different botanical affiliation [16].

There is a lack of data in the literature on the mineral composition of thyme grown in Bulgaria, which makes comparison difficult. All essential oils are pale yellow liquids except "Pagane" oil, which is almost transparent due to the high content of geraniol determining its color. The chemical composition of the essential oils from the different varieties of thyme grown in Bulgaria is shown in Table 3.

Table 3. Chemical composition of essential oils, %.

№	RI	Compound	Content, %			
			French	German Winter	Slava	Pagane
1	929	α -Thujene	0.55	0.47	nd*	nd
2	935	α -Pinene	0.57	0.43	nd	nd
3	948	Camphene	0.72	0.55	nd	nd
4	972	β -Pinene	0.20	0.23	nd	nd
5	977	1-Octen-3-ol	1.60	0.26	0.29	0.19
6	990	Myrcene	0.62	0.73	nd	nd
7	994	3-Octanol	0.33	nd	0.22	nd
8	1016	α -Terpinene	0.92	1.05	nd	nd
9	1022	p-Cimene	29.43	17.68	0.46	nd
10	1024	Limonene	0.35	0.25	nd	nd
11	1026	Eucalyptol	1.03	1.40	nd	nd
12	1057	γ -Terpinene	5.23	6.45	0.27	nd
13	1071	Camphenilone	1.50	1.17	nd	nd
14	1098	β -Linalool	4.46	3.16	0.52	0.53
15	1105	1-Octen-3-yl-acetate	nd	nd	nd	1.33
16	1146	Camphor	0.52	nd	0.60	nd
17	1157	Benzyl acetate	0.76	nd	nd	nd
18	1169	Borneol	2.97	1.83	0.28	nd
19	1178	1-Terpinen-4-ol	0.43	0.87	nd	nd
20	1190	α -Terpineol	0.19	0.30	nd	1.40
21	1226	Nerol	nd	nd	3.84	2.80
22	1233	Methyl thymyl ether	0.29	0.34	nd	nd
23	1237	Neral	nd	nd	8.53	1.51
24	1250	Geraniol	nd	nd	29.89	55.56
25	1266	Geranial	nd	nd	7.86	0.75
26	1291	Thymol	36.98	55.49	3.97	0.23
27	1300	Carvacrol	3.59	3.02	nd	nd
28	1344	α -Terpinyl acetate	nd	nd	0.35	3.22
29	1350	Thymyl acetate	0.12	0.10	nd	nd
30	1361	Neryl acetate	nd	nd	1.69	0.86
31	1382	Geranyl acetate	nd	nd	34.35	27.72
32	1395	β -Elemene	0.14	0.21	nd	nd
33	1420	β -Caryophyllene	3.21	1.54	1.65	0.22
34	1455	α -Caryophyllene	0.11	0.15	1.26	0.14
35	1468	9-epi-(E)-Caryophyllene	0.24	nd	nd	nd
36	1484	Germacrene D	0.30	nd	0.65	0.77
37	1514	γ -Cadinene	0.17	0.11	0.20	0.15
38	1525	β -Cadinene	0.25	0.14	0.37	1.64
39	1560	Elemicin	nd	nd	0.92	0.13
40	1590	Caryophyllene oxide	1.65	1.34	1.07	0.37
41	1624	10-epi- γ -Eudesmol	0.24	0.42	0.53	0.28
Essential oil, % (v/w)			0.18±0.98	0.1±0.04	0.1±0.01	0.18±0.04

* nd - not determined

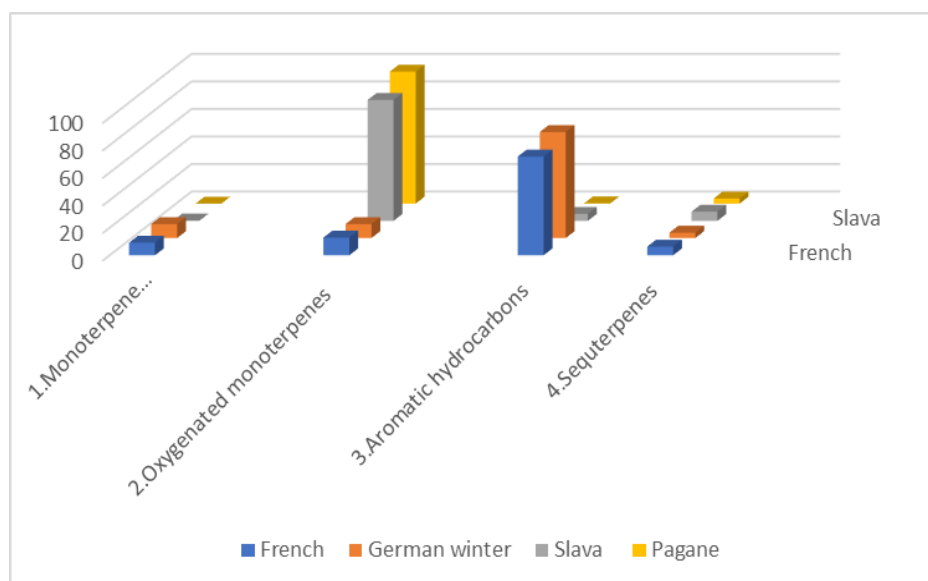


Fig. 1. Groups of components in thyme oils, %: 1 – monoterpene hydrocarbons; 2 – oxygenated monoterpenes; 3 – aromatic hydrocarbons; 4 – sesquiterpene hydrocarbons. In the essential oil of "French" variety (*Thymus vulgaris* cv. 'French'), 32 compounds were identified, representing 99.66% of the oil. The main components (over 3%) in oil from the aerial part are: thymol (36.98%), p-cimene (29.43%), γ -terpinene (5.23%), β -linalool (4.46%), carvacrol (3.59%), β -caryophyllene (3.21%).

In the oil of "German Winter" variety collected during the mass flowering phase, 27 components were identified constituting (99.72%) of the essential oil. The main compounds (over 3%) are: phenolic monoterpene thymol (55.49%), p-cimene (17.68%), monoterpene γ -terpinene (6.45%), oxygenated monoterpene β -linalool (3.16%), of these 27.

In the thyme oil of "Slava" variety, 23 components are observed, making up 99.76% of the total amount of oil with main compounds (over 3%) oxygen-containing monoterpenes: geranyl acetate (34.35%), geraniol (29.89%), neral (8.53%), geranial (7.86%), nerol (3.84%) and the aromatic monoterpene thymol (3.97%) as well.

20 components were found in the essential oil of "Pagane" variety, which are 99.8% of the total amount. The main compounds in the composition of the essential oil (over 3%) are the oxygen-containing monoterpenes: geraniol (55.56%), geranyl acetate (27.72%) and α -terpinyl acetate (3.22%).

The distribution of the identified aromatic compounds based on functional groups in these four essential oils is presented in Fig. 1.

In the essential oils of "French" and "German Winter" varieties, aromatic hydrocarbons predominate (71.72% and 77.07%, respectively), and in those of "Slava" and "Pagane" varieties, the oxygen-containing monoterpene hydrocarbons (87.81% and 95.87%, respectively). The content of sesquiterpenes in the essential oils of these four varieties is as follows: "French" - 6.3%; "German Winter" - 3.92%; "Slava" - 6.64% and "Pagane" - 3.7%.

CONCLUSION

Physical and chemical parameters of different varieties and chemotypes of thyme grown in Bulgaria were determined: variety "French", variety "German Winter", variety "Slava" and variety "Pagane". The different varieties are characterized by a different chemical composition of the essential oils, which also characterizes them as different chemotypes. The main component in the thyme oils of "French" and "German Winter" varieties is the aromatic monoterpene thymol (36.98% and 55.49%, respectively), which is decisive for their classification as a thymol chemotype. In "Slava" and "Pagane" varieties, oxygen-containing monoterpenes dominate. In the essential oil of "Slava" variety, the main components are geraniol (28.89%), nerol (3.84%) and geranyl acetate (34.35%), which define it as a citral chemotype. Main components in "Pagane" thyme oil are geraniol (55.56%) and geranyl acetate (27.72%), defining it as a geraniol chemotype. Both varieties of thyme have monoterpene hydrocarbons below 1%, which is positive for the perfumery industry.

Acknowledgement: This work was supported by Trakia University, Bulgaria under Project 2FTT/2022.

REFERENCES

1. L. Tabrizi, A. Koocheki, P. Rezvani Moghaddam, P. Nassiri Mahallati, *Chem. Nat. Compd.*, **46**, 121 (2010).

2. E. Stahl-Biskup, R. P. Venskutonis, Thyme. In Handbook of herbs and spices, 499. Woodhead Publishing, 2012.
3. P. Satyal, B. L. Murray, R. L. McFeeters, W. N. Setzer, *Foods*, **5** (4), 70 (2016).
4. O. Kosakowska, K. Bączek, J. L. Przybył, A. Pawelczak, K. Rolewska, Z. Węglarz, *Agron.*, **10** (6), 909 (2020).
5. E. Schmidt, J. Wanner, M. Höferl, L. Jirovetz, G. Buchbauer, V. Gochev, Geissler, *Nat. Prod. Commun.*, **7** (8), 1095 (2012).
6. F. A. Kaki, R. Benkiniouar, A. Touil, I. Demirtas, A. Merzoug, L. Khattabi, *Environ. Exp. Bot.*, **19** (2), 67 (2021).
7. A. K. Al-Asmari, M. T. Athar, A. A. Al-Faraidy, M. S. Almuhaiza, *Asia. Pac. J. Trop. Biomed.*, **7** (2), 147 (2017).
8. A. Touhami, A. Chefrour, N. Khellaf, A. Bukhari, I. J. Fadel, *Pharm. Pharmacol.*, **5**, 37 (2017).
9. M. Dalir, A. J. Safarnejad, *J. Medicinal Plants By-products*, **1**, 41 (2017).
10. I. Aneva, P. Zhelev, S. Stoyanov, Y. Marinov, K. Georgieva, *Ecol. Balk.*, **10** (2), 101 (2018).
11. A. Stefanaki, T. van Andel, in: Aromatic Herbs in Food, Academic Press, 93, 2021.
12. S. Stanev, Technology for Growing Thyme, 2015. https://bilki.naas.government.bg/doc/otglezdane/tehnologii/tehnologia_otglezdane_mashterka.pdf (available on 02.11.2023).
13. G. Zhekova, A. Dzhurmanski, M. Nikolova, *Agric. Sci. Technol.*, **3** (2), 123 (2011).
14. T. Atanasova, M. Perifanova-Nemska, A. Stoyanova, Raw material for vegetable fats and essential oils, Academic Publishing House of UFT Plovdiv, 2016.
15. S. Sandev, Chemical methods for feed analysis, Zemizdat, Sofia, 1979.
16. USDA, Agricultural Research Service, National Nutrient Database for Standard Reference Full Report (All Nutrients) 02027, Spices. 2018. (online).

Application of stable nitroxide radicals and their non-contrast forms in diagnostics of oxidative stress in patients with diabetes mellitus type 2 and non-alcoholic fatty liver disease

E. Georgieva^{1*}, D. Berbatov², Y. Karamalakova³, G. Nikolova³, M. Gulubova^{1,4}

¹Department of General and Clinical Pathology, Forensic Medicine, Deontology and Dermatovenerology, Medical Faculty, Trakia University, 11 Armeiska Str., 6000 Stara Zagora, Bulgaria

²Berbatov Medical Center, 8600 Yambol, Bulgaria

³Department of Chemistry and Biochemistry, Medical Faculty, Trakia University, 11 Armeiska Str., 6000 Stara Zagora, Bulgaria

⁴Department of Anatomy, Histology and Embryology and Pathology, Medical Faculty, Assen Zlatarov University, 8000 Burgas, Bulgaria

Received: November 3, 2023; Revised: April 11, 2024

Non-alcoholic fatty liver disease has emerged as one of the main causes of chronic liver damage, which occurs as a result of a wide range of complications such as obesity, T2DM, inflammation, fibrosis, and the development of non-alcoholic steatohepatitis, and cirrhosis. Elevated serum-free fatty acid concentrations, hepatic triglyceride accumulation, cytotoxic reactive oxygen species, and increased levels of oxidative stress are believed to be major contributors to the development and progression of the disease. The present study highlights the application of the stable nitroxide radical TEMPOL as an effective redox sensor for redox changes monitoring in T2DM and NAFLD patients. The oxidative stress levels and antioxidant status were investigated in T2DM and NAFLD patients (group 2) and healthy volunteers (group 1) by conventional EPR spectroscopy. The obtained data show a statistically significant increase in ROS levels and EPR signal intensity of nitroxide and hydroxylamine in patients with NAFLD and T2DM compared to the control group - healthy volunteers without metabolic disorders (post hoc test; (*) $p < 0.05$ vs. control). The spectroscopic analysis allows the prediction of diabetic complications and will guide the scientific community and clinicians to conduct effective antioxidant therapy.

Keywords: oxidative stress, antioxidant enzymes, ROS, NAFLD, EPR, nitroxide radicals, TEMPOL

INTRODUCTION

Non-alcoholic fatty liver disease

Non-alcoholic fatty liver disease (NAFLD) is a common liver disorder characterized by fat accumulation in the liver cells. It is one of the most prevalent liver conditions in the world and can range from relatively benign to more severe forms that can lead to liver damage and other health complications. Non-alcoholic fatty liver is the milder form of NAFLD, where there is excessive fat accumulation in the liver, but little or no inflammation or liver cell damage [1]. The main risk factors of NAFLD include excess body weight, especially around the abdomen, insulin resistance often associated with type 2 diabetes mellitus (T2DM), high blood triglyceride and cholesterol levels (hyperlipidemia), metabolic syndrome presenting as high blood pressure, high blood sugar, excess body fat, and abnormal lipid profiles, family history of NAFLD, etc. It is known that there exists a close relationship between NAFLD and diabetes.

with diabetes are at an increased risk of developing NAFLD, and on the other, the presence of NAFLD can exacerbate metabolic disease since diabetes type 2 increases the risk of NAFLD, and having NAFLD can make it more challenging to manage blood sugar levels in the body [2].

Role of inflammation and oxidative stress in diabetes-related NAFLD

Non-alcoholic fatty liver disease is one of the most common chronic liver diseases in obese and diabetic patients, and its incidence continues to rise. The disease ranges from mild hepatic steatosis to liver fibrosis and cirrhosis, which increase overall mortality in elderly patients and those with chronic diseases [3]. Several studies have shown that insulin resistance (IR) plays a critical role in the pathophysiology of NAFLD and the natural history of the disease [4-6]. Accelerated lipolysis associated with IR increases hepatic glucose production in NAFLD patients, which up-regulates de novo fat synthesis, accelerating NAFLD progression [7].

* To whom all correspondence should be sent:
E-mail: ekaterina.georgieva@trakia-uni.bg

Other pathogenic pathways such as changes in lipid metabolism, mitochondrial leakage, and activation of pro-inflammatory cascades have been described in disease progression [8].

It is known that the reactive oxygen species (ROS) and inflammation play a significant role in the pathogenesis of diabetes and the progression of NAFLD, and that is accompanied by the development of oxidative stress (OS) in the body [9]. When diabetes and NAFLD coexist, these two processes can interact and exacerbate each other, leading to more severe liver damage. Inflammation is one of the most common players of liver damage in NAFLD, especially in the more severe form of NAFLD - non-alcoholic steatohepatitis. In individuals with diabetes, there is often a chronic low-grade inflammation throughout the body, known as systemic inflammation. This systemic inflammation can also affect the liver and contribute to the non-alcoholic steatohepatitis (NASH). In the liver, inflammation can lead to the recruitment of immune cells and activation of pathways that promote cell damage, fibrosis, and cirrhosis. Another factor in the NAFLD pathogenesis is OS, which is presented as abnormal or high levels of ROS and reactive nitrogen species (RNS) and reduced antioxidant defenses, or a combination of both [10]. At the rule, OS is a physiological condition that occurs in an imbalance between ROS or free radicals production, and the body's ability to neutralize or detoxify them with antioxidants. In NAFLD, the excess fat in the liver can lead to the production of free radicals, the process as slow as lipid peroxidation, which can cause cellular damage and inflammation. In NASH, the inflammation and immune response in the liver can further promote OS [11].

Inflammation in diabetes is driven by various factors, including the release of pro-inflammatory cytokines from fat tissue, activation of the immune system, and accumulation of advanced glycation end-products (AGEs) that can stimulate inflammation [12]. Elevated blood sugar levels can lead to the overproduction of reactive oxygen species and reduce the body's antioxidant defenses. Hyperglycemia can also lead to the formation of AGEs, which not only promote inflammation but also contribute to OS [13]. In individuals with diabetes-related NAFLD, there is a synergistic effect between inflammation and OS. Inflammation can promote OS, which can further intensify inflammation [14]. This interplay can result in a vicious cycle where liver inflammation and OS can lead to NAFLD progression to more advanced stages, including fibrosis and cirrhosis [15].

Nitroxide radicals as a redox sensor in monitoring of diabetes and related complication

Nitroxides (aminoxyl radicals) are a class of paramagnetic heterocyclic nitroxide derivatives of piperidine, pyrrolidine, and pyrrolidine that possess an unpaired electron. The ability of nitroxides to interact with a wide range of free radicals determines their important biological significance [16]. They are characterized by unique antioxidant properties, the ability to modify OS and change the redox status of tissues by breaking down superoxide anion radicals and hydrogen peroxide, inhibiting Fenton reactions, and participating in radical-radical recombination reactions [17, 18]. The unpaired electron gives them paramagnetic properties, making them detectable by various spectroscopic techniques. By redox-transformation of one-electron transfer reaction, nitroxide becomes the reduced form hydroxylamine ($>N-OH$) and oxoammonium cation ($>N=O^+$), and donates an electron, returning the non-contrast form to the contrast oxidized nitroxide radical ($>N-O\bullet$) [17]. The involvement of nitroxide radicals in reversible redox reactions makes them valuable tools in studying redox processes at the cellular and molecular level in a wide range of fields, including chemistry, biochemistry, and biomedicine [19]. This is particularly important when studying the role of OS in the context of diseases such as cancer, neurodegenerative disorders, cardiovascular diseases, diabetes, etc [20]. As a redox-active species, nitroxide can provide information about the dynamic nature of redox processes in the body. This makes it useful tools in the development of diagnostic models, treatments, and interventions targeting diseases characterized by redox imbalance [21].

This study describes a new methodological protocol for the evaluation of redox imbalance in T2DM and non-alcoholic fatty liver disease and the application of EPR spectroscopy in monitoring the occur redox changes.

EXPERIMENTAL

Sample preparation

The study used whole blood from T2DM and NAFLD patients (n=50) and clinically healthy volunteers (n=20) (age 45-65 years). The blood samples (900 μ L) were mixed with 100 μ L of nitroxide standards in DMSO (Sigma-Aldrich, Germany) and incubated for 30 min at room temperature. All reagents are of high purity ("HPLC-grade"). Quartz non-heparinized capillaries were used, which were placed in the EPR cuvette, and the measurement was started. EPR spectral analysis was

performed at room temperature. All EPR measurements were performed at the following parameters: microwave frequency – 9.4 GHz, magnetic field strength – 336 mT, microwave power – 2.0 mW, field modulation frequency – 100 kHz, field modulation amplitude – 0.063 mT, time constant – 0.01 s, sweep width – 10 mT, scan time (sweep time) – 2 min. Each sample was scanned in triplicate, and spectral processing was performed using Simfonia software, Win-EPR (Bruker, Germany). Results are presented as a percentage of the nitroxide radical/DMSO control and a.u. in hydroxyl amine.

RESULTS AND DISCUSSION

As a result of normal metabolic processes, ROS are constantly produced in the human body, as the main source of oxidants are mitochondria. On the one hand, low levels of ROS are involved in the immune response to deal with various pathogens, modulating and maintaining physiologically important redox reactions. However, higher concentrations of ROS lead to OS, which can lead to oxidative damage to cells and provoke metabolic collapse, compromising their normal functions [12].

Determination of total OS levels by electron paramagnetic spectroscopy (CW-EPR spectroscopy)

X-band EPR was used to determine the total OS levels. Solutions of the nitroxide radicals TEMPOL (4-hydroxy-2,2,6,6-tetramethylpiperidine-N-oxyl, 4-hydroxy-TEMPO) (0.2 mM) and 3- carbamoyl-PROXYL (2,2,5,5-tetramethyl-1-pyrrolidinyloxy-3-carboxamide; 3-CP) (0.5 mM), which are characterized as suitable redox sensors for the determination of ROS levels ($O_2^{\bullet-}$, H_2O_2 , etc.). A

confirmatory assay was performed to determine superoxide radical levels using 0.5 mM hydroxyl amine 1-hydroxy-3-methoxycarbonyl-2,2,5,5-tetra-methylpyrrolidine (CMH) in DMSO. Pronounced changes in the EPR signal intensity of nitroxide radicals TEMPOL and 3-CP were observed in blood samples of patients with T2DM and NAFLD, compared to the control group (healthy volunteers, gray). The graph profile shows high levels of free radicals in patients with T2DM and NAFLD (Figure 1A and B), while normal redox status in healthy volunteers does not initiate a decrease in the signal intensity of the radical forms of nitroxide, as well as oxidation of the hydroxyl amine form (CMH). Values presented are mean \pm SEM. * $p < 0.05$ compared to control group.

Oxidative stress occurs as a result of metabolic reactions with the participation of oxygen and is expressed in a violation of the pro-oxidant-antioxidant balance of cells and tissues. As a result, a redox imbalance in favor of pro-oxidants is observed, which is due to the excessive production of reactive oxygen and/or nitrogen species and the inability to overcome this superproduction of oxidants by the body's antioxidant defense. Various macromolecules such as lipids, nucleic acids, and proteins are major targets of oxidative damage involving ROS [22-25].

The high ROS concentrations can initiate lipid peroxidation, DNA oxidation, and irreversible oxidative modifications of redox-sensitive residues in proteins (including enzymes), leading to structural and functional changes in various macromolecules [26]. The control group included patients without diabetes, renal, respiratory, or cardiovascular diseases.

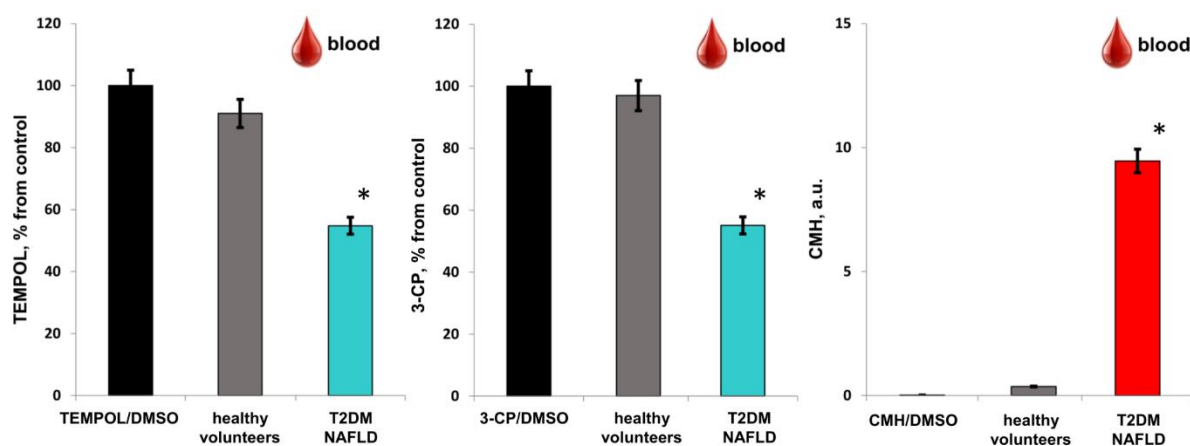


Figure 1. A, B, C. X-band EPR signal intensity in the T2DM and NAFLD patient blood samples, control nitroxide radical/DMSO (black) and healthy volunteers (in gray): (A) TEMPOL, (B) 3-Carbamoyl-PROXYL (3-CP), and (C) (CMH).

Oxidative stress plays a major role in the initiation and development of various pathological conditions such as diabetes mellitus (DM), cancer, atherosclerosis, neurodegenerative diseases, ischemia/reperfusion injury, aging, etc., and their resulting complications [27-29]. According to the literature data known to date, metabolic disorders are characterized by an increased production of ROS compared to a normal healthy organism. Hypoglycemia is believed to be involved in the production of free radicals, the initiation of OS, inflammation, hypercoagulation, and endothelial dysfunction and may lead to increased levels of oxidative markers of DNA damage, lipid peroxidation, etc. [9]. Diabetes is associated with several complications that are due to a higher production of free radicals and a sharp drop in the body's antioxidant defense expressed in reduced superoxide dismutase (SOD) and catalase (CAT) activity and leads to low concentrations of GSH and Vit E [30]. These complications are characterized by well-expressed changes in the normal redox balance and impaired activity of antioxidant protective enzymes, in conditions of hyperglycemia [12]. Disturbances in the normal metabolism of the body lead to a pronounced redox imbalance, which allows the use of nitroxide-enhanced EPR for monitoring OS and the degree of free-radical damage in patients with NAFLD and type 2 diabetes mellitus.

Abnormal levels of oxidants in these diseases can lead to a loss of the EPR signal of the nitroxide radical form (R-O•) and an increase in the EPR-silent hydroxylamine (R-OH) signal (Figure 1 A-C). The methodological approach presented in this article applies to direct and non-invasive assessment of OS in patients with NAFLD and T2DM. Diabetic patients have an increased risk of micro-, macro-vascular and cardiovascular complications, and increased mortality, with OS and cytokine expression considered to be one of the key sources of diabetic complications [9].

The EPR analysis with the participation of oxidized and reduced forms of nitroxides aims to show the application of their radical and hydroxylamine forms in determining the levels of free radicals and OS in patients with endocrine diseases. Through various acid and nitrogen radical and non-radical forms, transition metal ions, NAD(P)H, ascorbate, etc. the nitroxide radical, which gives an EPR signal, can be rapidly converted to the non-contrast form hydroxylamine or oxoammonium [31]. The presented results suggest that the nitroxide radicals TEMPOL and 3-CP can be successfully used for *in vitro* assessment of OS and redox imbalance in patients with T2DM and NAFLD. As a

result of the high levels of free radicals, the EPR signal intensity decreased after 30 minutes of incubation of the blood sample in T2DM and NAFLD patients relative to the nitroxide / DMSO control, while in healthy volunteers, the reduction in nitroxide signal intensity was about 10% (Figure 1A and B).

3-CP is a neutral membrane-permeable nitroxide that can be distributed in the intracellular and extracellular environment and can be used to measure the levels of oxygen radicals [32]. A high concentration of ROS leads to a downgraded EPR signal of paramagnetic 3-CPH due to the formation of non-contrast hydroxylamine (3-CPOH) or oxidation of protonated superoxide ($\bullet\text{OOH}$) to oxoammonium cation [33]. The results demonstrated that the intensity of 5-membered ring nitroxide 3-carbamoyl-proxy markedly reduced in diabetic patient blood samples, which can be a result of high ROS production, such as superoxide anion radicals and hydroxide radicals [34, 35] (Figure 1B).

The hydroxylamine 1-hydroxy-3-methoxy-carbonyl-2,2,5,5-tetramethylpyrrolidine (CMH) is the most effective centrifugation probe for measuring ROS production [31] and characterize as a neutral detector for intra- and extracellular production of superoxide radical levels [36]. The interaction of hydroxylamine with ROS ($\text{O}_2^{\bullet-}$ and H_2O_2) and RNS (peroxyl radicals or peroxyxynitrite) leads to the appearance of an EPR signal [37]. Abnormal levels of ROS in patients with T2DM, and in particular in oxidative stress-related diabetes and NAFLD, lead to oxidation of the hydroxylamine form of CMH and its conversion to the radical form (CM•). The normal redox state of the organism in healthy controls did not initiate the appearance of a significant EPR signal (Figure 1C). This result can be associated with low levels of ROS, well-coordinated redox regulation, and immune responses in healthy volunteers [38].

The results showed that EPR spectroscopy could be a powerful tool for assessing OS in endocrine conditions and their distinction. Based on this, the *in vitro* EPR could be successfully applied for the assessment of redox imbalance in oxidative stress-related metabolic diseases. Patients with T2DM and NAFLD are characterized by a completely different redox status compared to healthy people, which can be a basis for introducing antioxidant therapy to the main treatment.

CONCLUSION

The present study proposes a new reading of the application of nitroxide radicals and hydroxyl amines in monitoring of the patients redox status, in the context of T2DM and NAFLD-related OS. The

developed methodological protocol will allow a more detailed study of the dynamic nature of the disease and will contribute to the development of treatments and interventions aimed at limiting the effects of oxidative damage in patients with diabetes and its complications.

Acknowledgement: This research was funded by the scientific projects No.5/2023 and No.4/2022 Medical Faculty, Trakia University, Bulgaria and Ministry of Education and Science BG-RRP-2.004-0006 "Development of research and innovation at Trakia University in service of health and sustainable well-being".

Conflict of interest: The authors declared no potential conflicts of interest with respect to the research, authorship, and/or publication of this article.

REFERENCES

1. S. Pouwels, N. Sakran, Y. Graham, A. Leal, T. Pintar, W. Yang, R. Kassir, R. Singhal, K. Mahawar, D. Ramnarain, *BMC Endocr. Disord.*, **22**, 63 (2022).
2. R. Loomba, S. L. Friedman, G. I. Shulman, *Cell.*, **184**, 2537 (2021).
3. S. Mitra, A. De. Chowdhury, *Transl. Gastroenterol. Hepatol.*, **5**, 16 (2020).
4. S. Alam, G. Mustafa, M. Alam, N. Ahmad, *World J. Gastrointest. Pathophysiol.*, **7**, 211 (2016).
5. H. W. Chao, S. W. Chao, H. Lin, H. C. Ku, C. F. Cheng, *Int. J. Mol. Sci.*, **20**, 298 (2019).
6. H. Fujii, N. Kawada, *Int. J. Mol. Sci.*, **21**, 3863 (2020).
7. S. H. Koo, *Clin. Mol. Hepatol.*, **19**, 210 (2013).
8. Y. Shao, S. Chen, L. Han, J. Liu, *Nutr. & Metab.*, **20**, 30 (2023).
9. O. O. Oguntibeju, *Int. J. Physiol. Pathophysiol. Pharmacol.*, **11**, 45 (2019).
10. M. Martín-Fernández, V. Arroyo, C. Carnicero, R. Sigüenza, R. Busta, N. Mora, B. Antolín, E. Tamayo, P. Aspichueta, I. Carnicero-Frutos, H. Gonzalo-Benito, R. Aller, *Antioxidants*, **11**, 2217 (2022).
11. J. C. Arroyave-Ospina, Z. Wu, Y. Geng, H. Moshage, *Antioxidants*, **10**, 174 (2021).
12. E. Papachristoforou, V. Lambadiari, E. Maratou, K. Makrilakis. *J. Diabetes Res.*, **2020** (2020).
13. P. González, P. Lozano, G. Ros, F. Solano. *Int J Mol Sci.*, **24**, 9352 (2023).
14. A. P. Delli Bovi, F. Marciano, C. Mandato, M.A. Siano, M. Savoia, P. Vajrop, *Front. Med.*, **8**, 595371 (2021).
15. S. Ziolkowska, A. Binienda, M. Jabłkowski, J. Szemraj, P. Czarny, *Int. J. Mol. Sci.*, **22** (20), 11128 (2021).
16. B. P. Soule, F. Hyodo, K. Matsumoto, N. L. Simone, J. A. Cook, M. C. Krishna, J. B. Mitchell, *Free Radic. Biol. Med.*, **42** (11), 1632 (2007).
17. G. I. Likhtenshtein, Nitroxides: Brief History, Fundamentals, and Recent Developments, 2020.
18. S. Bujak-Pietrek, A. Pieniazek, K. Gwozdziński, L. Gwozdziński. *Molecules*, **28** (16), 6174 (2023).
19. G. Bačić, A. Pavićević, F. Peyrot, *Redox Biol.*, **8**, 226 (2016).
20. E. Zottler, G. Gescheidt, *J. Chem Res.*, **35**, 257 (2011).
21. C. Prescott, S. E. Bottle. *Cell Biochem. Biophys.*, **75** (2), 227 (2017).
22. H. Sies, V. V. Belousov, N. S. Chandel, M. J. Davies, D. P. Jones, G. E. Mann, M. P. Murphy, M. Yamamoto, C. Winterbourn, *Nature Reviews Molecular Cell Biology.*, **23** (7), 499 (2022).
23. M. Panayotova, K. Peeva, P. Chakarova, *Pediatrics*, **55** (3), 22 (2018).
24. M. Panayotova, M. Muhtarov, P. Dragomirova, V. Bangyozov, V. Boeva- Bangyozova, *Gen. Med.*, **20** (3), 47 (2018).
25. M. Muhtarov, V. Boeva-Bangyozova, M. Panayotova, D. Popov, *Gen Med*, **21** (1), 64 (2019).
26. C. A. Juan, J. M. Pérez de la Lastra, F. J. Plou, E. Pérez-Lebeña, *Int. J. Mol. Sci.*, **22** (9), 4642 (2021).
27. T. Rahman, I. Hosen, M. Islam, H. Shekhar, *Adv. Biosci. Biotechnol.*, **3**, 997 (2012).
28. I. Liguori, G. Russo, F. Curcio, G. Bulli, L. Aran, D. Della-Morte, G. Gargiulo, G. Testa, F. Cacciatore, D. Bonaduce, P. Abete, *Clin. Interv. Aging.*, **13**, 757 (2018).
29. S. Patergnani, E. Bouhamida, S. Leo, P. Pinton, A. Rimessi, *Biomed.*, **9** (2), 216 (2021).
30. S. C. Shabalala, R. Johnson, A. K. Basson, K. Ziqubu, N. Hlengwa, S. X. H. Mthembu, S. E. Mabhida, S. E. Mazibuko-Mbeje, S. Hanser, I. Cirilli, et al., *Antioxidants*, **11** (10), 2071 (2022).
31. S. I. Dikalov, Y. F. Polienko, I. Kirilyuk, *Antioxid. Redox Signal.*, **28** (15), 1433 (2018).
32. H. Zhang, in: Molecular Imaging and Contrast Agent Database (MICAD), 2010.
33. A. Haj-Yehia, T. Nassar, B. Kadery, C. Lotan, N. Da'as, Y. Kleinman, *Exp. Clin. Cardiol.*, **7** (2-3), 85 (2002).
34. H. Miyazaki, H. Shoji, M. C. Lee, *Redox Rep.*, **7** (5), 260 (2002).
35. M. Assayag, S. Goldstein, A. Samuni, A. Kaufman, N. Berkman, *Free Radic. Biol. Med.*, **177**, 181 (2021).
36. S.I. Dikalov, I. A. Kirilyuk, M. Voinov, I. A. Grigor'ev, *Free Radic. Res.*, **45** (4), 417 (2011).
37. N. Babić, F. Peyrot, *Magnetochem.*, **5** (1), 13 (2019)
38. R. Gorjão, H. K. Takahashi, J. A. Pan, S. Massao Hirabara, *J. Biomed. Biotechnol.*, 841983 (2012).

Evaluation of preliminary physico-chemical parameters and biometric characteristics of the "Stendesto" plum-apricot hybrid with reference to its parental lines

A. T. Popova^{1*}, D. S. Mihaylova², P. B. Doykina¹, S. Y. Pandova³

¹University of Food Technologies, Department of Catering and Nutrition, 26 Maritza Blvd., 4002 Plovdiv, Bulgaria

²University of Food Technologies, Department of Biotechnology, 26 Maritza Blvd., 4002 Plovdiv, Bulgaria

³Fruit Growing Institute, Agricultural Academy, Department of Breeding and Genetic Resources, 12 Ostromila Str., 4000 Plovdiv, Bulgaria

Received: November 3, 2023; Revised: April 11, 2024

Prunus spp. are economically important stone fruits with hybrid potential. The "Stendesto" is the only successful plum-apricot hybrid registered in Bulgaria. Information about its features is rather scarce in the available scientific databases. The "Stendesto" comes from the "Modesto" apricot and the "Stanley" plum. In this study, classical methods were used in order to provide preliminary knowledge about the hybrid, with reference to its parental lines. The color parameters, as well as total soluble solids, pH, ash and moisture contents, water activity, and biometric data (weight, size, thickness, length, and width) were evaluated. The results show that the moisture content is comparable between the three fruits, and the fruit weight had the highest values for the "Modesto" apricot, while the "Stendesto" stood in the middle. Microscopic images of the fruits were also provided for better evaluation. The results show that physically the "Stendesto" is more similar to the "Stanley" plum than to the "Modesto" apricot. This study considered a pilot on the topic of plum-apricot hybrids in Bulgaria and sets ground for further research on their phytochemical composition and related biological activities.

Keywords: *Prunus* spp., physico-chemical parameters, plumcot

INTRODUCTION

Stone fruits, and fruits in general, are important health and nutrition contributors due to their phytochemicals [1]. Phenolic compounds are major bioactive providers in stone fruits [2]. It is well-known that a diet rich in fruit and vegetables may contribute to the prevention of non-communicative diseases (hypertension, diabetes, obesity, several types of cancer, among others) [3]. However, consumers evaluate and make buying decisions based on primary physical characteristics like size, weight, shape, color, aroma. Fruit size is a qualitative feature that strongly influences consumer's preferences [4]. It can be partially controlled by water and nutrient availability, light and temperature [5]. The morphological description is recognized as a first important step in fruit characterization [6]. Additionally, the variability of the color parameters may determine appropriate maturity and fruit attractiveness in terms of the market selection [7]. Furthermore, the total soluble solids (TSS)/titratable acidity (TA) ratio gives important information about the fruit taste, and the possible content of sugars and organic acids. Higher TSS/TA ratios are associated with a higher eating quality [8].

Genus *Prunus* comprises important and well accepted fruits, e.g. peaches, plums, cherries, sour cherries, among others. Hybridization is recognized as a vital process in plant evolution [9]. Plum-apricot hybrids may result in plumcots, pluots, and apriums depending on the resemblance to their parent (plum or apricot, respectively) [10]. Globally, plum-apricot hybrids are not new [11] but to date, only one plum-apricot hybrid is registered in Bulgaria, and this is the "Stendesto".

Consequently, the present work aims at characterizing the "Stendesto" in terms of color parameters, total soluble solids, pH, ash and moisture contents, water activity, and biometric data (weight, size, thickness, length, and width), also making reference to its parental lines. This study is considered a pilot on the topic of plum-apricot hybrids in Bulgaria and sets ground for further research on their phytochemical composition and related biological activities.

MATERIALS AND METHODS

The fruits (apricots, plumcots, and plums) were harvested on three dates, at optimal ripeness, from the fields of the Fruit Growing Institute, Plovdiv, Bulgaria (lat. 42.10384828045957 and long.

* To whom all correspondence should be sent:
E-mail: popova_aneta@uft-plovdiv.bg

24.72164848814686). A total of sixty fruits were transported in pulp trays in an air-conditioned vehicle to the University of Food Technologies, where the fruits were randomly placed in new trays in order to minimize the differences in fruit quality and further analyses were applied. Twenty extra fruits per variety were selected in case there was decay or damage during/after the harvest.

Ash content was determined according to AOAC Official Method 940.26 [12]. The moisture content of the studied samples was measured using an infrared moisture analyzer PMB 53 (Adam Equipment Inc., Oxford, UK). The water activity (a_w) was measured using a LabSwift-aw, Novasina AG, Lachen, Bassersdorf, Switzerland. TSS (%) were evaluated using a digital handheld refractometer (Opti Brix 54, Bellingham + Stanley, Kent, UK). The pH was determined using an Orion 2 Star pH Benchtop (Thermo Scientific, Singapore) with the electrode standardized with pH 4.0 and 7.0 buffers (Sigma-Aldrich, Darmstadt, Germany). A PCE-CSM 2 (PCE-CSM instruments, Meschede, Deutschland) with a measuring aperture of 8 mm was used to analyze the color parameters (L, a, b, c, h) of the skin and flesh.

The fruits and pits were measured on a digital scale (KERN, EMB 600-2). Fruit was weight intact; afterwards the pit was extracted and evaluated. Fruit's and pit's sizes (length, width, thickness) were measured using a digital caliper. The microstructure of the fruit samples was examined with a Celestron LCD Digital II microscope. Micrographs were made by means of an 8MP digital camera, and further analyzed by ImageJ software [13].

MS Excel software was used for data analysis. All assays were performed at least in triplicate. Results are presented as mean \pm SD (standard deviation). The additional statistical analyses of the data were presented using one-way ANOVA and a Tukey–Kramer post hoc test ($\alpha = 0.05$), as described

by Assaad et al. [14].

RESULTS AND DISCUSSION

Information about the moisture and ash contents, TSS values, pH, and a_w is presented in Table 1.

The moisture content varied from 65.53 ± 6.18 to 74.55 ± 4.49 %. The lowest values belonged to the "Stanley" plum. Other authors reported 10% higher moisture content for apricot cultivars and comparable ash content [15]. Higher moisture content is also documented in papers about plums [16].

The TSS values of apricots range from 10 to 20 °Brix as established in another research [17]. The current result of 14.55 °Brix ("Modesto") is comparable to the ones established in ripe apricots [18]. European plum are characterized in literature with 8.2 to 18.4 °Brix values [19]. The "Stanley" plum shows much higher TSS. The plum-apricot hybrid had a TSS of 19.3 °Brix which was more similar to the plum than to the apricot. This is consistent with the morphological similarities of plumcot to plums compared to apricots [20]. A TSS report of plumcots [21] showed lower values which were more similar to the currently reported "Modesto" results.

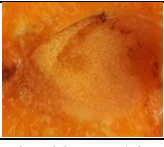
As fruit acidity is important to quality, it is related to two parameters, namely titratable acidity and pH value. Fruit acidity is mainly due to the organic acids and mineral cations in the vacuole [22]. Considering the pH values, the studied hybrid had the lowest values, while the apricot had the highest. The "Modesto" values are consistent with other reported in literature ranging from 3.90 to 4.70 [23]. Nicolas-Almansa et al. [11] reported lower pH values (3.08 to 3.75) for several plum-apricot hybrids. Information about the water activity of fresh fruit is scarce. Research teams report a_w of 0.966 ± 0.002 for plums [24] and showed an initial which is higher than the currently established results for "Stanley" plums.

Table 1. Physico-chemical characteristics of investigated fruit samples (n=3)

Fruit sample/ characteristic	"Modesto" apricot	"Stendesto" hybrid	"Stanley" plum
Moisture - fruit, %	72.95 ± 0.11^a	74.55 ± 4.49^a	65.53 ± 6.18^a
Moisture – stone, %	5.18 ± 1.51^{ab}	5.91 ± 1.69^a	2.24 ± 0.94^b
Ash - fruit, %	0.80 ± 0.15^a	0.66 ± 0.15^a	0.58 ± 0.24^a
Ash – stone, %	2.90 ± 0.57^a	1.27 ± 0.64^b	1.59 ± 0.60^{ab}
pH - fruit	4.50 ± 0.01^a	2.55 ± 0.01^c	3.80 ± 0.00^b
TSS - fruit	14.55 ± 0.21^b	19.3 ± 1.99^a	20.55 ± 0.63^a
a_w - fruit	0.875 ± 0.007^b	0.895 ± 0.007^a	0.905 ± 0.007^a
a_w - stone	0.85 ± 0.01^a	0.87 ± 0.01^a	0.785 ± 0.02^b

Different letters in the same row indicate statistically significant differences ($p < 0.05$), according to ANOVA (one-way) and the Tukey test.

Table2. CIE lab color parameters of the studied samples, (n=5)

Fruit sample/ parameter	"Modesto" apricot	"Stendesto" hybrid	"Stanley" plum
	<i>fruit skin</i>		
			
L	54.35 ± 4.38 ^a	44.86 ± 5.27 ^b	23.84 ± 3.59 ^c
a	24.14 ± 1.97 ^a	- 0.56 ± 2.34 ^b	1.25 ± 0.96 ^b
b	39.15 ± 5.97 ^a	- 7.58 ± 2.03 ^b	- 1.94 ± 0.91 ^b
c	46.26 ± 4.15 ^a	7.94 ± 1.76 ^b	2.50 ± 0.80 ^c
h	57.92 ± 6.30 ^c	269.01 ± 21.34 ^b	304.44 ± 21.54 ^a
	<i>fruit flesh</i>		
			
L	45.40 ± 5.19 ^a	31.61 ± 3.78 ^a	39.71 ± 17.56 ^a
a	11.34 ± 2.23 ^a	6.61 ± 6.55 ^a	-2.35 ± 4.53 ^b
b	41.67 ± 4.01 ^a	30.42 ± 4.01 ^b	27.46 ± 2.11 ^b
c	43.21 ± 4.33 ^a	30.79 ± 4.15 ^b	27.86 ± 1.99 ^b
h	74.83 ± 1.98 ^b	77.33 ± 11.85 ^b	94.92 ± 9.52 ^a

Different letters in the same row indicate statistically significant differences ($p < 0.05$), according to ANOVA (one-way) and the Tukey test.

Canakapalli *et al.* [25] have documented a water activity of 0.68 for pluots. These results are substantially lower than those currently reported about the "Stendesto" hybrid.

The plum-apricot hybrid has a water activity more similar to the plum than to the apricot. Lower water activity is usually associated with limited microbial growth. The results considering the fruit stones from the three studied samples are regarded as new data since information in the vastly available literature is not found.

Color is an important attribute especially when food is being evaluated. Table 2 holds information about the L*, a, b, c, and h parameters of the studied fruit skins and flesh. ΔE between the hybrid and its parents was calculated in order to demonstrate the differences in color perception. The calculated hybrid-plum (21.84) and hybrid-apricot (53.70) ΔE revealed that the "Stendesto" is more similar to the "Stanley" plum. However, color is not perceived as similar or is difficult to differentiate.

Visually the plum-apricot hybrid is more resembling to the plum (Figure 1). This is supported by the established "a" values of the fruit skin corresponding to a blue coloration. The lightness of the samples' skin varied between 23.84 ± 3.59 and 54.35 ± 4.38 . The apricot's skin was the lightest. The same trend was observed for the fruit flesh. The color parameters of the "Modesto" apricot are

comparable to other available in published papers [26, 27]. Vivid colors are desired for fruit. Plum peels can vary in color [28]. However, similarities to other results in established color attributes are present [29]. The great difference in the chroma of the fruit skin is due to the initial color of the fruit. High chroma values are associated with the change from green to yellow which is relevant to the "Modesto".

The microscopic images of the three studied fruits shed more light about their similarities. The plant cell is comprised of polysaccharides (cellulose, hemicellulose, pectin, among others) and proteins [31]. The dimensions (diagonal diameter) of the cells varied from $110.6 \pm 35.61 \mu\text{m}$ ("Stendesto") to $121.62 \pm 6.08 \mu\text{m}$ ("Stanley"). No statistically significant difference between the studied samples was established. Other authors have reported no correlation between cell size and attributes like firmness between fruit cultivars [32] although research papers had pointed out that cell size may be responsible for some textural differences (juiciness) [33].

The biometric data of the studied fruits are given in Table 3. Information about the weight of the fruit and stone, the dimensions of the fruit (length, width, thickness) and stone is used to better evaluate the differences and similarities between the hybrid and its parental lines.



Figure 1. Microscopic images of studied samples

Table 3. Biometric data of studied samples, (n=25)

Fruit sample/ parameter	"Modesto" apricot	"Stendesto" hybrid	"Stanley" plum
Fruit			
Weight, g	72.84 ± 6.55 ^a	47.84 ± 6.40 ^b	36.02 ± 3.54 ^c
Length, mm	53.18 ± 1.10 ^b	58.79 ± 2.65 ^a	48.09 ± 2.36 ^c
Width, mm	56.79 ± 2.83 ^a	41.01 ± 1.73 ^b	34.17 ± 1.59 ^c
Thickness, mm	48.75 ± 8.51 ^a	42.79 ± 2.15 ^b	36.01 ± 1.81 ^c
Stone			
Weight, g	3.28 ± 0.59 ^a	2.94 ± 0.56 ^b	2.22 ± 0.20 ^c
Length, mm	29.85 ± 1.53 ^b	33.34 ± 3.55 ^a	26.03 ± 1.83 ^c
Width, mm	23.58 ± 1.12 ^a	9.17 ± 0.88 ^c	14.61 ± 0.89 ^b
Thickness, mm	13.97 ± 1.07 ^b	15.51 ± 0.76 ^a	8.42 ± 0.64 ^c

Different letters in the same row indicate statistically significant differences ($p < 0.05$), according to ANOVA (one-way) and the Tukey test.

The heaviest of the three fruit is the apricot with an average of 72.84 ± 6.55 g. These measurements are in accordance with other published data about apricots from different cultivars [34]. The established biometry of the "Stanley" plum is comparable to the data published by Dimkova *et al.* [35] about nine cultivars, including "Stanley", which was used as a standard. The hybrid fruit had values for length, width, and thickness that are greater than those of the plum, and smaller than the same of the apricot. The same trend did not apply for the stones. The hybrid stone was visually more similar to the plum stone. The stone weight was comparable to the data published about apricot hybrids [36]. Some authors highlighted that very often plum-apricot hybrids were falsely regarded as plums due to the visual similarity [11].

CONCLUSION

The present study is considered a pilot on the topic of plum-apricot hybrids in Bulgaria. To date, the "Stendesto" is the only successful plum-apricot hybrid registered in Bulgaria. The color parameters, as well as total soluble solids, pH, ash and moisture contents, water activity, and biometric data (weight, size, thickness, length, and width) were evaluated. The studied plum-apricot hybrid showed more similarities to the plum than to the apricot, especially in terms of color. The hybrid fruit had values for length, width, and thickness greater than those of the plum, and smaller than the same of the apricot. Visually there was a greater resemblance to the plum. The current results set ground for further research on the phytochemical composition and related biological activities of plum-apricot hybrids.

Acknowledgement: We acknowledge the financial support by the Bulgarian National Science Fund, project KII06-H67/2.

REFERENCES

1. M. Lara, C. Bonghi, F. Famiani, G. Vizzotto, R. Walker, M. Drincovich, *Front. Plant Sci.*, **11**: 562252 (2020).
2. Y. Hong, Z. Wang, C. Barrow, F. Dunshea, H. Suleria, *Antioxidants*, **10**, 234 (2021).
3. D. Aune, E. Giovannucci, P. Boffetta, L. Fadnes, N. Keum, T. Norat, D. Greenwood, E. Riboli, L. Vatten, S. Tonstad, *Int. J. Epidemiol.*, **46**: 1029 (2017).
4. C. Crisosto, G. Costa, D.R. Layne, D. Bassi (eds.), CAB International, Cambridge, 2008, p. 536.
5. M. Cerri, A. Rosati, F. Famiani, L. Reale, *Scientia Horticulturae*, **255**, 1 (2019).
6. M. Baji, H. Hanine, S. En-Nahli, R. Company O. Kodad, *Int. J. Fruit Sci.*, **21**(1), 52 (2021).
7. A. Cirillo, L. De Luca, L. Izzo, M. Cepparulo, G. Graziani, A. Ritieni, R. Romano, C. Di Vaio, *Horticulturae*, **9**(5), 546 (2023).
8. A. Hegedüs, R. Engel, L. Abrankó, E. Balogh, A. Blázovics, R. Hermán, J. Halász, S. Ercisli, A. Pedryc, E. Stefanovits-Bányai, *J. Food Sci.*, **75**: 722-730 (2010).
9. B. Kerbs, J. Ressler, J. Kelly, M. Mort, A. Santos-Guerra, M. Gibson, J. Caujapé-Castells, D. Crawford, *AoB Plants*, **9**, 043 (2017).
10. A. Popova, D. Mihaylova, S. Pandova, P. Doykina, *Horticulturae*, **9**: 584 (2023).
11. M. Nicolás-Almansa, D. Ruiz, J. Salazar, A. Guevara, J. Cos, P. Martínez-Gómez M. Rubio, *Scientia Horticulturae*, **318**, 112131 (2023).
12. AOAC Official Method 940.26, Washington, DC, USA: AOAC International, 2003.
13. C. Schneider, W. Rasband, K. Eliceiri, *Nature Methods*, **9**(7), 671 (2012).
14. A. Hussein, A. El-Anssary, *Plants Secondary Metabolites*, Intech Open Limited; London, UK, 2019.
15. F. Khan, T. Khan, M. Arif, M. Tajudin, *Adv Food Technol. Nutr. Sci. Open J.*, **2**(1), 3 (2016).
16. H. Polatci, *Pak. J. Bot.*, **53**(2), 579 (2021).
17. B. Velardo-Micharet, F. Agudo-Corbacho, M. Ayuso-Yuste, M. Bernalte-García, *Agriculture*, **11**(7): 639 (2021).
18. J. Ayour, M. Sagar, H. Harrak, A. Alahyane, M. Alfeddy, M. Taourirte, M. Benichou, *Sci. Hortic.*, **215**, 72 (2017).
19. P. Roussos, N. Efstathios, B. Intidhar, N. Denaxa, A. Tsafouros, *Nutritional Composition of Fruit Cultivars (19-48)*, M. Simmonds, V. Preedy (eds.), Academic Press, 2016, p. 639.
20. M. Szymajda, M. Studnicki, A. Kuras, E. Zurawicz, *S. Afr. J. Bot.*, **146**: 624 (2022).
21. S-K. Jung, H-S. Choi, *Sustainability*, **13**(19), 10737 (2021).
22. A. Etienne, M. Génard, D. Bancel, S. Benoit, C. Bugaud, *Sci. Hortic. (Amsterdam)*, **162**, 125 (2013).
23. E. Mratinić, B. Popovski, T. Milošević, M. Popovska, *Czech J. Food Sci.*, **29**(2), 161–170 (2011).
24. M. Rodríguez, A. Rodríguez, R. Mascheroni, *J. Food Processing and Preservation*, **39**, 2647 (2015).
25. S. Canakapalli, L. Sheng, L. Wang, *LWT*, **154**, 112632 (2022).
26. C. Petrisor, *J. Horticulture*, **18**(4), 70 (2014).
27. J. Salazar, P. Martínez-Gómez, D. Ruiz, *Eur. J. Hortic. Sci.* **87**(1), 1 (2022).
28. E. Rampácková, M. Göttingerová, T. Kiss, I. Ondrášek, R. Venuta, J. Wolf, T. Necas, S. Ercisli, *Eur. J. Hortic. Sci.*, **86**, 453 (2021).
29. P. Drogoudi, G. Pantelidis, *Plants*, **11**, 1338 (2022).
30. A. Hegedüs, P. Pfeiffer, N. Papp, L. Abrankó, A. Blázovics, A. Pedryc, É. Stefanovits-Bányai, *Biol Res*, **44**, 339 (2011).
31. S. Uluisik, G. Seymour, *Food Chem.*, **309**, 125559 (2020).
32. P. McAtee, I. Hallett, J. Johnston, R. Schaffer, *Plant Methods* **5**(5), (2009).
33. H. Mann, D. Bedford, J. Luby, Z. Vickers, C. Tong, *Hort. Science*, **40**(6), 1815 (2005).
34. L. Septar, C. Moale, L. Tilinca, I. Stoli, *Current Trends in Natural Sciences*, **10**(19), 387 (2021).
35. S. Dimkova, D. Ivanova, S. Todorova, N. Marinova, *Bulgarian Journal of Agricultural Science*, **23**(6), 947 (2017).
36. M. Tufaru, D. Hoza, L. Chira, A. Peticilă, *Scientific Papers. Series B, Horticulture*, **LXV**(1), 270 (2021).

Chlorella and *Spirulina* dietary supplements as sources of biologically active lipids

V. Panayotova*, A. Merdzhanova, D. A. Dobрева, K. Peycheva, T. Stoycheva

Department of Chemistry, Faculty of Pharmacy, Medical University - Varna, 84 Tzar Osvoboditel Blvd., 9000 Varna, Bulgaria

Received: November 3, 2023; Revised: April 11, 2024

Increasing the knowledge about the relationship between the lipid quality of foods and health benefits suggests the need to utilize sustainable alternative food resources that impact human health beyond basic nutrition. Aquatic organisms, such as microalgae, are promising sources of bioactive compounds. Freshwater microalgae, namely *Spirulina spp* and *Chlorella spp*, contain a variety of functional compounds, such as polyunsaturated fatty acids (PUFAs), carotenoids and vitamins with antioxidant, antihypertensive and cardiovascular protective effects. In recent years, these species have been largely promoted as dietary supplements in Bulgaria.

The aim of the present study was to analyse total lipids, lipid classes, fatty acids, carotenoids, total cholesterol and fat-soluble vitamins (α -tocopherol and ergocalciferol) contents in dietary supplements (*Spirulina platensis* and *Chlorella vulgaris* powders) available on the Bulgarian market. Lipids were extracted according to Bligh and Dyer method and separated into neutral lipids, glycolipids and phospholipids by column chromatography. Cholesterol, carotenoids and fat-soluble vitamins were simultaneously analysed by HPLC/UV/FL. Total lipids accounted 3.8 g/100 g dry *Spirulina* powder and 5.1 g/100 g dry *Chlorella* powder. Glycolipids were the main lipid class in *Spirulina* (over 69% of TL), while neutral lipids predominated in *Chlorella* (over 58% of TL). In both species polyunsaturated fatty acid presented 50% of total lipids, whereas cholesterol showed a significantly low content – up to 7.3 mg/100 g dw. The results showed that *Spirulina* and *Chlorella* powders available in Bulgaria contain high amounts of unsaturated fatty acids and astaxanthin (67.93 – 127.56 μ g/100 g dw) and low cholesterol levels which could confirm the high nutritional values of both species.

Keywords: microalgae, fatty acids, fat-soluble vitamins, carotenoids

INTRODUCTION

Microalgae are photosynthetic eukaryotic organisms rich in functional nutrients [1-3] used to provide nourishment to humans and animals since ancient times. In the early 1940s microalgae emerged as attractive and promising alternative lipid, protein, pigment, and polymer sources [4]. *Spirulina*, or correctly *Arthrospira spp.*, and *Chlorella* are the two most important algal groups that deserve a thorough exploration for nutritional value. *Spirulina* and *Chlorella* are a renewable and sustainable source of high-value bioactive compounds. They are well-known as high-protein sources (55–60% of dry weight) with all essential amino acids and a high digestibility coefficient [2, 3, 5]. They are also a rich source of lipids (e.g., n-3 polyunsaturated fatty acids (PUFA), vitamins (B group, ascorbic acid, A, D, E, K), functional components (e.g., chlorophylls, which have antioxidant activity), as well as minerals (Ca, Cr, Cu, Fe, K, Na, P, Se, Zn) [6]. Lipid nutritional value of *Spirulina* and *Chlorella* is comparable to that of fish oil, which makes them alternative sources of n-3 fatty acids [7]. The interest in n-3 PUFA as health-promoting nutrients has expanded dramatically in recent years. During the process of photosynthesis,

some microalgae can accumulate large amounts of lipids in their cells [8]. Considering their beneficial chemical composition, microalgae are increasingly utilized as food additives, functional foods and dietary supplements.

The aim of the present study was to analyse total lipids, lipid classes, fatty acids, carotenoids, total cholesterol and fat-soluble vitamins (α -tocopherol and ergocalciferol) contents in dietary supplements (*Spirulina platensis* and *Chlorella vulgaris* powders) available on the Bulgarian market.

MATERIALS AND METHODS

Spirulina platensis and *Chlorella vulgaris* dietary supplements were purchased from health-food stores in Varna, Bulgaria. The samples were stored in plastic bags and kept refrigerated (4 °C) until analysis.

Lipid classes separation and fatty acids analysis

Total lipids were extracted according to Bligh and Dyer method [9] and were separated into neutral lipids, glycolipids and phospholipids by column chromatography using a glass column (10 × 200 mm) packed with silica gel 60 [10]. Individual lipid fractions were transmethylated using 2% H₂SO₄ in anhydrous methanol [11]. Analysis of fatty acids

* To whom all correspondence should be sent:

E-mail: veselina.ivanova@hotmail.com

methyl esters (FAME) was carried out using a Thermo Scientific FOCUS GC gas chromatograph equipped with a 30 m × 0.25 mm × 0.25 μm TR-5 MS capillary column and Polaris Q mass detector. Helium was used as a carrier gas at a flow rate of 1 ml/min and a temperature program – initial oven temperature of 40°C for 4 min, followed by a rate of 20°C/min from 40°C to 150°C, raised from 150°C to 235°C at a rate of 5°C/min, and next from 235°C to 280°C a rate of 10°C/min for 5 min. Corresponding peaks were identified based on the comparison of the retention times with the authentic standards (Supelco 37 Component FAME Mix and PUFA №3 from Menhaden oil). The results are expressed as the weight percent of an individual fatty acid to the total fatty acid (TFA) content.

Carotenoids, fat-soluble vitamins and total cholesterol analysis

Fat-soluble vitamins (A, D₃, E), astaxanthin, β-carotene and cholesterol were extracted and analysed by the method of Dobrova *et al.* [12].

RESULTS AND DISCUSSION

The results for the fatty acid profiles of total lipids (TL), neutral lipids (NL), glycolipids (GL) and phospholipids (PL) in *Spirulina* and *Chlorella* supplements are presented in Tables 1 and 2, respectively. Total lipid contents were 3.8 g/100 g in *Spirulina* powder and 5.1 g/100 g in *Chlorella* powder which is lower than data reported in the scientific literature [13, 14]. The distribution of the fatty acid groups differs between microalgae species and among the lipid subclasses. In *Spirulina* the most abundant fatty acid group was the PUFA group in TL and GL, and SFA in NL and PL. In *Chlorella* supplements PUFA was the most abundant group in TL and the lipid classes, except PL. The analysis of FAME showed that the major fatty acid in *Spirulina* was palmitic acid (C16:0) followed by γ-linolenic (GLA, C18:3 n-6), comprising together about 75% of the FAME in the TL fraction. The third main fatty acids in *Spirulina* lipids were palmitoleic (C16:1) and linoleic acid (LA, C18:2 n-6). Fatty acid profile of *Spirulina* is consistent with the literature data [3, 13].

Table 1. Fatty acids (as relative %) composition of TL, NL and PL in *Spirulina*

FA, % of TFA	TL	NL	GL	PL
C 8:0	tr	nd	tr	nd
C 10:0	tr	tr	tr	tr
C 12:0	tr	0.27±0.02	0.22±0.02	nd
C 14:0	1.39±0.15	0.48±0.03	1.06±0.05	1.73±0.20
C 16:0	35.47±1.67	27.54±0.85	31.17±2.04	42.57±2.50
C 17:0	tr	0.45±0.03	tr	0.20±0.01
C 18:0	2.69±0.05	11.65±0.64	2.81±0.30	12.14±0.55
C 20:0	tr	0.11±0.01	tr	0.23±0.01
C 21:0	nd	0.10±0.02	nd	nd
C 22:0	tr	3.43±0.10	0.31±0.02	5.42±0.65
ΣSFA	39.55	44.03	35.57	62.29
C 14:1	tr	0.41±0.03	nd	0.35±0.03
C 16:1	8.50±0.73	4.25±0.40	9.48±0.69	5.95±0.60
C 17:1	nd	0.45±0.02	0.26±0.02	0.29±0.01
C 18:1 n-9	3.50±0.20	12.67±0.75	4.21±0.34	3.21±0.50
C 24:1	tr	nd	nd	nd
ΣMUFA	12.00	17.78	13.95	9.80
γ-C 18:3 n-6	39.49±2.30	20.80±1.55	37.53±2.40	16.39±0.80
C 18:2 n-6	5.80±0.55	8.10±0.68	7.55±0.80	4.66±0.23
α-C 18:3 n-3	0.50±0.02	0.82±0.03	0.10±0.01	tr
C 20:4 n-6	0.65±0.03	nd	0.20±0.01	nd
C 20:3 n-6	0.92±0.01	3.92±0.30	1.56±0.40	nd
C 20:2	tr	nd	0.18±0.02	nd
C 20:3 n-3	0.10±0.01	nd	0.20±0.01	nd
C 22:2	0.27±0.02	4.48±0.29	2.98±0.34	6.74±0.45
ΣPUFA	47.73	38.12	50.30	27.79
Σn-3	0.60	0.82	0.30	0.09
Σn-6	46.86	32.82	46.64	21.05
PUFA/SFA	1.20	0.86	1.41	0.45

Results represent mean values ± standard deviation (n = 3); SFA: saturated fatty acids; MUFA: monounsaturated fatty acids; PUFA: polyunsaturated fatty acids; TFA – total fatty acids; TL – total lipids; NL – neutral lipids; GL – glycolipids; PL – phospholipids; nd—not detected; tr—trace levels were <0.1% of TFA.

Table 2. Fatty acids (as relative %) composition of TL, NL and PL in *Chlorella*

FA, % of TFA	TL	NL	GL	PL
C 8:0	tr	tr	tr	0.25±0.02
C 10:0	tr	0.26±0.02	tr	0.28±0.03
C 12:0	tr	tr	0.11±0.02	0.33±0.01
C 14:0	0.25±0.02	0.25±0.03	0.51±0.04	0.75±0.05
C 16:0	28.09±0.54	27.78±1.38	37.28±2.42	32.91±2.10
C 17:0	tr	0.10±0.02	0.15±0.02	0.94±0.32
C 18:0	5.12±0.07	3.13±0.30	1.86±0.04	6.87±0.56
C 20:0	tr	tr	tr	0.43±0.02
C 21:0	nd	nd	0.02±0.01	nd
C 22:0	0.48±0.03	0.38±0.04	0.16±0.01	2.32±0.30
C 24:0	tr	nd	0.26±0.02	0.70±0.04
∑SFA	33.94	31.90	40.35	45.78
C 14:1	tr	0.10±0.02	0.19±0.03	1.31±0.20
C 16:1	5.26±0.21	2.85±0.35	7.72±0.34	3.74±0.40
C 17:1	nd	0.10±0.02	tr	tr
C 18:1 n-9	16.21±0.67	20.29±1.39	10.31±0.45	11.81±0.60
C 20:1	nd	nd	tr	nd
C 24:1	0.13±0.02	nd	0.13±0.01	nd
∑MUFA	21.60	23.34	18.35	16.86
C 18:3 n-6	1.21±0.03	1.74±0.20	2.59±0.15	nd
C 18:2 n-6	9.90±0.43	5.65±0.37	3.47±0.13	2.85±0.40
C 18:3 n-3	30.48±2.54	32.26±2.10	18.71±1.20	23.57±0.95
C 20:5 n-3	nd	nd	2.52±0.06	nd
C 20:4 n-6	0.55±0.02	0.50±0.03	6.68±0.37	3.66±0.30
C 20:3 n-6	0.62±0.03	3.50±0.15	4.18±0.55	7.28±0.64
C 20:3 n-3	tr	nd	0.38±0.03	nd
C 22:2	0.40±0.02	0.94±0.05	2.58±0.15	nd
∑PUFA	43.16	44.59	41.11	37.36
∑n-3	37.56	32.26	21.61	23.57
∑n-6	12.68	11.39	19.50	13.79
PUFA/SFA	1.55	1.53	1.01	0.75

Results represent mean values ± standard deviation (n = 3); SFA: saturated fatty acids; MUFA: monounsaturated fatty acids; PUFA: polyunsaturated fatty acids; TFA – total fatty acids; TL – total lipids; NL – neutral lipids; GL – glycolipids; PL – phospholipids; nd—not detected; tr—trace levels <0.1% of TFA.

Table 3. Fat-soluble vitamins, carotenoids and cholesterol contents in *Spirulina* and *Chlorella* dietary supplements

	<i>Spirulina</i>	<i>Chlorella</i>
Astaxanthin, µg/100 g dw	127.56 ± 11.16	67.93 ± 7.16
β-Carotene, mg/100 g dw	18.80 ± 2.4	5.73 ± 0.44
Ergocalciferol, mg/100 g dw	0.30 ± 0.07	0.31 ± 0.02
α-Tocopherol, mg/100 g dw	1.03 ± 0.09	1.30 ± 0.07
Cholesterol, mg/100 g dw	7.31 ± 0.81	3.64 ± 0.74

Results represent mean values ± standard deviation (n = 3)

Previous studies have reported predominance of PUFAs (in particular C18:3 n-3) over SFA (in particular C16:0) grown under autotrophic conditions [14,15]. A striking feature of the *Spirulina* lipids was the relatively high level of γ-linolenic acid, while of the *Chlorella* lipids – α-linolenic acid. Other authors reported the presence of the long chain PUFAs arachidonic acid (ARA, C20:4 n-6), eicosapentaenoic acid (EPA, C20:5 n-3) and docosahexaenoic acid (DHA, C22:6 n-3) in *Spirulina* and *Chlorella* tissues [16,17], but EPA and DHA were not detected in our study.

Fatty acids patterns of NL and PL lipids of *Spirulina* did not differ significantly from each other with palmitic acid (27.54 – 42.57%) being the most abundant fatty acid. The GL fraction showed fatty acid profile similar to the TL. In *Chlorella*, NL fraction showed similar fatty acid profile as the TL, while GL – similar to PL, wherein palmitic acid was the main fatty acid.

The PUFA/SFA ratio was considerably higher in *Chlorella* supplements, in particular in the NL fraction. *Spirulina* had the highest PUFA/SFA ratio

in the GL fraction than in the corresponding neutral fraction.

Fatty acid profiles of *Spirulina* and *Chlorella* supplements evince the lipids as alternative sources of the nutritionally essential fatty acids – γ -linolenic acid and α -linolenic acid. Besides being an energy source and a metabolic precursor, γ -linoleic acid also exhibits anti-inflammatory, antioxidant, and anti-allergic properties [18, 19].

The results for the fat-soluble vitamins, cholesterol and carotenoids contents in *Spirulina* and *Chlorella* supplements are presented in Table 3. Astaxanthin is a xanthophyll carotenoid naturally synthesized by algae. Its antioxidant activity is 10 times higher than β -carotene and 100 times higher than α -tocopherol. Higher amounts of astaxanthin were detected in *Spirulina* supplements (127.56 $\mu\text{g}/100\text{ g dw}$). β -carotene is the primary plant-based source of dietary vitamin A. However, β -carotene is only partially able to ensure an optimal total vitamin A intake. In our study, 3 times higher amounts of β -carotene were found in *Spirulina* (18.80 $\text{mg}/100\text{ g dw}$) supplements compared to *Chlorella* supplements (5.73 $\text{mg}/100\text{ g dw}$). According to previous studies, *Spirulina* exhibited high vitamin A equivalency ratios for β -carotene to vitamin A conversion – from 2.3:1 to 7:1 [20, 21]. α -tocopherol, the most bioactive form of vitamin E, was detected in higher amounts in *Chlorella* supplements – 1.3 $\text{mg}/100\text{ g dw}$. The main role of vitamin E is as an antioxidant, scavenging free radicals that can damage living cells. Total cholesterol content was higher in *Spirulina* supplements – 3.64 and 7.31 $\text{mg}/100\text{ g dw}$, respectively. Although recent evidences suggest that dietary cholesterol does not significantly increase low-density lipoprotein cholesterol [22], consumers are advised to follow healthy dietary patterns, which are inherently low in cholesterol [23].

CONCLUSIONS

The results showed that *Spirulina* and *Chlorella* dietary supplements available in Bulgaria contain high amounts of unsaturated fatty acids, astaxanthin, β -carotene and low cholesterol levels which could confirm the high nutritional value of both microalgae species. From this study, it is safe to conclude that *Spirulina* and *Chlorella* can be good sources of these nutritionally essential components and used as food additives, functional foods and dietary supplements.

REFERENCES

1. N. Yan, C. Fan, Y. Chen, Z. Hu, *Int. J. Mol. Sci.*, **17**, 962 (2016).

2. I. Barkia, N. Saari, S. R. Manning, *Mar. Drugs*, **17**, 304 (2019).

3. G. Gentsheva, K. Nikolova, V. Panayotova, K. Peycheva, L. Makedonski, P. Slavov, P. Radusheva, P. Petrova, I. Yotkovska, *Life*, **13**(3), 845 (2023).

4. Food and Agriculture Organization of the United Nations: Rome, Italy, 2009; p. 35.

5. G. Parisi, F. Tulli, R. Fortina, R. Marino, P. Bani, A.D. Zotte, A. De Angelis, G. Piccolo, L. Pinotti, A. Schiavone, G. Terova, A. Prandini, L. Gasco, A. Roncarati, P. P. Danieli, *Ital. J. Anim. Sci.*, **19**(1), 1204 (2020).

6. B. da Silva Vaz, J. B. Moreira, M. G. de Moraes, J. A. V. Costa, *Curr. Opin. Food Sci.*, **7**, 73 (2016).

7. J. Sharma, P. Sarmah, N.R. Bishnoi, in: Market Perspective of EPA and DHA Production from Microalgae, N. J. Hoboken (ed.), John Wiley & Sons, Ltd., USA, 2020, p. 281.

8. H. Alishah Aratboni, N. Rafiei, R. Garcia-Granados, A. Alemzadeh, J.R. Morones-Ramírez, J.R., *Microb. Cell Fact.*, **18**, 178 (2019).

9. E. Bligh, W.J. Dyer, *Canad. J. Biochem and Phys.*, **37**, 913 (1959).

10. A. Merdzhanova, V. Panayotova, D. A. Dobрева, K. Peycheva, *Agricultural Science & Technology*, **10**(4), (2018).

11. BDS EN ISO 12966-2:2017. Animal and vegetable fats and oils - Gas chromatography of fatty acid methyl esters - Part 2: Preparation of methyl esters of fatty acids.

12. D. A. Dobрева, V. Panayotova, R. Stancheva, M. Stancheva, *Bulg. Chem. Commun.*, **49**(G), 112 (2017).

13. M. F. Ramadan, M. M. S. Asker, Z. K. Ibrahim, *Czech J. Food Sci.*, **26**(3), 211 (2008).

14. D. Couto, T. Melo, T. A. Conde, M. Costa, J. Silva, M.R.M. Domingues, P. Domingues, *Algal Res.*, **53**, 102128 (2021).

15. O. Perez-Garcia, F. M. E. Escalante, L.E. de-Bashan, Y. Bashan, *Water Res.*, **45**(1), 11 (2011).

16. S. Ötleş, R. Pire, *J. AOAC Int.*, **84**(6), 1708 (2001).

17. M.I. Jay, M. Kawaroe, H. Effendi, *Ser. Earth Environ. Sci.*, **141**, 012015 (2018).

18. R. K. Saini, Y.-S. Keum, *Life Sci.*, **203**, 255 (2018).

19. U. N. Das, *Curr Pharmaceut Biotechnol*, **7**(6), 457 (2006).

20. M. J. Haskell, *Am. J. Clin. Nutr.*, **96**(5), 1193S (2012).

21. J. Wang, Y. Wang, Z. Wang, L. Li, J. Qin, W. Lai, Y. Fu, P. M. Suter, R. M. Russell, M. A. Grusak, G. Tang, S. Yin, *Am. J. Clin. Nutr.*, **87**(6), 1730 (2008).

22. A. Zampelas, E. Magriplis, *Nutrients*, **11**, 1645 (2019).

23. J. A. S. Carson, A. H. Lichtenstein, C. A. M. Anderson, L. J. Appel, P. M. Kris-Etherton, K. A. Meyer, K. Petersen, T. Polonsky, L. Van Horn, *Circ.*, **141**, e39 (2020).

Pectic polysaccharides extracted from unprocessed and steam-distilled lavender biomass

G. I. Marovska*, A. M. Slavov

University of Food Technologies, Department of Organic Chemistry and Inorganic Chemistry, 26 Maritsa Blvd., 4000 Plovdiv, Bulgaria

Received: November 3, 2023; Revised: April 11, 2024

The present research is focused on the extraction of polysaccharides from lavender biomass. One sample of unprocessed lavender: L_UNTR_22_Z (GALEN-N, Zelenikovo, Bulgaria; 2022) and two by-products of lavender industrially processed by steam distillation: L_SD_22_M (ECOMAAT distillery, Mirkovo, Bulgaria; 2022 crop) and L_SD_22_Z (GALEN-N distillery, Zelenikovo, Bulgaria; 2022 crop) were investigated. The biomass was pretreated with 70% ethanol aiming at removal of low-molecular substances and secondary metabolites (pigments, sugars, polyphenols, etc.) which could interfere with further extraction process of polysaccharides. The obtained alcohol-insoluble parts were subjected to acid extraction and acid-soluble pectic polysaccharides were obtained. The highest yield was achieved for sample L_SD_22_M (7.54±0.11%). Furthermore, different pectic polysaccharides building the cell walls of lavender biomass, were extracted from the alcohol-insoluble parts by successive fractional extraction with hot water, 0.05 (NH₄)₂C₂O₄, 0.1 M HCl and cold 0.05 M NaOH. The oxalate extractable pectic polysaccharide predominated in all investigated samples suggesting that most of the pectins were ionically bound by Ca²⁺ bridges in the lavender cell walls. The highest total yield of pectic polysaccharides was obtained for L_SD_22_M (14.98±0.16%). The present research suggests that lavender biomass could be successfully valorized and pectic polysaccharides with total yield ranging from 10.55±0.12% to 14.98±0.16% could be obtained.

Keywords: *Lavandula angustifolia*, by-products, valorization, pectic polysaccharides, fractional extraction

INTRODUCTION

Lavender originates from the mountainous Mediterranean regions of Europe and North Africa. Today it is grown in many European, South American, North African, Southwest Asian countries, and Australia. Despite the fact that 32 species and numerous subspecies and varieties are known, only three of them: the ordinary lavender (*Lavandula angustifolia*), lavender aspic (*Lavandula spica* L.) and lavandin (*Lavandula hybrida* Rev.) play a major role in essential oil production [1, 2]. The essential oil obtained from *L. angustifolia* is distinguished from the others by its high quality and therefore, common lavender is the main type grown in Bulgaria [3]. What is more, during the last few years the lavender became among the most exploited species. Lavender is a plant that is used as an anti-erosion plantation, its inflorescences, as well as the essential oil are included in the composition of many preparations with application in medicine [4]. The concentration of essential oil in the fresh plant is low and large amounts of by-products remain after steam distillation. Disposal or composting is among the common practices for the treatment of the industrially processed lavender biomass. However,

it can also serve as a raw material for the extraction of valuable biologically active substances that can be used in the food, cosmetic and perfume industries [5].

Pectins or pectic polysaccharides are quite common multifunctional components in the cell walls of almost all higher plants. Pectin macromolecules are made up of more than 15 monosaccharides. Among these, α -D-galacturonic acid is the major building block. Pectin has a wide range of applications in the food and cosmetic industries as gelling agent, stabilizer and thickener [6]. Due to the scarce information in the literature on pectic polysaccharides extracted from lavender by-products the aim of the present work was to investigate two lavender by-products and one untreated lavender for obtaining of polysaccharides, as a possible method for by-products valorization.

MATERIALS AND METHODS

The solid by-products of lavender essential oil industry were kindly provided by: Galen-N Ltd. (Zelenikovo, Brezovo, Bulgaria; 2022 harvest); from steam distillation of *Lavandula angustifolia*, abbreviated as L_SD_22_Z; EKOMAAT Ltd.

* To whom all correspondence should be sent:
E-mail: gerii_vlaseva@abv.bg

(Mirkovo, Sofia, Bulgaria; 2022 harvest); from steam distillation of *Lavandula angustifolia*, abbreviated as L_SD_22_M. The raw untreated lavender was provided by Galen-N Ltd. (Zelenikovo, Brezovo, Bulgaria; 2022 harvest) and further referred to as L_UNTR_22_Z.

Preparation of alcohol-insoluble residues (AIR)

Lavender biomass was treated with 70% ethanol (v/v) and after filtration, AIRs of the initial raw materials were prepared as described in [7].

Acid extraction (0.1 M hydrochloric acid) of AIRs

The acid extraction was performed twice. The first extraction was performed with 1000 mL of 0.1 M aqueous hydrochloric acid (HCl). The extraction took place for 1 h at 85°C, pH 1.5 and continuous stirring. The slurry was filtered through a nylon cloth (250 mesh). The second extraction was carried out on the solid residue from the first extraction using 1000 mL of 0.1 M aqueous HCl under the same conditions. The two filtrates were precipitated with 96% ethanol (1:2 parts by volume) to obtain the acid-soluble pectic polysaccharides.

Determination of ash content

Ash is the total inorganic residue produced after combustion or complete oxidation of the organic matter in the various samples. 1 g of the sample (m_1) was placed in a pre-weighed porcelain crucible (m_C). The crucible was placed in an oven heated to 600°C and held for 4 h. The crucible was removed and after tempering in a desiccator, was weighed until a constant weight (m_2) was established.

The ash content (A , %) was calculated according to the formula:

$$A, \% = \frac{(m_C+m_1)-m_2}{m_C+m_1} \times 100 \quad (1)$$

Determination of protein content in the lavender raw materials

The determination of the protein content in the lavender raw materials was performed according to the AOAC Method 976.06 using automated Kjeldahl system MultiKjel K-365 with potentiometric titrator

Metrohm ECO (Büchi Labortechnik, Switzerland) and conversion factor 6.25 for converting the amount of nitrogen to protein. The polyuronide content PU and degree of esterification DE were determined as described in [8]. The protein content of the polysaccharides, the amounts of neutral sugars and the anhydrogalacturonic acid content were determined spectrophotometrically using the Bradford method with AMRESCO E535-KIT (AMRESCO, Solon, Ohio, USA) with bovine gammaglobuline as standard, the phenol-sulfuric acid method with D-galactose as standard and the m-hydroxydiphenyl method with D-galacturonic acid as standard, respectively, as described in details in [9]. The molecular mass of the isolated polysaccharides was determined using an ELITE LaChrome HPLC system (Hitachi) with a VWR Hitachi Chromaster 5450 light refraction detector and an OHPak SB-806M column (Shodex®). Samples and standards were eluted with 0.1 M NaNO₃ at an elution rate of 0.8 mL/min, column temperature of 30°C and detector temperature of 35°C. The column was equilibrated with standards of Shodex® pullulans (Showa DENKO, Japan) (2 mg/mL) with molecular weights of 6.2×10^3 , 10.0×10^3 , 21.7×10^3 , 48.8×10^3 , 113.0×10^3 , 200.0×10^3 , 366.0×10^3 , and 805.8×10^3 Da.

RESULTS AND DISCUSSION

The general characteristics of the by-products and untreated lavender are presented in Table 1.

Analyses of the main physicochemical parameters of the lavender biomass showed that L_SD_22_Z had the highest mineral content (7.45±0.20%) and the highest polyuronide content (8.0±0.2%) compared to the other two materials.

In the next experiments, the AIRs were subjected to an extraction with 0.1 M HCl in order to obtain pectic polysaccharides. This extraction is mimicking the industrial processing of the by-products from the fruit juice industry and obtaining of apple and citrus pectins [10]. The yield and the general physicochemical parameters of the isolated polysaccharides are presented in Table 2.

Table 1. General characteristics of lavender by-products and raw untreated lavender

Parameter \ By-product	L_SD_22_M	L_SD_22_Z	L_UNTR_22_Z
Ash, %	5.41±0.07 ^b	7.45±0.20 ^a	4.10±0.33 ^c
Protein, %	8.15 ± 1.6 ^a	6.72 ± 0.28 ^b	5.94 ± 0.12 ^c
PU, %	7.5±0.1 ^b	8.0±0.2 ^a	7.1±0.1 ^c
DE, %	83.9±0.5 ^a	78.9±0.5 ^c	81.6±0.3 ^b

PU - polyuronide content; DE – degree of esterification. The results are expressed as mean ± SD (n = 3). ^{a,b,c} Different letters in a row mean statistical difference (Tuckey’s test, p < 0.05).

Table 2. Yield and physico-chemical parameters of pectic polysaccharides extracted by 0.1 M HCl from lavender AIRs

	Yield, %	Crude protein, %	Neutral sugars, µg/mg	Molecular weight, ×10 ⁴ Da	Proteins, µg/mg
L_SD_22_M	7.54±0.15 ^a	5.32±0.24 ^a	599.71±24.26 ^b	2.47	nd
L_SD_22_Z	6.62±0.16 ^b	4.65±0.19 ^b	713.55±19.34 ^a	2.34	1.37±0.07
L_UNTR_22_Z	6.92±0.21 ^b	4.85±0.17 ^b	585.87±21.04 ^b	3.28	nd

The results are expressed as mean ± SD (n = 3). ^{a,b}Different letters in a column mean statistical difference (Tuckey's test, p < 0.05).

Table 3. Yield and physico-chemical parameters of pectic polysaccharides obtained by sequential fractional extraction with deionized water, 0.05 M (NH₄)₂C₂O₄, 0.1 M HCl and 0.05 M NaOH of L_SD_22_M, L_SD_22_Z and L_UNTR_22_Z AIRs

	Extractor	Yield, %	Neutral sugars, µg/mg	Molecular weight, × 10 ⁴ , Da	Proteins, µg/mg
L_SD_22_M	Deionized water	4.60	503.10	3.07	5.20
	0.05 M (NH ₄) ₂ C ₂ O ₄	7.59	391.52	8.31	0.85
	0.1 M HCl	2.28	551.13	2.23	nd
	0.05 M NaOH	0.59	446.04	2.01	nd
L_SD_22_Z	Deionized water	4.05	428.81	2.08	8.37
	0.05 M (NH ₄) ₂ C ₂ O ₄	7.12	523.16	7.26	nd
	0.1 M HCl	2.38	474.29	2.92	2.15
	0.05 M NaOH	0.62	431.35	1.91	5.65
L_UNTR_22_Z	Deionized water	0.99	252.25	3.51 1.19	4.92
	0.05 M (NH ₄) ₂ C ₂ O ₄	4.69	432.76	26.17	0.41
	0.1 M HCl	3.87	384.74	3.07	nd
	0.05 M NaOH	1.01	467.51	2.38	5.05

nd – not determined.

The highest yield of acid-soluble pectic polysaccharides was observed for alcohol-insoluble parts of lavender by-product L_SD_22_M: 7.54%. The highest amount of neutral sugars was found for L_SD_22_Z: 713.55 µg/mg polysaccharide. For all three polysaccharides the amount of proteins was very low.

The experiments employing sequential extraction with different extractants suggested that the highest pectin yield was observed for the ammonium oxalate as extractant and the percentage of pectin was around 7%, except for the L_UNTR_22_Z, where the yield was 4.69% (Table 3). These results could be explained by the ionic bonding by Ca²⁺ ions of the pectic polysaccharides present in the lavender cell walls. The yield of water-soluble pectic polysaccharides for L_UNTR_22_Z was quite low: 0.99%, compared to the two by-products (4.60 and

4.05% for the L_SD_22_M and L_SD_22_Z, respectively). This might suggest that the steam distillation serves as initial pretreatment, which disrupts the cell walls of lavender biomass and facilitates further extraction of pectic polysaccharides from the by-products.

The evaluation of the monosaccharide composition of the extracted polysaccharides (Table 4) showed that the major building monomer of the extracted polysaccharides from L_SD_22_M (with 0.1 M HCl): 717.62 µg/mg; L_SD_22_Z (with deionized water): 312.42 µg/mg; L_UNTR_22_Z (with 0.1 M HCl): 448.78 µg/mg, was galacturonic acid. Small amounts of glucuronic acid were also detected. The second most abundant monosaccharide was galactose. The other monosaccharides detected that are characteristic of pectic polysaccharides were arabinose and xylose.

Table 4. Uronic acids and monosaccharide composition of pectic polysaccharides extracted by deionized water, 0.05 M (NH₄)₂C₂O₄, 0.1 M HCl and 0.05 M NaOH of L_SD_22_M, L_SD_22_Z and L_UNTR_22_Z AIRs

	Extractor	GlcA	GalA	Gal	Ara	Fuc	Xyl	Man
		(Polysaccharide, µg/mg)						
L_SD_22_M	Deionized water	30.63	517.67	88.59	32.17	1.95	13.03	12.73
	0.05 M (NH ₄) ₂ C ₂ O ₄	12.38	331.90	54.23	33.77	nd	22.11	7.12
	0.1 M HCl	8.31	717.62	91.79	19.40	nd	20.45	5.26
	0.05 M NaOH	6.83	444.44	134.27	16.80	nd	16.08	9.03
L_SD_22_Z	Deionized water	25.51	312.42	56.41	20.04	1.10	15.99	19.59
	0.05 M (NH ₄) ₂ C ₂ O ₄	10.44	233.26	54.78	52.02	nd	17.02	4.07
	0.1 M HCl	4.81	272.23	52.00	12.15	nd	10.12	17.98
	0.05 M NaOH	5.22	165.77	69.74	14.59	nd	12.85	9.12
L_UNTR_22_Z	Deionized water	43.14	189.43	49.94	10.13	nd	9.58	25.71
	0.05 M (NH ₄) ₂ C ₂ O ₄	10.40	243.89	32.76	27.36	nd	10.17	15.60
	0.1 M HCl	11.16	448.78	76.22	26.58	nd	55.33	10.63
	0.05 M NaOH	7.48	221.73	69.11	10.88	nd	14.32	3.40

GlcA – D-Glucuronic acid; GalA – D-Galacturonic acid; Gal – D-Galactose; Ara – D-Arabinose; Fuc – L-Fucose; Xyl – D-Xylose; Man – D-Manose; nd – not determined.

CONCLUSION

The hypothesis of the present work was to investigate the lavender biomass as a potential source of pectic polysaccharides – a possible pathway for lavender by-products valorization. Two solid residues obtained after steam distillation (the traditional way of lavender processing) and one untreated lavender pulp were investigated. Composition analysis showed that lavender by-products were rich in pectic polysaccharides, proteins, neutral sugars, etc. The highest yield of acid-soluble pectic polysaccharides was observed for the alcohol-insoluble parts of lavender by-product L_SD_22_M: 7.54%. The highest yield from the sequential fractional extraction of polysaccharides was observed using ammonium oxalate as extractant. This could suggest that a large part of the pectic polysaccharides were present in the lavender cell wall biomass, ionically bonded by divalent cations (mostly Ca²⁺). We conclude that lavender residues after steam distillation could serve as a potential source of pectic polysaccharides, which combined with other approaches will allow valorization of the lavender by-products from essential oil industry.

Acknowledgement: We acknowledge the financial support from the National Science Fund (Ministry of

Education and Science) of Bulgaria, project KII-06-Austria/4.

REFERENCES

1. L. Lesage-Meessen, M. Bou, J.C. Sigoillot, C.B. Faulds, A. Lomascolo, *Applied Microbiology and Biotechnology*, **99**, 3375 (2015).
2. A. Stoyanova, A. Balinova-Tsvetkova, A. Georgiev, *Lavender – Obtaining of essential oil products in Bulgaria*, 1st edn. 7DAgency, Plovdiv, 2009.
3. G. Marovska, I. Vasileva, N. Petkova, M. Ognyanov, V. Gandova, A. Stoyanova, P. Merdzhanov, A. Simitchiev, A. Slavov, *Industrial Crops and Products*, **188**, 115678 (2022).
4. M. Atanasova, N. Nedkov, *Essential oil and medicinal crops*, Kameya, Sofia, 2004.
5. G. Marovska, I. Vasileva, A. Aggelidou, N. Yantcheva, A. Slavov, *Bulgarian Chemical Communications*, **54**(1), 81 (2022).
6. A. G. J. Voragen, W. Pilnik, J.F. Thibault, M. A. V. Axelos, C. M. G. C. Renard, in: *Food polysaccharides and their applications*, A. M. Stephen (ed.) Marcel Dekker, New York, 1995, p. 287.
7. G. Marovska, I. Hambarliyska, N. Petkova, I. Ivanov, I. Vasileva, A. Slavov, *Philippine Journal of Science*, **152**(3), 861 (2023).
8. M. Kratchanova, M. Nikolova, E. Pavlova, I. Yanakieva, V. Kussovski, *Journal of the Science of Food and Agriculture*, **90**(12), 2046 (2010).
9. A. Slavov, M. Ognyanov, I. Vasileva, *Food Hydrocolloids*, **101**, 105545 (2020).
10. C. D. May, *Carbohydrate Polymers*, **12**, 79 (1990).

Instructions about Preparation of Manuscripts

General remarks: Manuscripts are submitted in English by e-mail. The text must be prepared in A4 format sheets using Times New Roman font size 11, normal character spacing. The manuscript should not exceed 15 pages (about 3500 words), including photographs, tables, drawings, formulae, etc. Authors are requested to use margins of 2 cm on all sides.

Manuscripts should be subdivided into labelled sections, e.g. INTRODUCTION, EXPERIMENTAL, RESULTS AND DISCUSSION, etc. **The title page** comprises headline, author(s)' names and affiliations, abstract and key words. Attention is drawn to the following:

a) **The title** of the manuscript should reflect concisely the purpose and findings of the work. Abbreviations, symbols, chemical formulae, references and footnotes should be avoided. If indispensable, abbreviations and formulae should be given in parentheses immediately after the respective full form.

b) **The author(s)**' first and middle name initials and family name in full should be given, followed by the address (or addresses) of the contributing laboratory (laboratories). **The affiliation** of the author(s) should be listed in detail (no abbreviations!). The author to whom correspondence and/or inquiries should be sent should be indicated by an asterisk (*) with e-mail address.

The abstract should be self-explanatory and intelligible without any references to the text and containing up to 250 words. It should be followed by keywords (up to six).

References should be numbered sequentially in the order, in which they are cited in the text. The numbers in the text should be enclosed in brackets [2], [5, 6], [9–12], etc., set on the text line. References are to be listed in numerical order on a separate sheet. All references are to be given in Latin letters. The names of the authors are given without inversion. Titles of journals must be abbreviated according to Chemical Abstracts and given in italics, the volume is typed in bold, the initial page is given and the year in parentheses. Attention is drawn to the following conventions: a) The names of all authors of a certain publication should be given. The use of "et al." in the list of references is not acceptable; b) Only the initials of the first and middle names should be given. In the manuscripts, the reference to author(s) of cited works should be made without giving initials, e.g. "Bush and Smith [7] pioneered...". If the reference carries the names of three or more authors it should be quoted as "Bush et al. [7]", if Bush is the first author, or as "Bush and co-workers [7]", if Bush is the senior author.

Footnotes should be reduced to a minimum. Each footnote should be typed double-spaced at the bottom of the page, on which its subject is first mentioned. **Tables** are numbered with Arabic numerals on the left-hand top. Each table should be referred to in the text. Column headings should be as short as possible but they must define units unambiguously. The units are to be separated from the preceding symbols by a comma or brackets. Note: The following format should be used when figures, equations, etc. are referred to the text (followed by the respective numbers): Fig., Eqns., Table, Scheme.

Schemes and figures. Each manuscript should contain or be accompanied by the respective illustrative material, as well as by the respective figure captions in a separate file. As far as presentation of units is concerned, SI units are to be used. However, some non-SI units are also acceptable, such as °C, ml, l, etc. Avoid using more than 6 (12 for review articles) figures in the manuscript. Since most of the illustrative materials are to be presented as 8-cm wide pictures, attention should be paid that all axis titles, numerals, legend(s) and texts are legible.

The authors are required to submit the text with a list of three individuals and their e-mail addresses that can be considered by the Editors as potential reviewers. Please note that the reviewers should be outside the authors' own institution or organization. The Editorial Board of the journal is not obliged to accept these proposals.

The authors are asked to submit **the** final text (after the manuscript has been accepted for publication) in electronic form by e-mail. The main text, list of references, tables and figure captions should be saved in separate files (as *.rtf or *.doc) with clearly identifiable file names. It is essential that the name and version of the word-processing program and the format of the text files is clearly indicated. It is recommended that the pictures are presented in *.tif, *.jpg, *.cdr or *.bmp format. The equations are written using "Equation Editor" and chemical reaction schemes are written using ISIS Draw or ChemDraw programme.

EXAMPLES FOR PRESENTATION OF REFERENCES

REFERENCES

1. D. S. Newsome, Catal. Rev.–Sci. Eng., 21, 275 (1980).
2. C.-H. Lin, C.-Y. Hsu, J. Chem. Soc. Chem. Commun., 1479 (1992).
3. R. G. Parr, W. Yang, Density Functional Theory of Atoms and Molecules, Oxford Univ. Press, New York, 1989.
4. V. Ponec, G. C. Bond, Catalysis by Metals and Alloys (Stud. Surf. Sci. Catal., vol. 95), Elsevier, Amsterdam, 1995.
5. G. Kadinov, S. Todorova, A. Palazov, in: New Frontiers in Catalysis (Proc. 10th Int. Congr. Catal., Budapest (1992), L. Guzzi, F. Solymosi, P. Tetenyi (eds.), Akademiai Kiado, Budapest, 1993, Part C, p. 2817.
6. G. L. C. Maire, F. Garin, in: Catalysis. Science and Technology, J. R. Anderson, M. Boudart (eds.), vol. 6, Springer Verlag, Berlin, 1984, p. 161.
7. D. Pocknell, GB Patent 2 207 355 (1949).
8. G. Angelov, PhD Thesis, UCTM, Sofia, 2001, pp. 121-126.
9. JCPDS International Center for Diffraction Data, Power Diffraction File, Swarthmore, PA, 1991.
10. CA 127, 184 762q (1998).
11. P. Hou, H. Wise, J. Catal., in press.
12. M. Sinev, private communication.
13. <http://www.chemweb.com/alchem/articles/1051611477211.html>.

Texts with references which do not match these requirements will not be considered for publication!!!

CONTENTS

<i>M. H. Docheva, D. M. Kirkova, I. S. Stoyanova</i> , Factors affecting the 5-hydroxymethyl-2-furfural content in the gas-phase of tobacco smoke of commercial cigarette brands.....	5
<i>St. Georgieva, Zl. Peteva, S. Valkova</i> , Persistent pollutants in marine organisms: assessment of the state of the Black Sea environment.....	10
<i>Ts. Dimitrova, S. Ivanova, S. Stoycheva</i> , Fatty acid composition in kefir from milk of “Bulgarian White Dairy” goat breed and its crossings.....	20
<i>I. Nikolova, I. Kostova, M. Marinov</i> , Phenothiazine Schiff bases containing chlorine: synthesis, characterization and antimicrobial study.....	26
<i>G. Simeonova, B. Todorov</i> , The modification of [¹⁸ F] FDG for further click reactions.....	31
<i>Zh. Petkova, V. Popova, N. Petkova, T. Ivanova, P. Merdzhanov, A. Stoyanova</i> , phytonutrients in black nightshade fruit (<i>Solanum Nigrum</i> L.) growing in Bulgaria.....	38
<i>V. Gandova, O. Teneva, Zh. Petkova, I. Iliev, A. Stoyanova</i> , Lipid composition and investigation of the physicochemical characteristics at different temperatures of high oleic sunflower oil.....	44
<i>L. Stoyanova, M. Angelova-Romova</i> , Chemical composition of seeds from organically grown tobacco plants.....	49
<i>O. Teneva, Zh. Petkova, M. Angelova-Romova, G. Antova</i> , Comparative study on chemical composition and lipids of two species of quinoa seeds (<i>Chenopodium quinoa</i>).....	55
<i>T. Trifonova, St. Georgieva, Z. Peteva</i> , Persistent environmental contaminants in human milk samples from northeastern region of Bulgaria.....	60
<i>A. Merdzhanova, D. Dobрева, V. Panayotova, K. Peycheva, T. Hristova, R. Stancheva</i> , <i>Chamelea gallina</i> from the Black Sea (Bulgaria) as a sustainable source of macronutrients and fat-soluble vitamins.....	66
<i>A. Slavov, G. Marovska</i> , Characterization of by-products from industrial processing of the essential oil crops rose, hyssop, and thyme.....	71
<i>M. Brazkova, R. Koleva, G. Angelova, A. Krastanov</i> Degradation of pyrene by laccase from <i>Trametes versicolor</i>	78
<i>Y. Koleva, I. Iliev, V. Gandova, A. Stoyanova</i> , Potential toxicity, physicochemical properties and environmental behavior of L-carvone.....	84
<i>Y. Koleva, I. Iliev, V. Gandova, A. Stoyanova</i> , Predicting The potential absorption, distribution, metabolism and excretion of the aldehyde citral.....	92
<i>I. Ivanov, M. Todorova, N. Petkova, I. Dincheva</i> , Non-polar phytochemical compounds from dandelion (<i>Taraxacum officinale</i> Weber. ex F.H. Wigg.) flowers.....	96
<i>D. Vassilev, N. Petkova, D. Yaneva, P. Denev</i> , Application of “Green chemistry” principles to the modification of carbohydrates from natural sources for bio-additives in plastics	100
<i>K. V. Petkova-Parlapanska, E. D. Georgieva, Y. D. Karamalakova, P. I. Goycheva, G. D. Nikolova</i> , Type 2 diabetes mellitus and vascular complications.....	104
<i>Y. D. Karamalakova, E. D. Georgieva, K. V. Petkova-Parlapanska, V. B. Slavova, K.V. Ivanova, V. A. Ivanov, G. D. Nikolova</i> , <i>Silybum marianum</i> reduces acute kidneys injury by modifying biochemical changes and oxidative stress levels in glycerol-induced CRUSH syndrome.....	109
<i>Y. D. Karamalakova, E. D. Georgieva, K. V. Petkova-Parlapanska, V. A. Ivanov, G. D. Nikolova</i> , Neuroprotective effect of <i>Silybum marianum</i> in brain regions after experimental ochratoxicosis.....	116
<i>I. Hambarliyska, N. Petkova, P. Georgieva, A. Slavov, M. Ognyanov, D. Karashanova, B. Georgieva, Y. Tumbarski</i> , Green methods for inulin extraction from common salsify (<i>Tragopogon porrifolius</i> L.) roots and its application in metal nanoparticles synthesis.....	121
<i>V. Paskova, K. Dobрева, I. Dimitrova</i> , Investigation of the effect of ultrasound-assisted extraction on the yield and tannin content of white oregano extracts.....	129
<i>Ts. Valev, K. Dobрева, M. Dimov</i> , Phytochemical characterization of different varieties of thyme.....	133
<i>E. Georgieva, D. Berbatov, Y. Karamalakova, G. Nikolova, M. Gulubova</i> , Application of stable nitroxide radicals and their non-contrast forms in diagnostics of oxidative stress in patients with diabetes mellitus type 2 and non-alcoholic fatty liver disease.....	138

<i>A. Popova, D. Mihaylova, P. Doykina, S. Pandova</i> , Evaluation of preliminary physico-chemical parameters and biometric characteristics of the “Stendesto” plum-apricot hybrid with reference to its parental lines.....	143
<i>V. Panayotova, A. Merdzhanova, D. Dobрева, K. Peycheva, T. Stoycheva</i> , <i>Chlorella</i> and <i>Spirulina</i> dietary supplements as sources of biologically active lipids.....	148
<i>G. Marovska, A. Slavov</i> , Pectic polysaccharides extracted from unprocessed and steam-distilled lavender biomass.....	152
<i>Instructions to authors</i>	156